SELECTED TOPICS IN

Identification Modelling and Control

Volume 5, 1992

Edited by O.H. Bosgra and P.M.J. Van den Hof

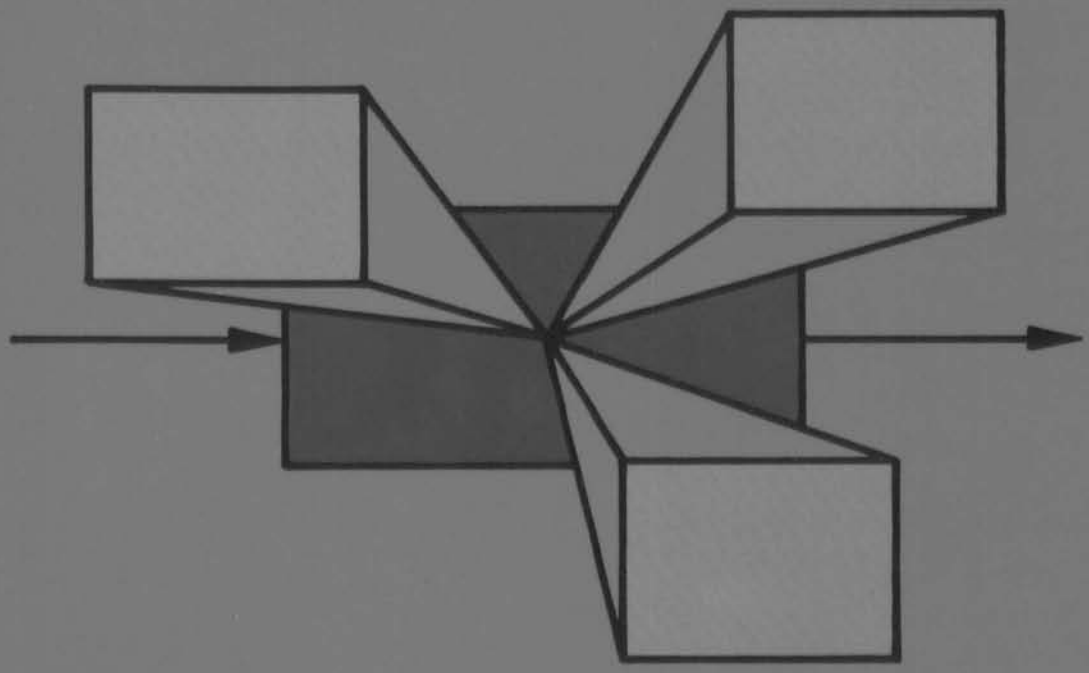

Delft University Press

IDENTIFICATION, MODELLING AND CONTROL

SELECTED TOPICS IN IDENTIFICATION, MODELLING AND CONTROL

Progress Report on Research Activities in the Mechanical Engineering Systems and Control Group

Edited by O.H. Bosgra and P.M.J. Van den Hof

Volume 5, December 1992

Mechanical Engineering Systems and Control Group
Delft University of Technology

Delft University Press/1992

Published and Distributed by

Delft University Press
Stevinweg 1
2628 CN Delft
The Netherlands
Tel.: (0)15 - 783254
Telefax: (0)15 - 781661

By order of

Mechanical Engineering Systems and Control Group
Delft University of Technology
Mekelweg 2, 2628 CD Delft
The Netherlands
Tel.: +31-15-786400; Telefax: +31-15-784717

CIP-GEGEVENS KONINKLIJKE BIBLIOTHEEK, DEN HAAG

Selected

Selected topics in identification, modelling and control:
progress report on research activities in the mechanical engineering
systems and control group. - Delft:Mechanical Engineering Systems and Control Group,
Delft University of Technology, Vol. 5-ed. by O.H. Bosgra and
P.M.J. Van den Hof.-ill. Met lit.opg.
ISBN 90-6275-834-7
SISO 656 UDC 531.7 + 681.5 NUGI 841

Cover design by Ruud Schrama

Contents

Volume 5, December 1992

Parametric uncertainty modelling using LFTs
P.F. Lambrechts, J. Terlouw, S. Bennani and M. Steinbuch 1

Robustness of feedback systems under simultaneous plant and controller perturbation
P.M.M. Bongers 11

Stability robustness for simultaneous perturbations of linear plant and controller: beyond the gap metric
R.J.P. Schrama, P.M.M. Bongers and O.H. Bosgra 19

Generalized frequency weighted balanced reduction
P.M.R. Wortelboer and O.H. Bosgra 29

On orthogonal basis functions that contain system dynamics
P.S.C. Heuberger, P.M.J. Van den Hof and O.H. Bosgra 37

Partial validation of a flexible wind turbine model
G.E. van Baars and P.M.M. Bongers 45

Heat balance reconciliation in chemical process operation
E.A.J.Ch. Baak, J. Krist and S. Dijkstra 53

Worst-case system identification in ℓ_1: error bounds, optimal models and model reduction
R.G. Hakvoort 63

Worst-case system identification in H_∞: error bounds, interpolation and optimal models
R.G. Hakvoort 73

A mixed deterministic-probabilistic approach for quantifying uncertainty in transfer function estimation
D.K. de Vries and P.M.J. Van den Hof 85

Iterative identification and control design: a worked out example
R.J.P. Schrama and P.M.J. Van den Hof 93

Editorial

The present issue of *Selected Topics in Identification, Modelling and Control* is the fifth volume in the series, reporting on ongoing research in the *Mechanical Engineering Systems and Control Group* at Delft University of Technology. We have eleven papers on a variety of subjects that completely cover the subjects of *Identification, Modelling and Control.*

In the area of *Modelling*, the issue of model uncertainty representation is considered by *Lambrechts et al.* with a contribution aimed at obtaining structured uncertainty models to be used in μ-synthesis controller design. *Wortelboer and Bosgra* consider extensions to frequency weighted balancing model reduction. The modelling of a wind power generation system is the subject of *Van Baars and Bongers* who present first results on the issue of experimental validation of their theoretical models. The real-time modelling of heat balances and the estimation of the relevant process variables on the basis of operational chemical process plant data is the subject of work reported by *Baak et al.*

The field of *Control* is covered in contributions by *Bongers* and by *Schrama et al.* Both papers consider robust control issues with both uncertainty in plant and in controller, and derive new results with respect to robust stability. The interplay between the requirements of robust high-performance control and the achievements of error-analysis-directed system identification is shown in the contribution by *Schrama and Van den Hof.*

In the area of *System Identification* we have two papers by *Hakvoort* addressing worst-case aspects of identification for two fundamentally different error criteria. The issue of guaranteed error bounds in system identification results is discussed and worked out by *De Vries and Van den Hof.* Finally, *Heuberger et al.* show the construction of orthogonal domains that may lead to advantageous signal and system representations in system identification.

The present issue contains results from applied projects and from theoretical studies. We appreciate the fact that results from collaborative projects performed in cooperation with external institutes and industrial research groups constitute a considerable part of this issue. Although most of the material presented here will eventually be published elsewhere in the open literature, we appreciate the efforts of our authors who in many cases have made available some of their most recent research results. We hope you enjoy the result.

Okko Bosgra
Paul Van den Hof
Editors

Selected Topics in Identification, Modelling and Control
Vol. 5, December 1992

Parametric uncertainty modeling using LFTs

Paul Lambrechts[‡], Jan Terlouw[‡], Samir Bennani[§] and Maarten Steinbuch[♯]

[‡] *Mechanical Engineering Systems and Control Group, Delft University of Technology, Mekelweg 2, 2628 CD Delft, The Netherlands*
[§] *Fac. of Aerospace Engineering, Section Stability and Control, Delft University of Technology, Kluyverweg 1, 2629 HS Delft, The Netherlands*
[♯] *Philips Research Laboratories, P.O.Box 80.000, 5600 JA Eindhoven, The Netherlands*

Abstract. In this paper a general approach for modelling structured real-valued parametric perturbations is presented. It is based on a decomposition of perturbations into linear fractional transformations (LFTs), and is applicable to rational multi-dimensional (ND) polynomial perturbations of entries in state-space models. Model reduction is used to reduce the size of the uncertainty structure. The procedure will be applied for the uncertainty modelling of an aircraft model depending on altitude and velocity (flight envelope).

1 Introduction

In both robustness analysis and robust control system design the concept of the structured singular value μ as introduced by Doyle (1982) is of great importance. It allows a high degree of detail in modelling the conditions under which the considered control system should operate satisfactorily, both in the sense of stability and performance. The calculation of μ for such models then results in a single number acting as an accurate measure in indicating whether the behaviour of the controlled system is satisfactory or not. The relevance of using the structured singular value instead of measures that do not reflect the structural properties of the plant uncertainties, like the ∞-norm or the 2-norm, can be found in literature; the latter may lead to arbitrarily conservative statements when practical examples are considered (see for instance Balas et al., 1990, Stein and Doyle, 1978, 1991, Doyle et al., 1986, Skogestad et al., 1988). In spite of this the use of μ has been seriously hampered by the considerable computational effort needed for its calculation with respect to a given uncertainty model. Recently developed methods for calculating close upper and lower bounds for the most general cases (Fan and Tits, 1986, 1991, Young et al., 1991) now motivate the effort of modelling uncertainties in great detail. The main issue of this paper is to offer a complete procedure for setting up the general structure for the calculation of μ when uncertainties like real-valued parameter variations in state-space models and variations in operational conditions occur.

First, we will give some preliminary results on the use of Linear Fractional Transformations (LFTs) and their importance for uncertainty modelling, followed by a definition of the structured singular value μ and some relevant uncertainty sets. Section 3 then will present a procedure for parametric uncertainty modelling based on a state-space model in which uncertain entries may be given as rational multi-dimensional polynomial functions of a set of parameters. The usefulness of this procedure for practical problems will be demonstrated by means of an extensive example in section 4, after which some concluding remarks follow in section 5.

2 Preliminaries

This section will review some of the properties of Linear Fractional Transformations (LFTs) and the structured singular value μ along the lines of Doyle

et al. (1987, 1991). First we will give a definition of upper and lower LFTs and discuss some important possibilities of combining and rearranging them. Next we will consider the LFT concept as a framework for uncertainty modelling and within this framework we will give a definition of μ and some relevant uncertainty sets.

2.1 Definition of LFTs

We will consider matrices with entries that are fractions of polynomials in a complex-valued variable s; the space of all such real rational functions will be denoted as $\mathrm{R}(s)$, $M \in \mathrm{R}(s)^{p\times q}$ will denote that M is a $p \times q$ matrix with entries in $\mathrm{R}(s)$. Suppose a matrix $M \in \mathrm{R}(s)$ is partitioned as:

$$M = \begin{bmatrix} M_{11} & M_{12} \\ M_{21} & M_{22} \end{bmatrix} \quad \in \mathrm{R}(s)^{(p_1+p_2)\times(q_1+q_2)} \qquad (1)$$

and let $\Delta_u \in \mathrm{R}(s)^{q_1\times p_1}$ and $\Delta_l \in \mathrm{R}(s)^{q_2\times p_2}$ be arbitrary. We will then define the *upper* and *lower* LFTs as operators on Δ_u and Δ_l respectively:

$$\begin{aligned} \mathcal{F}_u(M,\Delta_u) &:= M_{22}+ \\ &\quad M_{21}(I-\Delta_u M_{11})^{-1}\Delta_u M_{12} \\ \mathcal{F}_l(M,\Delta_l) &:= M_{11}+ \\ &\quad M_{12}(I-\Delta_l M_{22})^{-1}\Delta_l M_{21} \end{aligned} \qquad (2)$$

Either LFT will be called *well defined* if the concerning inverse exists: $\det(I-\Delta_u M_{11}) \neq 0$ and $\det(I-\Delta_l M_{22}) \neq 0$. The matrix M is sometimes referred to as the coefficient matrix of the LFT. Note that if s is interpreted as the Laplace variable, a matrix with entries in $\mathrm{R}(s)$ can be seen as a multivariable transfer function of a linear time invariant finite dimensional system. In that case LFTs can be seen as operations resulting from feedback structures as given in fig.1; eq.2 then defines a closed loop transfer functions from w_M to z_M in both cases.

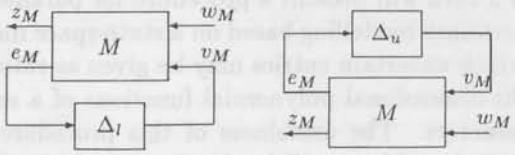

Fig. 1: Upper and lower LFT as feedback structure

An important reason for using the concept of LFTs in linear systems theory is that linear interconnections of LFTs can be rewritten as one single LFT. This implies that LFTs can be used to separately model specific details of the system under consideration after which a complete system description can be obtained by working out all connections. To demonstrate this we will first look at the two most basic connections between two LFTs: the cascade and parallel configurations. After that we will show a simple feedback configuration for one LFT which can also be rewritten into the standard form of fig.1. These three configurations will play an important role in the algorithmic approach to uncertainty modelling we will present in section 3.

Given matrices M and N partitioned as in eq.1: $M \in \mathrm{R}(s)^{p_M\times q_M)}$ and $N \in \mathrm{R}(s)^{p_N\times q_N}$, with $p_M := p_{M1}+p_{M2}$, $q_M := q_{M1}+q_{M2}$, $p_N := p_{N1}+p_{N2}$ and $q_N := q_{N1}+q_{N2}$. Let M and N be the coefficient matrices of the upper LFTs on $\Delta_M \in \mathrm{R}(s)^{q_{M1}\times p_{M1}}$ and $\Delta_N \in \mathrm{R}(s)^{q_{N1}\times p_{N1}}$ respectively and define the combined structure:

$$\Delta_{MN} = \begin{bmatrix} \Delta_M & 0 \\ 0 & \Delta_N \end{bmatrix} \quad \in \mathrm{R}(s)^{q_{MN}\times p_{MN}} \qquad (3)$$

with $p_{MN} := p_{M1}+p_{N1}$ and $q_{MN} := q_{M1}+q_{N1}$. Then the cascade connection obtained by setting $w_M = z_N$ with $r := q_{M2} = p_{N2}$ (see fig.2) results in an upper LFT on Δ_{MN} with coefficient matrix:

$$M_c = \left[\begin{array}{cc|c} M_{11} & M_{12}N_{21} & M_{12}N_{22} \\ 0 & N_{11} & N_{12} \\ \hline M_{21} & M_{22}N_{21} & M_{22}N_{22} \end{array}\right] \qquad (4)$$

$$M_c \in \mathrm{R}(s)^{(p_{MN}+r)\times(q_{MN}+r)}$$

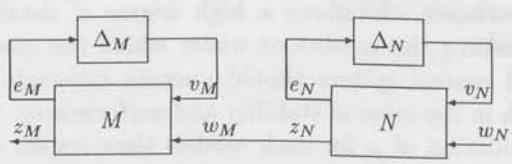

Fig. 2: Cascade connection of LFTs

The parallel connection obtained by setting $w_M = w_N$ and $z_{MN} = z_M + z_N$ with $r_q := q_{M2} = q_{N2}$ and $r_p := p_{M2} = p_{N2}$ (see fig.3) also results in an upper LFT on Δ_{MN}, this time with coefficient matrix:

$$M_p = \left[\begin{array}{cc|c} M_{11} & 0 & M_{12} \\ 0 & N_{11} & N_{12} \\ \hline M_{21} & N_{21} & M_{22}+N_{22} \end{array}\right] \qquad (5)$$

$$M_p \in \mathrm{R}(s)^{(p_{MN}+r_p)\times(q_{MN}+r_q)}$$

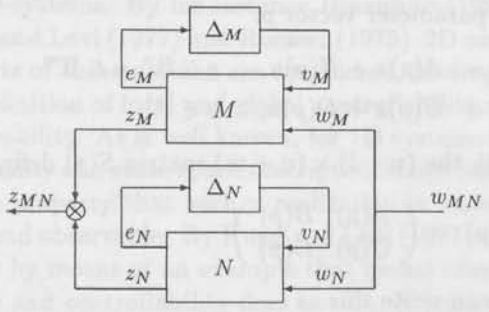

Fig. 3: Parallel connection of LFTs

Note that we have conveniently chosen the inputs and outputs of both LFTs to be compatible, but that it is also possible to connect only parts of input and output vectors by defining a further partitioning of M and N.

Next consider the feedback configuration given in fig.4 with M_{11} square ($p_1 = q_1$). In this case

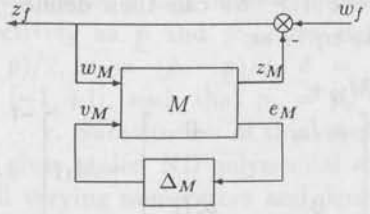

Fig. 4: An LFT in the feedback path

the coefficient matrix of the equivalent LFT can be calculated as:

$$M_f = \left[\begin{array}{c|c} M_{f11} & M_{f12} \\ \hline M_{f21} & M_{f22} \end{array}\right] \in \mathrm{R}(s)^{(p_2+p_1)\times(q_2+q_1)} \quad (6)$$

with:

$$\begin{array}{rcl} M_{f11} & := & M_{21}(I+M_{11})^{-1}M_{12} + M_{22} \\ M_{f12} & := & M_{21}(I+M_{11})^{-1} \\ M_{f21} & := & -(I+M_{11})^{-1}M_{12} \\ M_{f22} & := & (I+M_{11})^{-1} \end{array} \quad (7)$$

Clearly, for this coefficient matrix to be well defined we must have $\det(I + M_{11}) \neq 0$. A more general form of this structure is known as the 'Redheffer Star-Product' (Redheffer, 1959).

2.2 Uncertainty descriptions with LFTs and the structured singular value

Another main advantage of the LFT concept is that it provides a framework for uncertainty modelling. The coefficient matrix can be seen as the part of a linear model that is assumed to be correct: the nominal model then results as an LFT on $\Delta = 0$. By taking $\Delta \in \mathbf{\Delta}$ with $\mathbf{\Delta} \subset \mathrm{R}(s)$ a given subspace, it is then possible to specify a set of linear models rather than a single one. Especially if this set of models is closely related to physical properties of the system under consideration it thus provides a basis for non-conservative and trustworthy statements on robustness of controlled systems in the face of 'true' uncertainties.

For many relevant choices of the subspace $\mathbf{\Delta}$ it is possible to determine whether all models within the specified set are stable by calculating a single non-conservative measure. This measure was introduced by Doyle in 1982 as the structured singular value or μ and is based on a block-diagonal structure of $\mathbf{\Delta}$:

$$\begin{array}{rl} \mathbf{\Delta} = & \{\mathrm{diag}(\delta_1 I_{k_1}, \ldots, \delta_r I_{k_r}, \Delta_1, \ldots, \Delta_f) : \\ & \delta_i \in \mathrm{R}(s), \Delta_i \in \mathrm{R}(s)^{k_{r+i}\times k_{r+i}}\} \end{array} \quad (8)$$

in which $\delta_i I_{k_i}, i = 1 \ldots r$ denote *repeated scalar* blocks and $\Delta_i, i = 1 \ldots f$ denote *full* blocks. Note that for $\Delta \in \mathbf{\Delta}$ to be compatible with a coefficient matrix according to eq.1 we must have for an upper LFT $\sum_{i=1}^{r+f} k_i = p_1 = q_1$ and for a lower LFT $\sum_{i=1}^{r+f} k_i = p_2 = q_2$; extensions to the non-square case are reasonably straightforward. An often useful restriction of the set $\mathbf{\Delta}$ can be obtained by taking bounds for the ∞-norms of the sub-blocks of Δ, with the ∞-norm of a matrix $M \in \mathrm{R}(s)^{p\times q}$ defined as:

$$\|M\|_\infty := \sup_\omega \bar{\sigma}(M(j\omega)) \quad . \quad (9)$$

with $\bar{\sigma}$ denoting the largest singular value. Assuming that scaling factors are incorporated in the coefficient matrix of the LFT, Δ is an element of a unit ball in $\mathbf{\Delta}$:

$$\mathrm{B}\mathbf{\Delta} = \{\Delta \in \mathbf{\Delta} : \|\Delta\|_\infty \leq 1\} \quad (10)$$

For the block-diagonal structure of eq.8 we can now define the structured singular value as follows:

Definition 2.1 *Given an upper LFT with coefficient matrix M, partitioned as in eq.1 and given a compatible block-diagonal structure as in eq.8; $\mu_{\mathbf{\Delta}}(M)$ is then defined as:*

$$\begin{array}{l} \mu_{\mathbf{\Delta}}(M) := \\ \min\{\|\Delta\|_\infty : \Delta \in \mathbf{\Delta}, \det(I - \Delta M_{11}) = 0\}^{-1} \end{array} \quad (11)$$

unless no $\Delta \in \mathbf{\Delta}$ makes $I - \Delta M_{11}$ singular in which case $\mu_{\mathbf{\Delta}}(M) := 0$.

Clearly $\mu_{\mathbf{\Delta}}(M)$ determines the smallest $\Delta \in \mathbf{\Delta}$ for which the LFT under consideration is no longer well defined. If $\mathcal{F}(M, 0)$ and all $\Delta \in \mathbf{\Delta}$ are stable transfer function matrices, we may also interpret this Δ

as the smallest one such that $\mathcal{F}(M,\Delta)$ is unstable. Note that lower LFTs can easily be rewritten as upper LFTs such that we can use the same definition; furthermore we have that μ is also defined if in eq.1 we take $p_2 = q_2 = 0$.

With this definition we now have the possibility to test the properties of a *set* of systems by constructing an appropriate LFT, normalizing Δ such that $\Delta \in \mathrm{B}\boldsymbol{\Delta}$ and finally determining whether $\mu \leq 1$. For an overview of such tests in the general case of eq.8 we refer to Doyle et al. (1991). Furthermore, we will not go into detail on computational issues with respect to μ but simply refer to recent developments as reported by Fan and Tits (1986, 1991) and Young et al. (1991). We will concentrate on a further restricted set of Δs that directly results from real valued parameter variations in state-space models as considered in section 3. For this purpose we define the set of Δs that are *square* and *diagonal* and consist only of *real-valued repeated scalar blocks*:

$$\boldsymbol{\Delta}_{rr} := \{\mathrm{diag}(\delta_1 I_{k_1}, \ldots, \delta_r I_{k_r}) : \delta_i \in \mathrm{R}\} \tag{12}$$

In accordance with the general structure of eq.8 we can usually assume that scaling factors are incorporated in the coefficient matrix and that Δ is further restricted to the bounded set:

$$\begin{aligned} \mathrm{B}\boldsymbol{\Delta}_{rr} \;:=\; & \{\mathrm{diag}(\delta_1 I_{k_1}, \ldots, \delta_r I_{k_r}) : \\ & \delta_i \in [-1,+1]\} \end{aligned} \tag{13}$$

3 Parametric uncertainty modelling

In this paragraph we will consider the problem of state-space models with parametric uncertainty occurring as real rational ND-polynomials. This generalizes earlier results in parametric uncertainty modelling as given by Morton and McAfoos (1985) and Steinbuch et al. (1991, 1992). In section 3.1 the problem will be formulated, which turns out to be an ND-realization problem. Section 3.2 discusses the existence of a solution and section 3.3 provides an algorithm for solving the realization problem by constructing an appropriate LFT.

3.1 Transformation of a state-space model to an LFT

Consider a vector $p = (p_1, ..., p_r) \in \mathrm{R}^r$ containing r bounded scalar parameters. Let the model of the perturbed system be given as a state-space realization in which the entries of the matrices depend on the parameter vector p:

$$\begin{aligned} \dot{x} &= A(p)x + B(p)u, \quad x \in \mathrm{R}^n, u \in \mathrm{R}^m \\ y &= C(p)x + D(p)u, \quad y \in \mathrm{R}^l \end{aligned} \tag{14}$$

With the $(n+l)\times(n+m)$ matrix $S(p)$ defined as:

$$S(p) := \begin{pmatrix} A(p) & B(p) \\ C(p) & D(p) \end{pmatrix} \tag{15}$$

we can write this as

$$\begin{pmatrix} \dot{x} \\ y \end{pmatrix} = S(p) \begin{pmatrix} x \\ u \end{pmatrix} \tag{16}$$

Now we would like to rewrite eq.15 using an upper LFT:

$$S(p) = M_{22} + M_{21}(I - \Delta_u M_{11})^{-1}\Delta_u M_{12} \tag{17}$$

with $\Delta_u \in \mathrm{B}\boldsymbol{\Delta}_{rr}$ (eq.13) and the matrices $M_{22}, M_{21}, M_{11}, M_{12}$ independent of Δ_u.
If we consider only the non-trivial case that $\delta_i \neq 0$, $i = 1 \ldots r$ we can then define $\rho_i := 1/\delta_i$ and rewrite eq.17 as:

$$S(p) = M_{22} + M_{21}\left[\begin{bmatrix} \rho_1 I_{k_1} & & 0 \\ & \ddots & \\ 0 & & \rho_r I_{k_r} \end{bmatrix} - M_{11}\right]^{-1} M_{12} \tag{18}$$

Note that we now have transformed the problem of finding an LFT representation of eq.14 to an ND-realization problem (see Bose (1982)).

3.2 Existence of a solution

Using a constructive algorithm we are now able to prove the following theorem.

Theorem 3.1

A solution to the problem of transforming a state-space model with parametric uncertainty to an LFT exists if the state-space matrices can be given as real rational ND-polynomials in the parameters.

Proof:
Real rational varying entries in a state-space model can be described as LFTs individually. Based on the properties of the interconnection of LFTs, treated in subsection 2.1, these individual LFTs can be collected in one LFT afterwards. For details on the algorithm see section 3.3. □

Minimality of the obtained LFT can not be guaranteed since it is not straightforward to generalize the 1D concepts of controllability and observability

to ND-systems. By for instance Hinamoto (1980), Kung and Levi (1977) and Roesser (1975) 2D counterparts of these notions are considered, leading to the definition of local and global controllability and observability. As is well known, for 1D systems the minimality of a state-space description is equivalent to the property that such a realization is controllable and observable. By Kung and Levi (1977) it is shown by means of an example that global observability and controllability does not imply minimality. However, by removing locally unobservable and uncontrollable perturbations the dimensions of the obtained LFT can be reduced substantially. This approach has been implemented in the algorithm given in the next section.

3.3 A procedure for the transformation

1. **Scaling the varying parameters**
   Lower and upper bound vectors for the parameter vector p can be determined, denoted respectively as $\underline{p}$ and $\bar{p}$: Now define $p_o = (\underline{p} + \bar{p})/2$, $s = (\bar{p} - \underline{p})/2$, $\delta = (\delta_1 \dots \delta_r)$, $\delta_i \in [-1, +1]$, such that $p_i = p_{oi} + s_i\delta_i$ for $i = 1 \cdots r$. Substitution of this result in eq.14 then gives scaled ND-polynomial expressions for all varying numerators and denominators. For instance, suppose a numerator is given as $n_{ij}(p_1, p_2) = p_1 p_2$, with $p_1 = p_{o1} + s_1\delta_1$ and $p_2 = p_{o2} + s_2\delta_2$. Then the scaled numerator is

$$n_{ij}(\delta_1, \delta_2) = p_{o1}p_{o2} + p_{o2}s_1\delta_1 + p_{o1}s_2\delta_2 + s_1s_2\delta_1\delta_2 \qquad (19)$$

2. **Individual varying terms as LFTs**
   The varying parts of a numerator or denominator consist of a number of terms that can be written as seperate LFTs. For example, the scaled numerator $n_{ij}(\delta_1, \delta_2)$ given above has three varying terms resulting in three LFTs (see fig.5). Of course the same can be done with the varying terms in denominators.

3. **Numerators of varying entries**
   Using the fact that two parallel LFTs form again an LFT (see eq.5) the addition of all terms in each numerator can again be written as an LFT. Since we use upper LFTs, the nominal (constant) part of each numerator results in a feedthrough term, which can be incorporated in the M_{22} term of the combined LFT. The resulting LFT giving the numerator n_{ij} of eq.19 is depicted in fig.6.

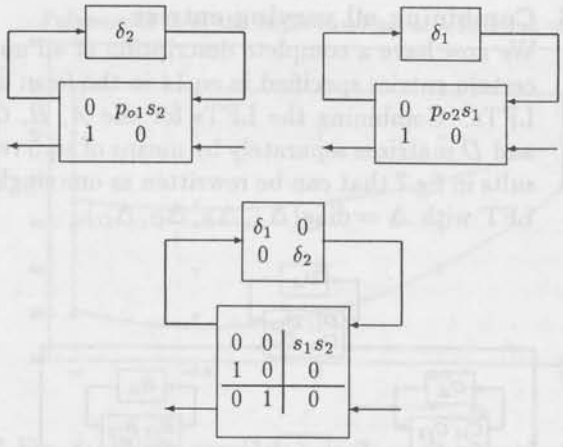

Fig. 5: The varying terms in the numerator n_{ij} written as LFTs

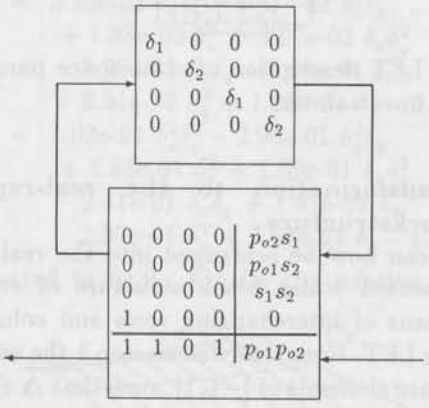

Fig. 6: The numerator n_{ij} given as a single LFT

4. **Denominators of varying entries**
   A similar procedure is followed for the denominators. However, there is a slight difference. In fact we are interested in an LFT-description of the *inverse* of the ND-polynomial denominator. This inverse can be thought of as a feedback structure as in fig.4, with the denominator minus 1 in the feedback path. According to eq.6 this structure can then be rewritten as an LFT under the condition that the term $M_{11}+1$ is invertible. This corresponds with the restriction that the nominal parts of all the varying denominators of a state-space model must be unequal to zero.

5. **Combining numerators and denominators of individual entries**
   Cascade connection of the LFTs of each numerator-denominator pair found in the previous steps can be performed as in eq.4.

6. **Combining all varying entries**
We now have a complete description of all uncertain entries specified in eq.14 in the form of LFTs. Combining the LFTs for the A, B, C and D matrices separately by means of eq.5 results in fig.7 that can be rewritten as one single LFT with $\Delta = \text{diag}(\Delta_A, \Delta_B, \Delta_C, \Delta_D)$.

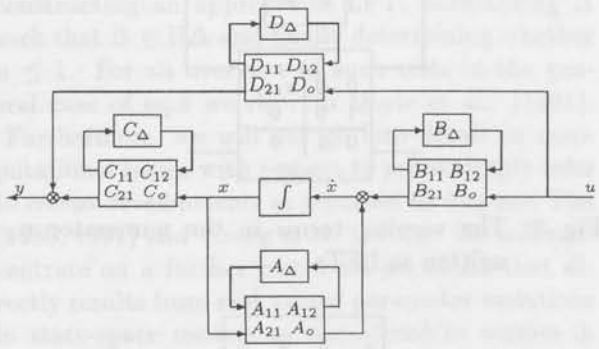

Fig. 7: LFT description of state-space parametric uncertainties

7. **Transformation to the real-repeated blockstructure**
Δ can now be rearanged into the real-valued repeated scalar block structure of eq.12 by means of interchanging rows and columns of the LFT. Note that due to step 1 the entries of Δ are elements of $[-1, 1]$, such that $\Delta \in \mathrm{B}\boldsymbol{\Delta}_{rr}$.

8. **Reducing the dimension of Δ**
The resulting LFT may now be reduced in dimension; if possible the individual repeated blocks are replaced by smaller blocks. The reduction procedure is started by seperating the first repeated block from the derived LFT resulting in a subsystem which has a state-space form. The remaining part of Δ may then be interpreted as an uncertainty block acting on this subsystem. Subsequently the uncontrollable and unobservable perturbations of the subsystem may be removed using a standard (1D) reduction technique. Rewriting the LFT such that the next repeated block is separated then allows to perform this reduction step for all blocks. Although a minimal realization can not always be obtained by this procedure, many examples have shown that an extensive reduction of dimensions can be achieved.

With these steps we now have an LFT description which is equivalent to the state-space system of eq.14. These steps have been implemented within the environment of PC Matlab such that the entire procedure can be performed interactively. In the next section an example is given.

4 Uncertainty modelling for the Phugoid approximation of the DHC2-Beaver aircraft.

The design example is based on the variations of aerodynamic coefficients and relative mass within the flight envelope, as they appear in the phugoid approximation of the Beaver aircraft. The phugoid motion is a low frequency badly damped oscillatory effect appearing in forward velocity and altitude of the aircraft. For good aircraft design it is important that the effect of the phugoid motion is minimized to ensure satisfactory handling and flying quality, especially under instrument flight rules. Also for controller design it is important to find an accurate characterization of this effect. We will therefore start with the definition of the analytical phugoid model in which stability derivatives are defined that have been quantified accurately over the whole flight envelope by Tjee and Mulder (1988).

In our example we are interested in modelling parameter variation of the aircraft in cruise flight conditions over the entire flight envelope. The flight envelope represents a set of flying conditions, in terms of velocity and altitude, under which the aircraft can operate. The goal of this exercise is to obtain an aircraft model that accurately represents all flight conditions that may occur and that may be used for stability and performance analysis and also can be used in robust controller synthesis. We will show that once the variations are explicitly defined, the model can be written as an LFT such that calculation of the structured singular value may provide a measure for the unwanted effect of the phugoid motion.

4.1 Modelling the phugoid motion

The aircraft model considered in this example is the linear approximation model of the phugoid motion and can be given in state-space form as:

$$\begin{aligned} \begin{bmatrix} \dot{u}(t) \\ \dot{\theta}(t) \end{bmatrix} &= A \begin{bmatrix} u(t) \\ \theta(t) \end{bmatrix} + \begin{bmatrix} 1 \\ 0 \end{bmatrix} w(t) \\ y(t) &= \begin{bmatrix} 0 & 1 \end{bmatrix} \begin{bmatrix} u(t) \\ \theta(t) \end{bmatrix} \end{aligned} \tag{20}$$

with:

$$A := \begin{bmatrix} \frac{V}{2\mu_c(\rho)\bar{c}} C_{X_u}(\rho, V) & -g_0/V \\ \frac{-V}{2\mu_c(\rho)\bar{c}} C_{Z_u}(\rho, V) & 0 \end{bmatrix} \tag{21}$$

The state vector $x = (u, \theta)$ represents the longitudinal component of the velocity vector (u) and the pitch angle (θ). The input vector w is added to demonstrate the possibility of modelling the effect of, for instance, air turbulence on the phugoid motion. As a measure of the effect of the phugoid motion we assume that the pitch angle θ can be measured. The terms C_{X_u} and C_{Z_u} represent the stablity derivatives which are known in terms of altitude (air density ρ) and velocity V. The acceller-ation of gravity is given as $g_0 = 9.80665$ m/s^2 and the factor $\mu_c = \frac{m}{\rho S \bar{c}}$ represents the relative aircraft mass with m denoting the nominal aicraft mass, S the wing area and $\bar{c}$ the mean aerodynamic chord of the wing profile. The air density ρ is assumed to depend on altitude h according to the Standard Atmosphere model:

$$\rho = \rho_0 \left[\frac{T_0}{T_0 + \lambda h} \right]^{\frac{M_0 g_0}{R_a \lambda} + 1} \tag{22}$$

with $T_0 = 288.15$ K, $\lambda = -0.0065$ K/m, $R_a = 8314.32$ J/K·kmol and $M_0 = 28.9644$ kg/kmol.

4.2 Fitting the stability derivatives

To obtain a parametric description of the stability derivatives C_{X_u} and C_{Z_u} as a function of ρ and V we will use a 2 dimensional polynomial fitting procedure. Data regarding the stability derivatives for several combinations of ρ and V within the flight envelope is available from Tjee and Mulder (1988).

Although the area of the flight envelope is not square it can be approximated by means of polynomial fits of the nominal value and deviation of V as a function of ρ. Both the approximation of the area and the surfaces defined by C_{X_u} and C_{Z_u} can then be given as a function of two new parameters δ_x and δ_y varying between -1 and 1. For the approximation of the area, second order polynomial fits have been determined resulting in:

$$\begin{aligned} h &= 4000\ \delta_x + 6000 \quad \text{[ft]} \\ \rho &= -1.25\text{e-}01\ \delta_x + 1.03 \quad \text{[kg/m}^3\text{]} \\ V &= -3.57\ \delta_x^2\delta_y + 3.57\ \delta_x^2 - 3.50\ \delta_x\delta_y \\ &\quad + 3.50\ \delta_x + 12.3\ \delta_y + 47.7 \quad \text{[m/s]} \end{aligned} \tag{23}$$

The flight envelope thus described is visualized in fig.8 as a function of δ_x. Polynomial fits for C_{X_u} and C_{Z_u} within this area and with terms having a

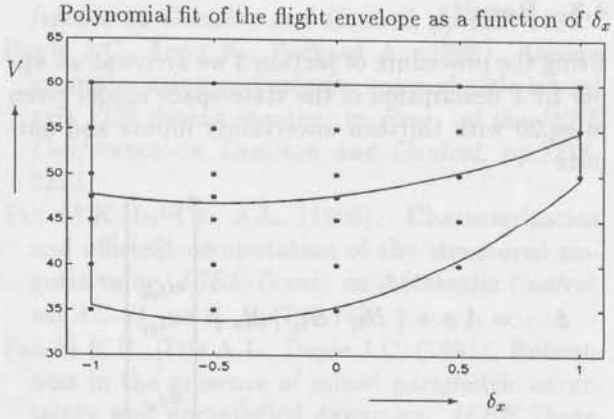

Fig. 8: Flight envelope and its approximation

maximal order of 2 are given by:

$$\begin{aligned} C_{X_u} &= 5.95\text{e-}02\ \delta_x^2\delta_y^2 - 6.37\text{e-}02\ \delta_x^2\delta_y \\ &\quad + 1.38\text{e-}02\ \delta_x^2 + 3.97\text{e-}02\ \delta_x\delta_y^2 \\ &\quad - 3.99\text{e-}02\ \delta_x\delta_y - 7.95\text{e-}04\ \delta_x \\ &\quad - 9.91\text{e-}02\ \delta_y^2 + 1.23\text{e-}01\ \delta_y - 0.14 \\ C_{Z_u} &= 1.02\text{e-}01\ \delta_x^2\delta_y^2 - 2.90\text{e-}01\ \delta_x^2\delta_y \\ &\quad + 1.83\text{e-}01\ \delta_x^2 + 1.09\text{e-}01\ \delta_x\delta_y^2 \\ &\quad - 2.41\text{e-}01\ \delta_x\delta_y + 1.91\text{e-}02\ \delta_x \\ &\quad - 2.37\text{e-}01\ \delta_y^2 + 7.68\text{e-}01\ \delta_y - 1.43 \end{aligned} \tag{24}$$

and plotted in fig.9. Finally the relative aircraft

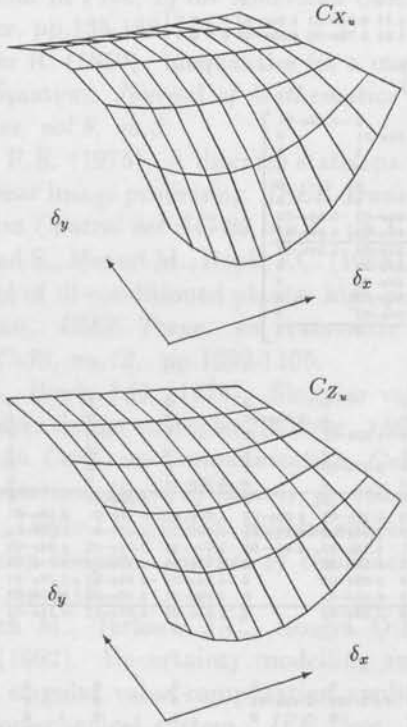

Fig. 9: Fitted surfaces of C_{X_u} and C_{Z_u}

mass can be determined as:

$$\mu_c = 7.43\ \delta_x + 60.9 \tag{25}$$

4.3 Results

Using the procedure of section 3 we arrive at an upper LFT description of the state-space model given in eq.20 with thirteen uncertainty inputs and outputs

$$\dot{x} = A\,x + [\,B_{\delta_1} \quad B_{\delta_2} \mid B_u\,] \begin{bmatrix} u_{\delta_{x1}} \\ \vdots \\ u_{\delta_{x6}} \\ u_{\delta_{y1}} \\ \vdots \\ u_{\delta_{y7}} \\ w \end{bmatrix}$$

$$\begin{bmatrix} y_{\delta_{x1}} \\ \vdots \\ y_{\delta_{x6}} \\ y_{\delta_{y1}} \\ \vdots \\ y_{\delta_{y7}} \\ y \end{bmatrix} = C\,x + [\,D_{\delta_1} \quad D_{\delta_2} \mid D_u\,] \begin{bmatrix} u_{\delta_{x1}} \\ \vdots \\ u_{\delta_{x6}} \\ u_{\delta_{y1}} \\ \vdots \\ u_{\delta_{y7}} \\ w \end{bmatrix} \tag{26}$$

with:

$$A = \begin{bmatrix} -3.47\text{e-}02 & -2.06\text{e-}01 \\ 3.54\text{e-}01 & 0 \end{bmatrix} \tag{27}$$

$$B_{\delta_1} = \begin{bmatrix} -1.018\text{e-}01 & 8.25\text{e-}03 & 1.45\text{e-}01 & 1.89\text{e-}02 & 9.92\text{e-}03 & 2.07\text{e-}02 \\ 0 & -1.22\text{e-}01 & 0 & -4.47\text{e-}01 & -1.54\text{e-}01 & -2.74\text{e-}01 \end{bmatrix} \tag{28}$$

$$B_{\delta_2} = \begin{bmatrix} -1.17 & 9.61\text{e-}01 & 1.94\text{e-}02 & 0 & 0 & 0 & 0 \\ 3.04 & 3.70\text{e-}01 & 6.68\text{e-}03 & 0 & 0 & 0 & 0 \end{bmatrix} \tag{29}$$

$$B_u = \begin{bmatrix} 1 \\ 0 \end{bmatrix} \tag{30}$$

$$C = \begin{bmatrix} 0 & -1.48\text{e-}01 \\ 1.81\text{e-}01 & 0 \\ 0 & 0 \\ 0 & 0 \\ 0 & 0 \\ 0 & 0 \\ -3.05\text{e-}02 & -5.88\text{e-}03 \\ -1.48\text{e-}02 & 5.08\text{e-}02 \\ \hline -4.11\text{e-}03 & -1.40\text{e-}01 \\ -1.85\text{e-}02 & 0 \\ -1.48\text{e-}02 & 0 \\ -3.87\text{e-}03 & 0 \\ 3.00\text{e-}03 & 0 \\ \hline 0 & 1 \end{bmatrix} \tag{31}$$

$$D_{\delta_1} = \left[\begin{array}{cccccc} 0 & 0 & 0 & 0 & 0 & 0 \\ -7.34\text{e-}02 & 0 & 1.05\text{e-}01 & 0 & 0 & 0 \\ 0 & -1.22\text{e-}01 & 0 & 0 & 0 & 0 \\ -7.14\text{e-}01 & 0 & 0 & 0 & 0 & 0 \\ 0 & 2.37\text{e-}01 & 0 & 0 & 0 & 0 \\ 0 & 0 & 0 & 5.57\text{e-}01 & 0 & 0 \\ \hline 0 & 0 & 0 & 0 & 5.20\text{e-}01 & 0 \\ -1.421\text{e-}02 & 5.29\text{e-}02 & 2.03\text{e-}02 & 1.90\text{e-}01 & 1.71\text{e-}01 & 2.16\text{e-}01 \\ 1.23\text{e-}01 & 1.98\text{e-}02 & -1.75\text{e-}01 & -5.00\text{e-}02 & 1.12\text{e-}01 & 1.36\text{e-}01 \\ -3.374\text{e-}01 & 4.96\text{e-}03 & 4.82\text{e-}01 & -2.62\text{e-}02 & 3.36\text{e-}02 & 4.04\text{e-}02 \\ 0 & 8.05\text{e-}02 & 0 & 4.15\text{e-}01 & -3.20\text{e-}01 & -2.81\text{e-}01 \\ 0 & 3.05\text{e-}02 & 0 & -4.24\text{e-}01 & -2.84\text{e-}01 & -2.78\text{e-}01 \\ 0 & -6.45\text{e-}02 & 0 & 1.79\text{e-}01 & 2.16\text{e-}02 & 2.55\text{e-}01 \\ \hline 0 & -7.33\text{e-}02 & 0 & 2.05\text{e-}01 & -8.07\text{e-}02 & -6.15\text{e-}01 \end{array}\right] \tag{32}$$

$$D_{\delta_2} = \left[\begin{array}{ccccccc} 0 & 0 & 0 & 0 & 0 & 0 & 0 \\ -1.02\text{e-}02 & 8.77\text{e-}02 & -2.41\text{e-}01 & 0 & 0 & 0 & 0 \\ 0 & 0 & 0 & 0 & 0 & 0 & 0 \\ 0 & 0 & 0 & 0 & 0 & 0 & 0 \\ 0 & 0 & 0 & 0 & 0 & 0 & 0 \\ 0 & 0 & 0 & 0 & 0 & 0 & 0 \\ 0 & 0 & 0 & 0 & 0 & 0 & 0 \\ \hline -1.33\text{e-}01 & -3.99\text{e-}01 & -1.50\text{e-}01 & 2.01\text{e-}01 & 1.55\text{e-}01 & 0 & 0 \\ 1.69\text{e-}01 & 4.06\text{e-}02 & 1.01\text{e-}01 & 3.56\text{e-}01 & -7.59\text{e-}02 & 0 & 0 \\ 5.64\text{e-}02 & 1.25\text{e-}01 & -2.14\text{e-}01 & 1.21\text{e-}01 & -3.41\text{e-}02 & 0 & 0 \\ 3.27\text{e-}02 & 1.01\text{e-}01 & 3.53\text{e-}02 & -4.95\text{e-}02 & -9.58\text{e-}02 & 8.18\text{e-}02 & 8.65\text{e-}02 \\ -1.80\text{e-}02 & -2.19\text{e-}01 & -7.88\text{e-}02 & 3.49\text{e-}02 & -1.65\text{e-}02 & 3.34\text{e-}01 & -2.12\text{e-}02 \\ -3.86\text{e-}02 & -4.12\text{e-}02 & -1.34\text{e-}02 & -4.40\text{e-}02 & -1.57\text{e-}01 & 2.64\text{e-}01 & 2.72\text{e-}01 \\ \hline 2.24\text{e-}02 & -1.39\text{e-}01 & -5.14\text{e-}02 & 1.62\text{e-}01 & 8.95\text{e-}02 & 2.62\text{e-}03 & -1.49\text{e-}01 \end{array}\right] \tag{33}$$

$$D_u = \left[\,0\;0\;0\;0\;0\;0 \mid 0\;0\;0\;0\;0\;0\;0 \mid 0\,\right]^T \tag{34}$$

To demonstrate the possibility of using the structured singular value μ as a measure for the worst case influence of disturbance input w on the phugoid motion, we will calculate μ for the interconnection structure given in eq.26. The structure of the uncertainty block Δ for this LFT can be given according to eq.8 as $\mathbf{\Delta} = \mathrm{diag}(\delta_x I_6, \delta_y I_7, \delta_w)$ with δ_x, δ_y the real parameter variations as defined before and δ_w a complex perturbation to express our demand to restrict the phugoid motion. We used a preliminary release of the MUSYN toolbox to calculate μ for this mixed real-repeated complex problem resulting in fig.10. Our choice of disturbance input

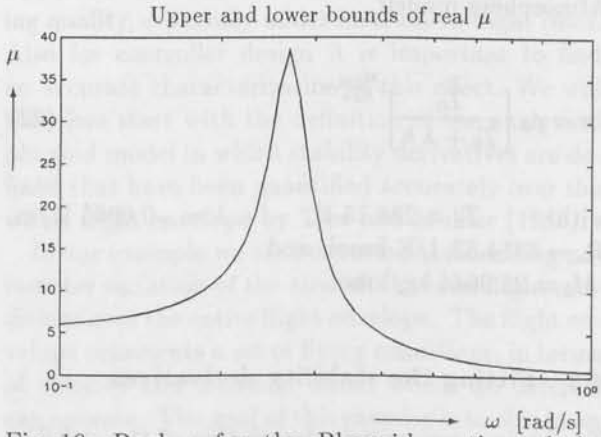

Fig. 10: Real μ for the Phugoid motion of the Beaver aircraft

w and output y was arbitrary and just to demonstrate the procedure. The value of μ of 38.6 can be interpreted as the maximal amplification occurring in the transfer function matrix from w to y under the worst case conditions within the flight envelope and with the worst case disturbance w (a sine of frequency 0.27 rad/s). A choice of inputs and outputs based on a physical interpretation of disturbances and the desired suppression of the phugoid motion is currently a research topic at the faculty of aerospace engineering.

5 Conclusions

The development of methods for analysis and design based on the structured singular value μ causes an increasing demand for the construction of accurate uncertainty models in the form of LFTs. Usually the knowledge concerning uncertainty in mathematical models of physical systems is available in terms of parameter variations. In state-space models this often appears as variations of entries that

can be approximated accurately by means of ratios of ND-polynomials in independent variables which have a physical interpretation. In this paper an algorithm is presented which is used to transform a state-space model with this type of parametric uncertainty to an LFT description with a real-repeated perturbation matrix. Although the dimension of this perturbation matrix may initially be very high, a reduction procedure is proposed that usually decreases it significantly. However, this procedure does not guarantee minimality of the resulting structure. The proposed procedure has been applied to the uncertainty modelling for the phugoid approximation of the DHC2-Beaver aircraft resulting in an LFT description allowing the analysis of the influence of disturbances over the entire flight envelope. The procedure has been implemented in MatLab, such that uncertainty models can be set up in an interactive user-friendly manner.

Acknowledgements

Maarten Steinbuch wants to thank Mathew Newlin and Peter Young, both from California Institute of Technology, for providing a test version of their μ-analysis software for real and complex structures.
The authors also wish to thank Paula Rocha from Delft University of Technology fac. of Mathematics for her help in gaining a better understanding of developments in the area of 2D and ND system representations.
This research was sponsored by Philips Research Laboratories in Eindhoven, Delft University of Technology and National Aerospace Laboratory (NLR) in Amsterdam.

References

Balas G.J., Packard A., Doyle J.C. (1990). Theory and applications of robust multivariable control. in *H_∞ and μ Short Course, Musyn inc., Delft, june 25-28.*

Bose N.K. (1982). *Applied multidimensional system theory.* Van Nostrand Reinhold Co., N.Y.,

Doyle J.C. (1982). Analysis of feedback systems with structured uncertainties. *IEE Proe., Part D, Control Theory and Applications, vol.129, no.6(nov),* pp.242-250.

Doyle J.C., Packard A. (1987). Uncertain multivariable systems from a state space perspective. in *Proc. of the American Control Conference,* pp.2147-2152.

Doyle J.C., Packard A., Zhou K. (1991). Review of LFTs, LMIs and μ. in *Proc. of the IEEE Conference on Decision and Control,* pp.1227-1232.

Doyle J.C., Lenz K., Packard A. (1986). Design examples using μ-synthesis: space shuttle lateral axis FCS during reentry. in *Proc. of the IEEE Conference on Decision and Control,* pp.2218-2223.

Fan M.K.H., Tits A.L. (1986). Characterization and efficient computation of the structured singular value. *IEEE Trans. on Automatic Control, vol.AC-31, no.8,* pp.734-743.

Fan M.K.H., Tits A.L., Doyle J.C. (1991). Robustness in the presence of mixed parametric uncertainty and unmodelled dynamics. *IEEE Trans. on Automatic Control, vol AC-36, no.1,* pp.25-38.

Hinamoto T. (1980). Realization of a state-space model from 2D input output map. *IEEE Trans. on Circuits & Systems, vol.CAS-27, no.1,* pp.36-44.

Kung S., Levi B.C. (1977). New results in 2D system theory, part II: 2D state-space models realisations and the notions of controllability, observability and minimality. in *Proc. of the IEEE, vol.65, no.6,* pp.945-961.

Morton B.G., McAfoos R.M. (1985). A μ-test for robustness analysis of a real-parameter variation problem. in *Proc. of the American Control Conference,* pp.135-138.

Redheffer R. (1959). Inequalities for a matrix Riccati equation. *Journal of Mathematics and Mechanics, vol.8, no.3.*

Roesser R.E. (1975). A discrete state-space model for linear image processing. *IEEE Trans. on Automatic Control vol AC-20, no.1,* pp.1-10.

Skogestad S., Morari M., Doyle J.C. (1988). Robust control of ill-conditioned plants: high-purity distillation. *IEEE Trans. on Automatic Control, vol.AC-33, no.12,* pp.1092-1105.

Stein G., Doyle J.C. (1978). Singular values and feedback: design examples. in *Proc. 16th Annual Allerton Conf. on Communication, Control and Computation, Univ. of Illinois,* pp.460-471.

Stein G., Doyle J.C. (1991). Beyond singular values and loop shapes. *Journal of Guidance, vol.14, no.1,* pp.5-16.

Steinbuch M., Terlouw J.C., Bosgra O.H., Smit S.G. (1992). Uncertainty modelling and structured singular value computation applied to an electromechanical system. *IEE Proc., Part D, Control Theory and Applications, vol.139, no.3,* pp.301-307.

Steinbuch M., Terlouw J.C., Bosgra O.H. (1991). Robustness analysis for real and complex perturbations applied to an electro-mechanical system.

in *Proc. of the American Control Conference, Boston,* pp.556-561.

Tjee R.T.H, Mulder J.A. (1988). Stability and control derivatives of the De Havilland DHC-2 'BEAVER' aircraft. in *Techn. Univ. Delft, Report LR-556.*

Young P.M., Newlin M.P., Doyle J.C. (1991). μ analysis with real parametric uncertainty. in *Proc. of the IEEE Conference on Decision and Control,* pp.1251-1256.

Selected Topics in Identification, Modelling and Control
Vol. 5, December 1992

Robustness of feedback systems under simultaneous plant and controller perturbation

Peter M.M. Bongers

Mechanical Engineering Systems and Control Group
Delft University of Technology, Mekelweg 2, 2628 CD Delft, The Netherlands.

Abstract. The aim of this paper is to derive a new robust stability margin for simultaneous perturbation of plant and controller which is less conservative than the gap-metric robustness. Known sufficient conditions for robust stability stated in the gap-metric contain inherent conservativeness in the formulation of the various steps. In this paper conservativeness in one of the steps is removed, resulting in a new and less conservative robustness margin. The key issue is that more information of the nominal feedback system is taken into consideration. The improvement of the new robustness margin will be illustrated by an example.

Keywords. robustness, simultaneous perturbations, coprime factorizations, gap-metric

1 Introduction

A perfect model of the real plant, if it is available, will in general be non-linear and of extremely high order. In engineering practice the plant will be approximated by a low order linear model. The discrepancy between the nominal model and the plant is then described by a set of plant uncertainty models. In the next step a controller will be synthesized in such a way that it robustly stabilizes the nominal model and the set of plant uncertainty models, for a pre-specified performance; Methods to design such robust controllers are for example given in (Doyle *et al.*(1989), McFarlane and Glover (1989), Bongers and Bosgra (1990)).

When dealing with industrial processes the control computers are calculating in finite word length arithmetics or even integer arithmetics, while for the controller limited time and space on the computer is available. Therefore the implemented controller is only an approximation of the designed controller. The discrepancy between the designed controller and the implemented controller can be described by a set of controller uncertainty models.

The feedback connection of plant model and controller will be called robustly stable if the feedback system remains stable for all plant variations described by the set of plant uncertainty models and all controller variations described by the set of controller uncertainty models.

In some recent papers by Georgiou and Smith (1990a), Bongers and Bosgra (1990) a sufficient condition for robust stability of a closed loop system has been stated for plant perturbations measured in the gap-metric. In Georgiou and Smith (1990b) gap-metric robustness under simultaneous plant and controller perturbations has been studied. In the gap-metric robustness the nominal plant (controller) is factorized in normalized coprime factors. The difference between a perturbed plant (controller) and the nominal plant (controller) is described by perturbations on the normalized coprime factors of the nominal plant (controller). Robustness of the closed loop for a class of perturbed plants and controllers is guaranteed if the norm of the perturbations on the normalized coprime factors is small enough. The maximum allowable norm of the perturbations is determined by the infinity norm of the feedback system. This means that in the gap-metric robustness only crude information

about the nominal feedback system is taken into consideration.

The main idea behind the new and less conservative robustness margin, to be considered in this paper, is to take into account more information about the nominal feedback system. One can think of this information as refinement of the infinity norm to a frequency dependent maximum singular value, and the directionality of the feedback loops in multivariable systems.

In order to take account of the closed loop characteristics a normalized coprime factorization of the nominal controller (plant) is used to define a specific coprime factorization of the nominal plant (controller).

The difference between a simultaneously perturbed plant and controller (P_Δ, C_Δ) and the nominal plant and controller (P, C) is now described by perturbations on the specific coprime factors of the nominal plant and nominal controller which includes detailed information about the nominal controller and plant respectively.

It will be shown that this new robustness margin allows a larger class of coprime factor plant and controller perturbations than allowed in the gap-metric.

The layout of this paper is as follows: after some preliminaries in Section 2, stability of a nominal closed loop system is discussed in section 3. Then the new robustness margin will be derived in Section 4, where it will be demonstrated that this margin is less conservative than the gap-metric. The whole procedure will be illustrated by an example in Section 5 followed by the conclusions

2 Preliminaries

In this note we adopt the ring theoretic setting of Desoer *et al.*(1980) and Vidyasagar *et al.*(1982) to study stable multivariable linear systems by considering them as transfer function matrices having all entries belonging to the ring $\mathcal{H}$. In this note we will identify the ring $\mathcal{H}$ with $\mathbb{RH}_\infty$, the space of stable real rational finite dimensional linear time–invariant continuous–time systems. We consider the class of possibly non–proper and/or unstable multivariable systems as transfer function matrices whose entries are elements of the quotient field $\mathcal{F}$ of $\mathcal{H}$ ($\mathcal{F} := \{a/b \mid a \in \mathcal{H},\ b \in \mathcal{H}\backslash 0\}$). The set of multiplicative units of $\mathcal{H}$ is defined as: $\mathcal{J} := \{h \in \mathcal{H} \mid h^{-1} \in \mathcal{H}\}$. In the sequel systems $P \in \mathcal{F}^{m\times n}$ are denoted as $P \in \mathcal{F}$.

Definition 2.1 (Vidyasagar (1982))

A plant $P \in \mathcal{F}$ has a right (left) fractional representation if there exist $N, M(\tilde{N}, \tilde{M}) \in \mathcal{H}$ such that

$$P = NM^{-1}\ (= \tilde{M}^{-1}\tilde{N})$$

*The pair $M, N(\tilde{M}, \tilde{N})$ is right (left) coprime fractional representation (*rcf *or* lcf *) if it is a right (left) fractional representation and there exists $U, V(\tilde{U}, \tilde{V}) \in \mathcal{H}$ such that:*

$$UN + VM = I\ (\tilde{N}\tilde{U} + \tilde{M}\tilde{V} = I)$$

*The pair $M, N(\tilde{M}, \tilde{N})$ is a normalized right (left) coprime fractional representation (*nrcf *or* nlcf *) if it is a coprime fractional representation and:*

$$M^*M + N^*N = I\ (\tilde{M}\tilde{M}^* + \tilde{N}\tilde{N}^* = I)$$

with $M^* = M^T(-s)$.

Definition of distance measures

Suppose P_1, P_2 are two plants with nrcf $(N_1, M_1), (N_2, M_2)$ respectively, and suppose C is a controller such that $T(P_1, C) \in \mathcal{H}$ with $(\tilde{X}, \tilde{Y})$ a nlcf of C.

The graph metric distance (Vidyasagar (1984)) $d(P_1, P_2)$ between the two plants is defined as

$$\begin{aligned} d(P_1, P_2) &= \max\{\vec{d}(P_1, P_2), \vec{d}(P_2, P_1)\} \\ \vec{d}(P_1, P_2) &= \inf_{Q\in\mathcal{H}, \|Q\|_\infty \le 1} \left\| \begin{bmatrix} M_1 \\ N_1 \end{bmatrix} - \begin{bmatrix} M_2 \\ N_2 \end{bmatrix} Q \right\|_\infty \end{aligned}$$

The gap metric distance (El-Sakkary (1985), Zames and El-Sakkary (1980)) $\delta(P_1, P_2)$ between the two plants is defined as

$$\begin{aligned} \delta(P_1, P_2) &= \max\{\vec{\delta}(P_1, P_2), \vec{\delta}(P_2, P_1)\} \\ \vec{\delta}(P_1, P_2) &= \inf_{Q\in\mathcal{H}} \left\| \begin{bmatrix} M_1 \\ N_1 \end{bmatrix} - \begin{bmatrix} M_2 \\ N_2 \end{bmatrix} Q \right\|_\infty \end{aligned}$$

The Λ-gap margin $\delta_\Lambda(P_1, P_2)$ between the two plants is defined as

$$\delta_\Lambda(P_1, P_2) = \inf_{Q\in\mathcal{H}} \left\| \begin{bmatrix} M_1 \\ N_1 \end{bmatrix} \Lambda^{-1} - \begin{bmatrix} M_2 \\ N_2 \end{bmatrix} Q \right\|_\infty$$

where $\Lambda = \begin{bmatrix} \tilde{X} & \tilde{Y} \end{bmatrix} \begin{bmatrix} M_1 \\ N_1 \end{bmatrix}$. Note that the nrcf of P_1 is shaped with Λ^{-1} to account for the closed loop operation of the plant. If there is no controller, Λ^{-1} will be M_1^{-1}, as can be checked easily, and the Λ-gap will be:

$$\delta_\Lambda(P_1, P_2) = \inf_{Q\in\mathcal{H}} \left\| \begin{bmatrix} I \\ P_1 \end{bmatrix} - \begin{bmatrix} M_2 \\ N_2 \end{bmatrix} Q \right\|_\infty$$

3 Closed loop stability

In this paper we will study the closed loop stability according to Fig. 1, where we assume that a stabilizing controller C has been designed for the nominal plant P.

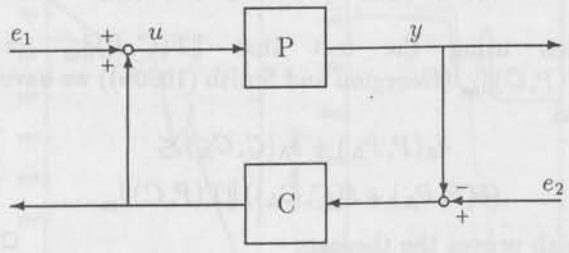

Fig. 1: Closed loop structure

The closed loop transfer function $T(P,C)$ mapping the external inputs (e_1, e_2) onto the outputs (u, y) is given by:

$$T(P,C) = \begin{bmatrix} I \\ P \end{bmatrix} (I + CP)^{-1} \begin{bmatrix} I & C \end{bmatrix}$$

For bounded exogeneous inputs (e_1, e_2), stability of the closed loop, i.e. the controller C internally stabilizes the plant P, is guaranteed if and only if $T(P,C) \in \mathcal{H}$. Now let $P = NM^{-1}$ with (N, M) a rcf of P and let $C = \tilde{X}^{-1}\tilde{Y}$ with $(\tilde{X}, \tilde{Y})$ a lcf of C then:

$$T(P,C) = \begin{bmatrix} M \\ N \end{bmatrix} \left(\tilde{X}M + \tilde{Y}N \right)^{-1} \begin{bmatrix} \tilde{X} & \tilde{Y} \end{bmatrix} \quad (1)$$

Theorem 3.1 (Vidyasagar *et al.*(1982))
Let $P \in \mathcal{F}$ be given as $P = NM^{-1}$ with (N, M) a rcf *of P and let the controller $C \in \mathcal{F}$ be given as $C = \tilde{X}^{-1}\tilde{Y}$ with $(\tilde{X}, \tilde{Y})$ a* lcf *of C or as $C = YX^{-1}$ with (Y, X) a* rcf *of C. Then the following statements are equivalent:*

1. *The closed loop is stable*
2. $\left(\begin{bmatrix} \tilde{X} & \tilde{Y} \end{bmatrix} \begin{bmatrix} M \\ N \end{bmatrix} \right) = \Lambda \in \mathcal{J}$
3. $U := \begin{bmatrix} M & -Y \\ N & X \end{bmatrix} \in \mathcal{J}$

For robust stability it is essential that the closed loop transfer function remains stable for plants P_Δ "close to" P controlled by controllers C_Δ "close to" C. Usually the controller C is designed with knowledge of P only.

4 Main result

In this section a sufficient condition for feedback stability under simultaneous plant and controller perturbations is presented. As a by-product we have sufficient conditions for only plant perturbations or only controller perturbations.
Next it will be shown that this robustness margin is less conservative than a similar margin based on the gap-metric distance between the nominal plant and perturbed plant summed with the gap-metric distance between the nominal controller and the perturbed controller, as derived by Georgiou and Smith (1990b) .
This will immediately imply that the gap-metric robustness margin is also less conservative than a margin based on graph-metric distances, as derived by Vidyasagar and Kimura (1986)
Finally it will be shown under what conditions the new robustness margin equals the gap-metric based robustness margin.

Theorem 4.1 *Suppose $T(P,C)$ is stable, and that both plant and controller are perturbed to P_Δ, C_Δ respectively. Then all pairs (P_Δ, C_Δ) form a stable closed loop $T(P_\Delta, C_\Delta)$, provided:*

$$\delta_\Lambda(P, P_\Delta) + \delta_\Lambda(C, C_\Delta) < 1 \quad (2)$$

Proof: Let $(N, M), (Y, X)$ be nrcf of P, C, respectively and let $(\tilde{M}, \tilde{N}), (\tilde{X}, \tilde{Y})$ be nlcf of P, C, respectively. Then from stability of $T(P,C)$ the matrix

$$U = \begin{bmatrix} M & -Y \\ N & X \end{bmatrix} \in \mathcal{J}.$$

Denote

$$U_o = \begin{bmatrix} M & -Y \\ N & X \end{bmatrix} \begin{bmatrix} \Lambda^{-1} & 0 \\ 0 & \tilde{\Lambda}^{-1} \end{bmatrix}$$

where $\Lambda = \begin{bmatrix} \tilde{X} & \tilde{Y} \end{bmatrix} \begin{bmatrix} M \\ N \end{bmatrix}, \tilde{\Lambda} = \begin{bmatrix} \tilde{M} & \tilde{N} \end{bmatrix} \begin{bmatrix} X \\ Y \end{bmatrix}$.
Then U_o^{-1} can be partitioned as

$$U_o^{-1} = \begin{bmatrix} \tilde{X} & \tilde{Y} \\ -\tilde{N} & \tilde{M} \end{bmatrix}$$

Now let $(N_\Delta, M_\Delta), (Y_\Delta, X_\Delta)$ be rcf of P_Δ, C_Δ, respectively. According to Theorem 3.1 $T(P_\Delta, C_\Delta) \in \mathcal{H}$ if and only if

$$U_\Delta = \begin{bmatrix} M_\Delta & -Y_\Delta \\ N_\Delta & X_\Delta \end{bmatrix} \in \mathcal{J}.$$

Select real numbers $\delta_p > \delta_\Lambda(P, P_\Delta), \delta_c > \delta_\Lambda(C, C_\Delta)$ such that $\delta_p + \delta_c < 1$.

Now if $\|(I - U_\Delta U_o^{-1}\|_\infty < 1$ then (according to Lemma A.1) $U_\Delta \in \mathcal{J}$ and thereby the pair (P_Δ, C_Δ) is stable. $U_o - U_\Delta = \left[\begin{array}{cc} A & B \end{array}\right]$, where

$$A = \left[\left[\begin{array}{c} M \\ N \end{array}\right]\Lambda^{-1} - \left[\begin{array}{c} M_\Delta \\ N_\Delta \end{array}\right]\right]$$

$$B = \left[\left[\begin{array}{c} -Y \\ X \end{array}\right]\tilde{\Lambda}^{-1} - \left[\begin{array}{c} -Y_\Delta \\ X_\Delta \end{array}\right]\right]$$

$$\begin{aligned} I - U_\Delta U_o^{-1} &= \left[\begin{array}{cc} A & B \end{array}\right] U_o^{-1} \\ &= A\left[\begin{array}{cc} \tilde{X} & \tilde{Y} \end{array}\right] + B\left[\begin{array}{cc} -\tilde{N} & \tilde{M} \end{array}\right] \end{aligned}$$

$$\begin{aligned} \left\|\left[\begin{array}{cc} A & B \end{array}\right] U_o^{-1}\right\|_\infty &\leq \left\|A\left[\begin{array}{cc} \tilde{X} & \tilde{Y} \end{array}\right]\right\|_\infty \\ &\quad + \left\|B\left[\begin{array}{cc} -\tilde{N} & \tilde{M} \end{array}\right]\right\|_\infty \\ &\leq \delta_p + \delta_c \end{aligned}$$

Now if $\delta_p + \delta_c < 1$ then $U_\Delta \in \mathcal{J}$ which proves that $T(P_\Delta, C_\Delta) \in \mathcal{H}$, which completes the proof. □

The robustness results of (Bongers (1991), Schrama *et al.*(1992)) are a special case of Theorem 4.1, which can be seen in the next corollary.

Corollary 4.2 *Suppose $T(P,C)$ is stable. There holds*

$$\text{if } \delta_\Lambda(P, P_\Delta) < 1 \text{ then } T(P_\Delta, C) \in \mathcal{H}$$

and

$$\text{if } \delta_\Lambda(C, C_\Delta) < 1 \text{ then } T(P, C_\Delta) \in \mathcal{H}.$$

In the next theorem it will be shown that a sufficient condition for stability according to Theorem 4.1 can be stated in terms of gap-metric distance. Thereby we will show that Theorem 4.1 is a generalization of the gap-metric robustness

Theorem 4.3 *Suppose $T(P,C)$ is stable, then a sufficient condition for $\delta_\Lambda(P, P_\Delta) + \delta_\Lambda(C, C_\Delta) < 1$ is given in the gap-metric by*

$$\delta(P, P_\Delta) + \delta(C, C_\Delta) < \|T(P,C)\|_\infty^{-1}$$

Proof:

$$\begin{aligned} \delta_\Lambda(P, P_\Delta) &= \inf_{Q \in \mathcal{H}} \left\| \left[\begin{array}{c} M \\ N \end{array}\right]\Lambda^{-1} - \left[\begin{array}{c} M_\Delta \\ N_\Delta \end{array}\right] Q \right\|_\infty \\ &= \inf_{\tilde{Q} \in \mathcal{H}} \left\| \left(\left[\begin{array}{c} M \\ N \end{array}\right] - \left[\begin{array}{c} M_\Delta \\ N_\Delta \end{array}\right]\tilde{Q} \right)\Lambda^{-1} \right\|_\infty \\ &\leq \inf_{\tilde{Q} \in \mathcal{H}} \left\| \left(\left[\begin{array}{c} M \\ N \end{array}\right] - \left[\begin{array}{c} M_\Delta \\ N_\Delta \end{array}\right]\tilde{Q} \right) \right\|_\infty \|\Lambda^{-1}\|_\infty \end{aligned}$$

Now assembling the pieces, using the definition of the gap-metric and Lemma A.3 we have that

$$\delta_\Lambda(P, P_\Delta) \leq \delta(P, P_\Delta)\,\|T(P,C)\|_\infty$$

Along the same lines we have

$$\delta_\Lambda(C, C_\Delta) \leq \delta(C, C_\Delta)\,\|T(C,P)\|_\infty$$

Then using the fact that $\|T(C,P)\|_\infty = \|T(P,C)\|_\infty$ (Georgiou and Smith (1990b)) we have that

$$\begin{aligned} &\delta_\Lambda(P, P_\Delta) + \delta_\Lambda(C, C_\Delta) \leq \\ &(\delta(P, P_\Delta) + \delta(C, C_\Delta))\,\|T(P,C)\|_\infty \end{aligned}$$

which proves the theorem □

The transfer function Λ^{-1} can be seen as a weighting function on the gap between the nominal plant and the perturbed plant. Only when $\Lambda = \alpha I$, with $\alpha \in \mathbb{R}$, the extraction of Λ^{-1} will not introduce conservatism. In that case the gap-metric robustness is not more conservative than the new robustness margin.
It can be shown (Bongers (1992)) that a specific choice of the controller order in a $\mathbb{RH}_\infty$-norm design based on normalized coprime factorizations will lead to $\Lambda = \alpha I$.
However in general the maximum singular value of Λ will be frequency dependent. For multivariable control designs the singular values of Λ will in general not be equal, which means that in Λ also directionality will be present.
The presented robustness margin takes both the features of directionality and frequency dependency into account. This implies that the presented robustness margin has practical benefits compared to the gap-metric robustness margin.

5 Example

In this section the application of the presented robustness margin will be illustrated using an example. For simplicity only SISO systems are considered, which implies that the improvement of the new robustness margin by taking into account directionality of the feedback loops can not be demonstrated.

In Fig. 2 the frequency responses of both the nominal plant model P of order 5 and a perturbed plant model P_Δ are shown.

Using the control design method described in Bongers and Bosgra (1990) a controller C of order 3 has been designed on P such that $\|T(P,C)\|_\infty$ is minimized. In Fig. 3 the frequency responses

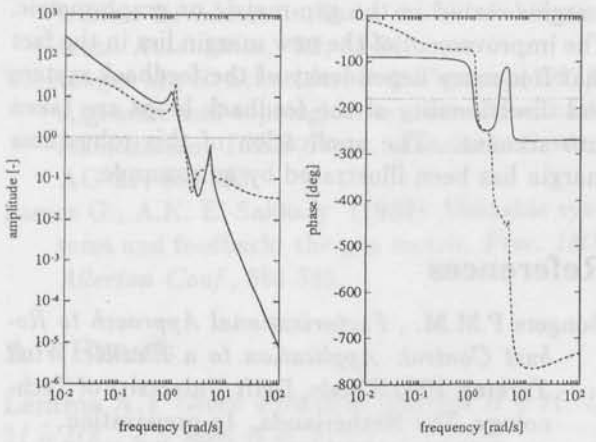

Fig. 2: Frequency response P (—) , P_Δ (- -)

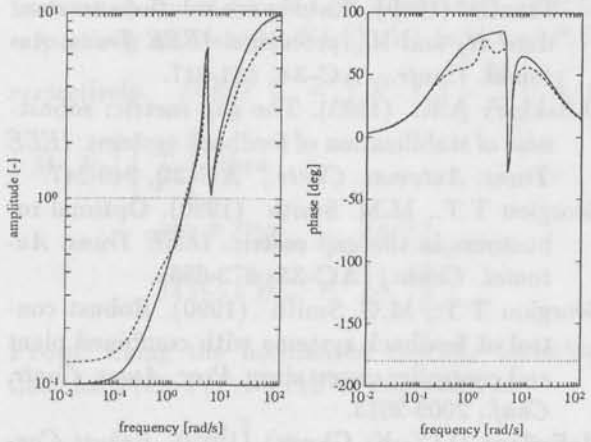

Fig. 3: Frequency response C (—) , C_Δ (- -)

of both the designed controller C and a perturbed controller C_Δ are shown.

If the robustness is measured in the gap-metric, the closed loop system $T(P_\Delta, C_\Delta)$ (Theorem 4.3) remains stable provided

$$\delta(P, P_\Delta) + \delta(C, C_\Delta) \leq \|T(P, C)\|_\infty^{-1}$$

The gap between the nominal plant and perturbed plant is:

$$\delta(P, P_\Delta) = 0.19,$$

and the gap between the nominal controller and the perturbed controller is:

$$\delta(C, C_\Delta) = 0.14$$

The nominal plant,controller pair imply a robustness margin of: $\|T(P, C)\|_\infty^{-1} = 0.1$ It is obvious that even the individual perturbations do not satisfy the robustness margin, therefore stability of the perturbed feedback system can not be guaranteed.

Next the refinement of the new robustness margin will be shown. The improvement of the new robustness margin, by taking into account the frequency dependency of the feedback system, is illustrated in Fig. 4.

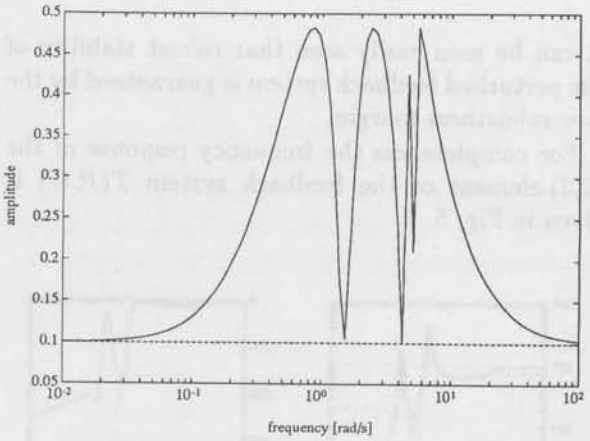

Fig. 4: Frequency response $\sigma(\Lambda)$ (—) , $\|T(P, C)\|_\infty^{-1}$ (- -)

Suppose, for a moment, only plant perturbations are present. Then stability of the closed loop in gap-metric sense is guaranteed provided that $\delta(P, P_\Delta)$ is smaller than the dashed line in Fig. 4.

The refinement towards the new robustness margin can be seen as follows: The frequency where the largest difference between P and P_Δ lies is not taken into account in $\delta(P, P_\Delta)$, it is in $\delta_\Lambda(P, P_\Delta)$. Let $\tilde{Q}$ be the optimal solution in Theorem 4.3, then

$T(P_\Delta, C)$ is stable if

$$\delta_\Lambda(P, P_\Delta) \leq \sigma\left(\begin{bmatrix} M \\ N \end{bmatrix} - \begin{bmatrix} M_\Delta \\ N_\Delta \end{bmatrix} \tilde{Q}\right) \sigma(\Lambda^{-1}) < 1$$

Next if the difference between P and P_Δ, defined as

$$\sigma\left(\begin{bmatrix} M \\ N \end{bmatrix} - \begin{bmatrix} M_\Delta \\ N_\Delta \end{bmatrix} \tilde{Q}\right)$$

is smaller than $\sigma(\Lambda)$, then $T(P_\Delta, C)$ is stable. Thereby the area of allowable $P'_\Delta s$ is extended towards the solid curve in Fig. 4.

When the stability robustness is measured in the new robustness margin (Theorem 4.1), the perturbed closed loop $T(P_\Delta, C_\Delta)$ remains stable provided:

$$\delta_\Lambda(P, P_\Delta) + \delta_\Lambda(C, C_\Delta) < 1$$

The lambda-gap between the nominal plant and the perturbed plant is

$$\delta_\Lambda(P, P_\Delta) = 0.5004$$

and the lambda-gap between the nominal controller and the perturbed controller is

$$\delta_\Lambda(C, C_\Delta) = 0.3220$$

It can be seen easily seen that robust stability of the perturbed feedback system is guaranteed by the new robustness margin.

For completeness the frequency response of the (2,2)-element of the feedback system $T(P, C)$ is given in Fig. 5.

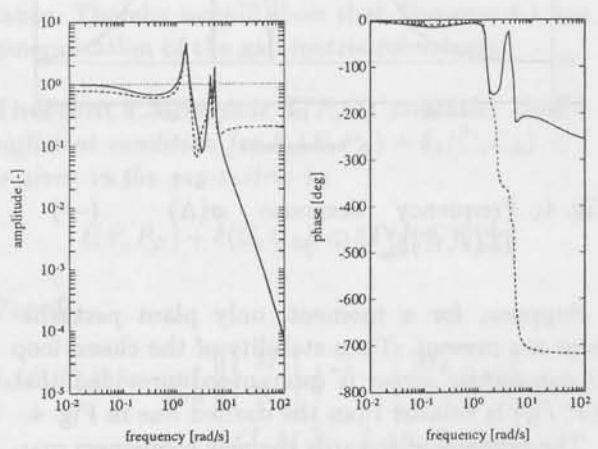

Fig. 5: Frequency response $P(I + CP)^{-1}C$ (—), $P_\Delta(I + C_\Delta P_\Delta)^{-1}C_\Delta$ (- -)

6 Conclusions

The derivation of a new robust stability margin for simultaneous perturbation of plant and controller has been presented. It has been shown that this margin is less conservative than similar robustness margins stated in the gap-metric or graph-metric. The improvement of the new margin lies in the fact that frequency dependency of the feedback system and directionality of the feedback loops are taken into account. The application of this robustness margin has been illustrated by an example.

References

Bongers P.M.M. , *Factorizational Approach to Robust Control: Application to a Flexible Wind Turbine.* PhD Thesis, Delft University of Technology, The Netherlands, In preparation, .

Bongers P.M.M. (1992). On a new robust stability margin. in *Recent Advances in Mathematical Theory of Systems, Control, Networks and Signal Processing, Proc. of the Int. Symp. MTNS-91,* H. Kimura, S. Kodama (Eds.), 377-382.

Bongers P.M.M., O.H. Bosgra (1990). Low order H_∞ controller synthesis. *Proc. 29th Conf. Desicion and Control,* Hawaii, USA, 194-199.

Desoer C.A., R.W. Liu, J. Murray, R. Saeks (1980). Feedback systems design: the fractional representation approach to analysis and synthesis. *IEEE Trans. Automat. Contr.,* **AC-25**, 399-412.

Doyle J.C., K. Glover, P.P. Khargonekar, B.A. Francis (1989). State-space solutions to standard H_2 and H_∞ problems. *IEEE Trans. Automat. Contr.,* **AC-34**, 831-847.

El-Sakkary A.K. (1985). The gap metric: robustness of stabilization of feedback systems. *IEEE Trans. Automat. Contr.,* **AC-30**, 240-247.

Georgiou T.T., M.M. Smith (1990). Optimal robustness in the gap metric. *IEEE Trans. Automat. Contr.,* **AC-35**, 673-686.

Georgiou T.T., M.C. Smith (1990). Robust control of feedback systems with combined plant and controller uncertainty. *Proc. Amer. Contr. Conf.,* 2009-2013.

McFarlane D.C., K. Glover (1989). *Robust Controller Design Using Normalized Coprime Factor Plant Descriptions.* Lecture Notes in Control and Information Sciences, vol.138, Springer Verlag, Berlin, Germany.

Schrama R.J.P., P.M.M. Bongers, D.K. de Vries (1992). Assessment of robust stability from experimental data. *Proc. Amer. Contr. Conf.,*

Chicago, Illinois, USA, 286-290.

Vidyasagar M. (1984). The graph metric for unstable plants and robustness estimates for feedback stability. *IEEE Trans. Automat. Contr.*, **AC-29**, 403-418.

Vidyasagar M., H. Kimura (1986). Robust controllers for uncertain linear multivariable systems. *Automatica,* **22**, 85-94.

Vidyasagar M., H. Schneider, B.A. Francis (1982). Algebraic and topological aspects of feedback stabilization. *IEEE Trans. Automat. Contr.*, **AC-27**, 880-893.

Zames G., A.K. El-Sakkary (1980). Unstable systems and feedback: the gap metric. *Proc. 18th Allerton Conf.,* 380-385.

A Proofs

Lemma A.1 *Given a transfer function $H \in \mathcal{H}$. If $\|I - H\|_\infty < 1$ then $H \in \mathcal{J}$.*

Proof: For an arbitrary function $F \in \mathcal{H}$, a sufficient condition for $I - F$ to have a stable inverse is given by the small gain condition $\|F\|_\infty < 1$. Define $H := I - F$ and the lemma is proved. □

Theorem A.2 *Let (N, M) be a* rcf *of P and (Y, X) be a* rcf *of C, then $T(P, C) \in \mathcal{H}$ if and only if*

$$U = \begin{bmatrix} M & -Y \\ N & X \end{bmatrix} \in \mathcal{J}.$$

Proof: Vidyasagar and Kimura (1986), lemma 5.1 □

Lemma A.3 *Let $(N, M), (Y, X)$ be* nrcf *of P, C, respectively and let $(\tilde{M}, \tilde{N}), (\tilde{X}, \tilde{Y})$ be* nlcf *of P, C, respectively. Define $\Lambda = \begin{bmatrix} \tilde{X} & \tilde{Y} \end{bmatrix} \begin{bmatrix} M \\ N \end{bmatrix}, \tilde{\Lambda} = \begin{bmatrix} \tilde{M} & \tilde{N} \end{bmatrix} \begin{bmatrix} X \\ Y \end{bmatrix}$, then*

$$\begin{aligned} \|T(P,C)\|_\infty &= \left\|\Lambda^{-1}\right\|_\infty \\ \|T(C,P)\|_\infty &= \left\|\tilde{\Lambda}^{-1}\right\|_\infty \end{aligned}$$

Proof: Using the normalized coprime factorizations for P, C, $T(P, C)$ can be expressed as

$$T(P,C) = \begin{bmatrix} M \\ N \end{bmatrix} \left(\tilde{X}M + \tilde{Y}N\right)^{-1} \begin{bmatrix} \tilde{X} & \tilde{Y} \end{bmatrix}$$

The fact that $\begin{bmatrix} M \\ N \end{bmatrix}$ is a nrcf , $\begin{bmatrix} \tilde{X} & \tilde{Y} \end{bmatrix}$ is a nlcf and $\left(\tilde{X}M + \tilde{Y}N\right)^{-1} = \Lambda^{-1}$ proves the first part. The second part can be proved similarly. □

Selected Topics in Identification, Modelling and Control
Vol. 5, December 1992

Stability robustness for simultaneous perturbations of linear plant and controller: beyond the gap metric

Ruud J.P. Schrama , Peter M.M. Bongers and Okko H. Bosgra ‡

Mechanical Engineering Systems and Control Group
Delft University of Technology, Mekelweg 2, 2628 CD Delft, The Netherlands.

Abstract. In this paper we study robust stability under simultaneous plant and controller perturbations. We use a Youla parameterization to represent the class of all possible plant perturbations that do not destabilize the nominal feedback system. A similar representation is used for the class of controller perturbations that do not destabilize the nominal feedback system. From these two Youla parameterizations we derive a sufficient condition for robust stability under simultaneous perturbations. This condition is shown to be less conservative than a condition for robust stability under simultaneous plant-controller perturbations measured in the gap metric. An example is provided in which the new condition guarantees robust stability for some simultaneous perturbations that are too large in view of the gap-metric condition.

Keywords. stability, robustness, closed loop systems, coprime fractions, gap metric.

1 Introduction

This paper is addressed to the robustness of feedback stability in the face of simultaneous plant and controller perturbations. Robust stability under plant perturbations has been widely studied in the robust control theory, see e.g. Francis (1987), Maciejowski (1989), Morari and Zafiriou (1989), Stein and Doyle (1991). Simultaneous controller perturbations play an important role in engineering applications, where an implemented controller usually differs from the designed controller.

A condition for robust stability under simultaneous perturbations must guarantee that each element of some "uncertainty domain" around the plant P is stabilized by each element of another "uncertainty domain" around the controller C. Hence only dynamically perturbed plants P_Δ that are stabilized by the nominal controller C are of interest. Likewise we have to consider only the dynamically perturbed controllers C_Δ that stabilize the nominal plant P. These classes of perturbed plants and controllers can be represented precisely with two Youla parameterizations based on the nominal P and C. From these two Youla parameterizations we derive a sufficient condition for robust stability in the presence of simultaneous plant and controller perturbations.

Conditions for robust stability under combined plant-controller perturbations have been derived by Vidyasagar (1984) and Vidyasagar and Kimura (1986) in terms of the graph metric. Georgiou and Smith (1990a, 1990b) have established a condition for robust stability under simultaneous perturbations measured by the gap metric. Each of these metrics induce sets of bounded plant perturbations that are independent of the nominal controller C: the graph and the gap between a nominal plant and a perturbed plant does not depend on C. Similarly, the induced sets of bounded controller perturbations are independent of the nominal plant P. In contrast with these approaches, we use the nominal plant *and* the nominal controller to define the plant perturbations of concern. The same applies

‡Author to whom all correspondence should be addressed.

to the class of controller perturbations that we consider. Consequently, our condition is less conservative than the stability conditions in terms of the graph and gap metrics. The significance of this reduction of conservatism is illustrated by an example.

The next section defines the classes of admissible plant and controller perturbations. Our stability result is derived in Section 3. In Section 4 it is shown to be less conservative than the condition for robust stability in the gap metric. In Section 5 we provide the example, and the paper ends with some concluding remarks in Section 6.

2 Admissible Dynamical Perturbations

We study linear time-invariant finite dimensional systems, and the set of proper stable systems is denoted $\mathbb{RH}_\infty$. We consider the feedback interconnection $H(P,C)$ shown in Fig. 1. In here P represents the plant and C represents the controller. The closed-loop dynamics of $H(P,C)$ are described by the transfer function

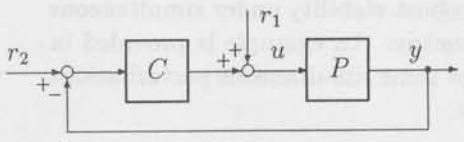

Fig. 1: Feedback interconnection $H(P,C)$.

$$T(P,C) = \begin{bmatrix} P \\ I \end{bmatrix} (I+CP)^{-1} \begin{bmatrix} C & I \end{bmatrix}, \qquad (1)$$

which maps the vector of variables $\mathrm{col}(r_2, r_1)$ into $\mathrm{col}(y,u)$. This transfer function is used to define the notion of stability of $H(P,C)$.

Definition 2.1 *The feedback system $H(P,C)$ of Fig. 1 is stable if and only if $T(P,C) \in \mathbb{RH}_\infty$.*

In order that plant and controller perturbations can be investigated individually, we introduce the following definition.

Definition 2.2 *A perturbed plant P_Δ (controller C_Δ) is* admissible *if and only if $H(P_\Delta, C)$ ($H(P, C_\Delta)$) is stable.*

Notice that perturbations of P and C at least must be admissible in order that the simultaneously perturbed feedback system $H(P_\Delta, C_\Delta)$ is *robustly* stable. Below we derive a neccessary and sufficient condition for a perturbed plant P_Δ (controller C_Δ) to be admissible.

The plant P admits normalized right and left coprime factorizations over $\mathbb{RH}_\infty$ (for definitions see Vidyasagar, 1985), i.e. there exist $N, D, \tilde{N}, \tilde{D}, X, Y, \tilde{X}, \tilde{Y} \in \mathbb{RH}_\infty$ such that

$$P(s) = N(s)D^{-1}(s) = \tilde{D}^{-1}(s)\tilde{N}(s) \qquad (2)$$

with

$$XN + YD = I, \quad \tilde{N}\tilde{X} + \tilde{D}\tilde{Y} = I \qquad (3)$$

and

$$N^T(-s)N(s) + D^T(-s)D(s) = I, \quad \forall s$$
$$\tilde{N}(s)\tilde{N}^T(-s) + \tilde{D}(s)\tilde{D}^T(-s) = I, \quad \forall s.$$

Likewise the controller C admits the normalized coprime factorizations

$$C(s) = N_c(s)D_c^{-1}(s) = \tilde{D}_c^{-1}(s)\tilde{N}_c(s) \qquad (4)$$

where $N_c, D_c, \tilde{N}_c, \tilde{D}_c \in \mathbb{RH}_\infty$. In Desoer *et al.* (1980), Vidyasagar *et al.* (1982) and Vidyasagar (1985) coprime factorizations of P and C have been used to establish necessary and sufficient conditions for stability of $H(P,C)$. For ease of referencing we state these results in terms of the above notation.

Lemma 2.3 *Let P and C have normalized coprime factorizations as in (2) and (4), and let $\Lambda, \tilde{\Lambda} \in \mathbb{RH}_\infty$ be defined as*

$$\Lambda = \tilde{N}_c N + \tilde{D}_c D, \quad \tilde{\Lambda} = \tilde{N} N_c + \tilde{D} D_c. \qquad (5)$$

Then the following statements are equivalent:

i. $H(P,C)$ *is stable,*

ii. $\Lambda^{-1} \in \mathbb{RH}_\infty$,

iii. $\tilde{\Lambda}^{-1} \in \mathbb{RH}_\infty$,

iv. $\begin{bmatrix} D & -N_c \\ N & D_c \end{bmatrix}^{-1} \in \mathbb{RH}_\infty$.

With this stability result it is easy to parameterize the set of all controllers that stabilize P (Vidyasagar, 1985). We state the dual result in terms of a perturbed plant P_Δ.

Proposition 2.4 *Let P and C have normalized coprime factorizations as in (2) and (4), and let $H(P,C)$ of Fig. 1 be stable. Then the perturbed feedback system $H(P_\Delta, C)$ is stable if and only if P_Δ admits the coprime factorization*

$$P_\Delta = (N + D_c\Delta_P)(D - N_c\Delta_P)^{-1} \qquad (6)$$

for some $\Delta_P \in \mathbb{RH}_\infty$.

Proof: By Lemma 2.3 the stability of $H(P,C)$ implies that $\Lambda^{-1}, \tilde{\Lambda}^{-1} \in \mathbb{RH}_\infty$. Coprimeness of $N+D_c\Delta_P$ and $D-N_c\Delta_P$ follows from $(\Lambda^{-1}\tilde{N}_c)(N+D_c\Delta_P)+(\Lambda^{-1}\tilde{D}_c)(D-N_c\Delta_P)=I$. Further, $\tilde{X}_c, \tilde{Y}_c, X_c$ and Y_c defined as

$$\tilde{X}_c = N\Lambda^{-1},\ \tilde{Y}_c = D\Lambda^{-1},\ X_c = \tilde{\Lambda}^{-1}\tilde{N},\ Y_c = \tilde{\Lambda}^{-1}\tilde{D}$$

belong to $\mathbb{RH}_\infty$ and

$$X_cN_c+Y_cD_c=I,\quad \tilde{N}_c\tilde{X}_c+\tilde{D}_c\tilde{Y}_c=I.$$

From here the result follows along the same lines as in Vidyasagar (1985), p.109. □

Combining Proposition 2.4 with Definition 2.2 yields the following necessary and sufficient condition for admissibility.

Lemma 2.5 *Let P and C have normalized coprime factorizations as in (2) and (4), and let $H(P,C)$ of Fig. 1 be stable. Then the perturbed plant P_Δ is admissible if and only if $|I+P_\Delta C| \neq 0$ and $\Delta_P \in \mathbb{RH}_\infty$ with*

$$\Delta_P = D_c^{-1}(I+P_\Delta C)^{-1}(P_\Delta - P)D. \qquad (7)$$

Proof: By Definition 2.2 and Proposition 2.4 P_Δ is admissible if and only if P_Δ admits the coprime factorization of (6). We rewrite the latter equation as

$$\begin{aligned}(N+D_c\Delta_P) &= P_\Delta(D-N_c\Delta_P)\\ \Leftrightarrow (D_c+P_\Delta N_c)\Delta_P &= (P_\Delta - ND^{-1})D\end{aligned}$$

from which (7) follows straightforwardly. □

Similarly a perturbed controller C_Δ is admissible if and only if $|I+C_\Delta P| \neq 0$ and $\Delta_C \in \mathbb{RH}_\infty$ with

$$\Delta_C = D(I+C_\Delta P)^{-1}(C_\Delta - C)D_c \qquad (8)$$

satisfying

$$C_\Delta = (N_c+D\Delta_C)(D_c-N\Delta_C)^{-1}. \qquad (9)$$

Remark 2.6 The property of admissibility has the following geometric interpretation. The operator associated with $T(P,C)$ is a projection on the graph of P (for details see Georgiou and Smith (1990a, 1990b)). As $T(P,C)T(P_\Delta,C)=T(P,C)$, an admissible perturbation of P results in a perturbation of the graph of P in a direction parallel along the projection that is associated with $T(P,C)$. □

3 Sufficient Condition for Robust Stability

The following lemma contains a sufficient condition for robust stability under simultaneous plant and controller perturbations.

Lemma 3.1 *Let P and C have normalized coprime factorizations as in (2) and (4), let $H(P,C)$ of Fig. 1 be stable, and let P_Δ and C_Δ be admissible. Then the feedback system $H(P_\Delta,C_\Delta)$ is stable if Δ_P of (7) and Δ_C of (8) satisfy*

$$\sigma_{max}(\Delta_C(j\omega)) \cdot \sigma_{max}(\Delta_P(j\omega)) < 1 \qquad (10)$$

for all frequencies $\omega \in \mathbb{R}$.

Proof: By Lemma 2.5 and Proposition 2.4 the admissibility of P_Δ and C_Δ implies that P_Δ and C_Δ admit the coprime factorizations of (6) and (9) with $\Delta_P \in \mathbb{RH}_\infty$ as in (7) and $\Delta_C \in \mathbb{RH}_\infty$ as in (8). By definition Definition 2.1 $H(P_\Delta,C_\Delta)$ is stable if and only if $T(P_\Delta,C_\Delta) \in \mathbb{RH}_\infty$. Applying Lemma 2.3 to the coprime factorizations of (6) and (9) yields

$$T(P_\Delta,C_\Delta) \in \mathbb{RH}_\infty \Leftrightarrow \begin{bmatrix} D-N_c\Delta_P & -N_c-D\Delta_C \\ N+D_c\Delta_P & D_c-N\Delta_C \end{bmatrix}^{-1} \in \mathbb{RH}_\infty. \qquad (11)$$

Next we use the fact that any $U, V \in \mathbb{RH}_\infty$ with $U^{-1} \in \mathbb{RH}_\infty$ satisfy

$$V^{-1} \in \mathbb{RH}_\infty \Leftrightarrow (UV)^{-1} \in \mathbb{RH}_\infty.$$

Together with facts ii.-iv. of Lemma 2.3 implied by the stability of $H(P,C)$ we can rewrite the stability condition of (11) as follows.

$$T(P_\Delta,C_\Delta) \in \mathbb{RH}_\infty \Leftrightarrow$$

$$\left[\begin{bmatrix} D & -N_c \\ N & D_c \end{bmatrix}^{-1}\begin{bmatrix} D-N_c\Delta_P & -N_c-D\Delta_C \\ N+D_c\Delta_P & D_c-N\Delta_C \end{bmatrix}\right]^{-1} \in \mathbb{RH}_\infty$$

$$\Leftrightarrow \left[\begin{bmatrix} \Lambda^{-1} & 0 \\ 0 & \tilde{\Lambda}^{-1} \end{bmatrix}\begin{bmatrix} \tilde{D}_c & \tilde{N}_c \\ -\tilde{N} & \tilde{D} \end{bmatrix}\cdot \begin{bmatrix} D-N_c\Delta_P & -N_c-D\Delta_C \\ N+D_c\Delta_P & D_c-N\Delta_C \end{bmatrix}\right]^{-1} \in \mathbb{RH}_\infty$$

$$\Leftrightarrow \begin{bmatrix} I & -\Delta_C \\ \Delta_P & I \end{bmatrix}^{-1} \in \mathbb{RH}_\infty.$$

Using the fact that $\mathbb{RH}_\infty$ is closed under addition, we add $\mathrm{diag}(0,-I)$ to the latter right hand side, so that

$$T(P_\Delta,C_\Delta) \in \mathbb{RH}_\infty \Leftrightarrow \qquad (12)$$

$$\Leftrightarrow \begin{bmatrix} I \\ -\Delta_P \end{bmatrix} (I+\Delta_C\Delta_P)^{-1} \begin{bmatrix} I & \Delta_C \end{bmatrix} \in \mathbb{RH}_\infty$$

$$\Leftrightarrow (I+\Delta_C\Delta_P)^{-1} \in \mathbb{RH}_\infty.$$

Finally, as Δ_P and Δ_C belong to $\mathbb{RH}_\infty$ by Lemma 2.5, the product $\Delta_C\Delta_P$ is a contraction if (10) holds. Then $I+\Delta_C\Delta_P$ is guaranteed to have a stable inverse by virtue of the small gain theorem, see Desoer and Vidyasagar (1975), which completes the proof. □

Remark 3.2 A robust stability test for any given couple of a perturbed plant P_Δ and a perturbed compensator C_Δ proceeds as follows. First $I+P_\Delta C$ and $I+C_\Delta P$ must be demonstrated to be nonsingular. Then it must be verified that Δ_P and Δ_C belong to $\mathbb{RH}_\infty$. Finally Lemma 3.1 is applied to ascertain robust stability. □

The fact that the factorizations (N, D) and (N_c, D_c) are normalized will be of use in the next section. This property has not been exploited in deriving the condition for robust stability of Lemma 3.1. Therefore we can readily extend this robust stability condition to other pairs of coprime factorizations of P and C. Such factorizations can always be represented as respectively (NQ, DQ) and (N_cQ_c, D_cQ_c), in which Q and Q_c are unimodular elements of $\mathbb{RH}_\infty$ (i.e. $Q^{-1}, Q_c^{-1} \in \mathbb{RH}_\infty$). By letting Q and Q_c vary freely over the space of unimodular elements of $\mathbb{RH}_\infty$ we can study all coprime factorizations of P and C at once. This results in the following general condition for robust stability under simultaneous plant and controller perturbations.

Theorem 3.3 *Let P and C have normalized coprime factorizations as in* (2) *and* (4)*, let $H(P,C)$ of Fig. 1 be stable, and let P_Δ and C_Δ be admissible. Then the feedback system $H(P_\Delta, C_\Delta)$ is stable if there exist some unimodular $Q, Q_c \in \mathbb{RH}_\infty$ such that Δ_P of* (7) *and Δ_C of* (8) *satisfy*

$$\sigma_{max}\left(Q^{-1}(j\omega)\Delta_C(j\omega)Q_c(j\omega)\right) \cdot \cdot\sigma_{max}\left(Q_c^{-1}(j\omega)\Delta_P(j\omega)Q(j\omega)\right) < 1 \quad (13)$$

for all frequencies $\omega \in \mathbb{R}$.

Proof: We define the coprime factorizations $(\bar{N}, \bar{D})$ of P and $(\bar{N}_c, \bar{D}_c)$ of C as

$$\bar{N} = NQ,\ \bar{D} = DQ,\ \bar{N}_c = N_cQ_c,\ \bar{D}_C = D_cQ_c$$

for any particular unimodular $Q, Q_c \in \mathbb{RH}_\infty$. Similar to (7) and (8) we define $\bar{\Delta}_P, \bar{\Delta}_C$ as

$$\begin{aligned} \bar{\Delta}_P &= \bar{D}_c^{-1}(I+P_\Delta C)^{-1}(P_\Delta - P)\bar{D} \\ \bar{\Delta}_C &= \bar{D}^{-1}(I+C_\Delta P)^{-1}(C_\Delta - C)\bar{D}_c \end{aligned}$$

so that $\bar{\Delta}_P = Q_c^{-1}\Delta_P Q$, $\bar{\Delta}_C = Q^{-1}\Delta_C Q_c$. Like in Proposition 2.4 and Lemma 2.5 the perturbed P_Δ and C_Δ are admissible if and only if $\bar{\Delta}_P, \bar{\Delta}_C \in \mathbb{RH}_\infty$. And $H(P,C)$ is robustly stable under simultaneous perturbations if the admissible perturbations $\bar{\Delta}_P, \bar{\Delta}_C$ satisfy

$$\sigma_{max}\left(\bar{\Delta}_C(j\omega)\right) \cdot \sigma_{max}\left(\bar{\Delta}_P(j\omega)\right) < 1 \quad (14)$$

for all frequencies $\omega \in \mathbb{R}$. The proof hereof is the same as that of Lemma 3.1 except that $\bar{N}, \bar{D}, \bar{N}_c, \bar{D}_c, \bar{\Delta}_P$ and $\bar{\Delta}_C$ have to be substituted for respectively N, D, N_c, D_c, Δ_P and Δ_C. Finally (13) follows by replacing $\bar{\Delta}_P$ and $\bar{\Delta}_C$ in (14) by respectively $Q_c^{-1}\Delta_P Q$ and $Q^{-1}\Delta_C Q_c$. □

Remark 3.4 A robust stability test based on Theorem 3.3 proceeds as in Remark 3.2, except that the freedom of the unimodular Q, Q_c can be exploited to ascertain robust stability. □

Notice that Theorem 3.3 contains a condition for robust stability of $H(P,C)$ under simultaneous perturbations, and not just a condition for stability of $H(P_\Delta, C_\Delta)$. In this perspective the admissibility of P_Δ and C_Δ incurs no restriction, since we want $H(P_\Delta, C_\Delta)$ to remain stable if the perturbation of either the plant or the controller vanishes. Further, as Δ_P and Δ_C must belong to $\mathbb{RH}_\infty$ for robust stability, following corollary follows from Theorem 3.3.

Corollary 3.5 *Let P and C have normalized coprime factorizations as in* (2) *and* (4)*, let $H(P,C)$ of Fig. 1 be stable, and let P_Δ and C_Δ be admissible. Then the feedback system $H(P_\Delta, C_\Delta)$ is stable if there exist some unimodular $Q, Q_c \in \mathbb{RH}_\infty$ such that Δ_P of* (7) *and Δ_C of* (8) *satisfy*

$$\|Q^{-1}\Delta_C Q_c\|_\infty \|Q_c^{-1}\Delta_P Q\|_\infty < 1. \quad (15)$$

This condition for robust stability has the following attractive property. If the controller perturbation Δ_C converges to 0 in $\mathbb{RH}_\infty$, then the stability condition of (15) admits every plant perturbation $\Delta_P \in \mathbb{RH}_\infty$. In that case we retrieve precisely the set of *all* plants that are stabilized by the nominal controller C (see Proposition 2.4). The dual result holds in case of a vanishing plant perturbation Δ_P in $\mathbb{RH}_\infty$. Hence our condition for robust stability under simultaneous perturbations involves only very little conservatism if either the plant perturbation or the controller perturbation is relatively small.

Finally we mention that all results in this section have a dual counterpart framed in terms of left coprime factorizations.

4 Relation to the gap metric

In this section we show that the condition of Theorem 3.3 is less conservative than a condition for robust stability under simultaneous plant-controller perturbations measured in the gap metric. In order to adopt the gap metric results from Georgiou (1988) and Georgiou and Smith (1990a), we introduce the following notation. The perturbed plant P_Δ and controller C_Δ admit the normalized coprime factorizations

$$P_\Delta = N_\Delta D_\Delta^{-1}, \quad C_\Delta = N_{c\Delta} D_{c\Delta}^{-1}. \tag{16}$$

Further, the *gap* between P and P_Δ is denoted $\delta(P, P_\Delta)$, and the *directed gap* is denoted $\vec{\delta}(P, P_\Delta)$ (see Georgiou, 1988, and Georgiou and Smith, 1990a, for definitions).

Proposition 4.1 (Georgiou (1988)) *Let P and P_Δ have normalized coprime factorizations as in* (2) *and* (16). *Then*

$$\delta(P, P_\Delta) = \max\{\vec{\delta}(P, P_\Delta),\ \vec{\delta}(P_\Delta, P)\}$$

and

$$\vec{\delta}(P, P_\Delta) = \inf_{Q \in H_\infty} \left\| \begin{bmatrix} N \\ D \end{bmatrix} - \begin{bmatrix} N_\Delta \\ D_\Delta \end{bmatrix} Q \right\|_\infty \tag{17}$$

where H_∞ denotes the standard Hardy space.

Theorem 4.2 (Georgiou and Smith (1990a)) *Let $H(P, C)$ be stable. Then $H(P_\Delta, C_\Delta)$ is stable if*

$$\delta(P, P_\Delta) + \delta(C, C_\Delta) < \|T(P, C)\|_\infty^{-1}. \tag{18}$$

Now we can state the main result of this section: if a perturbed *couple* P_Δ,C_Δ satisfies the gap-metric robust stability condition of (18), then this couple P_Δ,C_Δ satisfies also the robust stability condition of Corollary 3.5 (and of Theorem 3.3).

Theorem 4.3 *Let $H(P, C)$ be stable and let P_Δ,C_Δ satisfy* (18). *Then there exist unimodular $Q, Q_c \in \mathbb{R}\mathrm{H}_\infty$ such that* (15) *is satisfied.*

The opposite of this theorem is not true, and thus our robust stability condition is less conservative than the gap-metric condition. That is, if P_Δ,C_Δ comply with our robust stability condition of (15), then the gap-metric condition of (18) is not necessarily satisfied. An example thereof will be provided in the next section.

The sequel of this section is merely addressed to proving Theorem 4.3. First we establish some preliminary facts. Thereafter we list several properties of P_Δ and C_Δ that are implied by the gap-metric robust stability condition of (18). Then we provide the proof of Theorem 4.3. In conclusion of the section we relate our results to the condition for robust stability under simultaneous perturbations measured in the graph metric.

Fact 4.4 *Let P and C have normalized coprime factorizations as in* (2) *and* (4), *and let $H(P, C)$ of Fig. 1 be stable. Then*

i. $\|T(P, C)\|_\infty = \|T(C, P)\|_\infty$,

ii. $\|T(P, C)\|_\infty = \|\Lambda^{-1}\|_\infty = \|\tilde{\Lambda}^{-1}\|_\infty$.

Proof:
(i.) Corollary 1 of Georgiou and Smith (1990a).
(ii.) By substituting ND^{-1} and $N_c D_c^{-1}$ for P and C in (1) we get

$$\|T(P, C)\|_\infty = \left\| \begin{bmatrix} N \\ D \end{bmatrix} \Lambda^{-1} \begin{bmatrix} \tilde{N}_c & \tilde{D}_c \end{bmatrix} \right\|_\infty = \|\Lambda^{-1}\|_\infty,$$

since $\begin{bmatrix} N \\ D \end{bmatrix}$ is inner and $\begin{bmatrix} \tilde{N}_c & \tilde{D}_c \end{bmatrix}$ is co-inner (see Francis, 1987). Similarly $\|T(C, P)\|_\infty = \|\tilde{\Lambda}^{-1}\|_\infty$, and the result is complete by fact i. □

Proposition 4.5 *Let M be a square complex matrix. Then*

$$\sigma_{max}(I - M) < 1 - b \Rightarrow \sigma_{min}(M) > b \tag{19}$$

for any $b \in [0, 1)$, and

$$\sigma_{max}(I - M) \leq 1 - d \Rightarrow \sigma_{min}(M) \geq d \tag{20}$$

for any $d \in (0, 1]$.

Proof: Let v be any non-zero vector such that

$$\frac{\|Mv\|_2}{\|v\|_2} = \sigma_{min}(M)$$

where $\|\cdot\|_2$ is the usual Euclidian vector norm. As $\|(I-M)v\|_2 + \|Mv\|_2 \geq \|v\|_2$ we have

$$\sigma_{min}(M) \geq 1 - \frac{\|(I-M)v\|_2}{\|v\|_2}.$$

We use the inequality
$\sigma_{max}(I-M) \geq \|(I-M)v\|_2 / \|v\|_2$ to obtain

$$\sigma_{min}(M) \geq 1 - \sigma_{max}(I - M)$$

from which (19) and (20) are immediate. □

Having established these preliminaries, now we reveal several implications of the gap-metric robust stability condition of (18).

Lemma 4.6 *Let $H(P,C)$ be stable, and let P_Δ,C_Δ satisfy* (18). *Define*

$$\tau = \|\Lambda^{-1}\|_\infty \vec{\delta}(C, C_\Delta), \tag{21}$$

then

$$\|\tilde{\Lambda}^{-1}\|_\infty \vec{\delta}(P, P_\Delta) < 1-\tau \tag{22}$$

and $\tau \in [0,1)$.

Proof: As the gap $\delta(P, P_\Delta)$ is the maximum of two directed gaps, cf. Proposition 4.1, the inequality

$$\vec{\delta}(P, P_\Delta) + \vec{\delta}(C, C_\Delta) < \|T(P,C)\|_\infty^{-1} \tag{23}$$

is satisfied if (18) holds. Application of Fact 4.4.ii yields

$$\|\tilde{\Lambda}^{-1}\|_\infty \vec{\delta}(P, P_\Delta) + \|\Lambda^{-1}\|_\infty \vec{\delta}(C, C_\Delta) < 1,$$

which implies that $\tau < 1$, and (22) follows straightforwardly. □

Proposition 4.7 *Let $H(P,C)$ be stable, and let P_Δ,C_Δ satisfy* (18). *Then P_Δ and C_Δ admit the right coprime factorizations $(N_{\Delta G}, D_{\Delta G})$ and $(N_{c\Delta G}, D_{c\Delta G})$ such that*

$$\begin{aligned} \vec{\delta}(P, P_\Delta) &= \| \begin{bmatrix} N \\ D \end{bmatrix} - \begin{bmatrix} N_{\Delta G} \\ D_{\Delta G} \end{bmatrix} \|_\infty \\ \vec{\delta}(C, C_\Delta) &= \| \begin{bmatrix} N_c \\ D_c \end{bmatrix} - \begin{bmatrix} N_{c\Delta G} \\ D_{c\Delta G} \end{bmatrix} \|_\infty. \end{aligned} \tag{24}$$

Proof: We prove only the expression for $\vec{\delta}(P, P_\Delta)$, as the proof of the other part is completely analogous.

By Theorem 6.1.1 of Francis (1987) the infimum of (17) is actually reached for some $\bar{Q} = Q_G \in \mathbb{RH}_\infty$, i.e.

$$\vec{\delta}(P, P_\Delta) = \| \begin{bmatrix} N \\ D \end{bmatrix} - \begin{bmatrix} N_\Delta \\ D_\Delta \end{bmatrix} Q_G \|_\infty \tag{25}$$

with (N_Δ, D_Δ) as in (16). We define $(N_{\Delta G}, D_{\Delta G})$ as $(N_\Delta Q_G, D_\Delta Q_G)$, which is a right coprime factorization of P_Δ if and only if $Q_G \in \mathbb{RH}_\infty$ is unimodular. So it remains to be shown that $Q_G^{-1} \in \mathbb{RH}_\infty$.

The robust stability of $H(P_\Delta, C_\Delta)$ implies that $H(P_\Delta, C)$ is stable, which implies that Λ_Δ, defined as

$$\Lambda_\Delta = \tilde{N}_c N_\Delta + \tilde{D}_c D_\Delta,$$

is a unimodular element of $\mathbb{RH}_\infty$ by virtue of Lemma 2.3. Next, for notational convenience, we define

$$\begin{bmatrix} \Delta_N \\ \Delta_D \end{bmatrix} = \begin{bmatrix} N \\ D \end{bmatrix} - \begin{bmatrix} N_\Delta \\ D_\Delta \end{bmatrix} Q_G, \tag{26}$$

so that

$$\begin{aligned} &[\ \tilde{N}_c \ \ \tilde{D}_c\ ] \begin{bmatrix} N_\Delta \\ D_\Delta \end{bmatrix} Q_G = \\ &= [\ \tilde{N}_c \ \ \tilde{D}_c\ ] \left[\begin{bmatrix} N \\ D \end{bmatrix} - \begin{bmatrix} \Delta_N \\ \Delta_D \end{bmatrix} \right] \end{aligned}$$

from which we obtain

$$Q_G = \Lambda_\Delta^{-1} \Lambda (I + \Psi)$$

with $\Psi \in \mathbb{RH}_\infty$ satisfying

$$\Psi = -\Lambda^{-1} [\ \tilde{N}_c \ \ \tilde{D}_c\ ] \begin{bmatrix} \Delta_N \\ \Delta_D \end{bmatrix}.$$

As Λ_Δ and Λ are unimodular, Q_G has a stable inverse if and only if $(I+\Psi)$ has a stable inverse. By the small gain theorem (Desoer and Vidyasagar, 1975) $(I+\Psi)$ has a stable inverse if $\Psi \in \mathbb{RH}_\infty$ is a contraction. And (18) implies that $\|\Psi\|_\infty < 1$, because by Fact 4.4.ii and (25)

$$\begin{aligned} \|\Psi\|_\infty &\le \|\Lambda^{-1}\|_\infty \| [\ \tilde{N}_c \ \ \tilde{D}_c\ ] \|_\infty \| \begin{bmatrix} \Delta_N \\ \Delta_D \end{bmatrix} \|_\infty = \\ &= \|T(P,C)\|_\infty \vec{\delta}(P, P_\Delta) \end{aligned}$$

and $\|T(P,C)\|_\infty \vec{\delta}(P, P_\Delta) < 1$ by (23). □

Lemma 4.8 *Let $H(P,C)$ be stable, and let P_Δ,C_Δ satisfy* (18). *Define $Q, Q_c \in \mathbb{RH}_\infty$ as*

$$\begin{aligned} Q &= \Lambda^{-1} [\ \tilde{N}_c \ \ \tilde{D}_c\ ] \begin{bmatrix} N_{\Delta G} \\ D_{\Delta G} \end{bmatrix} \\ Q_c &= \tilde{\Lambda}^{-1} [\ \tilde{N} \ \ \tilde{D}\ ] \begin{bmatrix} N_{c\Delta G} \\ D_{c\Delta G} \end{bmatrix} \end{aligned} \tag{27}$$

with $(N_{\Delta G}, D_{\Delta G})$, $(N_{c\Delta G}, D_{c\Delta G})$ as in (24). *Then $Q^{-1}, Q_c^{-1} \in \mathbb{RH}_\infty$ and*

$$\|\Delta_P Q\|_\infty < 1-\tau, \quad \|\Delta_C Q_c\|_\infty \le \tau$$

with Δ_P of (7), *Δ_C of* (8) *and τ as defined in* (21).

Proof: From (18) and the stability of $H(P,C)$ it follows that $H(P_\Delta, C)$ and $H(P, C_\Delta)$ are stable. This means that P_Δ and C_Δ are admissible, so that by Lemma 2.5 Δ_P and Δ_C belong to $\mathbb{RH}_\infty$. Further, by Lemma 2.3 the admissibility of P_Δ and C_Δ implies that $\tilde{N}_c N_{\Delta G} + \tilde{D}_c D_{\Delta G}$ and

$\tilde{N}N_{c\Delta G}+\tilde{D}D_{c\Delta G}$ are unimodular, since $(N_{\Delta G}, D_{\Delta G})$ and $(N_{c\Delta G}, D_{c\Delta G})$ are right coprime factorizations by virtue of Proposition 4.7. Consequently Q and Q_c have stable inverses.
Next we use the equivalences

$$\begin{bmatrix} N+D_c\Delta_P \\ D-N_c\Delta_P \end{bmatrix} Q =$$

$$= \begin{bmatrix} N+D_c\Delta_P \\ D-N_c\Delta_P \end{bmatrix} \Lambda^{-1} \begin{bmatrix} \tilde{N}_c & \tilde{D}_c \end{bmatrix} \begin{bmatrix} N_{\Delta G} \\ D_{\Delta G} \end{bmatrix}$$

$$= T(P_\Delta, C) \begin{bmatrix} N_{\Delta G} \\ D_{\Delta G} \end{bmatrix}$$

$$= \begin{bmatrix} N_{\Delta G} \\ D_{\Delta G} \end{bmatrix} (\tilde{N}_c N_{\Delta G}+\tilde{D}_c D_{\Delta G})^{-1} \cdot \cdot \begin{bmatrix} \tilde{N}_c & \tilde{D}_c \end{bmatrix} \begin{bmatrix} N_{\Delta G} \\ D_{\Delta G} \end{bmatrix}$$

$$= \begin{bmatrix} N_{\Delta G} \\ D_{\Delta G} \end{bmatrix}$$

and similarly

$$\begin{bmatrix} N_c+D\Delta_C \\ D_c-N\Delta_C \end{bmatrix} Q_c = \begin{bmatrix} N_{c\Delta G} \\ D_{c\Delta G} \end{bmatrix}$$

to obtain

$$\begin{bmatrix} N \\ D \end{bmatrix} (I-Q) + \begin{bmatrix} -D_c \\ N_c \end{bmatrix} \Delta_P Q =$$

$$= \begin{bmatrix} N \\ D \end{bmatrix} - \begin{bmatrix} N_{\Delta G} \\ D_{\Delta G} \end{bmatrix} \tag{28}$$

$$\begin{bmatrix} N_c \\ D_c \end{bmatrix} (I-Q_c) + \begin{bmatrix} -D \\ N \end{bmatrix} \Delta_C Q_c =$$

$$= \begin{bmatrix} N_c \\ D_c \end{bmatrix} - \begin{bmatrix} N_{c\Delta G} \\ D_{c\Delta G} \end{bmatrix}. \tag{29}$$

Multiplying (28) to the left with $\tilde{\Lambda}^{-1} \begin{bmatrix} -\tilde{D} & \tilde{N} \end{bmatrix}$ yields

$$\Delta_P Q = \tilde{\Lambda}^{-1} \begin{bmatrix} -\tilde{D} & \tilde{N} \end{bmatrix} \left[\begin{bmatrix} N \\ D \end{bmatrix} - \begin{bmatrix} N_{\Delta G} \\ D_{\Delta G} \end{bmatrix} \right].$$

Making use of Proposition 4.7, Lemma 4.6 and the fact that $\begin{bmatrix} -\tilde{D} & \tilde{N} \end{bmatrix}$ is co-inner we obtain

$$\|\Delta_P Q\|_\infty \leq \|\tilde{\Lambda}^{-1}\|_\infty \vec{\delta}(P, P_\Delta) < 1-\tau.$$

Similarly the inequality

$$\|\Delta_C Q_c\|_\infty \leq \|\Lambda^{-1}\|_\infty \vec{\delta}(C, C_\Delta) = \tau$$

results after multiplying (29) to the left with $\Lambda^{-1} \begin{bmatrix} -\tilde{D}_c & \tilde{N}_c \end{bmatrix}$. □

Lemma 4.9 *Let $H(P,C)$ be stable, and let P_Δ,C_Δ satisfy* (18). *Then Q, Q_c defined in* (27) *satisfy*

$$\|Q^{-1}\|_\infty < \frac{1}{\tau}, \quad \|Q_c^{-1}\|_\infty \leq \frac{1}{1-\tau}$$

with τ defined in (21).

Proof: Similar to the proof of Lemma 4.8 we multiply (28) to the left by $\Lambda^{-1} \begin{bmatrix} \tilde{N}_c & \tilde{D}_c \end{bmatrix}$, which results in

$$I - Q = \Lambda^{-1} \begin{bmatrix} \tilde{N}_c & \tilde{D}_c \end{bmatrix} \left[\begin{bmatrix} N \\ D \end{bmatrix} - \begin{bmatrix} N_{\Delta G} \\ D_{\Delta G} \end{bmatrix} \right].$$

Since $\begin{bmatrix} \tilde{N}_c & \tilde{D}_c \end{bmatrix}$ is co-inner

$$\|I - Q\|_\infty \leq \|\Lambda^{-1}\|_\infty \vec{\delta}(P, P_\Delta) < 1-\tau,$$

by virtue of (24), Fact 4.4.ii and Lemma 4.6 . Likewise, multiplication of (29) by $\tilde{\Lambda}^{-1} \begin{bmatrix} \tilde{N} & \tilde{D} \end{bmatrix}$ results in

$$\|I - Q_c\|_\infty \leq \|\tilde{\Lambda}^{-1}\|_\infty \vec{\delta}(C, C_\Delta) = \tau.$$

The two latter inequalities imply that

$$\sigma_{max}(I - Q(j\omega)) < 1-\tau, \quad \sigma_{max}(I - Q_c(j\omega)) \leq \tau$$

for all $\omega \in \mathbb{R}$. For any particular frequency $\omega \in \mathbb{R}$ we replace M, b of (19) with $Q(j\omega)$ and τ, and M, d of (20) with $Q_c(j\omega)$ and $1-\tau$, so that

$$\sigma_{min}(Q(j\omega)) > \tau, \quad \sigma_{min}(Q_c(j\omega)) \geq 1-\tau.$$

Using the fact that $1/\sigma_{min}(M) = \sigma_{max}(M^{-1})$ for every invertible complex matrix M, Proposition 12.9.4. in Lancaster and Tismenetsky (1985), we get

$$\sigma_{max}(Q^{-1}(j\omega)) < \frac{1}{\tau}, \quad \sigma_{max}(Q_c^{-1}(j\omega)) \leq \frac{1}{1-\tau}$$

for any particular frequency $\omega \in \dot{\mathbb{R}}$, which proves the lemma. □

By now the gap-metric condition for robust stability of (18) has been sufficiently exploited to prove Theorem 4.3. Especially the latter two lemmas greatly facilitate the following proof.

Proof of Theorem 4.3: By Lemma 4.8 the stability of $H(P,C)$ and the inequality (18) together imply that $Q, Q_c \in \mathbb{R}\mathrm{H}_\infty$ of (27) are unimodular. For these particular Q, Q_c we have

$$\|Q_c^{-1}\Delta_P Q\|_\infty \leq \|Q_c^{-1}\|_\infty \|\Delta_P Q\|_\infty < \frac{1-\tau}{1-\tau} = 1$$

$$\|Q^{-1}\Delta_C Q_c\|_\infty \leq \|Q^{-1}\|_\infty \|\Delta_C Q_c\|_\infty \leq \frac{1}{\tau} \cdot \tau = 1$$

by Lemma 4.8 and Lemma 4.9, so that there indeed exist unimodular $Q, Q_c \in \mathbb{R}\mathrm{H}_\infty$ such that (15) is satisfied. □

In conclusion we relate our robust stability condition of Corollary 3.5 to the graph metric condition introduced by Vidyasagar and Kimura (1986):

$$\|T(P,C)\|_\infty d(P,P_\Delta) + \|T(C,P)\|_\infty d(C,C_\Delta) < 1,$$

where $d(P,P_\Delta)$ denotes the distance between P and P_Δ in the graph metric. Using Fact 4.4.i we rewrite the latter condition as

$$d(P,P_\Delta) + d(C,C_\Delta) < \|T(P,C)\|_\infty^{-1}, \qquad (30)$$

which bears great similarity to the gap-metric condition of (18). Moreover, as $\delta(P,P_\Delta) \leq d(P,P_\Delta)$ by Corollary 1 of Georgiou (1988), the gap-metric condition of (18) is less conservative than the graph-metric condition of (30). Hence our condition of Corollary 3.5 is less conservative than both the gap- and graph-metric conditions for robust stability under simultaneous perturbations.

5 Example

Having demonstrated that the new robust stability condition is less conservative than the gap-metric condition, now we provide an example in which robust stability under simultaneous perturbations is guaranteed by our condition of (15), but not by the gap-metric condition of (18). The systems of concern have the following transfer functions:

$$P = \frac{-s+1}{4s^3+0.4s^2+4s}$$

$$C = \frac{17s^2-2.3s+10}{s^2+3.3s+11}$$

$$P_\Delta = \frac{0.2s^7+3s^6+5.4s^5+7.8s^4-22s^3+5.2s^2-21s+3.2}{10s^7+31s^6+150s^5+123s^4+218s^3+87s^2+69s+7.1}$$

$$C_\Delta = \frac{30s^7+87s^6+131s^5+148s^4+130s^3+63s^2+41s+9.3}{s^7+8.3s^6+38s^5+83s^4+107s^3+97s^2+62s+13}$$

The Bode diagrams of these systems have been depicted in Fig. 2.d.

The Figures 2.d.a and c display that P (—) and P_Δ (--) are strikingly different. The difference P–P_Δ (····) is quite large: its frequency response magnitude is at least 40% of $|P(j\omega)|$ over all frequencies, and it is even larger than 60% at those frequencies where $|P(j\omega)C(j\omega)| \approx 1$. The controller perturbation seems to be moderate, but $|C(j\omega)-C_\Delta(j\omega)|$ is larger than 15% of $|C(j\omega)|$ over all frequencies, and it is up to 70% at the frequencies where $|PC| \approx 1$.

Like in (6), (9) we model P_Δ, C_Δ as perturbations of the normalized coprime factors of P, C. The corresponding plant and controller perturbations Δ_P and Δ_C are shown in Fig. 3.

The H_∞-norms of these perturbations are $\|\Delta_P\|_\infty = 0.968$ and $\|\Delta_C\|_\infty = 0.764$. The product of these norms is 0.734, so that even larger plant and controller perturbations are allowed in view of Corollary 3.5 (and Theorem 3.3).

For the robust stability test based on the gap-metric condition of (18) we have the following numbers:

$$\begin{aligned} \delta(P,P_\Delta) &= 0.917 \\ \delta(C,C_\Delta) &= 0.286 \\ \|T(P,C)\|_\infty^{-1} &= 5.73 \cdot 10^{-2}. \end{aligned}$$

Clearly $\delta(P,P_\Delta) + \delta(C,C_\Delta)$ is much larger than $\|T(P,C)\|_\infty^{-1}$. Hence from (18) it cannot be concluded that $H(P_\Delta, C_\Delta)$ is robustly stable. Moreover, as $\delta(P,P_\Delta) > \|T(P,C)\|_\infty^{-1}$ and $\delta(C,C_\Delta) > \|T(P,C)\|_\infty^{-1}$, the gap-metric condition fails even to guarantee stability of $H(P_\Delta, C)$ or of $H(P, C_\Delta)$. Finally, the small value of $\|T(P,C)\|_\infty^{-1}$ indicates that $H(P,C)$ has poor robustness properties in gap metric sense, while $H(P,C)$ is robustly stable against rather large perturbations as shown in Fig. 2.d.

6 Concluding remarks

We have used two Youla parameterizations to derive a new condition for robust stability in the face of simultaneous perturbations of the nominal plant and controller. By a number of theorems we have demonstrated that this new condition is less conservative than a condition for robust stability under simultaneous perturbations measured in the gap metric. An example has been provided in which robust stability under simultaneous perturbations is guaranteed by our condition, but not by the gap-metric condition.

In addition, our robustness condition is non-conservative if either the plant perturbations or the controller perturbations vanish. The utility of this stability result for control design has been demonstrated in Schrama (1992), where a robust controller is designed for a plant with uncertain dynamics. A geometric interpretation of the new robust stability condition remains a topic for future research.

References

Desoer, C.A., R.-W. Liu, J. Murray and R. Saeks (1980). Feedback system design: the fractional

representation approach to analysis and synthesis. *IEEE Trans. Automat. Contr., vol. AC-25*, 399–412.

Desoer, C.A. and M. Vidyasagar (1975). *Feedback Systems: Input-Output Properties.* Academic Press Inc., New York.

Francis, B.A. (1987). *A Course in H_∞ Control Theory.* Springer Verlag, Berlin.

Georgiou, T.T. (1988). On the computation of the gap metric. *Syst. Control Lett.*, 253–257.

Georgiou, T.T. and M.C. Smith (1990a). Optimal robustness in the gap metric. *IEEE Trans. Automat. Contr., vol. AC-35*, 673–686.

Georgiou, T.T. and M.C. Smith (1990b). Robust control of feedback systems with combined plant and controller uncertainty. *Proc. American Control Conf., San Diego, CA*, 2009–2013.

Lancaster, P. and M. Tismenetsky (1985). *The Theory of Matrices, Second Edition.* Academic Press Inc., London.

Maciejowski, J.M. (1989). it Multivariable Feedback Design. Addison-Wesley Publ. Comp.

Morari, M. and E. Zafiriou (1989). *Robust Process Control.* Prentice-Hall Inc., Englewood Cliffs, NJ.

Schrama, R.J.P. (1992). it Approximate Identification and Control Design with Application to a Mechanical System. PhD Thesis, Delft University of Technology, The Netherlands.

Stein, G. and J.C. Doyle (1991). Beyond singular values and loop shapes. it J. Guidance, Control and Dynamics, 14, 5–16.

Vidyasagar, M. (1984). The graph metric for unstable plants and robustness estimates for feedback stability. *IEEE Trans. Automat. Contr., AC-29*, 403–417.

Vidyasagar, M. (1985). it trol System Synthesis: A Factorization Approach. M.I.T. Press, Cambridge, MA.

Vidyasagar, M. and H. Kimura (1986). Robust controllers for uncertain linear systems. it Automatica, 22, 85–94.

Vidyasagar, M., H. Schneider and B.A. Francis (1982). Algebraic and topological aspects of feedback stabilization. it IEEE Trans. Automat. Contr., AC-27, 880–894.

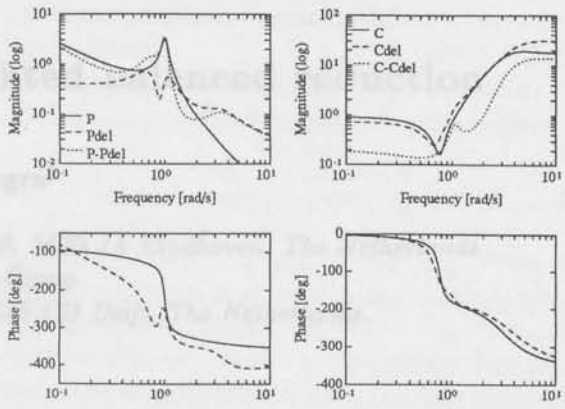

Fig. 2: Bode diagrams of the nominal and perturbed plants and controllers.
a: Magnitudes of P (—), P_Δ (--) and $P-P_\Delta$ (····).
b: Magnitudes of C (—), C_Δ (--) and $C-C_\Delta$ (····).
c: Phases, see a.
d: Phases, see b.

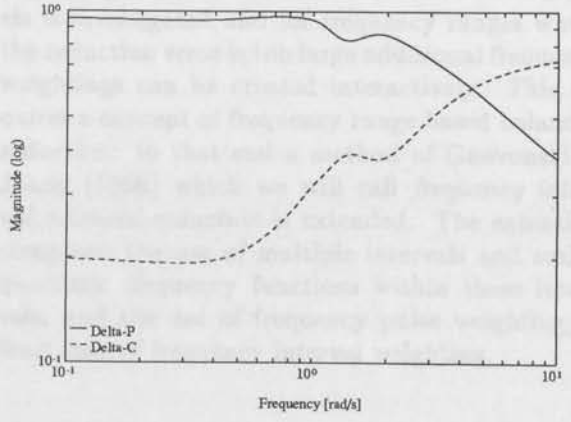

Fig. 3: Plant perturbation Δ_P (—) and controller perturbation Δ_C (--).

Selected Topics in Identification, Modelling and Control
Vol. 5, December 1992

Generalized frequency weighted balanced reduction

Pepijn M.R. Wortelboer [‡] **, Okko H. Bosgra**[§]

[‡] *Philips Research Laboratories, P.O.Box 80.000, 5600 JA Eindhoven, The Netherlands*
[§] *Mechanical Engineering Systems and Control Group*
Delft University of Technology, Mekelweg 2, 2628 CD Delft, The Netherlands.

Abstract. A generalization of frequency weighted balanced reduction is worked out that comprises: the original frequency weighted balanced reduction of Enns (1984b), and frequency interval balanced reduction of Gawronski & Juang (1990). The latter is extended with scalar quadratic frequency weightings per frequency interval. Weighting in frequency points is also developed. This generalization provides a very direct and flexible way of specifying frequency weightings. In a MATLAB implementation the frequency weightings can be adjusted and refined until the reduction error after weighted balanced reduction is satisfactory. The procedure is illustrated by means of two examples.

Keywords. model reduction; frequency weighted balancing.

1 Introduction

Frequency domain robust controller design methods require some quantification of the expected deviation of the nominal controller design model from the real system. The smaller the deviations, the easier a robust high-performance controller can be found. The contribution of model reduction to the deviations in the frequency domain is more or less free after the introduction of frequency weighted model reduction methods such as frequency weighted balanced reduction (FWBR). In FWBR (Enns 1984), the standard balanced reduction procedure is followed, the difference is that instead of the standard controllability Gramian P and observability Gramian Q (6), frequency weighted (FW) Gramians P_{W_i} (10) and Q_{W_o} are used (12). FWBR can be used to approximate the original model specifically good in a bandwidth related frequency range where relatively small errors are known to endanger robust controller design. It is by no means clear however what frequency weighting should be used to keep the reduction error below a certain frequency dependent bound. A clear guideline for the construction of appropriate frequency weighting functions is lacking. This stimulated the development of a step by step FWBR procedure: after each FWBR step the performance of a number of reduced models is investigated and for frequency ranges where the reduction error is too large additional frequency weightings can be created interactively. This requires a concept of frequency range based balanced reduction: to that end a method of Gawronski & Juang (1990) which we will call *frequency interval balanced reduction* is extended. The extension comprises the use of multiple intervals and scalar quadratic frequency functions within these intervals, and the use of frequency pulse weighting, a limit case of frequency interval weighting.

In Section 2 balanced reduction is reviewed. Enns' frequency weighted model reduction method is discussed in Section 3. Section 4 extends the frequency interval Gramians to weighted frequency interval Gramians. A special limit case, the frequency point Gramians are introduced next in Section 5. In Section 6 the (MATLAB) implementation of all methods is discussed. Its ease of use and effectiveness in FWBR are illustrated by means of two examples.

2 Balanced reduction

Balanced reduction finds its origin in the work of Moore (1981), a self-contained treatise can be found in Glover (1984).

Consider the linear time-invariant system of order n with m inputs and p outputs

$$\begin{aligned} \dot{x} &= Ax + Bu \\ y &= Cx + Du \end{aligned}$$

$x \in \mathbb{R}^{n\times 1}$, $u \in \mathbb{R}^{m\times 1}$, and $y \in \mathbb{R}^{p\times 1}$. Matrices A, B, C, D have compatible sizes. (A, B, C, D) and $G_n(s) = C(sI - A)^{-1}B + D$ will both be used as system description.

Balanced reduction is the truncation of a balanced state space realization. It is restricted to stable systems.

2.1 balancing

The balancing state-space transformation is such that

$$\breve{T}^{-1} P \breve{T}^{-H} = \breve{T}^H Q \breve{T} = \Sigma$$

with P, Q the controllability, observability Gramian

$$\begin{aligned} P &= \int_0^\infty e^{At} B B^H e^{A^H t}\, \mathrm{d}t \\ Q &= \int_0^\infty e^{A^H t} C^H C e^{At}\, \mathrm{d}t \end{aligned} \qquad (1)$$

and Σ a diagonal matrix with the so-called Hankel singular values (HSVs) $\sigma_i = \sqrt{\lambda_i(PQ)}$ in decreasing order. The balanced realization $(\breve{A}, \breve{B}, \breve{C}, D) = (\breve{T}^{-1}A\breve{T}, \breve{T}^{-1}B, C\breve{T}, D)$ thus has equal and diagonal Gramians and σ_i measures how controllable/observable state $\breve{x}_i$ is.

2.2 reduction

The actual reduction step is as follows: let R denote the first n_r columns of $\breve{T}$ and L the first n_r rows of $\breve{T}^{-1}$. The n_r^{th} order balanced truncation then is:

$$(\breve{A}, \breve{B}, \breve{C}, D) = (LAR, LB, CR, D)$$

Denote $G_r(s)$ the reduced system. $G_r(s)$ has HSVs $\sigma_1, \ldots, \sigma_{n_r}$, and the realization $(\breve{A}, \breve{B}, \breve{C}, D)$ is balanced. The truncated HSVs determine a reduction error bound:

$$\|G_n(j\omega) - G_r(j\omega)\|_\infty \leq 2(\sigma_{n_r+1} + \ldots + \sigma_n) \qquad (2)$$

2.3 algorithms

Many procedures for calculating $\breve{T}$ have been proposed. The standard approach uses a Cholesky decomposition of P or Q but this is not recommended because P and Q are often almost singular (in the reduction of high-order systems Hankel singular values close to zero are no exception). A singular value decomposition of P and Q is a more robust alternative for the Cholesky decomposition. Since we know that P and Q are non-negative definite the following factorizations must exist:

$$\begin{aligned} P &= pp^H \\ Q &= qq^H \end{aligned}$$

with $p \in \mathbb{R}^{n\times n_p}$ of rank n_p and $q \in \mathbb{R}^{n\times n_q}$ of rank n_q. Let $r = \min(n_p, n_q)$. Then we have r non-zero Hankel singular values:

$$\lambda_i^{\frac{1}{2}}(PQ) = \sigma_i(p^H q) \quad i = 1, \ldots, r$$

The singular value decomposition of $p^H q$ gives both the r largest Hankel singular values and the corresponding right (R_r) and left (L_r) eigenvectors of PQ that define the minimal balanced realization of order r $(L_r A R_r, L_r B, C R_r, D)$

$$\begin{aligned} p^H q &= U_{n_p r} \Sigma_r V_{n_q r}^H \\ R_r &= p U_{n_p r} \Sigma_r^{-\frac{1}{2}} \\ L_r &= (q V_{n_q r} \Sigma_r^{-\frac{1}{2}})^H \end{aligned}$$

$\Sigma_r = \mathrm{diag}(\sigma_1, \ldots, \sigma_r)$, $U_{n_p r}^H U_{n_p r} = V_{n_q r}^H V_{n_q r} = I_r$, $R_r \in \mathbb{R}^{n\times r}$ and $L_r \in \mathbb{R}^{r\times n}$.

A second alternative for Cholesky factorizations is used in the block-balancing iteration (Wortelboer 1991): it operates directly on PQ and finds a balanced realization of some fixed order n_1 by iteration. If the first n_1 HSVs are all greater than zero, no singularity problems can occur.

The Gramians P and Q are usually not calculated by evaluating the time integrals in (1). Instead a pair of linear matrix equations is solved:

$$\begin{aligned} AP + PA^H &= \int_0^\infty \mathrm{d}(e^{At} B B^H e^{A^H t}) = -BB^H \\ A^H Q + QA &= \int_0^\infty \mathrm{d}(e^{A^H t} C^H C e^{At}) = -C^H C \end{aligned} \qquad (3)$$

These are the controllability and observability Lyapunov equations. The solution is straightforward for system realizations with A in triangular form.

2.4 time domain interpretation

The controllability Gramian can be interpreted as follows:

$$\begin{aligned} P &= \sum_{i=1}^m \int_0^\infty x_{u_i} x_{u_i}^H\, \mathrm{d}t \stackrel{\mathrm{def}}{=} \sum_{i=1}^m p_i \\ x_{u_i} &= e^{At} B e_i \end{aligned} \qquad (4)$$

with x_{u_i} the state response to an impulsive input at channel i ($e_i \in \mathbb{R}^m$ is the i^{th} unit vector). This

is a direct consequence of the fact that $BB^H = B\sum_{i=1}^{m} e_i e_i^H B^H$.

The observability Gramian measures the energy at the output when the system is released from $x(0) = x_0$ while keeping the inputs equal to zero,

$$\int_0^\infty y^H(t)y(t)\,\mathrm{d}t = x_0^H Q x_0$$

Q can also be interpreted as a summation of p separate parts:

$$\begin{aligned} Q &= \sum_{i=1}^{p}\int_0^\infty y_{i,x_0}^H y_{i,x_0}\,\mathrm{d}t \stackrel{\text{def}}{=} \sum_{i=1}^{p} q_i \qquad (5)\\ y_{i,x_0} &= e_i^H C e^{At} \end{aligned}$$

with y_{i,x_0} the response of the i^{th} output to a state impulse at $t = 0$ and $e_i \in \mathbb{R}^p$ the i^{th} unit vector.

2.5 frequency domain interpretation

In the sequel the frequency domain counterpart of (1) will be of special importance (Skelton 1988)

$$\begin{aligned} P &= \tfrac{1}{2\pi}\textstyle\int_{-\infty}^{\infty}\Phi(j\omega)BB^H\Phi^H(j\omega)\mathrm{d}\omega\\ Q &= \tfrac{1}{2\pi}\textstyle\int_{-\infty}^{\infty}\Phi^H(j\omega)C^HC\Phi(j\omega)\mathrm{d}\omega \end{aligned} \qquad (6)$$

with $\Phi(s) = (sI - A)^{-1}$. These equations are a direct consequence of Parseval's theory. In the time domain the inputs were impulses, here the inputs can be seen as white noise processes with unit intensity.

2.6 practical use

The steps to be performed are

1) calculate the Gramians P and Q
2) calculate the balancing transformation
3) calculate the balanced realization
4) truncate the balanced realization

For stable systems balanced reduction is a very practical reduction method. Each truncation of a balanced realization is stable and balanced and the reduction error is bounded (2). In practice the reduction error is often evaluated based on the maximum singular value of $G_n(j\omega) - G_r(j\omega)$ and it is often true that the reduction error has a unniform distribution over frequency.

If we want non-uniform error distributions, frequency weighted versions of balanced reduction can be used. The common approach is to define frequency weighted Gramians (modification of step 1) and to leave the other steps unchanged. For all methods step 2 should be performed with care. The next sections discuss the construction of FW Gramians.

3 Frequency weighted Gramians according to Enns

For a thorough discussion of FWBR we refer to Enns (1984a).

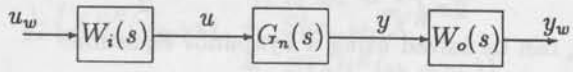

Fig. 1: Series connection for input and output weighting

In normal balanced reduction the inputs are assumed to be unit intensity white noise processes. Colored noise processes can be generated by means of a weighting function $W_i(s)$ receiving white noise inputs. Now $W_i(s)$ can be placed in series with the system, but reduction of this series connection applies to both original and filter states. Similarly filtering the output can be modeled by premultiplying the system with $W_o(s)$, the output weighting. The idea of Enns was to calculate the controllability Gramian of $G_n(s)W_i(s)$, the observability Gramian of $W_o(s)G_n(s)$ and to look only at the part related to the system states. These Gramian parts determine the FW-balancing transformation and the subsequent reduction.

Let (A_i, B_i, C_i, D_i) be an order n_i state space realization of $W_i(s)$ and (A_o, B_o, C_o, D_o) an order n_o state space realization of $W_o(s)$.

The frequency response of the states of (A, B, C, D) to the new inputs u_w is

$$\begin{aligned} x(s) &= (sI - A)^{-1}BW_i(s)u_w(s)\\ &= \Pi_{si}(sI - A_{si})^{-1}B_{si}u_w(s) \qquad (7) \end{aligned}$$

with

$$\Pi_{si} = \begin{bmatrix} O_{n,n_i} & I_n \end{bmatrix}$$

$$A_{si} = \begin{bmatrix} A_i & O_{n_i,n} \\ BC_i & A \end{bmatrix} \qquad (8)$$

$$B_{si} = \begin{bmatrix} B_i \\ BD_i \end{bmatrix} \qquad (9)$$

For x driven by unit intensity white noise u_w the weighted controllability Gramian is

$$P_{W_i} = \frac{1}{2\pi}\int_{-\infty}^{\infty} x(j\omega)x^H(j\omega)\mathrm{d}\omega$$

Using (7) and the fact that $u_w(j\omega)u_w^H(j\omega) = I$ we find

$$\begin{aligned} P_{W_i} &= \frac{1}{2\pi}\int_{-\infty}^{\infty}\Phi BW_iW_i^HB^H\Phi^H\mathrm{d}\omega\\ &= \Pi_{si}P_{si}\Pi_{si}^H \qquad (10) \end{aligned}$$

with

$$P_{si} = \frac{1}{2\pi}\int_{-\infty}^{\infty} \Phi_{si} B_{si} B_{si}^H \Phi_{si}^H \mathrm{d}\omega$$
$$\Phi_{si}(s) = (sI - A_{si})^{-1}$$

Since

$$\frac{1}{2\pi}\int_{-\infty}^{\infty} (j\omega I - A_s)^{-1}\mathrm{d}\omega = \frac{I}{2}$$

P_{si} can be solved using a Lyapunov equation:

$$(j\omega I - A_{si})P_{si} + P_{si}(j\omega I - A_{si})^H = -A_{si}P_{si} - P_{si}A_{si}^H = B_{si}B_{si}^H \qquad (11)$$

Output weighting with $W_o(s)$ means

$$Q_{W_o} = \frac{1}{2\pi}\int_{-\infty}^{\infty} \Phi^H C^H W_o^H W_o C \Phi \mathrm{d}\omega = \Pi_{so} Q_{so} \Pi_{so}^H \qquad (12)$$

with

$$\Pi_{so} = \begin{bmatrix} I_n & O_{n,n_o} \end{bmatrix}$$
$$A_{so} = \begin{bmatrix} A & O_{n,n_o} \\ B_o C & A_o \end{bmatrix} \qquad (13)$$
$$C_{so} = \begin{bmatrix} D_o C & C_o \end{bmatrix} \qquad (14)$$
$$Q_{so} = \frac{1}{2\pi}\int_{-\infty}^{\infty} \Phi_{so}^H C_{so}^H C_{so} \Phi_{so} \mathrm{d}\omega$$
$$\Phi_{so}(s) = (sI - A_{so})^{-1}$$

Q_{so} is solved from the observability Lyapunov equation,

$$A_{so}^H Q_{so} + Q_{so} A_{so} + C_{so}^H C_{so} = 0 \qquad (15)$$

The FW-balancing transformation is defined as

$$\breve{T}_W^{-1} P_{W_i} \breve{T}_W^{-H} = \breve{T}_W^H Q_{W_o} \breve{T}_W = \Sigma_W = \mathrm{diag}(\sigma_{W,i})$$

Expressions (10,12) clearly show that the influence of the weightings is fully determined by $W_i(j\omega)W_i(j\omega)^H, W_o(j\omega)^H W_o(j\omega)$. The state-space realizations of $W_i(s), W_o(s)$ are irrelevant and thus the FW HSVs $\sigma_{W,i}$ are system invariants for given (W_i, W_o). As expected intuitively weighting with all-pass systems has no effect.

3.1 stability

The truncation of the FW-balanced model is not necessarily stable for stable systems as was the case with balanced reduction, nor is it FW-balanced.

Stability is guaranteed for the following two cases:

i) if the input weighting is a constant matrix D_i and (A, BD_i) is a controllable pair with A stable, then FWBR results in a stable reduced-order model. (A, BD_i) is a controllable pair if and only if (A, B) is a controllable pair and $D_i D_i^H$ is nonsingular. The output weighting $W_o(s)$ is allowed to be dynamic.

ii) also for dynamic input weighting $W_i(s)$, and constant output weighting D_o, observability of $(A, D_o C)$ is sufficient for stability of the reduced-order model. Observability of (A, C) implies observability of $(A, D_o C)$ provided $D_o^H D_o$ is nonsingular.

3.2 practical use

In FWBR the normal balanced reduction procedure is applied to (A, B, C, D) using P_{W_i}, Q_{W_o} to define the FW-balancing transformation. P_{W_i} is solved via (10) and (11), and Q_{W_o} is solved via (12) and (15). In general the reduced models are not FW-balanced and stability is not guaranteed. The advantage over balanced reduction is that the reduction error can be shaped more or less as a function of frequency. A structured way of defining W_i and W_o for this purpose however is lacking. Also for practical use the order of W_i and W_o may not be too large.

4 Frequency weighted interval Gramians

The idea of defining Gramians over a fixed frequency interval is due to Gawronski and Juang (1990). They introduced new Gramians by limiting the time evolution in (1) and/or the frequency range in (6). Here we use the frequency interval Gramians as a starting point for our generalization.

4.1 frequency interval Gramians

In frequency interval balanced reduction it is assumed that the frequency content of the input signals is limited to a specific frequency band and similarly the output is only of concern in the same frequency band. Note that the interval is in fact a pair. Define

$$[\![\omega_a, \omega_b]\!] = [-\omega_b, -\omega_a] \cup [\omega_a, \omega_b] \quad \text{for} \quad \omega_b > \omega_a > 0$$

$$\eta(\omega, [\![\omega_a, \omega_b]\!]) = 1 \text{ for } \omega \in [\![\omega_a, \omega_b]\!] \quad = 0 \text{ for } \omega \notin [\![\omega_a, \omega_b]\!] \qquad (16)$$

The frequency interval Gramians then are

$$P_\eta = \tfrac{1}{2\pi}\int_{-\infty}^{\infty} \Phi(j\omega) B \eta(\omega, [\![\omega_a, \omega_b]\!]) B^H \Phi^H(j\omega)\, \mathrm{d}\omega$$
$$Q_\eta = \tfrac{1}{2\pi}\int_{-\infty}^{\infty} \Phi^H(j\omega) C^H \eta(\omega, [\![\omega_a, \omega_b]\!]) C \Phi(j\omega)\, \mathrm{d}\omega$$

P_η and Q_η are not computed via numerical integration but via standard Lyapunov equations and an additional matrix logarithm as will be shown in 4.3.

Experiments with frequency interval balanced reduction revealed that a large interval is needed to ensure that the reduced order model is stable. In

that case the advantage over standard balanced reduction is minimal. A valuable extension however is created by using more intervals each equipped with some frequency weighting function.

4.2 definition of FW interval Gramians

Let's write our generalized FW Gramians as

$$\begin{aligned} P_{\Omega_i} &= \tfrac{1}{2\pi}\int_{-\infty}^{\infty} \Phi(j\omega)B\Omega_i(\omega)B^H\Phi^H(j\omega)\,\mathrm{d}\omega \\ Q_{\Omega_o} &= \tfrac{1}{2\pi}\int_{-\infty}^{\infty} \Phi^H(j\omega)C^H\Omega_o(\omega)C\Phi(j\omega)\,\mathrm{d}\omega \end{aligned} \quad (17)$$

For $\Omega_i(\omega) = W_i(j\omega)W_i^H(j\omega)$ and $\Omega_o(\omega) = W_o^H(j\omega)W_o(j\omega)$ we have Enns' (W_i, W_o)-weighted Gramians. For $\Omega_i(\omega) = I_m\eta(\omega, [\![\omega_a, \omega_b]\!])$ and $\Omega_o(\omega) = I_p\eta(\omega, [\![\omega_a, \omega_b]\!])$ we have the plain interval case of Gawronski & Juang (1990).

We are looking for well defined Ω functions

$$\begin{aligned} \Omega(-\omega) &= \overline{\Omega(\omega)} \\ \Omega^H(\omega) &= \Omega(\omega) > 0 \end{aligned} \quad (18)$$

that can be specified easily and that allow a solution to (17) based on Lyapunov equations.

A piecewise quadratic frequency function is proposed:

$$\Omega(\omega) = \textstyle\sum_k(\Gamma_{0k} + \Gamma_{1k}|\omega| + \Gamma_{2k}\omega^2)\ \eta(\omega, [\![\omega_a, \omega_b]\!]_k) \quad (19)$$

For each interval k, the constants Γ_0, Γ_1 and Γ_2 should be such that (18) is satisfied.

The derivation of the weighted observability Gramian is similar to the derivation of the controllability Gramian that will be given next. We can concentrate on one frequency interval $[\omega_a, \omega_b]$ with $\omega_b > \omega_a \geq 0$. The associated $[-\omega_b, -\omega_a]$ part of the weighted controllability Gramian can be obtained by substitution.

4.3 solution of the weighted controllability Gramian

For the solution of

$$\begin{aligned} P_{\Gamma,[\omega_a,\omega_b]} &= \frac{1}{2\pi}\int_{\omega_a}^{\omega_b} \Phi(j\omega)Y\Phi^H(j\omega)\,\mathrm{d}\omega \quad (20) \\ \text{with} \quad Y &= B(\Gamma_0 + \Gamma_1\omega + \Gamma_2\omega^2)B^H \end{aligned}$$

we write Y as

$$\begin{aligned} &(j\omega I - A)X + X^H(j\omega I - A)^H \\ &+(j\omega I - A)B\Gamma_2B^H(j\omega I - A)^H \end{aligned}$$

with X the solution to the following linear matrix equation

$$\begin{aligned} &AX + XA^H + BF^H = 0 \quad (21) \\ &F = B\Gamma_0^H - jAB\Gamma_1^H - A^2B\Gamma_2^H \end{aligned}$$

Next the integration (20) can be executed term by term:

$$\begin{aligned} P_{\Gamma,[\omega_a,\omega_b]} &= \tfrac{1}{2\pi}\textstyle\int_{\omega_a}^{\omega_b} X(j\omega I - A)^{-H}\mathrm{d}\omega + \\ &\quad \tfrac{1}{2\pi}\textstyle\int_{\omega_a}^{\omega_b}(j\omega I - A)^{-1}X^H\mathrm{d}\omega + \\ &\quad \tfrac{1}{2\pi}\textstyle\int_{\omega_a}^{\omega_b} B\Gamma_2B^H\mathrm{d}\omega = \\ \tfrac{1}{2\pi}\big\{XS^H(\omega_a,\omega_b) &+ S(\omega_a,\omega_b)X^H \\ &+ B\Gamma_2B^H(\omega_b - \omega_a)\big\} \end{aligned} \quad (22)$$

with $S(\omega_a, \omega_b) = -j\ \ln[(j\omega_a I - A)^{-1}(j\omega_b I - A)]$. The matrix logarithm $S(\omega_a, \omega_b)$ can be solved by first transforming A to diagonal form.

For the interval case with $\Gamma_0 = I$ (21) simplifies to the standard (unweighted) controllability Lyapunov equation yielding $X = P$. The interval weighted controllability Gramian then is

$$\begin{aligned} P_{[\omega_a,\omega_b]} = \frac{1}{2\pi}\{\ &P[S^H(\omega_a,\omega_b) + S^H(-\omega_b,-\omega_a)] + \\ &[S(\omega_a,\omega_b) + S(-\omega_b,-\omega_a)]P\ \} \end{aligned}$$

A similar solution can be derived for

$$\Omega(\omega) = \textstyle\sum_k\left(\sum_{p\in\mathbb{Z}}\Gamma_{pk}|\omega|^p\right)\ \eta(\omega, [\![\omega_a, \omega_b]\!]_k) \quad (23)$$

4.4 practical use

For each interval with a quadratic frequency function given by $\Gamma_0, \Gamma_1, \Gamma_2$, (21) is solved and X is substituted in (22). For the associated negative interval the same Γ's are used. $Q_{\Gamma,[\![\omega_a,\omega_b]\!]}$ is handled similarly. The sum over all frequency interval pairs yields the FW Gramians P_{Ω_i} and Q_{Ω_o}. In the FW-balanced form we have $\breve{P}_{\Omega_i} = \breve{Q}_{\Omega_o} = \Sigma_\Omega = \mathrm{diag}(\sigma_{\Omega,i})$. In general the reduced models are not FW-balanced and stability is not guaranteed. Compared to Enns' FWBR the freedom in specifying $\Omega(\omega)$ is large. No realizations for $W_i(s)$ and $W_o(s)$ are needed.

5 Frequency pulse Gramians

Suppose we have an interval function bounding a unit area $(\omega_b - \omega_a)^{-1}\eta(\omega, [\omega_a, \omega_b])$. For $\omega_a \to \omega_b$ this function deforms into a Dirac delta function $\delta(\omega - \omega_b)$. For $\omega_b \neq 0$ a frequency pulse pair is used to satisfy (18): $\Omega(\omega) = \Gamma_\delta(\delta(\omega - \omega_b) + \delta(\omega + \omega_b))$ with Γ_δ real and positive definite. Let $\omega_b|$ represent a frequency pulse at ω_b and $\omega_b\|$ a frequency pulse pair at $\{-\omega_b, +\omega_b\}$. With (17) we find for the pulse weighted controllability Gramian

$$\begin{aligned} P_{\omega_b\|} &= P_{\omega_b|} + P_{-\omega_b|} \\ P_{\omega_b|} &= \frac{1}{2\pi}(j\omega_b I - A)^{-1}B\Gamma_\delta B^H(j\omega_b I - A)^{-H} \end{aligned}$$

This can be computed straightforwardly.

The rank of this matrix cannot exceed m, the number of inputs. By choosing n_k pairs of frequency pulses (at positive and negative frequencies) the order of the controllability Gramian will be $2n_k m$. If we require positive definite Gramians for minimal systems we have to take $n_k \geq \frac{1}{2}n/m$.

6 Generalized framework

In the most general case we start with input and output weighting W_i and W_o and apply the interval based frequency weightings to the inputs u_w and outputs y_w (see Fig.1). On the input side we have A_{si}, B_{si} (8,9) and by means of piecewise quadratic and pulse weightings the FW controllability Gramian is built up. At the end the original system-state part is extracted using the projection Π_{si} and the *un*weighted controllability Gramian P is added with a scaling factor β

$$P_{W\Omega_i} = \beta P + \Pi_{si} P_{si,\Omega_i} \Pi_{si}^H \qquad (24)$$

$$P_{si,\Omega_i} = \sum_{j=1}^{m_i} \left(\sum_k P_{si,([\Gamma,[\omega_a,\omega_b]])_{jk}} + \sum_l P_{si,(\Gamma_\delta,\omega_b])_{jl}} \right)$$

Thus we have a sum over intervals (k), a sum over frequency points (l) and all these summed over the inputs u_w of W_i (see Fig.1 and (4)). On the output side we have A_{so}, C_{so} (13,14) and the same approach is followed to build $Q_{W\Omega_o}$.

A MATLAB model reduction tool has been developed that builds weighted controllability and observability Gramian in steps, showing the reduction result (frequency response, reduction error) after each step and allowing the user to specify additional weightings. One can start with a small factor β to analyse normal balanced reduction. Next a scalar piecewise quadratic function or a series of pulses can be specified for each input and output separately. For quadratic weighting within a single interval three frequency function values are required. The lowest and highest frequencies determine the interval, Γ_0, Γ_1 and Γ_2 result from an interpolation through the three function values. Continuation in neighbouring intervals requires two additional function values. For a frequency pulse one function value $(\omega_b, \Gamma_\delta)$ is needed. The input of the frequency function values can be performed graphically. Picking points in a frequency response plot has the advantage that the weighting can be tuned to the system frequency characteristics. The reduction error and the scalar weightings are plotted together after each step. This gives the user a clue for applying additional weightings.

6.1 example 1

First frequency weighted reduction of a 34^{th}-order siso model (Fig.2) of the tracking mechanism in a Compact Disc player is analysed. The reduced order model will be used for the design of a controller that achieves a bandwidth of about 1 kHz. The lightly damped system poles turn unstable if the model reduction error near 1 kHz is too large. Here it will be shown that our frequency weighting concept is very efficient for controller-relevant reduction. Let us first analyse standard balanced reduction (unweighted case).

The HSVs (Fig.3) are used to calculate the error bounds (2) for all possible reduced orders. Figure 4 shows that only with $n_r \geq 30$ sufficiently accurate results can be expected, due to the magnitude of the transfer function in the bandwidth frequency range. To force a better fit around 1 kHz a quadratic frequency function is added. Figure 2 shows the three points that were picked and the quadratic fit within the chosen interval. The frequency weighted HSVs (Fig.3) point to a 12^{th} order reduced model. Normalized LQG control design on a 12^{th} order frequency weighted reduced model gave a controller that performed well on the 34^{th} order model whereas the same design on a balanced approximation of order 12 resulted in a controller that destabilized the original model. Figures 5 and 6 show the results for $n_r = 12$ in the unweighted and weighted case. Balanced reduction gives reduction errors distributed almost uniformly over all frequencies, but the dynamics in the bandwidth frequency range are not included. In the weighted case the accuracy is clearly improved within the interval. At low frequencies the fit is worse than with normal balanced reduction, but this does not hamper successful control design.

Weighting only with the quadratic part, the 3.5 Hz mode turns unstable in most reduced models. Plain frequency interval balanced reduction shows similar stability problems.

6.2 example 2

The second example shows the use of the Dirac pulse frequency weighting on a stable single input single output all-pass system:

$$g_4(s) = \frac{(s-1)(s-2)(s-3)(s-4)}{(s+1)(s+2)(s+3)(s+4)} \qquad (25)$$

This academical system provides no basis for balanced reduction since all HSVs are equal to one. FWBR gives distinct FW HSVs and thus a basis for reduction. Choosing a frequency weighting

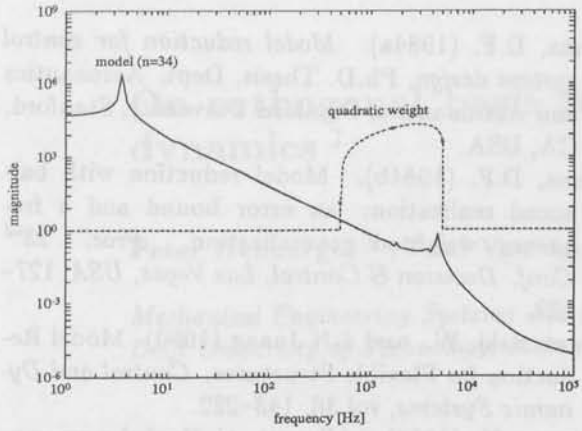

Fig. 2: Magnitude 34^{th}-order model and piecewise quadratic frequency weighting function

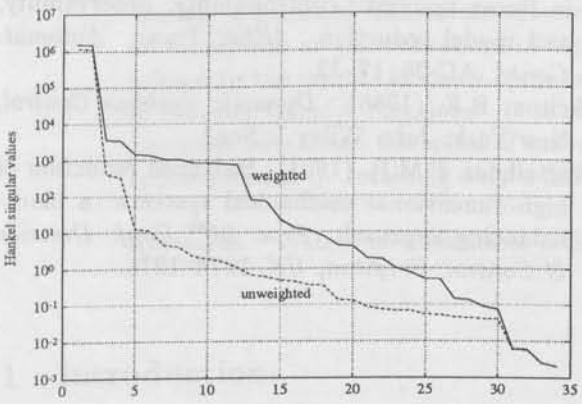

Fig. 3: frequency weighted HSVs σ_Ω, and unweighted HSVs σ

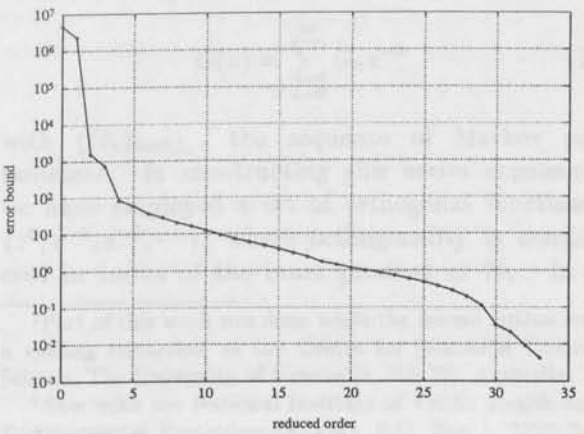

Fig. 4: error bounds as a function of the reduced order n_r

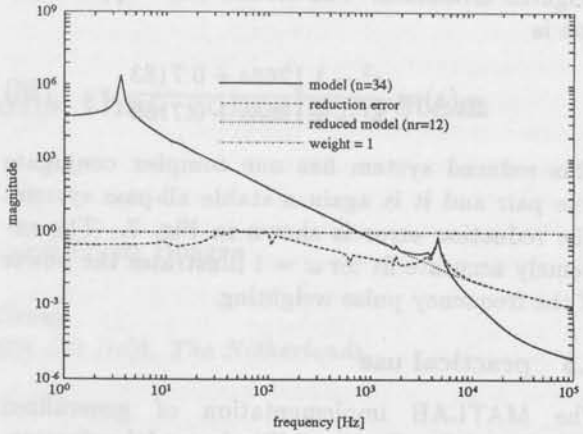

Fig. 5: Unweighted balanced reduction to order $n_r = 12$

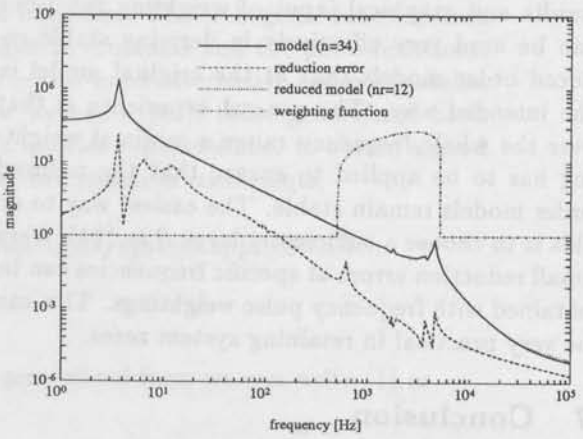

Fig. 6: Weighted balanced reduction to order $n_r = 12$

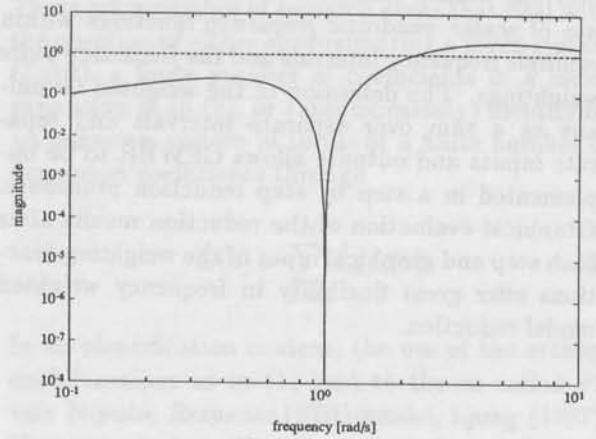

Fig. 7: Reduction error for weighting with frequency pulse at $\omega = 1$

$\Omega_i(\omega) = \Omega_o(\omega) = \hat{\delta}(\omega+1) + \hat{\delta}(\omega-1)$ gives rank 2 weighted Gramians. The second order approximation is

$$g_2(s) = \frac{s^2 - 1.1268s + 0.7183}{s^2 + 1.1268s + 0.7183} \qquad (26)$$

This reduced system has one complex conjugate pole pair and it is again a stable all-pass system. The reduction error is shown in Fig. 7. The extremely accurate fit for $\omega = 1$ illustrates the power of the frequency pulse weighting.

6.3 practical use

The MATLAB implementation of generalized FWBR mainly offers flexibility in model reduction. Balanced reduction, Enns' frequency weighted balanced reduction, and frequency interval balanced reduction are all special cases. The step by step approach with graphical evaluation of the reduction results and graphical input of weighting functions can be used very effectively in deriving stable reduced order models that fit the original model in the intended way. The general experience is that over the whole frequency range a minimal weighting has to be applied to ensure that the reduced order models remain stable. The easiest way to do this is to choose a sufficiently large β in (24). Very small reduction errors at specific frequencies can be obtained with frequency pulse weightings. This can be very practical in retaining system zeros.

7 Conclusion

Generalized frequency weighted balanced reduction (GFWBR) is introduced. It merges Enns' frequency weighted balanced reduction and frequency interval balanced reduction of Gawronski & Juang into one unified framework. New features are the use of scalar *quadratic frequency* functions within *multiple* frequency intervals and the frequency *pulse* weightings. The definition of the weighted Gramians as a sum over separate intervals and separate inputs and outputs allows GFWBR to be implemented in a step by step reduction procedure. Graphical evaluation of the reduction results after each step and graphical input of the weighting functions offer great flexibility in frequency weighted model reduction.

References

Enns, D.F. (1984a). *Model reduction for control system design,* Ph.D. Thesis, Dept. Aeronautics and Astronautics, Stanford University, Stanford, CA, USA.

Enns, D.F. (1984b). Model reduction with balanced realization: an error bound and a frequency weighted generalization. *Proc.* 23^{rd} *Conf. Decision & Control, Las Vegas, USA,* 127–132.

Gawronski, W., and J-N Juang (1990). Model Reduction for Flexible Structures. *Control and Dynamic Systems,* vol.36, 143–222.

Glover, K. (1984). All optimal Hankel-norm approximations of linear multivariable systems and their L_∞-error bounds. *Int. J. Contr.*, vol. 39, 1115–1193.

Moore, B.C. (1981). Principal component analysis in linear systems: controllability, observability, and model reduction. *IEEE Trans. Automat. Contr.*, AC-26, 17–32.

Skelton, R.E. (1988). *Dynamic Systems Control,* New York: John Wiley & Sons.

Wortelboer, P.M.R. (1991). Balanced reduction of high-dimensional mechanical systems: a block-balancing approach. *Proc.* 30^{th} *Conf. Decision & Control, Brighton, UK,* 1974–1975.

Selected Topics in Identification, Modelling and Control
Vol. 5, December 1992

On orthogonal basis functions that contain system dynamics [‡]

Peter Heuberger [§] , Paul Van den Hof [♯] and Okko Bosgra

Mechanical Engineering Systems and Control Group
Delft University of Technology, Mekelweg 2, 2628 CD Delft, The Netherlands.

Abstract. In many areas of signal, system and control theory orthogonal functions play an important role in issues of analysis and design. In this paper it is shown that there exist orthogonal functions that, in a natural way, are generated by stable linear dynamical systems, and that compose an orthonormal basis for the signal space ℓ_2^n. To this end use is made of balanced realizations of inner transfer functions. The orthogonal functions can be considered as generalizations of e.g. the Laguerre functions and the pulse functions, related to the use of the delay operator, and give rise to an alternative series expansion of rational transfer functions. It is shown how we can exploit these generalized basis functions to increase the speed of convergence in a series expansion, i.e. to obtain a good approximation by retaining only a finite number of expansion coefficients.

Keywords. system identification, orthogonal functions, system approximation.

1 Introduction

Consider a finite-dimensional linear time-invariant discrete-time system G, represented by its transfer function $G(z)$ in the Hilbert space $\mathcal{H}_2$, i.e. $G(z)$ is analytic outside the unit circle, $|z| \geq 1$. A general and common representation of $G(z)$ is in terms of its Laurent expansion around $z = \infty$, as

$$G(z) = \sum_{k=0}^{\infty} G_k z^{-k} \qquad (1)$$

with $\{G_k\}_{k=0,1,\ldots}$ the sequence of Markov parameters. In constructing this series expansion we have employed a set of orthogonal functions: $\{z^0, z^{-1}, z^{-2}, \cdots\}$, where orthogonality is considered in terms of the inner product in $\mathcal{H}_2$. In a generalized form we can write (1) as

$$G(z) = \sum_{k=0}^{\infty} L_k f_k(z) \qquad (2)$$

with $\{f_k(z)\}_{k=0,1,2,\ldots}$ a sequence of orthogonal functions.

There are a number of research areas that deal with the question of either approximating a given system G with a finite number of coefficients in a series expansion as in (2), or (approximately) identifying an unknown system in terms of a finite number of expansion coefficients through

$$\hat{G}(z) = \sum_{k=0}^{N} \hat{L}_k f_k(z) \qquad (3)$$

In an identification context, the use of the orthogonal functions as in (1) lead to the so called *Finite Impulse Response* (FIR)-model, Ljung (1987). However, it is well known that for moderately damped systems, and/or in situations of high sampling rates, it may take a large value of N, the

[‡] Part of this work was done while the second author was a visiting researcher at the Centre for Industrial Control Science, The University of Newcastle, N.S.W., Australia.

[§] Now with the National Institute of Public Health and Environmental Protection (RIVM), P.O. Box 1, 3720 BA Bilthoven, The Netherlands.

[♯] Author to whom all correspondence should be addressed.

number coefficients to be estimated, in order to capture the essential dynamics of the system G into its model.

In this paper we consider the problem of constructing orthogonal functions $f_k(z)$ in such a way that a series expansion of the system G, as in (2) becomes very simple, i.e. the number of coefficients L_k that is needed becomes small. In dealing with this problem, we have considered the question whether a linear system in a natural way gives rise to a set of orthogonal functions. The answer to this question appears to be affirmative. It will be shown that every stable system gives rise to a complete set of orthonormal functions based on input (or output) balanced realizations, or equivalently based on a singular value decomposition of a corresponding Hankel matrix.

The use of orthogonal functions with the aim to adapt the system and signal representation to the specific properties of the systems and signals at hand has a long history. The classical work of Lee and Wiener during the 1930's on network synthesis in terms of Laguerre functions is summarized in Lee (1960). During the past decades, the use of orthogonal functions has been studied in problems of e.g. filter synthesis, King and Paraskevopoulos (1977), and system identification, King and Paraskevopoulos (1979), Nurges and Yaaksoo (1981), Nurges (1987). In these approaches to system identification, the input and output signals are transformed to an (Laguerre) transformed domain and standard identification techniques are applied to the signals in this domain. Data reduction has been the main motivation in these studies. In recent years, a renewed interest in Laguerre functions has emerged. The approximation of (infinite dimensional) systems in terms of Laguerre functions has been considered in Mäkilä (1990), Glover *et al.*(1990) and Gu and Khargonekar (1989). In the identification of coefficients in finite length series expansions, Laguerre function representations have been considered from a statistical analysis point of view in Wahlberg (1991). The use of Laguerre-function-based identification in adaptive control and controller tuning is studied in Zervos *et al.*(1988). A second-order extension to the basic Laguerre functions using the so called Kautz functions is subject of discussion in Wahlberg (1990).

In section 3 we will show how inner functions generate two sets of orthonormal functions that are complete in the signal space ℓ_2. Next the interpretation of these results is given in terms of balanced state space representations. After showing the relations of the new basis functions with existing ones, we will focus on the dynamics that implicitly are involved in the inner functions generating the basis. It will be shown that if the dynamics of a stable system match the dynamics of the inner function that generates the basis, then the representation of this system in terms of this basis becomes extremely simple. Consequences for a related identification and approximation problem are discussed in a final section. For the proofs of the results the reader is referred to Heuberger *et al.*(1992).

2 Preliminaries

We will denote $(\cdot)^*$ as the complex conjugate transpose of a matrix, $\mathbf{Z}_+$ as the set of nonnegative integers. $\ell_2[0,\infty)$ is the space of squared summable sequences on the time interval $\mathbf{Z}_+$, $\ell_2^{m\times n}[0,\infty)$ the space of matrix sequences $\{F_k, k=0,1,2,\cdots\}$ such that $\sum_{k=0}^{\infty} tr(F_k^* F_k)$ is finite. $\|\cdot\|_2$ is the induced 2-norm or spectral norm of a matrix, i.e. its maximum singular value. We will consider discrete-time signals and systems. A linear time-invariant finite-dimensional system will be represented by its rational transfer function $G(z) \in \mathbb{R}^{p\times m}(z)$, with m the number of inputs in u, and p the number of outputs in y. (A,B,C,D) is a realization of G if $G(z) = C(zI-A)^{-1}B + D$. A realization is stable if $|\sigma(A)| < 1$, where $\sigma(A)$ is the set of eigenvalues of A. If a realization is stable, the controllability Gramian P and observability Gramian Q are defined as the solutions to the Lyapunov equations $APA^* + BB^* = P$ and $A^*QA + C^*C = Q$ respectively. A stable realization is called (internally) balanced if $P = Q = \Sigma$, with $\Sigma = diag(\sigma_1,\cdots,\sigma_n)$, $\sigma_1 \geq \cdots \geq \sigma_n$, a diagonal matrix with the positive Hankel singular values as diagonal elements. A stable realization is called input balanced if $P = I$, $Q = \Sigma^2$, and output balanced if $P = \Sigma^2$, $Q = I$.

A square system ($p = m$) is called all-pass if it satisfies $G^T(z^{-1})G(z) = I$, or equivalently $G(z)G^T(z^{-1}) = I$. An inner transfer function matrix is an all-pass transfer function that is stable, i.e. it is analytic outside and on the unit circle. When dealing with inner functions in this paper, we will implicitly assume that the inner function G is proper, i.e. it has a Laurent series expansion $\sum_{k=0}^{\infty} G_k z^{-k}$. The (block) Hankel matrix associated with G is denoted by $\mathcal{H}(G)$, and is constructed from the Markov parameters $\{G_k\}_{k=1,2,\cdots}$.

3 Orthonormal functions generated by inner transfer functions

In this section we will show that a square and inner transfer function gives rise to an infinite set of orthonormal functions. This derivation is based on the fact that a singular value decomposition of the Hankel matrix associated to a linear system induces a set of left (right) singular vectors that are orthogonal. Considering the left (right) singular vectors as discrete time functions, they are known to be orthogonal in ℓ_2-sense, thus generating a number of orthogonal functions being equal to the McMillan degree of the corresponding system. We will embed an inner function with McMillan degree n into a sequence of inner functions with McMillan degree kn, for which the left (right) singular vectors of the Hankel matrix span a space with dimension kn. If we let $k \to \infty$ the set of left (right) singular vectors will yield an infinite number of orthonormal functions, which can be shown to be complete in ℓ_2.

The Hankel matrix of an inner transfer function has some specific properties, reflected in the following two results.

Proposition 3.1 *Let $G(z)$ be an inner function with McMillan degree $n > 0$. Then a singular value decomposition (svd) of $\mathcal{H}(G)$ satisfies $\mathcal{H}(G) = U_0 V_0^*$ with $U_0, V_0 \in \mathbf{C}^{\infty \times n}$ unitary matrices, and the pair (U_0, V_0) is unique modulo postmultiplication with a unitary matrix $T \in \mathbf{C}^{n \times n}$.*

Proposition 3.2 *Let $G(z)$ be an inner function, having a Laurent expansion $G(z) = \sum_{k=0}^{\infty} G_k z^{-k}$. Denote the block Toeplitz matrices*

$$T_v = \begin{bmatrix} G_0 & G_1 & G_2 & \cdots & \cdots \\ 0 & G_0 & G_1 & G_2 & \cdots \\ 0 & 0 & G_0 & G_1 & \cdots \\ \vdots & \vdots & 0 & G_0 & \ddots \\ \vdots & \vdots & \vdots & \vdots & \ddots \end{bmatrix} \tag{4}$$

$$T_u = \begin{bmatrix} G_0 & 0 & 0 & \cdots & \cdots \\ G_1 & G_0 & 0 & \cdots & \cdots \\ G_2 & G_1 & G_0 & \ddots & \cdots \\ \vdots & \vdots & G_1 & G_0 & \cdots \\ \vdots & \vdots & \vdots & \ddots & \ddots \end{bmatrix} \tag{5}$$

Then $T_v T_v^T = T_u^T T_u = I$.

Lemma 3.3 *Let $G(z)$ be an inner function with McMillan degree n. Then for all $k \in \mathbf{Z}_+$, $G^k(z)$ is an inner function with McMillan degree kn.* □

Considering Proposition 3.1, it follows that the rows of V_0^*, and the columns of U_0, are n mutually orthonormal vectors of infinite dimension. Additionally Lemma 3.3 shows that we can construct an inner transfer function with increasing McMillan degree, by repeatedly multiplying the transfer function with itself, and thus implicitly creating an increasing number of orthogonal vectors. The following result shows how we can increase this number of vectors, by embedding the svd of $\mathcal{H}(G)$ into a sequence of svd's of $\mathcal{H}(G^k)$.

Theorem 3.4 *Let $G(z)$ be an inner function with McMillan degree $n > 0$. Then*

(a) There exist unitary matrices $U_i, V_i \in \mathbf{C}^{\infty \times n}$, $i = 0, 1, \cdots$, such that for every $0 \neq k \in \mathbf{Z}_+$, the matrices

$$\Gamma_k^o = [\, U_{k-1} \ \cdots \ U_1 \ U_0] \text{ and } \Gamma_k^c = \begin{bmatrix} V_0^* \\ V_1^* \\ \vdots \\ V_{k-1}^* \end{bmatrix} \tag{6}$$

constitute a singular value decomposition of $\mathcal{H}(G^k)$, through $\mathcal{H}(G^k) = \Gamma_k^o \Gamma_k^c$;

(b) Let $G(z)$ have a Laurent expansion $G(z) = \sum_{i=0}^{\infty} G_i z^{-i}$, and consider the block Toeplitz matrices T_u, T_v as in (4), then this matrix sequence $\{U_i, V_i\}_{i=0,1,\cdots}$ satisfies

$$V_k^* = V_{k-1}^* T_v \tag{7}$$

$$U_k = T_u U_{k-1} \qquad \text{for } k = 1, 2, \cdots \tag{8}$$

The theorem shows the construction of orthogonal matrices Γ_k^o, Γ_k^c that have a nesting structure. The suggested svd of $\mathcal{H}(G^k)$ incorporates svd's of $\mathcal{H}(G^i)$ for all $i < k$. In this way orthogonal matrices Γ_k^o and Γ_k^c are constructed with an increasing rank. Note that the restriction on the structure of the consecutive svd's is so strong that, according to (b), given a singular value decomposition $\mathcal{H}(G) = U_0 V_0^*$, the matrix sequence $\{U_i, V_i,\ i = 1, 2, \cdots\}$ is uniquely determined. Note also that there is a clear duality between the controllability part Γ_k^c and the observability part Γ_k^o. In order to keep the exposition and the notation as simple as possible we will further restrict attention to the controllability part of the problem. Dual results exist for the observability part.

Proposition 3.5 *Let $G(z) \in \mathbf{R}^{m \times m}(z)$ be an inner function with McMillan degree $n > 0$, and consider a sequence of unitary matrices $\{V_i\}_{i=0,1,\cdots}$ as*

meant in Theorem 3.4. Denote

$$V_k(z) = \sum_{i=0}^{\infty} M_k(i) z^{-i}, \quad \textit{with } M_k(i) \textit{ defined by}$$
$$V_k^* = [M_k(0)\ M_k(1)\ M_k(2)\ \cdots] \tag{9}$$

and $M_k(i) \in \mathbf{C}^{n\times m}$, $k \in \mathbf{Z}_+$.
Then $V_k(z) = V_0(z)G^k(z)$. □

The proposition actually is a z-transformequivalent of the result in Theorem 3.4. It shows the construction of the controllability matrix Γ_k^c. In the next stage we show that this controllability matrix generates a sequence of orthogonal functions that is complete in ℓ_2^n.

Theorem 3.6 *Let* $G(z) \in \mathbb{R}^{m\times m}(z)$ *be an inner function with McMillan degree* $n > 0$, *such that* $\|G_0\|_2 < 1$; *consider a sequence of unitary matrices* $\{V_i\}_{i=0,1,\cdots}$ *as meant in Theorem 3.4. For each* $k \in \mathbf{Z}_+$ *consider the function* $\phi_k : \mathbf{Z}_+ \to \mathbf{C}^n$, *defined by:*

$$[\phi_k(0)\ \phi_k(1)\ \phi_k(2)\ \cdots] = V_k^*.$$

Then the set of functions $\Psi(G) := \{\phi_k\}_{k=0}^{\infty}$ *constitutes an orthonormal basis of the signal space* $\ell_2^n[0,\infty)$. □

Remark 3.7 *This basis has been derived from the singular value decomposition of the Hankel matrix* $\mathcal{H}(G)$. *As stated in Proposition 3.1 this svd is unique up to postmultiplication of* U_0, V_0 *with a unitary matrix. Consequently - within this context - both* V_k^*, $V_k(z)$ *and the corresponding basis functions* $\{\phi_k\}$ *are unique up to unitary premultiplication.*

For use later on we will formalize two classes of inner functions.

Definition 3.8 *We define the classes of functions:*

$\mathcal{G}_1$:= {*all inner functions* G *with McMillan degree* > 0 *such that* $\|G_0\|_2 < 1$};
$\mathcal{G}_2$:= {*all inner functions* G *with McMillan degree* > 0 *such that* $G_0^*G_0 = G_0G_0^*$}.

As a result of the fact that the proposed orthonormal functions constitute a basis of ℓ_2^n, each square inner function generates an orthonormal basis that provides a unique transformation of ℓ_2^q-signals to an orthogonal domain. Similarly, when given such an orthonormal basis, each stable rational function can be expanded in a series expansion of basis functions $V_k(z)$ as defined in proposition 3.5.

Corollary 3.9 *Let* G *be an inner function,* $G \in \mathcal{G}_1$, *and let* $\Psi(G)$ *be as defined in theorem 3.6. Then for every proper stable transfer function* $H(z) \in \mathbb{R}^{p\times m}(z)$ *there exist unique* $D \in \mathbb{R}^{p\times m}$, *and* $L = \{L_k\}_{k=0,1,\cdots} \in \ell_2^{p\times n}[0,\infty)$, *such that*

$$H(z) = D + z^{-1}\sum_{k=0}^{\infty} L_k V_k(z) \tag{10}$$

We refer to D, L_k *as the orthogonal expansion coefficients of* $H(z)$. □

We will refer to the sequence $\{V_k(z)\}_{k=0,1,\cdots}$ as the sequence of generating transfer functions for the orthonormal basis $\Psi(G)$. In order to find appropriate ways to calculate the orthogonal functions, as well as to determine the transformation as meant in the corollary, we will now first analyse the results presented so far in terms of state space realizations.

4 Balanced state space representations

In order to represent the orthogonal controllability matrix in a state space form, we will use a balanced state space realization of G.

Proposition 4.1 *Let* G *be a transfer function with minimum balanced realization* (A,B,C,D), *Then* $G(z)G^T(z^{-1}) = I$ *if and only if (i)* $P = Q = I$; *(ii)* $BD^* + AC^* = 0$, *and (iii)* $DD^* + CC^* = I$. □

Note that for this proposition there also exists a dual form, concerning the transfer function G^T with realization (A^*, C^*, B^*, D^*). The class of functions $\mathcal{G}_1$ can simply be characterized in terms of a balanced realization.

Proposition 4.2 *Let* $G \in \mathbb{R}^{m\times m}(z)$ *be an inner function with minimal balanced realization* (A,B,C,D). *Then* $G \in \mathcal{G}_1$ *if and only if rank* $B = m$, *or equivalently rank* $C = m$.

The following proposition shows that we can use a balanced realization of G to construct a balanced realization for any power of G.

Proposition 4.3 *Let* G *be an inner transfer function with minimal balanced realization* (A,B,C,D) *having state dimension* $n > 0$. *Then for any* $k > 1$ *the realization* (A_k, B_k, C_k, D_k) *with*

$$A_k = \begin{bmatrix} A & 0 & \cdots & \cdot & 0 \\ BC & A & 0 & \cdot & 0 \\ BDC & BC & \cdot & \cdot & 0 \\ \vdots & \vdots & \cdot & \ddots & 0 \\ BD^{k-2}C & BD^{k-1}C & \cdots & BC & A \end{bmatrix} \tag{11}$$

$$B_k = \begin{bmatrix} B \\ BD \\ BD^2 \\ \vdots \\ BD^{k-1} \end{bmatrix} \quad (12)$$

$$C_k = \begin{bmatrix} D^{k-1}C & D^{k-2}C & \cdots & D^2C & DC & C \end{bmatrix} \quad (13)$$

$$D_k = D^k \quad (14)$$

is a minimal balanced realization of G^k with state dimension $n \cdot k$. □

Examining the realization in the above proposition, reveals a similar structure of observability and controllability matrices, as has been discussed in the previous section. E.g. taking the situation $k = 2$, it shows that the controllability matrix of (A_2, B_2) contains the controllability matrix of (A, B) as its first block row.

Proposition 4.4 *Let $G(z) \in \mathbb{R}^{m\times m}(z)$ be an inner transfer function with McMillan degree $n > 0$, whose Hankel matrix has an svd $\mathcal{H}(G) = U_0 V_0^*$, and let (A, B, C, D) be a minimal balanced realization of G such that $V_0^* = [B\ AB\ A^2B\ \cdots]$. Then the unique sequence of orthogonal matrices $\{\Gamma_k^c\}_{k=1,2,\cdots}$ as meant in theorem 3.4 is determined by*

$$\Gamma_k^c = [B_k\ A_kB_k\ A_k^2B_k\ \cdots] \quad (15)$$

with A_k, B_k as defined in (12). □

The above result shows how a minimal balanced realization of G actually generates the sequence of orthogonal matrices Γ_k^c, the rows of which are the basis functions in our orthonormal basis of ℓ_2^n. For inner functions in $\mathcal{G}_2$ specific properties in terms of their balanced state space representation can be derived.

Proposition 4.5 *Let $G \in \mathbb{R}^{m\times m}(z)$ be an inner function with minimal balanced realization (A, B, C, D). Then $G \in \mathcal{G}_2$ if and only if there exists a unitary matrix R such that $C = B^*R$.* □.

There exist recursive formulae for constructing the orthogonal functions.

Proposition 4.6 *Let G be an inner function, $G \in (\mathcal{G}_1 \cap \mathcal{G}_2)$, and consider the assumptions and notation as in Theorem 3.4 and Proposition 4.4. Denote $X = BC$, and $P = -RA^*$, with R according to Proposition 4.5. Then*

(a) the elements of Γ_k^c are determined by the following recursive equations

$$\begin{aligned} M_0(0) &= B \\ M_k(i+1) &= AM_k(i) + \sum_{j=1}^{k} P^{j-1}XM_{k-j}(i) \\ M_k(0) &= PM_{k-1}(0) \end{aligned}$$

with Γ_k^c as in (6) *and* (9).

(b) Γ_k^c is unique, i.e. it is not dependent on the specific choice of R in case R is nonunique. □

The recursive equations show how we can simply construct the set of orthogonal functions. We now come to the construction of a series expansion of any stable proper rational transfer function, in terms of the new orthonormal basis.

Theorem 4.7 *Let G be an inner function $G \in (\mathcal{G}_1 \cap \mathcal{G}_2)$ with a minimal balanced realization (A, B, C, D). Let this inner function generate an orthonormal basis with corresponding generating functions $V_k(z)$, as defined in Proposition 3.5. Let $H \in \mathbb{R}^{p\times m}(z)$ be any proper and stable transfer function with a minimal realization (A_s, B_s, C_s, D_s). Then*

$$H(z) = D_s + z^{-1}\sum_{k=0}^{\infty} L_kV_k(z) \quad (16)$$

with $L_k \in \mathbf{C}^{p\times n}$ determined by:

$$\begin{aligned} L_k &= C_sQ_k & (17)\\ Q_0 &= A_sQ_0A^* + B_sB^* & (18)\\ Q_{i+1} &= A_sQ_{i+1}A^* + A_sQ_iR^* - Q_iAR^* & (19) \end{aligned}$$

In section 6 we will show that specific choices of $G(z)$ in relation with $H(z)$, i.e. specific relations between the inner function G producing the orthonormal basis and a transfer function H that should be described in this basis, will lead to very simple representations.

5 A generalization of classical basis functions

In this section we show two examples of well known sets of orthogonal functions that are frequently used in the description of linear time-invariant dynamical systems, and that occur as special cases in the framework that is discussed in this paper.

Pulse functions

Consider the inner function $G(z) = z^{-1}$, $G \in \mathcal{G}_1$. The Hankel matrix of G satisfies:

$$\mathcal{H}(G) = \begin{bmatrix} 1 & 0 & \cdots & \cdot & 0 \\ 0 & 0 & 0 & \cdot & 0 \\ 0 & 0 & 0 & \cdot & 0 \\ \vdots & \vdots & \cdot & \ddots & \cdot \end{bmatrix} = \begin{bmatrix} 1 \\ 0 \\ 0 \\ \vdots \end{bmatrix} \begin{bmatrix} 1 & 0 & \cdots \end{bmatrix}$$
$$= U_0 V_0^* \qquad (20)$$

As a result $V_0(z) = 1$, and with proposition 3.5 the generating transfer functions $V_k(z)$ satisfy $V_k(z) = G^k(z) = z^{-k}$, $k = 0, 1, \cdots$. The corresponding set of basis functions $\Psi(G)$ is determined by $\phi_k(t) = \delta(t-k)$ with $\delta(\tau)$ the Kronecker delta function.
The inner function G can be realized by the minimal balanced realization $(A, B, C, D) = (0, 1, 1, 0)$, showing that $DD^* = D^*D$ and so $G \in \mathcal{G}_2$. Applying theorem 4.7 with $R = 1$ shows the classical result that $L_k = C_s A_s^k B_s$.

Laguerre functions

Consider the inner function $G(z) = \dfrac{1-az}{z-a}$, with some real-valued a, $|a| < 1$, and denote $\eta = 1 - a^2$. Since $G_0 = -a$ it is clear that $G \in (\mathcal{G}_1 \cap \mathcal{G}_2)$.
A minimal balanced realization of G is given by $(A, B, C, D) = (a, \sqrt{\eta}, \sqrt{\eta}, -a)$, leading to $R = 1$. Application of Proposition 4.6 gives $X = \eta$, $P = -a$, and taking account of the fact that for one-dimensional scalar G, $M_k(i) = \phi_k(i)$, it follows that

$$\begin{aligned} \phi_0(0) &= \sqrt{\eta} \\ \phi_k(i+1) &= a\phi_k(i) + \eta \sum_{j=1}^{k} (-a)^{j-1} \phi_{k-j}(i) \\ \phi_k(0) &= -a\phi_{k-1}(0) \end{aligned}$$

These equations exactly match the equations that generate the normalized discrete-time Laguerre polynomials with discount factor a (Nurges and Yaaksoo, 1981).
The corresponding generating transfer functions $V_k(z)$ can be analysed with the result of proposition 3.5:

$$V_k(z) = \sqrt{\eta} z \frac{(1-az)^k}{(z-a)^{k+1}} \qquad (21)$$

This exactly fits with the formulation of the generating transfer functions of discrete-time Laguerre polynomials in e.g. King and Paraskevopoulos (1979).

6 Orthonormal functions originating from general dynamical systems

We have shown that any square inner transfer function $G \in \mathcal{G}_1$ generates an orthonormal basis for the signal space ℓ_s^n. One of the reasons for developing this generalized bases was to find out whether we can yield a more suitable representation of a general dynamical system, when the basis within which we describe the system is more or less adapted to the system dynamics. In view of the results presented so far, this aspect relates to the question whether we can construct an inner transfer function generating a basis, that incorporates dynamics of a general system to be represented within this basis.
There are several ways of connecting general transfer functions to inner functions, as e.g. inner/outer factorization (Francis, 1987), normalized coprime factorization (Vidyasagar, 1985), or inner-unstable factorization (Baratchart and Olivi, 1991). In this paper we will explore a different connection, where a general stable dynamical system with input balanced realization $(A, B, \tilde{C}, \tilde{D})$ will induce a inner function through retaining the matrices (A, B) and constructing (C, D) such that (A, B, C, D) is inner. This implies that the poles of the stable dynamical system are retained in the corresponding inner function.

Proposition 6.1 *Let $H \in \mathbb{R}^{p\times m}(z)$ be a proper stable transfer function, with input balanced realization $(A, B, \tilde{C}, \tilde{D})$ having state dimension $n > 0$. Then*

(a) there exist matrices C, D such that (A, B, C, D) is a minimal balanced realization of an inner function G;

(b) This G satisfies $G \in \mathcal{G}_2$ if and only if (i) $C = B^*R$, (ii) $BD^* + AC^* = 0$ and (iii) $D^*D + B^*B = I$, with $R = UV^*$, and U, V any square unitary matrices such that $A = USV^*$ is an svd of A. □

In the proposition all inner functions in $\mathcal{G}_1 \cap \mathcal{G}_2$ are characterized that can be constructed in the way as decribed above, by retaining the matrices (A, B) of any given stable system. Note that the extension with C, D is not necessarily unique. For an analysis of this see Heuberger *et al.*(1992).
We will now present a result that is very appealing. It shows that when we want to describe the dynamical system H in terms of the basis that it has generated, as presented in Proposition 6.1, then

the series expansion in the new orthogonal basis becomes extremely simple.

Theorem 6.2 *Let $H \in \mathbb{R}^{p\times m}(z)$ be a proper stable transfer function, with input balanced realization (A_s, B_s, C_s, D_s), having all controllability indices > 0. Let $G \in \mathcal{G}_1$ be an inner function with minimal balanced realization (A, B, C, D) such that $A = A_s$ and $B = B_s$, generating an orthonormal basis with generating transfer functions $V_k(z)$. Then*

$$H(z) = D_s + z^{-1}\sum_{k=0}^{\infty} L_k V_k(z) \qquad (22)$$

with $L_0 = C_s$ and $L_k = 0$ for $k > 0$. □

The theorem shows that when we use a general stable and proper dynamical system to generate an orthonormal basis as described above, then the system itself has a very simple representation in terms of this basis. It is represented in a series expansion with only two nonzero expansion coefficients, being equal to the system matrices C_s and D_s. In the next section we will discuss the results of this paper in regard of their relevance to problems of system identification and system approximation.

It has to be stressed that so far, we have only used the generalized orthonormal basis to study the series expansion of a given stable transfer function. Similar to the case of the pulse functions and Laguerre functions, the presented generalized functions induce a transformation of ℓ_2-signals to a transform domain, compare e.g. with the z-domain when pulse functions are used. In the transform domain dynamical system equations can be derived, leading to transform pairs of time-domain and orthogonal-domain system representations (Heuberger and Bosgra, 1990; Heuberger, 1991).

7 Identification and System Approximation

We will now take a look at the question how we can utilize the results to problems of identification and system approximation. As mentioned in the introduction, identification of a finite impulse model (FIR) fails to be successful when the number of coefficients to be estimated becomes large. An alternative way to attain the advantages of this identification method, is to exploit the model structure

$$y(t) = D(\theta) + \sum_{k=0}^{N-1} L_k(\theta) V_k(q) u(t) + \varepsilon(t) \qquad (23)$$

where $\varepsilon(t)$ is the one step ahead prediction error, $D(\theta), L_k(\theta)$ the parametrized expansion coefficients, and with $V_k(z)$ representing an appropriately chosen basis.
Identifying θ through least squares optimization of $\varepsilon(t)$ over the time interval, is a similar problem as in the case of an FIR-model. However, with appropriately chosen basis functions, the convergence rate of the series expansion can become extremely fast, i.e. the number of coefficients to be estimated can become very small. Note that the result of Theorem 6.2 shows an ultimate result of only two expansion coefficients that are nonzero.

There is another point of interest, being the a priori knowledge that very often is available in an identification situation. Very often the experimenter has a -rough- knowledge about the dynamics of the system under consideration, and it would be favourable to exploit this knowledge in the identification procedure. The method suggested above, shows that this a priori knowledge can be exploited in terms of the basis functions that are chosen. The more precise the a priori knowledge is, the better we can adapt the basis functions to the system dynamics, and the simpler will become the identification problem; the latter effect, due to the smaller number of expansion coefficients that essentially contribute to the expression (23).
In order to justify this identification/approximation method we will present some results showing that the speed of convergence in an orthogonal series expansion can be quantified, showing the increase of speed as the dynamics of system and basis approach eachother.

Theorem 7.1 *Let $H(z) \in \mathbb{R}^{p\times 1}(z)$ be a proper stable transfer function with an input balanced realization (A_s, B_s, C_s, D_s), and let (A, B) be an input balanced pair that generates an inner transfer function $G \in \mathbb{R}(z)$ with $G \in (\mathcal{G}_1 \cap \mathcal{G}_2)$, leading to an orthonormal basis $\Psi(G)$. Let*
μ_i, $i = 1, \cdots, n_s$ denote the eigenvalues of A_s, and ρ_j, $j = 1, \cdots, n$ denote the eigenvalues of A.

and denote $|\lambda_i| = \prod_{j=1}^{n} \left| \frac{\mu_i - \rho_j}{1 - \mu_i \rho_j} \right|$ and $\lambda := \max_i |\lambda_i|$.

Then for any $\eta \in \mathbb{R}$, $\eta > \lambda$, there exists a finite $c \in \mathbb{R}$ such that

$$\|H(z) - \hat{H}^N(z)\|_\infty \leq c\frac{\eta^{N+1}}{1-\eta} \qquad (24)$$

with $\hat{H}^N(z) = D + z^{-1}\sum_{k=0}^{N-1} L_k V_k(z)$ □

The above theorem shows that we can draw conclusions on the convergence rate of the sequence

of expansion coefficients $\{L_k\}_{k=0,\cdots}$, when given the eigenvalues of the original system $H(z)$ and the eigenvalues of the inner function $G(z)$ that generates the basis. Note that when the sets of eigenvalues $\{\mu_i\}$, $\{\rho_j\}$ coincide, then $\lambda_i = 0$, for all i. Since λ is a measure for the "closeness" of system dynamics and basis dynamics, the above theorem shows that the error that is made when neglecting the tail of a series expansion, becomes smaller as λ becomes smaller.

Conclusions

We have developed a theory on orthogonal functions as basis functions for general linear time-invariant stable systems. The basic ingredient is that every square inner transfer function in a very natural way induces two sets of orthogonal functions that form a basis of the signal space ℓ_2. The ordinary pulse functions and the classical Laguerre polynomials are special cases in this theory of inner functions.

With this concept it follows that any connection between a linear system and an inner function, e.g. through inner/outer factorization, normalized coprime factorization, leads to bases of specific system based orthonormal functions. In this paper we have explored a factorization in which the poles of the system determine the inner factor. An important property of the resulting orthonormal functions is that they - to some extent - incorporate the dynamic behavior of the underlying system, leading to an increasing speed of convergence in a series expansion.

References

Baratchart, L. and M. Olivi (1991). Inner-unstable factorization of stable rational transfer functions. In G.B. DiMasi, A. Gombani and A.B. Kurzhanski (Eds.), *Modeling, Estimation and Control of Systems with Uncertainty*, Birkhäuser Verlag, Boston, MA, pp. 22-39.

Francis, B.A. (1987). *A Course in H_∞ Control Theory.* Lecture Notes in Contr. Inform. Sc., vol. 88, Springer Verlag, Berlin.

Glover, K., J. Lam and J.R. Partington (1990). Rational approximation of a class of infinite-dimensional systems. I. Singular values of Hankel operators. *Mathem. of Control Signals and Systems, vol. 3*, no. 4, pp. 325-344.

Gu, G., P.P. Khargonekar and E.B. Lee (1989). Approximation of infinite-dimensional systems. *IEEE Trans. Autom. Contr., vol. AC- 34*, no. 6, pp. 610-618.

Heuberger, P.S.C. and O.H. Bosgra (1990). Approximate system identification using system based orthonormal functions. *Proc. 29th IEEE Conf. Decision and Control*, Honolulu, HI, December 1990, pp. 1086-1092.

Heuberger, P.S.C. (1991). *On Approximate System Identification with System Based Orthonormal Functions.* Dr. Dissertation, Delft University of Technology, The Netherlands, 1991.

Heuberger, P.S.C., P.M.J. Van den Hof and O.H. Bosgra (1992). *A Generalized Orthonormal Basis for Linear Dynamical Systems.* Report N-404, Mech. Eng. Systems and Control Group, Delft Univ. Techn., October 1992.

King, R.E. and P.N. Paraskevopoulos (1977). Digital Laguerre filters. *Int. J. Circuit Theory and Appl., 5*, pp. 81-91.

King, R.E. and P.N. Paraskevopoulos (1979). Parametric identification of discrete time SISO systems. *Int. J. Control, 30*, 1023-1029.

Lee, Y.W. (1960). *Statistical Theory of Communication.* John Wiley & Sons, Inc., New York, NY.

Ljung, L. (1987). *System Identification - Theory for the User.* Prentice Hall, Englewood Cliffs, NJ.

Mäkilä, P.M. (1990). Approximation of stable systems by Laguerre filters. *Automatica, 26*, pp. 333-345.

Nurges, Y. (1987). Laguerre models in problems of approximation and identification of discrete systems. *Autom. and Remote Contr., 48*, 346-352.

Nurges, Y. and Y. Yaaksoo (1981). Laguerre state equations for a multivariable discrete system. *Autom. and Remote Contr., 42*, 1601-1603.

Vidyasagar, M. (1985). *Control Systems Synthesis: A Factorization Approach.* MIT Press.

Wahlberg, B. (1990). On the use of orthogonalized exponentials in system identification. Report LiTH-ISY-1099, Dept. Electr. Eng., Linköping University, Sweden.

Wahlberg, B. (1991). System identification using Laguerre models. *IEEE Trans. Automat. Contr., 36*, 551-562.

Zervos, C., P.R. Bélanger and G.A. Dumont (1988). On PID controller tuning using orthonormal series identification. *Automatica, 24*, 2, pp. 165-175.

Selected Topics in Identification, Modelling and Control
Vol. 5, December 1992

Partial validation of a flexible wind turbine model ‡

Gregor E. van Baars and Peter M.M. Bongers

Mechanical Engineering Systems and Control Group
Delft University of Technology, Mekelweg 2, 2628 CD Delft, The Netherlands.

Abstract. In this paper validation results of a flexible wind turbine model are presented. The paper starts with the description of a modular structured theoretical model for flexible wind turbines. Such a model can contribute essentially when designing wind turbine systems that have to behave properly at low construction costs. Experiments on a real life wind turbine system have been performed to obtain experimental models which can serve for validation of parts of the theoretical model. System identification techniques have been used to find the input-output relations in the experimental data. Because the wind plays an important role in the behavior of the system an independently parametrized stochastic part of the experimental models is needed to obtain accurate models. Considering step responses the theoretical model predicts approximately the same outputs as the experimental model. Hence the theoretical model can be used to describe this part of the wind turbine behaviour.

Keywords. Experimental modelling, wind power plants, System identification, Validation

1 Introduction

Wind turbine systems, or wind energy conversion systems (WECS), are developed in order to utilize, in some way, the energy present in the wind. In most cases this energy source is exploited to produce electrical power and feed it into the public grid. At this moment the efficiency of this conversion can not compete completely with the price of electrical power generated using fossile fuels. This can be improved by reduction of construction costs, achieving a long life time of the construction, and highly efficient conversion of wind power. Such improvement is needed to achieve a significant contribution of wind generated power to public demand of electical power. This is a desirable goal because the environmental aspects, which are expected to become more important in the future, compare favourably with conventional power plants.

It is expected that low cost WECS can be developed if *flexibility* is allowed in the different subsystems that compose the complete wind turbine system (Bongers *et al.* (1990)). Examples are: flexible blades in the rotor, shafts with low torsional stiffness in the transmission, and electrical conversion systems that can buffer energy before feeding it into the grid. The design should also aim at long life time. This is directly related to fatigue which can also be reduced when flexible components are used.

As a consequence of these flexibilities the dynamic behavior will become more complex. This poses a more complicated *design* and *control* problem for a flexible wind turbine compared to conventional rigid wind turbines. Such a design must be carried out very carefully otherwise the benefits of applying flexible components will be lost or even reversed. The control design pursues optimal energy production without an excess of mechanical

‡This research was supported by the CEC under grant JOUR-0110 and the Netherlands agency for energy and environment under grant 40.35-001.10

loads, to maintain a reasonable operational life of the wind turbine. Therefore the design of well controlled flexible wind turbines seems to be attractive for commercial applications.
To solve these design problems an accurate *model* describing the relevant dynamics of the complete wind turbine is necessary in the design phase of a well controlled flexible wind turbine system.
There is an abundance of publications concerning dynamic models of wind turbines. Typical aero-elastic rotor models are for example found in (Kirchgasner (1986)), typical models describing mainly the rotating machinery are for example found in Mattson (1984), Steinbuch (1989). Often these models more or less concentrate on one component of the wind turbine system using simplified descriptions of the other turbine parts. In Bongers *et al.* (1990) an *integrated* dynamic model of a flexible wind turbine is presented which takes into account both the aero-elastic rotor parts as well as the rotating machinery. Models of this kind are scarce and only have been developed recently.
For these models to produce reliable predictions they need to be *validated* with respect to their dynamics for different configurations. Some of these dynamic models have been partly validated by quasi-stationairy measurements. A model of a rigid wind turbine described in Bongers *et al.* (1989) is also validated with respect to its dynamics. The integrated dynamic model has not been validated with measurements yet.
This paper describes the first steps made in investigating the validity of this theoretical model. These steps include the estimation of experimental models by means of black box system identification. In the field of wind energy research this technique has only been applied rarely, but in helicopter and flight dynamics testing it has been succesfully used in many cases. For example the identification of helicopter rotor dynamics has been succesfully performed by Tischler (1986) and Du Val *et al.* (1989) .
Validation obviously requires an experimental site. The UNIWEX experimental wind turbine offers the possibility to emulate a large set of (flexible) wind turbine configurations (Müller (1989)) . The benefits of this experimental wind turbine lie in the fact that there are no hardware changes involved when switching between different configurations.
As stated earlier it is expected that the application of components with flexible characteristics will introduce a more complex dynamic behavior. The validation procedure should therefore cover more phenomena, and a more detailed examination of particular phenomena that did not play a role in the rigid case. In order to be valid for a diversity of flexible configurations the dynamics should be examined over a range of flexibilities. Therefore one may expect the amount of work related to the validation to be a great deal more in comparison to the dynamically more simple case of a rigid system.
In this paper the validation procedure for the most rigid configuration will be dealt with first. If this validation turns out to be successfull some confidence about the more flexible configurations will be justified.

The layout of this paper is as follows: Section 2 presents a description of the UNIWEX experimental wind turbine. Both the theoretical model as well as the experimental model structure of the wind turbine are discussed. In Section 3 preliminary results are presented, which consist of the identification experiments and the validation results of the integrated dynamic wind turbine model. The paper is ends with conclusions in Section 4.

2 Wind turbine description

In this section various descriptions of the UNIWEX experimental wind turbine are presented. First some details about the UNIWEX wind turbine itself will be given. After that the dynamics of the wind turbine will be approximated by an integrated model derived by laws of first principles. This model will be referred to as the theoretical model. Finally a procedure to approximate the dynamics by means of system identification on measurement data is discussed. This procedure will provide experimental models.

UNIWEX experimental wind turbine

The UNIWEX experimental wind turbine Fig. 1 is located near the city of Stuttgart, Germany. It is operated by the Institute for Computer Applications of the University of Stuttgart. The construction of the UNIWEX turbine can be seen as a series of linked rigid bodies which are : the two rotor blades, the tower and hub connected to each other by joints. Hydraulic cylinders are mounted across these joints and act like virtual springs and dampers. By adjusting the joint characteristics a family of flexible wind turbines can be emulated without hardware manipulations that could consume considerable time and financial effort.
The blades, with a length of $8m$ and a weigth of $75kg$, are mounted to the hub by a three degrees of freedom joint allowing the blades to hinge in plane

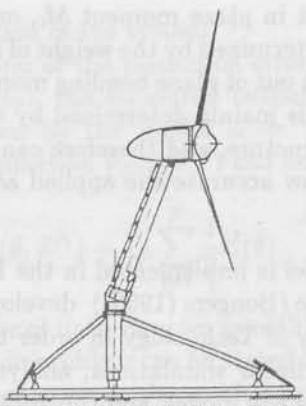

Fig. 1: drawing of UNIWEX wind turbine

of rotation (*lead-lag*), out of plane (*flap*), and rotate around their own axis (*pitch*). This rotor system is able to emulate almost every two bladed rotor concept known for horizontal axis wind energy conversion systems (rigid, flexible flap and/or lead-lag, teeter). Changes between concepts can be executed within a short time span because only software parameter adjustments are needed. This can save a considerable amount of time and effort and can thereby make fluent measurement sessions possible. The parameter values themselves can also vary over a reasonable range. For example the flexible flap rotor stiffness can vary between almost rigid to extremely flexible. Hereby it is possible to test a sequence of different rotor systems exposed to approximately the same wind regime. In that case differences in dynamic behavior probably can be identified in a more decisive way.

The nacelle is mounted to the tower ($height \approx 15m$) with a 2 degrees of freedom joint allowing the nacelle to rotate in the horizontal plane (*yaw*), and in the vertical plane (*tilt*). The tower is mounted to the ground by a 2 degrees of freedom joint allowing tower bending in one direction and rotation around its axis.

The rotor system converts the absorbed wind energy to mechanical energy and the transmission increases the rotational speed to a value that is suitable for the generator.

The UNIWEX turbine is not grid connected and has no electrical conversion system. Instead, a hydraulic pump is used to dissipate the mechanical energy of the rotoating shafts into heat. This pump can be controlled to have different torque-rotational speed characteristics. This opens the possibility to operate the turbine in such a way that the pump behaves globally corresponding to electrical conversion systems usually applied in grid-connected wind turbine systems. Thereby the dynamic behavior of one turbine with different conversion systems can be studied without the financial investments to actually buy these systems, and without losing time needed to mount and dismount them on the turbine.

Theoretical model

In this part we will introduce a model describing the dynamic behaviour of a wind turbine. The complete model consists of a description of each of the wind turbine parts in separate modules and mutual connections between these modules by interaction variables. This modular structure of wind turbine modelling together with the interaction variables can provide an appropriate way of describing different wind turbine configurations (Bongers *et al.* (1990), Steinbuch (1989)). If, for example, the impact of changes in the transmission is of interest, only this module has to be changed or a new transmission module can be linked to the other parts of the complete model.

Here we will apply this modelling approach to describe the dynamic behaviour of the UNIWEX turbine. As stated in Section 1 we consider the most rigid configuration first. Fig. 2 is a schematic representation of the UNIWEX wind turbine. The

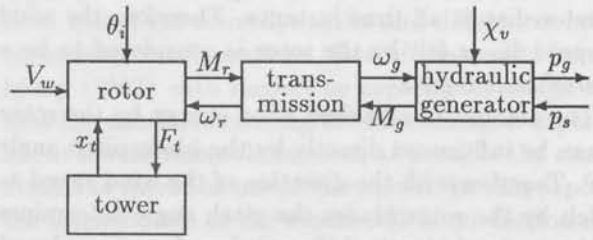

Fig. 2: Block scheme of UNIWEX turbine

mathematical model of this wind turbine consists of the interconnection of submodels having the following characteristics:

The **rotor** has two blades, without flexibility in the joints. Only pitch angle movements were allowed by the controller. The complete rotor system has additional freedom in yaw and tilt directions. The equations of motion are derived using Kane's method as described in Kane and Levinson (1985) .

The aerodynamic behavior of the rotor is described as follows. Each blade is divided into 10 sections, each section has its own corde, mass, twist and profile. The local wind velocity depends on wind shear

(i.e. variations of wind speed with height), the wake of the wind turbine and the velocity of the blades. Based on the local wind velocity and angle of inflow of each section the aerodynamic forces are calculated using the blade element theory (Glauert (1959)) . The UNIWEX wind turbine operates in down wind position. This means that wind passes the tower first before meeting the rotor disc, so there will be a significant tower wake. The rotor system is mounted on a rigid **tower** so no flexibility in the tower system is assumed. Torsional movements in the **transmission** are described by the first torsional mode of the rotor shaft. The dynamics of the **hydraulic generator** are not known in detail. In the model it is described by a spring characteristic.

The block scheme Fig. 2 shows various signals going in and coming out of the modules just described above. Out of these signals the following input and output signals have been defined for the complete wind turbine system.

input signals:

The wind speed obviously is the driving input of the wind turbine system. But unfortunately it is not a controllable input. Besides that it is impossible to measure the wind speed over the complete rotor disc at all time instants. Therefore the wind speed V_w as felt by the rotor is considered to be a *stochastic* input.
The amount of absorbed wind energy by the rotor can be influenced directly by the blade pitch angle θ. Together with the direction of the wind speed as felt by the rotor blades the pitch angle determines the angle of attack. Lift and drag forces produced by each blade element are functions of this angle. For the UNIWEX turbine the pitch angle of the blades can be controlled and therefore can be seen as the first *deterministic* input.
The counter torque M_g generated by the hydraulic generator can be adjusted by manipulating the valve position χ_v which is the second *deterministic* input.

output signals:

In order to gain insight in the dynamic behaviour of the wind turbine the following outputs are measured. The rotor shaft speed ω_r, and the rotor shaft torque M_r. These are important output variables when the overall behavior of the complete system is considered.
Other output signals are the following two. The blade root in plane moment M_l, or lag moment,is mainly determined by the weight of the blades. The blade root out of plane bending moment M_f, or flap moment, is mainly determined by the wind thrust on the structure, and therefore can give an indication of how accurate the applied aerodynamic formulas are.

This model is implemented in the DUWECS computer code (Bongers (1990)) developed at the Delft University of Technology in order to perform nonlinear or linear simulations, analysis of linearized versions of the model, and controller design.

Experimental model

This section introduces the system identification technique which is used to obtain linear experimental models known as the prediction error method (Ljung (1987)) because it has proven to be successful. Based on prior experiments with a rigid wind turbine (Bongers *et al.* (1989)) we assume that the measured data can be explained by the following Box-Jenkins model structure:

$$\hat{y}_t = \frac{\hat{B}(q^{-1},\theta)}{\hat{F}(q^{-1},\theta)}u_t + \frac{\hat{C}(q^{-1},\theta)}{\hat{D}(q^{-1},\theta)}e_t \qquad (1)$$

with:

θ parameter vector	$\hat{y}_t$ predicted output at time t
u_t input at time t	e_t white noise
q^{-1} backward shift operator	

$B(q^{-1},\theta), C(q^{-1},\theta), D(q^{-1},\theta), F(q^{-1},\theta)$ are polynominals in the backward shift operator q^{-1} with unknown coefficients that are lined up in the parameter vector θ. Based on measurements of the system inputs and outputs these parameters have to be estimated. The deterministic part, in this model structure $\frac{\hat{B}(q^{-1},\theta)}{\hat{F}(q^{-1},\theta)}$, describes the influence which the deterministic input has on the output. The stochastic part $\frac{\hat{C}(q^{-1},\theta)}{\hat{D}(q^{-1},\theta)}$ models the way in which noise affects the system. For an accurate experimental model of a wind turbine system a parametrized stochastic part will be necessary because the stochastic input (mainly the wind velocity) is expected to have a complicated dynamic impact on the system output. Furthermore the wind velocity itself can not be represented by white noise (van Baars (1991)).
This model structure has the important advantage that the deterministic transfer function $\frac{\hat{B}(q^{-1},\theta)}{\hat{F}(q^{-1},\theta)}$ can be estimated consistently even when the noise model set is not rich enough to admit a completely

correct description of the system.
Using a definition of the prediction error ϵ_t as the difference between the measured output and the output predicted by the model $\epsilon_t = y_t - \hat{y}_t$ a quadratic cost function $V_N(\theta, Z^N)$ can be defined:

$$V_N(\theta, Z^N) = \frac{1}{N} \sum_{t=1}^{N} \frac{1}{2} \epsilon_t^2(\theta) \qquad (2)$$

N is the number of data samples available.
The identification problem can be stated as follows. Find the parameter vector $\hat{\theta}_N$, guided by the measured data Z^N, such that the criterium (2) is minimized:

$$\hat{\theta}_N = \arg\min V_N(\theta, Z^N) \qquad (3)$$

In case of the used Box-Jenkins model structure the minimization problem has no analytic solution. The minimizing solution has to be found in an iterative way.

3 Identification and validation results

In this section results obtained from system identification on the measured wind turbine data as well as validation results are presented.
The organization of this section is as follows: First the approach of the identification and validation is sketched. Next the identification experiment is described, followed by the identification results obtained from the measured data. At the end of the section first validation results are discussed.

The approach is to measure the same wind turbine configuration exposed to different average wind speeds applying the same input signal. Each average wind speed defines a different point of operation. Based on the measurements we want to identify reliable experimental models for those points of operation seperately.
The theoretical model introduced in Section 2 is linearized in the same points of operation as the experiments. The validation consists of the comparison between the experimental model and the theoretical model for each point of operation covered by the experiments.
If this turns out to be succesful the validation holds not only for a single point of operation, but pointwise over the whole operational range of the wind turbine system. Obviously this is a far more powerful result than partial validation in a single point of operation.
As a start this paper discusses only validation in one point of operation by looking at step responses of both experimental and theoretical model. Since this is only the beginning of the validation the evaluation of stepresponses can provide an global idea of how the dynamics of both models compare to each other. If results turn out to be encouraging more detailed validation can be pursued.

Identification experiment

There was practically no a priori information about the UNIWEX turbine, hence detailed experiment design could not be performed. The possibility to measure the turbine with the desired average wind speed depends of course on the presence of such wind speeds at the time experiments can be performed. Since the wind speed cannot be controlled this means that the point of operation of the experiments cannot be dictated and one possibly has to wait until the suitable average wind speed occurs (this can take weeks or months). In practice measurements were recorded with the wind velocity available at that time.
Out of the system input and output relations of interest (discussed in Section 2) we will first investigate the transfer function from blade pitch angle θ to rotor speed ω_r and rotor shaft torque M_r. Because the blade pitch angle directly influences the rotor system it is expected that these transfer functions reveal the rotor dynamics and differences between rotor configurations. One of the results from Ljung (1987) with respect to experiment design is that the conditions during the identification experiment should resemble as much as possible the conditions of intended use of the model. In this paper the intended use of the model will be prediction of open loop dynamical behavior in order to validate the theoretical model. Therefore open loop experiments are preferable.
Feedback of the system outputs has been disabled which means that open loop experimental conditions have been created.
Using the experimental wind turbine some identification experiments were performed. During a series of experiments the set point of the blade pitch angle was changed according to a Pseudo Random Binary Sequence (PRBS) and the position of the generator valve was kept constant. In this experiment the blade pitch angle of the two blades was changed stepwise over a range of 4°. This is only a moderate excitation which introduces no heavy loads and therefore no safety problems. Moreover normal operation can continue during the identification experiment which can be a serious economic advantage for example in case of experimental modelling

a commercial grid connected wind turbine system. We have chosen to elaborate the data set of the series of experiments which has the most constant wind speed and a reasonable effect of the pitch angle on the outputs. The relatively constant wind speed indicates more or less constant point of operation which increases the possibility to identify a reliable linear model out of the data. The experiment lasted about 200 seconds while the signals were sampled at 50Hz. This implies that theoretically the wind turbine dynamics up to 25Hz can be identified. This should be enough to cover the relevant dynamics of the wind turbine, especially since the blade pitch angle primarily effects the aerodynamics and thereby the slow dynamics of the wind turbine.
Fig. 3 gives an overview of such an identification experiment.

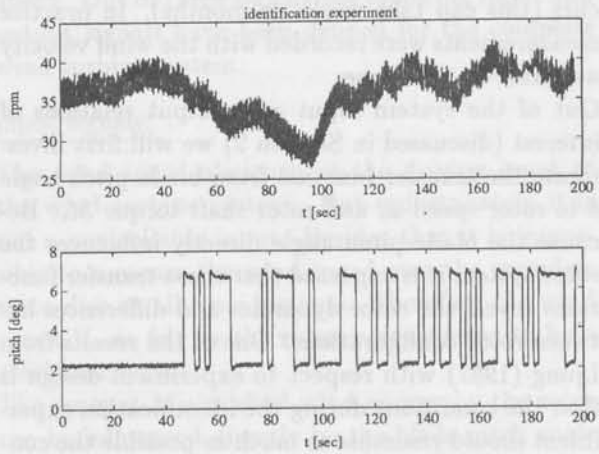

Fig. 3: Identification experiment (fragment) input: pitch angle, output: rotor speed

This figure shows that the excitation of the pitch angle does not disturb normal operation drastically therefore abortion of normal operation is superfluous. At first sight no clear relation between the input and its effect on the output can be detected.

Identification results

Given the measured data the experimental transfer functions from blade pitch angle to rotor shaft speed, rotor shaft torque and flap moment are estimated. Here the identification result for the transfer function from pitch angle to rotor speed is discussed. Investigation of the other transfer functions leads to approximately the same conclusions.
Different choices of model orders have been investigated (that is the order of the polynomials in the Box-Jenkins model structure (1)), both for the deterministic part as well as the stochastic part. The accuracy of the models was evaluated by looking at the loss criterion (2) and stepresponses of the different models. For deterministic orders > 5 and stochastic orders > 8 both the loss criterium and the model step responses show no significant improvement, they only differ slightly. Residual analysis pointed out that there was no information left in the data and therefore it may be assumed that all significant linear relations in the data are explained by the model.
Identification results in time and frequency domain are presented in Fig. 4.

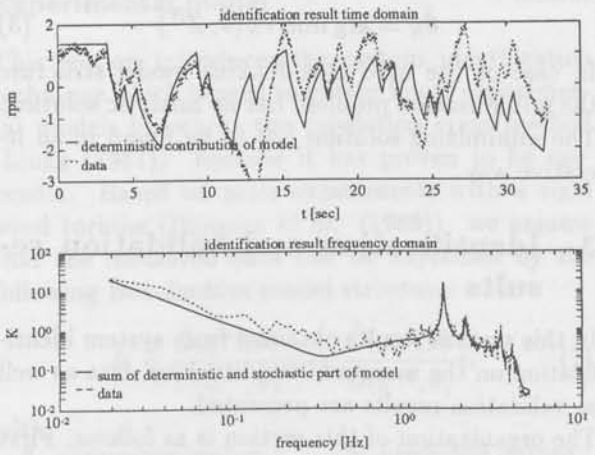

Fig. 4: Identification result in time and frequency domain

The upper half of Fig. 4 confronts the prediction of the deterministic part of the model with the measured data. Just for visual convenience the measured rotor speed has been filtered to remove the 1P effect (i.e. a phenomenon that is related to one times the rotational frequency of the rotor) which has nothing to do with the identified transfer function. The deterministic response can be explained by physical reasoning: the stepwise change of pitch angle alters the aerodynamic efficiency of the rotor. Because of rotor inertia and aerodynamic effects the rotor slowly accelerates or decelerates towards a new stationary value. Before this value is reached the pitch angle has changed again and a new transient is induced. Because of this physical interpretation we are quite confident about the reliability of the deterministic part.
The difference between the measured output and the output of the deterministic part of the model, driven by the applied input signal, is assumed to be mainly due to variations of wind speed. These variations are of random nature and need to be covered by the stochastic part of the model. The output

signals are modelled as the summation of a deterministic and stochastic contribution. Because we are also interested in a proper description of the wind influence on the wind turbine system we want to validate the stochastic part also. Since the input signal of the stochastic part is typically unknown in the time domain we have to pursue validation in the frequency domain. The lower half of Fig. 4 displays the spectrum of the output signal and the sum of spectra of both deterministic and stochastic part of the model. As it can be seen there are no serious discrepancies between the data and the total model. Referring to the upper half again we can state that the difference between the predicted deterministic part and the measured data is almost entirely covered by the stochastic part of the model. This is a support to the assumption that the influence of the wind speed on the system should be acccounted for by the stochatic part of the model.

validation results

In this subsection the validity of the theoretical model with respect to the transfer function from blade pitch angle to rotor speed and torque will be investigated.

As stated in the first part of this section the validation consists of the confrontation of stepresponse obtained from both the theoretical model and the experimental model. Performing the validation on the basis of experimental and theoretical model simulations yields some profits. First of all extreme situations can be investigated without putting the real wind turbine in danger. Moreover it is possible to devide the responses in deterministic and stochastic contributions to the output and validation can focus on each part separately. Since both models involved in the validation are linear models also system properties such as location of eigenvalues and frequency responses can be compared.

In this paper the validation is restricted to one point of operation. The theoretical model is linearized, using DUWECS (Bongers (1990)) , in an operating condition corresponding to the experimental condition from which the experimental data were obtained. In order to account partly for non-linearities in the experimental data two different linear models are obtained from the non-linear theoretical model, one at $\theta = 7^o$ and one at $\theta = 3^o$. In Fig. 5 step responses (to an increase of the blade pitch angle of one degree) of different experimental models and the two linearized theoretical models are given.

It can be seen in Fig. 5 that the experimental

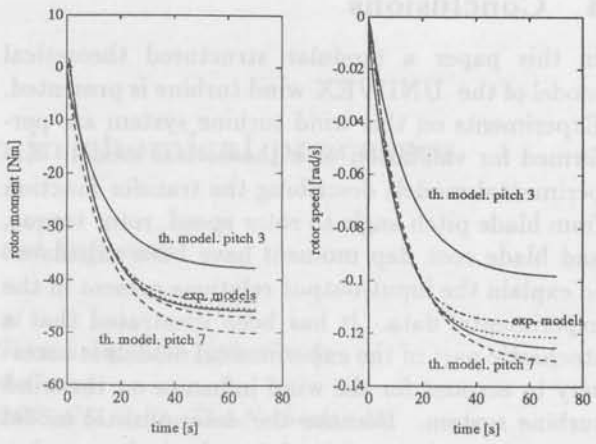

Fig. 5: Rotor shaft angular velocity, rotor shaft torque

models are squeezed between the two linear responses of the theoretical model. This can be explained by reasoning that the experimental model, which is linear, is the best compromise between the non-linearities in the experimental data.

In order to investigate the validity of the aerodynamics in the rotor model the transfer function between the blade pitch angle and the flap moment is estimated. By changing the blade pitch angle the absorbed wind energy and thereby the aerodynamic forces acting on the blades change. These forces are best observable looking at the flap moments of the blades. Despite serious tower wake and effects of unbalance of the blades on the flap moment a clear cut deterministic influence can be identified from the data, which corresponds rather well with the theoretical model. The instantaneous part at the step moment and the slower transient behaviour are found in both the theoretical model as well as the experimental model when comparing the magnitudes, which strengthens the confidence in the mathematical description of the aerodynamics.

Of course the validity is not ultimately established by comparison of step responses, but as a first result it is encouraging. This validation procedure has to be repeated for other points of operation (e.g. different average wind speed) to be able to draw the conclusion that the theoretical model of this configuration is valid over the complete wind regime from low to high wind speed. After that the validity of the model for other (more flexible) configurations can be investigated the same way.

4 Conclusions

In this paper a modular structured theoretical model of the UNIWEX wind turbine is presented. Experiments on this wind turbine system are performed for validation of a theoretical model. Experimental models describing the transfer function from blade pitch angle to rotor speed, rotor torque, and blade root flap moment have been calculated to explain the input-output relations present in the experimental data. It has been illustrated that a stochastic part of the experimental models is necessary to account for the wind influence on the wind turbine system. Because the deterministic model response can be explained by physical reasoning and because the summation of deterministic and stochastic part covers the frequency content in the data almost completely there is reasonable confidence that the identified models are suitable to describe the measured data. As a validation result of the theoretical model it has been shown that, for the transfer functions under consideration, the theoretical model predicts approximately the same outputs as the experimental model in one point of operation. Hence the theoretical model can be used to describe the wind turbine in open-loop behaviour.

Further research will focus on the validation of the same transfer function in different wind regimes, the transfer functions related to the generator valve, and validation of more flexible configurations of the UNIWEX wind turbine.

acknowledgements

The authors wish to thank the ICA of the universtity of Stuttgart for the possibility to experiment with the UNIWEX turbine, and in particular the people working at the test site for the pleasant coöperation during the measurement sessions.

References

Bongers P.M.M. (1990). *DUWECS Reference Guide, Delft University Wind Energy Conversion Simulation Program.* Delft University of Technology, The Netherlands, .

Bongers P.M.M., W.A.A.M. Bierbooms, Sj. Dijkstra, Th. van Holten (1990). *An Integrated Dynamic Model of a Flexible Wind Turbine.* Delft University of Technology, The Netherlands, .

Bongers P.M.M., T.G. van Engelen, Sj. Dijkstra, Z.D.Q.P. Kock (1989). Optimal control of a wind turbine in full load. *Proc. European Wind Energy Conference 1989, Glasgow, UK,* .

Glauert H. (1959). *The elements of airfoil and airscrew theory, (second ed.).* Cambridge University Press.

Kane T.R., D.A. Levinson (1985). *Dynamics, theory and applications.* McGraw-Hill series in mechanical engineering.

Kirchgaßner B. , *Linearisierte aeroelastische analyse einer Windturbine mit zweiblattrotor.* PhD Thesis, Universität von Stuttgart, 1986.

Ljung L. (1987). *System Identification: theory for the user.* Prentice Hall,, Inc. Englewood Cliffs, New jersey.

Mattson S.E. , *Modelling and control of large horizontal axis wind power plants.* PhD Thesis, Lund-Sweden, 1984.

Müller M. (1989). Experimental investigations with the universal test wind turbine. *Proc. European Wind energy Conf. 1989.,* Glasgow, Schotland, 832-836.

Steinbuch M. , *Dynamic modelling and robust control of a wind energy conversion system.* PhD Thesis, Delft University of Technology, The Netherlands, 1989.

Tischler, M. B. Leung, J. G. M. Dugan, D. C. (1986). Identification and verification of frequency-domain models for XV-15 tilt-rotor aircraft dynamics in cruising flight. *Journal of Guidance, Control, and Dynamics,* **9**, 446-453.

Amrani, A. O., Du Val, R. (1990). Parameter identification of aeroelastic modes of rotary wings from transient time histories. *Journal of Guidance, Control, and Dynamics,* **13**, 669-674.

Selected Topics in Identification, Modelling and Control
Vol. 5, December 1992

Heat balance reconciliation in chemical processes

Emile A.J.Ch. Baak[§], John Krist[‡] , Sjoerd Dijkstra[§]

[‡]*Process Development and Control Department*
DOW Benelux N.V., P.O. box 48, 4530 AA Terneuzen, The Netherlands.
[§]*Mechanical Engineering Systems and Control Group*
Delft University of Technology, Mekelweg 2, 2628 CD Delft, The Netherlands.

Abstract. Measurement data from chemical plants, in general, contain randomly distributed errors. Due to these errors, the measured variables do not exactly obey the theoretically existing balance equations. For the application of an *on-line* optimization algorithm it is neccessary to reduce these errors as much as possible. So far, only a technique was available to correct mass flow measurements with mass balances, the so called *mass balance reconciliation.* In this paper the extention of this theory towards the field of correcting temperature measurements with heat balances will be presented.

Keywords. heat balance reconciliation, data reconciliation, on-line optimization, correcting measurements.

1 Introduction

Chemical processes are often controlled by local controllers, supervised by a host computer. The controllers regulate the operation of the process, using flowrate, pressure, temperature and composition measurements. An optimization program, running on the host computer, uses the same inputs to determine the setpoints for the local controllers. Unfortunately, process measurements are never perfect and sometimes they are even quite wrong due to instrument drift, plugging up, failing or to the non-ideal character of the measurement devices. As a consequence, an optimization program will find a wrong optimum and money is wasted. To correct the measurement data in order to improve the quality of the measurements, à priori knowledge can be helpful. This information is mainly available in the form of mass and heat balances. The physical conservation laws for material and energy are, in general, suitable for chemical equipment like distillation columns, reactors and heat exchangers. For *steady state* conditions, the static balances can easely be derived. Although the assumption of *steady state* is not always essential, it is usually permitted to assume that large chemical processes, excluding start-up or shut down situations, are operating at, or near steady state.

A statistical procedure which enables the adjustment of measurements is *data reconciliation.* In general, data reconciliation is only applicable in overspecified situations with regard to the number of measurements taken or information sources, i.e. a certain level of redundancy. This procedure minimizes the differences between the *theoretically calculated* and the *real measured* values. Instead of arbitrarily replacing measurements by theoretically calculated values, the smallest or the *most likely* corrections to *all* measurements are selected. The origin of information can be both the direct measurement and a value resulting from other measurements (Romagnoli and Stephanopoulos(1980), Tamhane and Mah (1985), Heenan and Serth(1986)). Besides this, it is also possible to reconcile measurements with à priori knowledge about the correlation between variables in time. Here it is important to have an impression of the relative inaccuracy. This last method, called *dynamic*

data reconciliation (Grinten, van der (1971)) uses *Kalman-filtering* (Barham and Humphries (1970)) and assumes *quasi* steady state situation. The method to be described here is based on measurements only. Due to the fact that only steady state balances are used to correct the data, this method can be seen as *static* Kalman filtering.

Until now, only measurements of mass flows were involved in data reconciliation techniques and it had to be assumed that temperature measurements were reliable. This was basically because no general theory was available to reconcile these measurements with energy or heatbalances. The technique of heatbalance reconciliation is based on a non-linear model that arises from the fact that energy, in most cases, can not be measured directly but can only be determined by considering it as a product of mass flow and specific enthalpy.

2 Preliminaries

First the key assumptions are listed for the purpose of this study. For a more detailed description of some of these items see the literature survey made by Baak (1991). These assumptions are valid until otherwise is stated:

- The *random errors* are independent and normally distributed.
- All *process variables* are measured with known uncertainty.
- No *gross errors* are present in the measurements (i.e. errors due to calibration defects, wear of measurement devices or fouling).
- Only *one* set of measurements is taken.
- The process is operating at *steady state.*

3 Linear data reconciliation

The method to be presented first is used concerning *mass balance* reconciliation and is based on the theory of *Lagrange multipliers.* In Figure 1, a simple distillation column is depicted and to simplify, only mass flows are taken into account. In general, the steady state mass balance equation can simply be derived, considering :

$$\sum Flow_{in} - \sum Flow_{out} = 0 \qquad (1)$$

With the real measured flowrates, in general, equation (1) will not be equal to zero. So one, two or

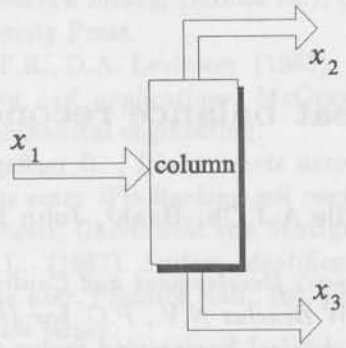

Fig. 1: Mass flows round distillation unit.

perhaps all three of the measured flowrates show errors and these errors will typically yield the inconsistent mass balance. Random errors can be reconciled by the following procedure. The mass balance of the distillation column given, can be derived through applying equation (1):

$$x_1 - x_2 - x_3 = 0 \qquad (2)$$

With the measured values of these variables, $\tilde{x}_1$, $\tilde{x}_2$ and $\tilde{x}_3$, the right hand-side (i.e. the imbalance) of equation (2) will not be equal to zero. After adding corrections Δx_1, Δx_2 and Δx_3, the mass balance is:

$$(\tilde{x}_1 + \Delta x_1) - (\tilde{x}_2 + \Delta x_2) - (\tilde{x}_3 + \Delta x_3) = 0 \qquad (3)$$

The problem here is to find the *most likely* corrections Δx_i, which satisfy equation (3). Most likely can be interpreted as the smallest possible corrections, taking into account some weighing factor defined as σ_i. The weighing factors for each measurement are derived from the error variances. The value of σ_i is normally independently estimated, using the manufacturer's specifications together with the engineer's knowledge of the performance of the measurement device. Often, the error variances are found by a statistical analysis of the measurement data (Heenan and Serth (1986)). The most likely corrections are found by minimizing the following *constrained least squares* criterion:

$$L_{const.} = \frac{\Delta^2 x_1}{\sigma_1^2} + \frac{\Delta^2 x_2}{\sigma_2^2} + \frac{\Delta^2 x_3}{\sigma_3^2} \qquad (4)$$

This expression reaches a minimum value if all the derivatives with respect to Δx_i, are zero. The use of a least squares criterion as objective function in data reconciliation problems is based on the assumption that the measurement errors have

a *normal* distribution, without taking into account *gross errors* that may be present (Tjoa and Biegler (1991)). Then, one of the Δx_i-values can be eliminated using equation (3). For example, solving the *linear* equations for Δx_1, leads to:

$$\Delta x_1 = \frac{\sigma_1^2\{\tilde{x}_2 + \tilde{x}_3 - \tilde{x}_1\}}{\sigma_1^2 + \sigma_2^2 + \sigma_3^2} = \frac{-\varepsilon}{1 + \frac{\sigma_2^2}{\sigma_1^2} + \frac{\sigma_3^2}{\sigma_1^2}} \qquad (5)$$

Here ε is defined as: $\varepsilon \stackrel{\text{def}}{=} \{\tilde{x}_1 - \tilde{x}_2 - \tilde{x}_3\}$, the imbalance of the distillation column. As can be seen from equation (5) that the corrections on the measurements are proportional to the imbalance and the relative inaccuracies, the ratios of the σ_i^2's.

Minimizing criterion (4) with equation (3) as constraint can properly be done with the help of a *Lagrange multiplier*, represented by λ. In general, the number of Lagrange multipliers equals the number of constraints or balance equations. With these multipliers, the *constrained* least squares criterion can be transformed to an *unconstrained* criterion. If the system becomes more complicated it can be recommended to pass on to matrix representations. The topological balance structure is represented by A, the so called *incidence* or *system* matrix (Romagnoli and Stephanopoulos (1980)). An element a_{ji} of matrix A is either a 1, if stream i is an input of unit j or -1 in case stream i is an output. If there are n streams and m units, consequently m balances can be derived:

$$A\underline{x} = 0 \qquad A \in \mathbb{R}^{m \times n} \qquad (6)$$

Here $\underline{x}$ is a vector with all the measured process variables. If we apply the same substitution as before, $x_j = \tilde{x}_j + \Delta x_j$, the matrix representation of the constrained least squares criterion is:

$$\begin{aligned} \textit{minimize}: \quad & L_{constr.} = \Delta\underline{x}^T P^{-1} \Delta\underline{x} & (7) \\ \textit{constraints}: \quad & \underline{0} = A(\underline{\tilde{x}} + \Delta\underline{x}) & (8) \end{aligned}$$

The weighing matrix is represented by P, with elements σ_i^2 on the diagonal (assuming no correlation between measurement errors). With the introduction of the *Lagrange multipliers* the problem can be reduced to the following *unconstrained* criterion:

$$\begin{aligned} &\textit{minimize}: \\ &L_{unconstr.} = \Delta\underline{x}^T P^{-1} \Delta\underline{x} + 2\underline{\lambda}^T A(\underline{\tilde{x}} + \Delta\underline{x}) \qquad (9) \end{aligned}$$

The vector $\underline{\lambda}$ contains the m Lagrange multipliers. Differentiating this expression with respect to the corrections $\Delta\underline{x}$ and the Lagrange multipliers $\underline{\lambda}$, leads to:

$$\begin{aligned} \frac{\partial L_{unconstr.}}{\partial \Delta\underline{x}} &= \Delta\underline{x}^T P^{-1} + \underline{\lambda}^T A = \underline{0} & (10) \\ \frac{\partial L_{unconstr.}}{\partial \Delta\underline{\lambda}} &= A(\underline{\tilde{x}} + \Delta\underline{x}) = \underline{0} & (11) \end{aligned}$$

This system must be solved in order to find the *most likely* corrections. By eliminating $\Delta\underline{x}$, the following expression gives the values of the Lagrange multipliers:

$$\underline{\lambda} = \{APA^T\}^{-1} A\underline{\tilde{x}} \qquad (12)$$

This is a system of m linearily independent equations, and consequently $\underline{\lambda}$ can be uniquely solved. Substituting this solution in (10) leads to the desired corrections:

$$\Delta\underline{x} = -PA^T\{APA^T\}^{-1} A\underline{\tilde{x}} \qquad (13)$$

It can be shown that the accuracy improves, under the theoretical assumptions. The reconciliation procedure estimates the *random* measurement error. If the estimates of the process variable is represented by $\underline{\hat{x}}$ the variances are given below:

$$E\{\underline{\tilde{x}}\underline{\tilde{x}}^T\} = P \qquad (14)$$

$$\begin{aligned} E\{\underline{\hat{x}}\underline{\hat{x}}^T\} &= E\{(\underline{\tilde{x}} + \Delta\underline{x})(\underline{\tilde{x}} + \Delta\underline{x})^T\} \\ &= E\{\underline{\tilde{x}}\underline{\tilde{x}}^T\} - E\{\Delta\underline{x}\Delta\underline{x}^T\} \\ &= P - PA^T\{APA^T\}^{-1} AP \qquad (15) \end{aligned}$$

This immediately shows that the variance decreases after reconciliation.

4 Non-linear data reconciliation

As referred to in the introduction, there are circumstances in which the method of linear data reconciliation has severe shortcomings. The values of flow variables, for example, are mostly *directly* measured by *orifice* or *vortex* devices. Measurements can then be reconciled by applying the described linear reconciliation theory. If the variable *is* not or *can* not be directly measured, a *non-linear* data reconciliation technique might be neccesary. Heat or energy are generally not directly measurable but have to be calculated from mass flow and specific enthalpy (temperature) measurements. This leads to *non-linear* balance equations. The phenomenon non-linear data reconciliation also arises in case of the reconciliation of *component* measurements. The global difference between linear and non-linear cases is in fact that the linear approach is not useful when entries of a certain balance are composed

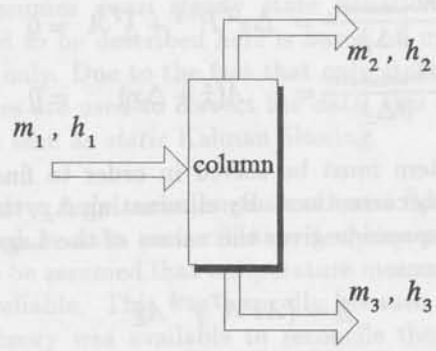

Fig. 2: Mass and specific enthalpy flows round distillation unit.

out of two or more measurements. Entries of heat balances are calculated as follows:

$$\tilde{E} = \tilde{m}\tilde{h} = (m + \delta_m)(h + \delta_h) \qquad (16)$$

with m as mass flow and h as specific enthalpy. the measurement error is represented by δ.

Essential for this non-linear method is the introduction of *ratio numbers*. These numbers are the link between the mass balance and the heat balance. The treatment of these ratio numbers is equal to the treatment of the process variables. This is possible due to the weighing phenomenon. To present the method of non-linear reconciliation, the distillation unit of Figure 1 is considered, but now specific enthalpies are added as in Figure 2. The author was inspired by Duyfjes and Swenker (1976) where component balance reconciliation is discussed. The mass and heat balances are:

$$m_1 - m_2 - m_3 = 0 \qquad (17)$$

$$m_1h_1 - m_2h_2 - m_3h_3 = 0 \qquad (18)$$

Respectively. A change to a new vector $\underline{x}$ will be made. The elements for this vector $\underline{x}$ are, as in the example of Figure 2:

$$x_1 = m_1 \quad x_5 = h_1 \quad x_4 = 1$$
$$x_2 = m_2 \quad x_7 = h_2 \quad x_6 = 1$$
$$x_3 = m_3 \quad x_9 = h_3 \quad x_8 = 1$$

The numbering method for this vector will soon be clear while considering the balances or the reconciliation *model*. For the simple distillation column, three extra balances are introduced, representing the interaction between the mass flow and heat flow in one particular stream. In these balances, the ratio numbers play an important role. In this case, the variables x_4, x_6 and x_8 are set equal to one but they can have any value as long as the values of these variables are equal. The corrections of all the measurements are then scaled in the same way. The reconciliation model for the distillation column is:

$$\begin{aligned}
x_1 \quad & -r_1x_4 \quad & & & = 0 \\
-x_2 \quad & & +r_2x_6 \quad & & = 0 \\
-x_3 \quad & & & +r_3x_8 \quad & = 0 \\
x_1 - x_2 - x_3 \quad & & & & = 0 \\
& r_1x_5 \quad & -r_2x_7 \quad & -r_3x_9 & = 0
\end{aligned} \qquad (19)$$

The flexibility of the approach allows to define the variance of the variables x_4, x_6 and x_8 to be zero. This implies that the value of these variables remains the same and consequently the interaction of the balances does not change during reconciliation.

The reason to write the reconciliation model in the form above is that the balance system (19) can be divided into blocks. Actually every flowsheet can be written in form (19). The first n balances refer to the n streams involved. In case of the simple column, three streams occur so three *ratio equations* are needed. The remaining two equations are the physical balances, respectively the mass and heat balance round the column. If we divide the system (vertically) into four, i.e. $(n + 1)$, blocks, it is possible to present the system in the following form:

$$A_0\underline{x}_0 + r_1A_1\underline{x}_1 + r_2A_2\underline{x}_2 + r_3A_3\underline{x}_3 = \underline{0} \qquad (20)$$

The four parts are in accordance with the blocks in (20) after defining:

$$\underline{x}_0 = \begin{bmatrix} x_1 \\ x_2 \\ x_3 \end{bmatrix}, \underline{x}_1 = \begin{bmatrix} x_4 \\ x_5 \end{bmatrix}, \underline{x}_2 = \begin{bmatrix} x_6 \\ x_7 \end{bmatrix}, \underline{x}_3 = \begin{bmatrix} x_8 \\ x_9 \end{bmatrix} \qquad (21)$$

$$A_0 = \begin{bmatrix} 1 & 0 & 0 \\ 0 & -1 & 0 \\ 0 & 0 & -1 \\ 1 & -1 & -1 \\ 0 & 0 & 0 \end{bmatrix} A_1 = \begin{bmatrix} -1 & 0 \\ 0 & 0 \\ 0 & 0 \\ 0 & 0 \\ 0 & 1 \end{bmatrix} A_2 = \begin{bmatrix} 0 & 0 \\ 1 & 0 \\ 0 & 0 \\ 0 & 0 \\ 0 & -1 \end{bmatrix} A_3 = \begin{bmatrix} 0 & 0 \\ 0 & 0 \\ 1 & 0 \\ 0 & 0 \\ 0 & -1 \end{bmatrix} \qquad (22)$$

To match the new situation, the criterion function must be changed. In the particular case of the column, once more with the assumption $\underline{x}_i = \hat{\underline{x}}_i + \Delta\,\underline{x}_i$, the constrained least squares

criterion is:

$$minimize: \quad L_{constr.} = \sum_{i=1}^{3n} \left(\frac{\Delta x_i}{\sigma_i}\right)^2 = \sum_{j=0}^{n=3} \Delta \underline{x}_j^T P_j^{-1} \Delta \underline{x}_j \quad (23)$$

Here P_j are the variance matrices of the variables in the vectors respectively $\underline{x}_j$ and serve again as weighing matrices. In the variance matrices, the variances σ_4, σ_6 and σ_8 are set equal to zero.

So far, the presented theory concerned only the flowsheet of Figure 2. However, the theory can be applied to any flowsheet as long as *steady state* situations are considered. Every system is convertible to the reconciliation model of type (19). Hence the general least squares problem is:

$$minimize: L_{constr.} = \sum_{j=0}^{n} \Delta \underline{x}_j^T P_j^{-1} \Delta \underline{x}_j \quad (24)$$

$$constraints: \quad \underline{0} = \sum_{j=0}^{n} r_j (A_j \underline{\tilde{x}}_j + A_j \Delta \underline{x}_j) \quad (25)$$

Here, by definition: $r_0 \stackrel{\text{def}}{=} 1$ Again, this problem can be solved with the help of Lagrange multipliers $\underline{\lambda}$. Transforming the constrained least squares criterion into an unconstrained, leads to:

$$minimize: \quad L_{unconstr.} = \sum_{j=0}^{n} \Delta \underline{x}_j^T P_j^{-1} \Delta \underline{x}_j + 2\underline{\lambda}^T \sum_{j=0}^{n} r_j (A_j \underline{\tilde{x}}_j + A_j \Delta \underline{x}_j) \quad (26)$$

Differentiating this criterion with respect to $\Delta \underline{x}_j$, j=0,..., n, the ratio numbers r_j, j=1,..., n and the Lagrange multipliers λ, leads to the optimal corrections:

$$\Delta \underline{x}_j = -r_j P_j A_j^T \underline{\lambda} \qquad j = 0, \ldots, n \quad (27)$$

Substituting (27) in the equations providing the optimal solution leads to:

$$\sum_{j=0}^{n} r_j A_j \underline{\tilde{x}}_j - \sum_{j=0}^{n} r_j^2 A_j P_j A_j^T \underline{\lambda} = \underline{0} \quad (r_0 = 1) \quad (28)$$

$$(A_j \underline{\tilde{x}}_j - r_j A_j P_j A_j^T \underline{\lambda})^T \underline{\lambda} = 0 \quad j = 1, \ldots, n \quad (29)$$

This solvable, *non-linear* system, has the ratio numbers r_j and the elements of the multiplier vector $\underline{\lambda}$ as unknowns, resulting in a total of n plus $(n+2m)$ so $2(n+ m)$ unknowns, respectively. The number of non-linear equations is also $2(n + m)$, $n + 2m$ from equation (28) and n from (29). This set of equations can be solved in two different ways. The set may either be solved directly with the help of numerical equation solver routines like those in the flowsheet simulation package SPEEDUP. After the values of the Lagrange multipliers and the ratio numbers are found, the optimal corrections can be found by applying equation (27). The other way is to linearize the equations and solve the set iteratively.

5 Solving the system

In a practical environment, such as a chemical plant, a robust reconciliation algorithm is needed. The reconciled measurements must be reliable and consequently the solution must converge to a set of consistent process values under all circumstances. Although the procedure of linearizing the set equations (28) and (29), and succesively coming to a solution via an iterative approach works fine in all the investigated examples, a flowsheet simulation package can add a number of advantages. First of all, in the case of data deduced from large process flowsheets, it is not easy to transform this flowsheet into a corresponding reconciliation model. As can be seen from (19), even for a very simple flowsheet example, there are a lot of equations involved. Transforming a flowsheet into the required reconciliation model can automatically be done while approaching the problem with a flowsheet simulation package. Secondly, solving the non-linear equations via succesively solving linear subproblems may not be robust enough in practical situations. However, after adjusting the flowsheet to a flowsheet program, this program returns with the optimal corrections and shows to be very robust. Temporarily or permanent not measured process variables are estimated during the calculation. This is important as measurements with so called *gross errors* are not to be taken into account in the reconciliation procedure.

6 Experimental results

As the original formulation of the problem required, after reconciliation, the imbalance of the mass and heat balances must be reduced to zero. This is done in such a way that the weighed adjustments to the measurement values will always be as small as possible. With the help of a random generator in a FORTRAN routine, 105 data sets were created. Besides the heat balances, also the component balances were taken into account in the same

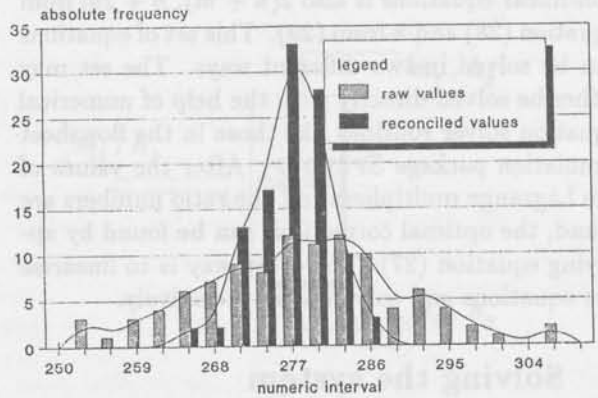

Fig. 3: The dispersion reduction of a mass flow measurement.

way. After reconciliation, the standard deviation of the imbalances of all the units is reduced to zero with zero mean. This is obvious since the problem was put in that way. Besides this, there is the desired effect on the accuracy of the measurement values. Adding information, by means of the balances, the dispersion of the measurement values will be reduced. For a particular mass flow value, this phenomenon is shown in Figure 3. A statistical program is used to count the absolute frequencies of the values within certain numerical intervals. Then by means of non-linear regression techniques, the *normal* or *bell-shaped* curve is constructed. Figure 3 shows that after reconciliation, the curve becomes narrower (the standard deviation decreases). In this case the standard deviation is reduced with 67%. The reduction rates of the other mass flow measurements are conform this value, depending on location and relative inaccuracies or weighing. Also the *redundancy* plays an important role. The accuracy improvement is larger the more the system is overspecified. The reduction rates of the temperature measurements although significant ($\pm 15\%$), are smaller due to two reasons. First of all, it is always possible to derive more mass balances than heat balances in the reconciliation model, due to the fact that in normal cases, heat leaks for more easier from pipes or reactors than mass does. Consequently, there is more additional information about the mass flows than about the temperature values and so the effect of reconciliation is more observable. Secondly, as can be seen from (19), mass flow measurements are entries of both the mass balances and heat balances. These measurements have to obey two restrictions instead of one if specific enthalpy or temperature mesurements are considered. Again, more additional information causes a bigger accuracy improvement.

In real application the *steady state* assumption will not be fulfilled completely. However, dynamic effects are normally very small and can be neglected in comparison to the measurements errors. In case of steady state optimization, steady state detectors are mostly installed and no optimization and reconciliation will be carried out without steady state situation.

7 Discussion

While data reconciliation via the Lagrange multiplier method yield good, i.e. consistent, mass and heat balances, the adjusted measurements will be erroneous if there are *gross errors* present in the used data set. Therefore, such errors have to be identified, the offending measurements removed, before preceeding the with data reconciliation procedure. In the following, two general types of statistical tests are considered:

(I) Methods for analyzing least squares residuals.
Here, the idea is to adjust the data using the described least squared error analysis and then calculate a set of residuals:

$$\varepsilon_i = x_i - \tilde{x}_i \tag{30}$$

The outliers among the ε_i values are those that exceed some number of standard deviations, for example: 1.96 for a 95% confidence level. Thus, a given residual is an outlier if the following is true:

$$\left|\frac{\varepsilon_i}{\sigma_i}\right| > 1.96 \tag{31}$$

where σ_i is the standard deviation of the residual. The outliers, if any, are considered to be result of gross errors. Besides this, another approach based on observation of the residuals can be made. Due to the fact that the measurement values are normally distributed, the residuals will be normally distributed with a mean zero and a certain variance. In case of involved gross errors, this mean differs from zero while observing a sufficient number of samples. Thus another way of detecting gross errors is by observing the mean of the residuals.

(II) Methods for analyzing nodal imbalances.
The imbalance ε_j for a node or unit j (with K

inputs and L outputs) is defined by:

$$\varepsilon_j = \sum_{k=1}^{K} input_k - \sum_{l=1}^{L} output_l \qquad (32)$$

This value is divided by the nodal *standard deviation* σ_j, which is the squared root of the nodal variance:

$$\sigma_j = \sqrt{\sum_{k=1}^{K} \sigma_k^2 + \sum_{l=1}^{L} \sigma_l^2} \qquad (33)$$

Here, the summation extends over all the streams connected to node j. Equation (33) is directly applicable while considering mass flows only. In case of heat flows however, the variances of the balance entries must be calculated from variances of the temperature and possible fraction measurements. This functionality is mostly *non-linear*. Due to this, the determination of the nodal variance is normally a result of some kind of linearization. Again for a 95% confidence interval, there are one or more gross errors present in the measurements if the following expression for the normalized imbalance of node j is valid:

$$\left| \frac{\varepsilon_j}{\sigma_j} \right| > 1.96 \qquad (34)$$

Once a gross error has been identified, the corresponding measurement is eliminated from the data by a process called *nodal aggregation*. For example consider the small flowsheet shown in Figure 4. If there is a gross error detected in stream 3, this stream can be eliminated by combining nodes A and B to yield the aggregate node shown in Figure 5. The random errors in an aggregated network can be reconciled in the normal way. This leads to corrected measurements for all streams except stream 3. The reconciled value for stream 3 can

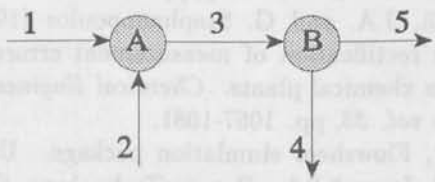

Fig. 4: The process before nodal aggregation.

be found afterwards by solving the balance equation for node A or node B. These method has two

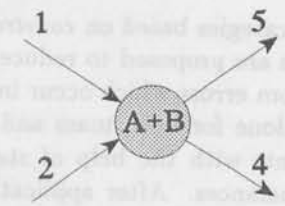

Fig. 5: The process after nodal aggregation.

principal drawbacks. First the least squares procedure tends to spread the error over all the data. So, even the best measurements can have fairly high residuals. If these residuals fail the test for outliers, then the corresponding measurements are erroneously identified as having gross errors. The second drawback is that there is no provision to prevent unrealistic flowrates or temperatures from being computed. If the algorithm fails to identify all the gross errors, the data reconciliation procedure may generate for example negative flowrates or absurdly large positive ones. In modern flowsheet simulation programs however, it is possible to overcome this by placing certain bounds on the variables.

8 Future research

In view of the application: *steady state optimization*, only steady state systems are considered. In the future, research can be extended towards the dynamic case. For dynamic systems extended and augmented *Kalman* filters have been used to reconcile process data and estimate parameters. The recursive nature of the Kalman filter makes it very efficient and well-suited for *on-line* applications. However, these methods are based on linear approximations which may not be suitable for chemical engineering systems which are operating in highly non-linear regions. In addition, if the data reconciliation objective function is not weighed least squares, the Kalman filter is not applicable. Kim *et al.*(1991) presented a method to extend the data reconciliation and parameter estimation to the field of *non-linear* dynamic systems. This is done based on numerical integration nested within a non-linear programming algorithm. A moving data horizon is defined which extends back to a certain number of time steps from the current time. Unfortunately, these techniques have recently been developed and no general tests have been carried out of how these algorithms perform in practice.

9 Conclusions

Reconciliation strategies based on *constrained least squares* criterions are proposed to reduce the influence of the random errors which occur in measurements. This is done for both mass and temperature measurements with the help of steady state mass and heat balances. After application, fairly high imbalances of several units disappeared. Entries of both mass and heat balances are in equilibrium. As a second result, the accuracy of all the involved measurements improved more or less. The improvement in accuracy of the measurements depents on the location in the topologic structure of the flowsheet and the level of redundancy. Temperature measurements show a smaller improvement then mass flows, in all the cases.

In practice, the reduction of the inaccuracies will be smaller then the obtained results. This arises from the fact that no accurate information is present about the parameters of the distributions. Since the standard deviation is used as a weighing factor in the procedure, this can cause problems. Besides this, the used balances are derived from the assumption that the chemical plant is operating at steady state, which is not always upheld in practice. However, this will hardly influence the results.

Finally the conclusion can be drawn that, normally, heatbalance reconciliation is possible since robust *numerical* optimization tools are available. Both mass and heat measurements descended from fairly complicated and multi-component flowsheets can easily be reconciled in case the criterion is properly formulated and the weighing factors are determined. However, gross errors will always lead to erroneous results. Therefore, these errors have to be detected and removed from the data set. The aspect of gross errors and their remedies could eventually be subject of further research pending the implementation of the presented reconciliation techniques.

Glossary of symbols

A	incidence or system matrix
h	specific enthalpy
m	mass flow, number of balances
n	number of process variables
P	weighing matrix
r	ratio number
$\tilde{x}$	measurement value of variable x
Δx	correction on measurement $\tilde{x}$
δ	error
ε	imbalance, residual
λ	Lagrange multiplier
σ	standard deviation, weighing factor

References

Baak, E.A.J.Ch. (1991). Meetwaardenvereffening voor de procesindustrie (Dutch). *Literature survey S-577 Delft University of Technology, Faculty of Mechanical Engineering.*

Barham, P.M. and D.E. Humphries (1970). Derivation of the Kalman filtering equations from elementairy statistical principles. *Agardograph No 139*, pp. 12-31.

Duyfjes, G and A.G. Swenker (1976). Het vereffenen van overtallige informatie (Dutch). *Polytechnisch Tijdschrift P(31) No 9*, pp. 535-546.

Edgar, T.G. and D.M. Himmelblau (1988). Optimization of chemical processes. *M^{c}Graw-Hill Chemical Engineering Series.*

Grinten, P.M.E.M. van der (1971). Statische en dynamische vereffening van meetgegevens (Dutch). *De Ingenieur No 21*, pp. 70-72.

Heenan, W.H. and R.W. Serth (1986). Detecting errors in process data. *Chemical Engineering No 11*, pp. 99-103.

IMSL, Fortran subroutines for statistical analysis. User's manual. 3rd vol. version 1.1. Houston, January 1989.

Kim, I.W., M.J. Liebman and T.F. Edgar (1991). A sequential error-in-variables method for nonlinear dynamic systems. *Computers in Chemical Engineering vol. 15 No 9*, pp. 663-670.

Lawrence, P.J. (1989). Data reconciliation: Getting better information. *Hydrocarbon Processing No 6 June*, pp. 55-66.

Mah, S.H. (1981). Design and analysis of process performance monitoring systems. *Chemical Process Control No 1 January*, pp. 525-540.

Romagnoli, J.A. and G. Stephanopoulos (1980). On the rectification of measurement errors for complex chemical plants. *Chemical Engineering Science vol. 35*, pp. 1067-1081.

SPEEDUP, Flowsheet simulation package. User's manual, Issue 5.3.1. Prosys Technology, Cambridge. January 1991.

Stephenson, G.R. and C.F. Shewchuk (1986). Reconciliation of process data with process simulation. *AIChE Journal vol.32 No 2 February*, pp. 247-254.

Tamhane, A.C. and S.H. Mah (1985). Data reconciliation and gross error detection in chemical process networks. *Technometrics november vol. 27 No 4*, pp. 409-422.

Tjoa, I.B. and L.T. Biegler (1991). Simultenious strategies for data reconciliation and gross error detection of non-linear systems. *Computers in Chemical Engineering vol. 15 No 10*, pp. 679-690.

Selected Topics in Identification, Modelling and Control
Vol. 5, December 1992

Worst–case system identification in ℓ_1: error bounds, optimal models and model reduction ‡

Richard G. Hakvoort

Mechanical Engineering Systems and Control Group
Delft University of Technology, Mekelweg 2, 2628 CD Delft, The Netherlands.

Abstract. In ℓ_1-robust control design model uncertainty can be handled if an upper-bound on the ℓ_1-norm of the model error is known. In this paper a procedure is developed which yields such an upper bound for a given nominal model, using measurement data and a priori information consisting of a time domain bound on the noise and information about the decay–rate of the pulse response of the model error. The upper bound is calculated by solving a set of linear programming problems.
Moreover a procedure is presented to derive a new nominal model which is optimal in an ℓ_1-sense, i.e. has a minimal upper bound on the ℓ_1-norm of the model error. This is performed in two steps, in the first step the so–called central estimate is computed and in the second step model reduction in ℓ_1-norm is performed. For the latter problem a solution is given for the case that the reduced order model is linear in the parameters.

Keywords. worst–case identification, ℓ_1-norm, linear programming

1 Introduction

Analogous to H_∞-control theory the ℓ_1-optimal feedback design problem has been formulated and solved (Dahleh and Pearson, 1987; McDonald and Pearson, 1991). In this setting knowledge of an ℓ_1-bound on the model error can be utilized for the analysis and design of robust controllers (Khammash and Pearson, 1991). Consequently identification strategies are being developed that are compatible with the ℓ_1-control design, i.e. yield an upper bound on the ℓ_1-norm of the model error and an ℓ_1-optimal nominal model (Chen *et al.*, 1992; Jacobson and Nett, 1991; Mäkilä, 1990, 1991; Tse *et al.*, 1991).

The algorithms so far available have a restricted applicability due to the fact that often only additive uncertainty is considered and that specific experimental conditions have to be met, e.g. the input signal is required to be a step, an impulse or a Galois sequence, and the initial conditions are assumed to be zero. However in many practical situations the input signal can not be specified arbitrarily, for example if the system is operating in closed loop.

In the present paper worst–case identification in ℓ_1-norm is considered. First the problem is considered of the estimation of an error bound. An identification algorithm is developed that yields an upper bound on the ℓ_1-norm of the model error for a given nominal model. There are no restrictions on the experimental conditions, i.e. the shape of the input signal. A general uncertainty description is adopted, weighted additive uncertainty, which includes the multiplicative uncertainty description. The main prior information assumed available is a bound on the pulse response of the model error and a time domain bound on the noise. No model order assumption on the true system is made, nor any statistical properties of the noise are assumed. The resulting error bound is a hard bound, which means that the true model error is guaranteed to be

‡This paper is also presented at the 31st Conference on Decision and Control, Tucson, U.S.A., December 16–18, 1992.

smaller than the calculated upper bound, provided the prior information that is used is correct.

Next in the same setting a second problem is considered, the problem of identifying an ℓ_1-optimal nominal model, i.e. a nominal model with minimal corresponding guaranteed error bound. After a problem simplification a solution is shown to be obtainable in two steps. In the first step the so–called central estimate is computed, which is in general a high order model. In the second step this high order model is reduced to a model of the desired order applying model reduction in ℓ_1-norm. For this model reduction problem a solution is given in case the reduced order model is parametrized linearly.

The outline of the paper is as follows. In the next section the a priori information assumed available is summarized. In section 3 it is described how this information, including the measurement data, is processed, such that it can be used in the worst–case analysis. Then in section 4 a solution is given for the problem of identifying an upper bound for the ℓ_1-norm of the model error. In section 5 we consider the problem of identifying an ℓ_1-optimal model. Then in section 6 an example is given of the entire procedure developed. The paper ends with conclusions.

2 A Priori Knowledge

We consider a discrete time, asymptotically stable, linear, time-invariant, causal SISO system $G_0(q) = \sum_{k=0}^{\infty} g_0(k)q^{-k}$ (where q is the forward shift operator) with additive bounded output noise. The input–output behaviour of the plant is assumed to be given by the equation

$$y(t) = G_0(q)u(t) + H(q)e(t), \quad e(t) \in [e_l(t), e_u(t)], \tag{1}$$

where $u(t)$ is the measured input signal, $y(t)$ is the measured output signal, $e(t)$ is the noise, only known to be bounded by $e_l(t)$ and $e_u(t)$. $H(q)$ is some (a priori given) noise model, that can be used to bring in a priori knowledge about the frequency distribution of the noise.

For identification purposes we need measurements of the input signal $u(t)$ and the output signal $y(t)$ acting on the system, $t = 1, 2, \ldots, N$. There are no prior restrictions whatsoever on $u(t)$, it may for example be generated in closed loop. Here the situation is considered that one data sequence is available. It is however straightforward to extend to the case that more measurement sequences are available.

We consider the uncertainty configuration

$$G_0(q) = \hat{G}(q) + \Delta_{\hat{G}}(q)W(q), \tag{2}$$

where $\hat{G}(q)$ is some a priori given nominal model, constructed by any identification or modelling procedure and $W(q)$ is an a priori specified fixed weighting function. The system $G_0(q)$ and the model error $\Delta_{\hat{G}}(q)$ are unknown. All transfer functions in (2) are assumed to be stable. We require the weighting function $W(q)$ and the noise model $H(q)$ to be minimum–phase. Without loss of generality we further require $W(q)$ to be biproper. The (possibly infinite) pulse response sequences of the transfer functions will be denoted by the corresponding lower–case characters. Hence (2) defines the pulse responses g_0, $\hat{g}$, $\delta_{\hat{G}}$ and w.

Next we assume to know an $M > 0$ and $\rho > 1$ such that

$$|\delta_{\hat{G}}(k)| \leq M\rho^{-k}, \quad \forall\, k \geq 0. \tag{3}$$

If more information is available about the pulse response of the model error this may be included as well. It is for example possible to consider an interval bound on $\delta_{\hat{G}}(k)$ independent of the bound for other values of k.

Finally we assume to know upper bounds on past (unmeasured) data $u(t)$ and $y(t)$,

$$|u(t)| \leq \bar{u}, \ |y(t)| \leq \bar{y}, \quad \forall\, t \leq 0. \tag{4}$$

If the system is at rest at $t = 0$, $\bar{u}$ can be chosen to be equal to 0.

Note that no model order assumption has been imposed on the system $G_0(q)$, neither any statistical properties have been assumed for the noise $e(t)$.

The information obtained so far does not uniquely determine the system $G_0(q)$ and the model error $\Delta_{\hat{G}}(q)$. There is a set of systems $G(q)$ and corresponding model errors $\Delta(q)$ consistent with the data and the prior information. We accordingly define

$$\begin{aligned}\mathbf{\Delta}_{\hat{G},C} = \{\Delta(q) \mid &(1),\ t = 1, \ldots, N,\\ &(2),\ (3) \text{ and } (4) \text{ are satisfied}\},\end{aligned} \tag{5}$$

with the property $\Delta_{\hat{G}}(q) \in \mathbf{\Delta}_{\hat{G},C}$.

3 Processing the Information

The idea now is to formulate the identification problems as constrained optimization problems. However the set $\mathbf{\Delta}_{\hat{G},C}$ has a complicated (implicit) structure and is not well suited for numerical optimization techniques. In this section it is described

how a set $\Delta_{\hat{G},B}$ can be obtained that is a simple (outer) box–approximation of the set $\Delta_{\hat{G},C}$. For that purpose as an intermediate result first a set $\Delta_{\hat{G},L}$, consisting of linear constraints, is calculated. This set $\Delta_{\hat{G},L}$ outer bounds the set $\Delta_{\hat{G},C}$. Then the set $\Delta_{\hat{G},B}$ is calculated using linear programming. This set $\Delta_{\hat{G},B}$ is a tight outer bounding orthotope of the set $\Delta_{\hat{G},L}$.

3.1 Construction of $\Delta_{\hat{G},L}$

In order to obtain a finite dimensional optimization problem, the number of unknowns in $\Delta_{\hat{G}}(q)$ has to be reduced to some finite number $n+1$. For that reason the (pulse response of the) model error $\Delta_{\hat{G}}(q)$ is split into two parts:

$$\Delta_{\hat{G}}(q) = \bar{\Delta}_{\hat{G}}(q) + \tilde{\Delta}_{\hat{G}}(q),$$

$$\bar{\Delta}_{\hat{G}}(q) = \sum_{k=0}^{n} \delta_{\hat{G}}(k) q^{-k},\ \tilde{\Delta}_{\hat{G}}(q) = \sum_{k=n+1}^{\infty} \delta_{\hat{G}}(k) q^{-k}, \tag{6}$$

where n is a design variable which influence will be discussed later on.

We substitute (2) into (1), divide by $H(q)$ and introduce $\tilde{H}(q) = H^{-1}(q)$, $\tilde{G}(q) = H^{-1}(q)\hat{G}(q)$ and $\tilde{W}(q) = H^{-1}(q)W(q)$, yielding

$$\tilde{H}(q)y(t) = \tilde{G}(q)u(t) + \Delta_{\hat{G}}(q)\tilde{W}(q)u(t) + e(t),$$

$$e(t) \in [e_l(t), e_u(t)]. \tag{7}$$

When calculating various signals a distinction will be made between the known part of a signal and the unknown part. Bounds will be calculated for these unknown parts and their influence will be captured in the bounded output noise. Using (4) in order to calculate the worst–case influence of the initial conditions, we write for the terms appearing in (7),

$$\tilde{H}(q)y(t) = x(t) + a(t),\ \ x(t) = \sum_{k=0}^{t-1} \tilde{h}(k)y(t-k),$$

$$|a(t)| \le \bar{a}(t) = \sum_{k=t}^{\infty} |\tilde{h}(k)|\bar{y},\ \ t = 1, \ldots, N, \tag{8}$$

$$\tilde{G}(q)u(t) = v(t) + b(t),\ \ v(t) = \sum_{k=0}^{t-1} \tilde{g}(k)u(t-k),$$

$$|b(t)| \le \bar{b}(t) = \sum_{k=t}^{\infty} |\tilde{g}(k)|\bar{u},\ \ t = 1, \ldots, N,$$

$$\tilde{W}(q)u(t) = w(t) + c(t),\ \ w(t) = \sum_{k=0}^{t-1} \tilde{w}(k)u(t-k),$$

$$|c(t)| \le \bar{c}(t) = \sum_{k=t}^{\infty} |\tilde{w}(k)|\bar{u},\ \ t = -n+1, \ldots, N,$$

with the additional property that

$$\bar{c}(-t) = \ldots = \bar{c}(0) \ge \bar{c}(1) \ge \ldots \ge \bar{c}(t),$$

$$w(-t) = 0,\ \forall\, t \ge 0.$$

In fact $\bar{a}(t)$, $\bar{b}(t)$ and $\bar{c}(t)$ are decreasing functions of t.

We now obtain

$$\Delta_{\hat{G}}(q)\tilde{W}(q)u(t) = (\tilde{\Delta}_{\hat{G}}(q) + \bar{\Delta}_{\hat{G}}(q))(w(t) + c(t)) =$$

$$= \tilde{\Delta}_{\hat{G}}(q)w(t) + d(t) + f(t),$$

$$d(t) = \tilde{\Delta}_{\hat{G}}(q)c(t),\ \ f(t) = \bar{\Delta}_{\hat{G}}(q)(w(t) + c(t)),$$

where, using (3), $d(t)$ can be bounded by

$$|d(t)| \le \sum_{k=0}^{n} |\delta_{\hat{G}}(k)||c(t-k)| \le$$

$$\le \sum_{k=0}^{n} M\rho^{-k}\bar{c}(t-k) = \bar{d}(t),\ \ t = 1, \ldots, N,$$

which is also a decreasing function of t, and $f(t)$ can be bounded by

$$|f(t)| \le \sum_{k=n+1}^{\infty} |\delta_{\hat{G}}(k)|(|w(t-k)| + |c(t-k)|) \le$$

$$\le \sum_{k=n+1}^{\infty} M\rho^{-k}(|w(t-k)| + \bar{c}(t-k)) =$$

$$= \sum_{k=n+1}^{t-1} M\rho^{-k}(|w(t-k)| + \bar{c}(t-k)) + \sum_{k=t}^{\infty} M\rho^{-k}\bar{c}(0) =$$

$$= \sum_{k=n+1}^{t-1} M\rho^{-k}(|w(t-k)| + \bar{c}(t-k)) +$$

$$+ M\rho^{-t+1}(\rho - 1)^{-1}\bar{c}(0) = \bar{f}(t),\ \ t = 1, \ldots, N,$$

that will generally not vanish for increasing t, especially due to the contribution of $|w(t-k)|$.

With these results equation (7) can be written as

$$x(t) + a(t) = v(t) + b(t) + \tilde{\Delta}_{\hat{G}}(q)w(t) +$$

$$+ d(t) + f(t) + e(t),\ \ t = 1, \ldots, N,$$

$$e(t) \in [e_l(t), e_u(t)],\ |a(t)| \le \bar{a}(t),\ |b(t)| \le \bar{b}(t),$$

$$|d(t)| \le \bar{d}(t),\ |f(t)| \le \bar{f}(t). \tag{9}$$

If we now introduce extended noise bounds

$$\begin{aligned} n_l(t) &= x(t) - v(t) - e_u(t) - \bar{a}(t) - \bar{b}(t) + \\ &\quad - \bar{d}(t) - \bar{f}(t), \\ n_u(t) &= x(t) - v(t) - e_l(t) + \bar{a}(t) + \bar{b}(t) + \\ &\quad + \bar{d}(t) + \bar{f}(t), \end{aligned}$$

then (3) and (9) yield a set of (linear inequality) constraints for the unknown pulse response parameters $\delta_{\hat{G}}(k)$, $\Delta_{\hat{G}}(q) \in \mathbf{\Delta}_{\hat{G},L}$, where

$$\mathbf{\Delta}_{\hat{G},L} = \{\Delta(q) \mid n_l(t) \leq$$

$$\leq \sum_{k=0}^{n} \delta(k) w(t-k) \leq n_u(t),\ t = 1, \ldots, N,$$

$$-M\rho^{-k} \leq \delta(k) \leq M\rho^{-k},\ k = 0, \ldots, \infty\}.$$

The set $\mathbf{\Delta}_{\hat{G},L}$ has been constructed in such a way that $\mathbf{\Delta}_{\hat{G},C} \subseteq \mathbf{\Delta}_{\hat{G},L}$ as each $\Delta(q)$ satisfying the constraints in (5) also satisfies the constraints of the set $\mathbf{\Delta}_{\hat{G},L}$. In general the set $\mathbf{\Delta}_{\hat{G},L}$ will be a fairly tight approximation of the set $\mathbf{\Delta}_{\hat{G},C}$ provided n has been chosen large enough, as in that case the signals $\bar{a}(t)$, etc. remain small (compared to the noise level $e_l(t)$, $e_u(t)$). The set $\mathbf{\Delta}_{\hat{G},L}$ is even identical to $\mathbf{\Delta}_{\hat{G},C}$ if $\bar{u} = 0$, $H(q) = 1$ and $n \geq N-1$ as in that case the signals $\bar{a}(t)$, $\bar{b}(t)$, $\bar{c}(t)$, $\bar{d}(t)$ and $\bar{f}(t)$ are zero $\forall t$.

3.2 Construction of $\mathbf{\Delta}_{\hat{G},B}$

Applying the box–bounding procedure of Milanese and Belforte (1982) we calculate

$$\delta_l(k) = \min_{\Delta \in \mathbf{\Delta}_{\hat{G},L}} \delta(k),$$

$$\delta_u(k) = \max_{\Delta \in \mathbf{\Delta}_{\hat{G},L}} \delta(k),\ \ k = 0, \ldots, n,$$

which requires solving $2(n+1)$ linear programming problems for $n+1$ unknowns subject to $2(N+n+1)$ linear inequality constraints. This can be done using standard linear programming software available. See Luenberger (1984) for an extensive treatment of the linear programming problem and numerical algorithms to solve it. Here we notice the price for choosing a large value of n in (6) as in that case more and larger linear programming problems have to be solved.

We thus obtain the outer–bounding box–description

$$\mathbf{\Delta}_{\hat{G},B} = \{\Delta(q) \mid \delta_l(k) \leq \delta(k) \leq \delta_u(k), k = 0, \ldots, n,$$

$$-M\rho^{-k} \leq \delta(k) \leq M\rho^{-k},\ k = n+1, \ldots, \infty\},$$

which has the property $\mathbf{\Delta}_{\hat{G},L} \subseteq \mathbf{\Delta}_{\hat{G},B}$. The box $\mathbf{\Delta}_{\hat{G},B}$ is tight in the sense that there does not exist a box (with the same orientation) of smaller size which contains the set $\mathbf{\Delta}_{\hat{G},L}$. The set $\mathbf{\Delta}_{\hat{G},B}$ has been calculated on the basis of the set $\mathbf{\Delta}_{\hat{G},L}$ which has in turn been constructed from the data and the prior information. Hence the quality of the data and prior information directly influences the size of $\mathbf{\Delta}_{\hat{G},B}$. If e.g. many measurements are available with a low noise level, the set $\mathbf{\Delta}_{\hat{G},B}$ will be relatively small. The simple box–structure of $\mathbf{\Delta}_{\hat{G},B}$ will be utilized later on when solving the problems of identification in ℓ_1.

4 Identification of an Upper Bound for the ℓ_1-norm of the Model Error

The first problem we focus on is the estimation of an upper bound on the ℓ_1-norm of the model error, $\|\Delta_{\hat{G}}\|_1$. This will only be an upper bound as the true model error is unknown. Using the results of the previous section such an upper bound is given by the following result.

Theorem 4.1

$$\|\Delta_{\hat{G}}\|_1 = \sum_{k=0}^{\infty} |\delta_{\hat{G}}(k)| \leq \max_{\Delta \in \mathbf{\Delta}_{\hat{G},C}} \|\Delta\|_1 \leq$$

$$\leq \max_{\Delta \in \mathbf{\Delta}_{\hat{G},L}} \|\Delta\|_1 \leq \max_{\Delta \in \mathbf{\Delta}_{\hat{G},B}} \|\Delta\|_1 =$$

$$= \sum_{k=0}^{n} \max\{-\delta_l(k), \delta_u(k)\} + \frac{M\rho^{-n}}{\rho - 1}.$$

Proof: The first equality is the definition of the ℓ_1-norm. The inequalities are direct implications of the construction of the sets involved, where $\Delta_{\hat{G}}(q) \in \mathbf{\Delta}_{\hat{G},C} \subseteq \mathbf{\Delta}_{\hat{G},L} \subseteq \mathbf{\Delta}_{\hat{G},B}$. The last equality finally follows from the fact that for any $\Delta(q) \in \mathbf{\Delta}_{\hat{G},B}$,

$$\|\Delta\|_1 = \sum_{k=0}^{\infty} |\delta(k)| = \sum_{k=0}^{n} |\delta(k)| + \sum_{k=n+1}^{\infty} |\delta(k)| \leq$$

$$\leq \sum_{k=0}^{n} \max\{-\delta_l(k), \delta_u(k)\} + \sum_{k=n+1}^{\infty} M\rho^{-k},$$

which yields the desired result by noting that there is a worst–case model error in the set $\mathbf{\Delta}_{\hat{G},B}$ for which the ℓ_1-norm equals this upper bound. □

The upper bound obtained in this way has been calculated using information from the data and the prior information. In general however it is not the minimal upper bound that can (theoretically) be derived from this information. By definition this smallest upper bound is given by $\max_{\Delta \in \mathbf{\Delta}_{\hat{G},C}} \|\Delta\|_1$, which generally can not be calculated. In Hakvoort (1991) an approach has been proposed to calculate $\max_{\Delta \in \mathbf{\Delta}_{\hat{G},L}} \|\Delta\|_1$ although in that paper this set has been defined slightly different. If that procedure is carried out in general a tighter bound for

$\|\Delta_{\hat{G}}\|_1$ will be obtained than given by theorem 4.1, however the procedure is computationally very involved. In section 6 an example is given of the calculation of an upper bound according to theorem 4.1 which shows that this can be carried out with some computational effort.

5 Identification of an ℓ_1-Suboptimal Model

5.1 Introduction

In the previous section we have presented a procedure to determine an upper bound on the ℓ_1-norm of the model error. A natural way to continue is now to determine a new nominal model $\hat{G}_N(q)$ that minimizes the ℓ_1-norm of the worst-case model error. We will consider that problem in this section.

For a fixed weigth $W(q)$ the newly identified model satisfies the equation

$$\hat{G}_N(q) + \Delta_{\hat{G}_N}(q)W(q) = G_0(q) = \\ = \hat{G}(q) + \Delta_{\hat{G}}(q)W(q).$$

Accordingly the new uncertainty set $\mathbf{\Delta}_{\hat{G}_N,L}$ is given by

$$\mathbf{\Delta}_{\hat{G}_N,L} = \{\Delta_N(q) \mid \Delta_N(q) = \Delta(q) + \\ + \left(\hat{G}(q) - \hat{G}_N(q)\right) W^{-1}(q),\ \Delta(q) \in \mathbf{\Delta}_{\hat{G},L}\}.$$

This new set has a dependence on the old nominal model $\hat{G}(q)$ as the prior information (3), which is used in the construction of the sets, is dependent on this old nominal model. The new box-bounding set $\mathbf{\Delta}_{\hat{G}_N,B}$ is now immediately found to be

$$\mathbf{\Delta}_{\hat{G}_N,B} = \{\Delta_N(q) \mid \Delta_N(q) = \Delta(q) + \\ + \left(\hat{G}(q) - \hat{G}_N(q)\right) W^{-1}(q),\ \Delta(q) \in \mathbf{\Delta}_{\hat{G},B}\},$$

which hence does not require the solution of a new set of linear programming problems.

We can formulate our problem of finding an optimal nominal model $\hat{G}_N(q)$ as

$$\hat{G}_N(q) = \arg \min_{\hat{G}'_N \in \mathcal{M}} \max_{\Delta_N \in \mathbf{\Delta}_{\hat{G}'_N,B}} \|\Delta_N\|_1, \qquad (10)$$

where $\mathcal{M}$ is a prespecified model set. By formulating the optimization problem over the set $\mathbf{\Delta}_{\hat{G}'_N,B}$ instead of the set $\mathbf{\Delta}_{\hat{G}'_N,C}$ the results will be suboptimal rather than optimal. We will show that the problem (10) is solvable in two steps. In the first step a high order nominal model is calculated without any model order restrictions. In the second step model reduction in ℓ_1-norm is performed, reducing the high order model to a model of the desired order. This is formalized in the next theorem.

Theorem 5.1 *The optimal model $\hat{G}_N(q)$ defined in (10) satisfies*

$$\hat{G}_N(q) = \arg \min_{\hat{G}'_N \in \mathcal{M}} \left\|(\hat{G}_C - \hat{G}'_N)W^{-1}\right\|_1, \qquad (11)$$

where

$$\hat{G}_C(q) = \arg \min_{\hat{G}'_C \in \mathcal{A}} \max_{\Delta_C \in \mathbf{\Delta}_{\hat{G}'_C,B}} \|\Delta_C\|_1, \qquad (12)$$

and $\mathcal{A}$ denotes the algebra of BIBO stable, linear, time-invariant, causal operators on l_∞.

Proof: Given in the proof of theorem 5.2. □

5.2 The Central Estimate

In this subsection we consider sub-problem (12) of identifying an optimal model $\hat{G}_C(q)$ without any model order restrictions. The solution to this problem is given by the so-called central estimate, as formulated in the next theorem.

Theorem 5.2 *The optimal model $\hat{G}_C(q)$ defined in (12) satisfies*

$$\hat{G}_C(q) = \hat{G}(q) + \hat{\Delta}_C(q)W(q), \qquad (13)$$

where

$$\hat{\Delta}_C(q) = \textstyle\sum_{k=0}^{n} \hat{\delta}_C(k)q^{-k}, \\ \hat{\delta}_C(k) = \tfrac{1}{2}(\delta_l(k) + \delta_u(k)),\ k = 0, \ldots, n.$$

Proof: First we note that $\hat{G}_C(q)$ as given by (13) is stable as it is the sum and product of stable transfer functions. Next, making use of the fact that

$$\Delta(q) + \left(\hat{G}(q) - \hat{G}_C(q)\right) W^{-1}(q) = \Delta(q) - \hat{\Delta}_C(q)$$

and hence the set $\mathbf{\Delta}_{\hat{G}_C,B}$ is a symmetric box with $\Delta_C(q) = 0$ as center, we obtain that for any nominal model $\hat{G}'_N(q)$,

$$\max_{\Delta_N \in \mathbf{\Delta}_{\hat{G}'_N,B}} \|\Delta_N\|_1 = \\ = \max_{\Delta \in \mathbf{\Delta}_{\hat{G},B}} \left\|\Delta + (\hat{G} - \hat{G}'_N)W^{-1}\right\|_1 = \\ \max_{\Delta \in \mathbf{\Delta}_{\hat{G},B}} \left\|\Delta + (\hat{G} - \hat{G}_C)W^{-1} + (\hat{G}_C - \hat{G}'_N)W^{-1}\right\|_1 \\ = \max_{\Delta_C \in \mathbf{\Delta}_{\hat{G}_C,B}} \left\|\Delta_C + (\hat{G}_C - \hat{G}'_N)W^{-1}\right\|_1 = \\ = \max_{\Delta_C \in \mathbf{\Delta}_{\hat{G}_C,B}} \|\Delta_C\|_1 + \left\|(\hat{G}_C - \hat{G}'_N)W^{-1}\right\|_1 \geq \qquad (14) \\ \geq \max_{\Delta_C \in \mathbf{\Delta}_{\hat{G}_C,B}} \|\Delta_C\|_1 =$$

$$= \sum_{k=0}^{n} \frac{1}{2}(\delta_u(k) - \delta_l(k)) + \frac{M\rho^{-n}}{\rho - 1},$$

and equality is achieved by choosing $\hat{G}'_N(q) = \hat{G}_C(q)$, which proves the theorem. Moreover,

$$\min_{\hat{G}'_N \in \mathcal{M}} \max_{\Delta_N \in \mathbf{\Delta}_{\hat{G}'_N,B}} \|\Delta_N\|_1 =$$

$$= \max_{\Delta_C \in \mathbf{\Delta}_{\hat{G}_C,B}} \|\Delta_C\|_1 + \min_{\hat{G}'_N \in \mathcal{M}} \left\|(\hat{G}_C - \hat{G}'_N)W^{-1}\right\|_1$$

which proves theorem 5.1. □

Note that for any new nominal model $\hat{G}_N(q)$ the ℓ_1-norm of the worst-case model error can be calculated using equation (14).

We will shortly discuss the optimality of the central estimate $\hat{G}_C(q)$ when evaluated over the set $\mathbf{\Delta}_{\hat{G},L}$. The following proposition says that this central model is in any norm optimal within a factor 2 when evaluated over this set of linear constraints.

Proposition 5.3 *Consider the central model $\hat{G}_C(q)$ defined in (12), then*

$$\max_{\Delta_C \in \mathbf{\Delta}_{\hat{G}_C,L}} \|\Delta_C\| \leq 2 \min_{\hat{G}'_C \in \mathcal{A}} \max_{\Delta'_C \in \mathbf{\Delta}_{\hat{G}'_C,L}} \|\Delta'_C\|.$$

Proof: First we note that due to the convexity of the set $\mathbf{\Delta}_{\hat{G},L}$ and the fact that $\mathbf{\Delta}_{\hat{G},B}$ is a tight outer bounding orthotope of this set, the central estimate $\hat{\Delta}_C(q)$ is a feasible point of the set $\mathbf{\Delta}_{\hat{G},L}$, i.e. $\hat{\Delta}_C(q) \in \mathbf{\Delta}_{\hat{G},L}$. Next define

$$\hat{G}^*_C(q) = \arg \min_{\hat{G}'_C \in \mathcal{A}} \max_{\Delta'_C \in \mathbf{\Delta}_{\hat{G}'_C,L}} \|\Delta'_C\|$$

and

$$\hat{\Delta}^*_C(q) = \left(\hat{G}^*_C(q) - \hat{G}(q)\right) W^{-1}(q),$$

then

$$\max_{\Delta_C \in \mathbf{\Delta}_{\hat{G}_C,L}} \|\Delta_C\| = \max_{\Delta \in \mathbf{\Delta}_{\hat{G},L}} \left\|\Delta - \hat{\Delta}_C\right\| =$$

$$= \max_{\Delta \in \mathbf{\Delta}_{\hat{G},L}} \left\|\Delta - \hat{\Delta}^*_C + \hat{\Delta}^*_C - \hat{\Delta}_C\right\| \leq$$

$$\leq \max_{\Delta \in \mathbf{\Delta}_{\hat{G},L}} \left\|\Delta - \hat{\Delta}^*_C\right\| + \left\|\hat{\Delta}_C - \hat{\Delta}^*_C\right\| \leq$$

$$\leq 2 \max_{\Delta \in \mathbf{\Delta}_{\hat{G},L}} \left\|\Delta - \hat{\Delta}^*_C\right\| = 2 \max_{\Delta_C \in \mathbf{\Delta}_{\hat{G}^*_C,L}} \|\Delta_C\|.$$

□

Hence the central estimate $\hat{G}_C(q)$ is optimal with respect to the set $\mathbf{\Delta}_{\hat{G},B}$ but only suboptimal with respect to the set $\mathbf{\Delta}_{\hat{G},L}$.

5.3 Model Reduction in ℓ_1-Norm

In this subsection we consider the model reduction in ℓ_1-norm problem (11). To the author's knowledge no results have been published so far that provide a solution for the ℓ_1-model reduction problem. This is in contrast with the H_∞-model reduction problem, which has been extensively studied (Glover, 1984), but only approximately solved. In this section an exact solution is given for the model reduction problem in ℓ_1-norm, but only for a restricted class of estimation models. We restrict to linearly parametrized models, i.e. we consider the model set

$$\mathcal{M}: \quad \hat{G}'_N(q) = \frac{x(q)}{d(q)}, \quad x(q) = \sum_{k=0}^{p} x(k)q^{-k}, \quad (15)$$

where $d(q)$ is an a priori given denominator of order p with all roots within the unit circle and $x(q)$ is the parametrized numerator polynomial.

Next we assume that $\hat{G}_C(q)$ and $W(q)$ are finite dimensional rational transfer functions, given by

$$\hat{G}_C(q) = \frac{g_n(q)}{g_d(q)}, \quad W(q) = \frac{w_n(q)}{w_d(q)}, \quad (16)$$

where $g_n(q)$, $g_d(q)$, $w_n(q)$ and $w_d(q)$ are polynomials in q^{-1}.

Then by introducing the error function $\Delta(q)$ the model reduction problem (11) can be reformulated as,

$$\min_{x,\Delta} \|\Delta\|_1 \text{ s.t.}$$

$$\Delta(q) = \sum_{k=0}^{\infty} \delta(k)q^{-k} = \left(\frac{g_n(q)}{g_d(q)} - \frac{x(q)}{d(q)}\right) \frac{w_d(q)}{w_n(q)},$$

or equivalently

$$\min_{x,\Delta} \sum_{k=0}^{\infty} |\delta(k)| \text{ s.t.}$$

$$g_d(q)d(q)w_n(q)\Delta(q) + g_d(q)w_d(q)x(q) +$$

$$- g_n(q)d(q)w_d(q) = 0. \quad (17)$$

The standard procedure (Lu and Wang, 1988) now is to introduce a new parametrization,

$$\Delta(q) = \Delta_p(q) - \Delta_n(q), \ \delta_p(k) \geq 0, \ \delta_n(k) \geq 0, \ \forall k,$$

which transforms the (infinite dimensional) nonlinear optimization problem (17) into an (infinite dimensional) linear programming problem. The result is given in the next proposition.

Proposition 5.4 *The solution of the model reduction problem in ℓ_1-norm as defined by (11) and (15), (16) is given by the solution of the (infinite dimensional) linear programming problem*

$$\min_{x,\delta_p,\delta_n} \sum_{k=0}^{\infty} (\delta_p(k) + \delta_n(k)) \text{ s.t.}$$

$$g_d(q)d(q)w_n(q)\left(\Delta_p(q) - \Delta_n(q)\right) + \\ + g_d(q)w_d(q)x(q) - g_n(q)d(q)w_d(q) = 0,$$

$$\delta_p(k) \geq 0,\ \delta_n(k) \geq 0,\ k = 0, \ldots, \infty. \qquad (18)$$

Proof: Follows from the fact that in the optimum for each k either $\delta_p(k) = 0$ or $\delta_n(k) = 0$, and therefore $\delta_p(k) + \delta_n(k) = |\delta(k)|$, which makes the optimization problems (17) and (18) identical. □

Now we can explain why the model has been chosen linear in the parameters. In case $d(q)$ needs to be calculated as well, problem (18) would be a very unattractive non–linear programming problem.

For a practical implementation the problem (18) is truncated to a finite dimensional linear programming problem, analogous to the truncation performed in the context of ℓ_1-optimal controller design (McDonald and Pearson, 1991). We choose some (large) value for the truncation parameter l and calculate

$$a(q) = \sum_{k=0}^{l} a(k)q^{-k} = g_d(q)d(q)w_n(q),$$
$$b(q) = \sum_{k=0}^{l} b(k)q^{-k} = g_d(q)w_d(q),$$
$$c(q) = \sum_{k=0}^{l} c(k)q^{-k} = g_n(q)d(q)w_d(q),$$

where l should be at least equal to the maximum order of the transfer functions appearing at the right–hand sides (and consequently $a(q)$, $b(q)$ and $c(q)$ may end with trailing zeros). Then the truncated linear programming problem can be formulated as

$$\min_{x,\delta_p,\delta_n} \sum_{k=0}^{l} (\delta_p(k) + \delta_n(k)) \text{ s.t.}$$

$$\sum_{j=0}^{k} a(k-j)(\delta_p(j) - \delta_n(j)) + \sum_{j=0}^{\min(p,k)} b(j-k)x(j) + \\ - c(k) = 0,\ \delta_p(k) \geq 0,\ \delta_n(k) \geq 0,\ \ k = 0, \ldots, l, \qquad (19)$$

which is a linear programming problem with $p + 2l + 3$ unknowns subject to $3(l+1)$ linear equality and inequality constraints.

It is possible to obtain insight in how close the solution of the truncated problem (19) is to the solution of the infinite dimensional problem (18). This is formalized in the next proposition.

Proposition 5.5 *Let the solution of the truncated problem (19) be given by $x_{t,o}(q)$, $\Delta_{t,o}(q) = \sum_{k=0}^{l} \delta_{t,o}(k)q^{-k}$ and let the solution of the infinite dimensional problem (18) be given by $x_o(q)$, $\Delta_o(q) = \sum_{k=0}^{\infty} \delta_o(k)q^{-k}$, then the optimal criterion value $\|\Delta_o\|_1$ for the infinite dimensional problem is bounded by*

$$\|\Delta_{t,o}\|_1 \leq \|\Delta_o\|_1 \leq \left\| \left(\hat{G}_C - \frac{x_{t,o}}{d} \right) W^{-1} \right\|_1 .$$

Proof: As $x_o(q)$, $\Delta_o(q)$ is a feasible solution for (18), $x_o(q)$, $\tilde{\Delta}_o(q) = \sum_{k=0}^{l} \delta_o(k)q^{-k}$ is a feasible solution for (19). Hence, as $\Delta_{t,o}$ is optimal, $\|\Delta_{t,o}\|_1 \leq \left\|\tilde{\Delta}_o\right\|_1 \leq \|\Delta_o\|_1$, which proves the left–hand inequality. The right–hand inequality is a direct implication of optimality of $x_o(q)$, $\Delta_o(q)$. □

The bounds provided in this proposition can be used to check if the truncation parameter l has been chosen large enough.

The model reduction problem considered and solved in this section requires a fixed denominator. There are several possible ways to arrive at such a denominator. One may for example take the denominator of a model resulting from any other identification procedure, or apply a Laguerre or Kautz model structure (Heuberger, 1991; Wahlberg, 1991). Finally it is also possible to first do Hankelnorm or balanced model reduction and after that tune the numerator in an ℓ_1-optimal way.

6 Example

In this section a simulation example is presented which shows the applicability of the theory developed. First an upper bound will be calculated for the ℓ_1-norm of the model error for a given nominal model. Next an ℓ_1-suboptimal model will be identified by first calculating the central estimate and then applying model reduction to this high–order model.

In figure 1 a Bode diagram is given of the 5th order system $G_0(q)$, the 3rd order nominal model $\hat{G}(q)$ and the 7th order weighting function $W(q)$ that have been chosen (quite randomly). The ℓ_1-norm of the true model error $\Delta_{\hat{G}}$ defined by (2) is equal to 0.8997. Starting from zero–initial conditions ($\bar{u} = 0$), a simulation experiment has been performed with a Gaussian white noise input signal (variance 1) and a uniformly distributed additive output noise ($e(t) \in [-0.3, 0.3]$, $H(q) = 1$, hence the choice of $\bar{y}$ is irrelevant as $\bar{a}(t) = 0$, $\forall t$ in (8)). We chose $M = 2$, $\rho = 1.1$, which are conservative

values. We used 1000 samples for identification purposes and chose $n = 80$, which means that to obtain the set $\Delta_{\hat{G},B}$ 162 linear programming problems had to be solved for 81 unknowns subject to 2162 linear inequality constraints. This has been done on a VAX workstation 3100 using the linear programming software in the Fortran NAG library. Solving one such linear programming problem takes about 4 minutes CPU time.

The result is shown in figure 2, where the calculated upper and lower bound of the pulse response sequence of the model error are plotted together with the pulse response of the true model error. The worst–case ℓ_1-norm found in this way is 1.8787, a factor 2 larger than the ℓ_1-norm of the true model error.

Next we calculated the central estimate and did model reduction in ℓ_1-norm. We reduced the 90th order central estimate $\hat{G}_C(q)$ to a 10th order model $\hat{G}_N(q)$ with all poles a priori fixed to 0.5. In figure 3 a Bode diagram is given of the resulting model. We see that the model bears a great resemblance to the system, except for extreme high frequencies (see phase–plot). The upper bound on the model error of this new nominal model is 1.0437, whereas the ℓ_1-norm of the new true model error $\Delta_{\hat{G}_N}(q)$ is 0.0518, a lot smaller. In this case the model is a lot closer to the true system than expected from the worst–case analysis.

7 Conclusions

An identification procedure has been developed which yields for a given nominal model $\hat{G}(q)$ and weight $W(q)$ an upper bound for the ℓ_1-norm of the model error, starting from measurement data and some a priori information. This prior information consists of a time domain bound on the noise and information about the decay rate of the pulse response of the model error. There are no restrictions on the shape of the input signal. Numerically it requires solving a set of linear programming problems.

Moreover a procedure has been developed to identify a new nominal model $\hat{G}_N(q)$ that is optimal in the sense that it yields a minimal upper bound on the ℓ_1-norm of the model error as computed above. This is performed in two steps, in the first step the central estimate is straightforwardly computed and in the second step model reduction in ℓ_1-norm is performed. For the latter problem a solution is given for the case that the reduced order model is linear in the parameters.

An example showed the applicability of the procedure. It appeared that the estimated optimal model $\hat{G}_N(q)$ may be a lot closer to the true system than expected from the worst–case analysis. This is due to the worst–case character of the analysis (the noise is always assumed to have the worst possible value) and the fact that conservativeness has been introduced in the procedure by bounding the set $\Delta_{\hat{G},L}$ by the set $\Delta_{\hat{G},B}$. A smaller upper bound on the model error may be obtained by using more data and more (and more accurate) prior information. Current investigations show that it is possible to utilize the fact that the noise $e(t)$ is uncorrelated to the input signal $u(t)$ (under open loop conditions) or some external reference signal $r(t)$ (under closed loop conditions). This is done by adding certain linear constraints to the set $\Delta_{\hat{G},L}$.

In the companion paper Hakvoort (1992) the same time domain setting is applied to the problem of worst–case identification in H_∞. In that paper the problem is considered of identifying an upper bound on the H_∞-norm of the model error for a given nominal model. Also the problem is considered of identifying a new nominal model with minimal upper bound on the H_∞-norm of the model error. The problems are solved using linear programming techniques.

This paper has been considering the SISO case. However the MIMO case is basically not more difficult and it is quite straightforward to extend the problem formulation and the solutions presented here to the MIMO case.

References

Chen, J., C.N. Nett and M.K.H. Fan (1992). Optimal non–parametric system identification from arbitrary corrupt finite time–series: a control oriented approach. *Proc. Am. Contr. Conf.*, Chicago, U.S.A., pp. 279–285.

Dahleh, M.A. and J.B. Pearson (1987). ℓ_1-Optimal feedback controllers for MIMO discrete–time systems. *IEEE Trans. Autom. Contr.*, Vol. AC–32, pp. 314–322.

Glover, K. (1984). All optimal Hankel–norm approximations of linear multivariable systems and their L_∞-error bounds. *Int. J. of Contr.*, Vol. 39, pp. 1115–1193.

Hakvoort, R.G. (1991). Identification of an upper bound for the ℓ_1-norm of the model uncertainty. *Sel. Topics in Id., Mod. and Contr.*, Vol. 3, eds. O.H. Bosgra and P.M.J. Van den Hof, Delft Univ. Press, pp. 51–58.

Hakvoort, R.G. (1992). Worst–case system identification in H_∞: error bounds and optimal models.

Sel. Topics in Id., Mod. and Contr., Vol. 5, eds. O.H. Bosgra and P.M.J. Van den Hof, Delft Univ. Press.

Heuberger, P.S.C. (1991). On approximate system identification with system based orthonormal functions. PhD. thesis, Mech. Eng. Syst. and Contr. Group, Delft Univ. of Techn., The Netherlands.

Jacobson, C.A. and C.N. Nett (1991). Worst case system identification in ℓ_1: optimal algorithms and error bounds. *Proc. Am. Contr. Conf.,* Boston, U.S.A., pp. 3152–3157.

Khammash, M. and J.B. Pearson (1991). Performance robustness of discrete-time systems with structured uncertainty. *IEEE Trans. Autom. Contr.,* Vol. AC–36, pp. 398–412.

Lu, L.C. and Y. Wang (1988). A variable transformation method for solving linear absolute–value objective–function problems with linear constraints. *J. of Comp. and Appl. Math.,* Vol. 21, pp. 111–113.

Luenberger, D.G. (1984). *Linear and Nonlinear Programming,* Addison Wesley, U.K., 2nd edition.

Mäkilä, P.M. (1990). On ℓ_1-approximation and identification of discrete–time systems. Techn. rep., Proc. Contr. Lab., Dept. Chem. Eng. Univ. of Åbo, Finland.

Mäkilä, P.M. (1991). Robust identification and Galois–sequences. Techn. rep., Proc. Contr. Lab., Dept. Chem. Eng. University of Åbo, Finland.

McDonald, J.S. and J.B. Pearson (1991). ℓ_1-Optimal control of multivariable systems with output norm constraints. *Automatica,* Vol. 27, pp. 317–329.

Milanese, M. and G. Belforte (1982). Estimation theory and uncertainty intervals evaluation in presence of unknown but bounded errors: linear families of models and estimators. *IEEE Trans. Autom. Contr.,* Vol. AC–27, pp. 408–414.

Tse, D.N.C., M.A. Dahleh and J.N. Tsitsiklis (1991). Optimal asymptotic identification under bounded disturbances. *Proc. 30th Conf. Dec. and Contr.,* Brighton, England, pp. 623–628.

Wahlberg, B. (1991). System identification using Laguerre models. *IEEE Trans. Autom. Contr.,* Vol. AC–36, pp. 551–562.

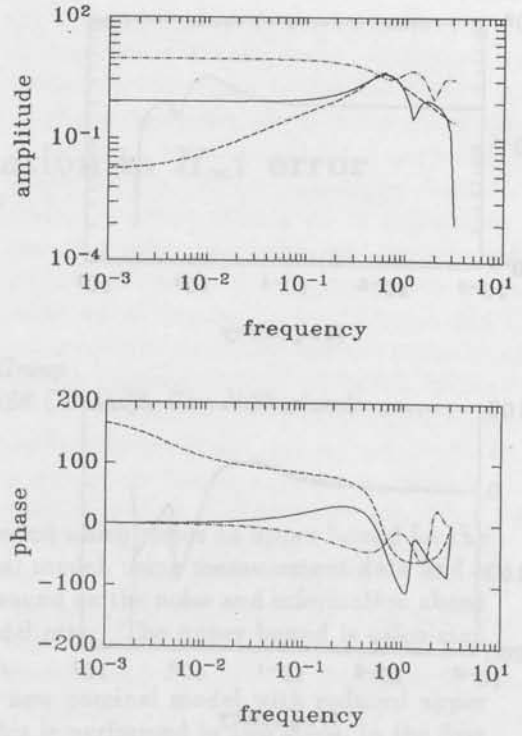

Fig. 1: Bode diagram system $G_0(q)$ (solid), nominal model $\hat{G}(q)$ (dashed) and weight $W(q)$ (dash–dotted)

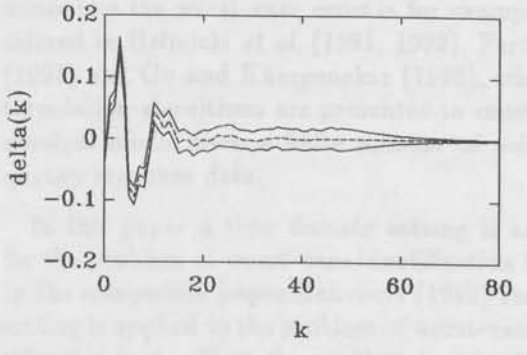

Fig. 2: Pulse response true model error $\delta_{\hat{G}}(k)$ (dashed) and identified lower bound $\delta_l(k)$ and upper bound $\delta_u(k)$ (solid)

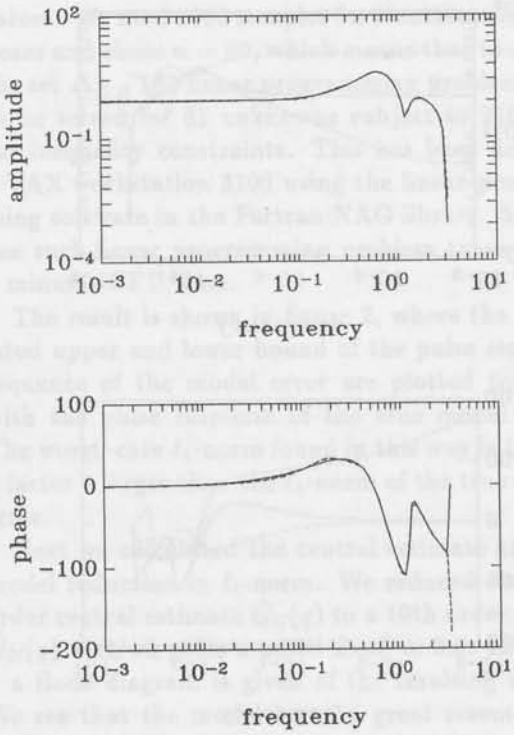

Fig. 3: Bode diagram system $G_0(q)$ (solid) and identified reduced order nominal model $\hat{G}_N(q)$ (dashed)

Selected Topics in Identification, Modelling and Control
Vol. 5, December 1992

Worst–case system identification in H_∞: error bounds and optimal models

Richard G. Hakvoort

Mechanical Engineering Systems and Control Group
Delft University of Technology, Mekelweg 2, 2628 CD Delft, The Netherlands.

Abstract. An identification procedure is developed which yields an upper bound for the H_∞-norm of the model error for a given nominal model, using measurement data and a priori information consisting of a time domain bound on the noise and information about the decay rate of the pulse response of the model error. The upper bound is calculated by solving a set of linear programming problems.
Moreover a procedure is presented to derive a new nominal model with reduced upper bound on the H_∞-norm of the model error. This is performed in two steps, in the first step frequency response data are generated and in the second step a nominal model is identified with a curve–fit procedure, minimizing a maximum absolute value criterion function.

Keywords. worst–case identification, H_∞-norm, linear programming

1 Introduction

H_∞-control theory is able to cope with a system representation consisting of a nominal model and an H_∞-bound on the model error (Maciejowski, 1989). Consequently identification strategies are being developed that are compatible with the H_∞-control design, i.e. yield an upper bound on the H_∞-norm of the model error and an optimal nominal model.

The problem of quantification of model errors is considered by many authors. Bai (1991) and Lamaire *et al.* (1991) investigate procedures for use in adaptive control. Lau *et al.* (1990) and Younce and Rohrs (1992) consider a combined parametric–nonparametric uncertainty approach. In Wahlberg and Ljung (1991) the least–squares algorithm is used to derive frequency domain error bounds. Goodwin *et al.* (1990) and Ninness *et al.* (1992) adopt a stochastic approach to the problem. Finally in Van den Boom *et al.* (1991) and De Vries and Van den Hof (1992) frequency domain error bounds are derived assuming the noise is bounded in the frequency domain.

The problem of identifying a nominal model that minimizes the worst–case error is for example considered in Helmicki *et al.* (1991, 1992), Partington (1991) and Gu and Khargonekar (1992), where interpolation algorithms are presented to construct a nominal model from a finite number of noisy frequency response data.

In this paper a time domain setting is adopted for the problem of worst–case identification in H_∞. In the companion paper Hakvoort (1992) the same setting is applied to the problem of worst–case identification in ℓ_1. First the problem is considered of identifying an upper bound for the H_∞-norm of the model error. A new identification algorithm is developed that yields a frequency dependent bound on the model error for a given nominal model, from which the H_∞-bound can readily be derived. There are no restrictions on the experimental conditions, i.e. the shape of the input signal. The main prior information assumed available is a bound on the pulse response of the model error and a time domain bound on the noise. No model order assumption on the true system is made, nor any statistical

properties of the noise are assumed.

In the identification procedure the model error is parametrized and the actual worst–case perturbation is calculated using linear programming techniques. On the one hand the resulting error bound is a hard bound, which means that the true model error is guaranteed to be smaller than the calculated upper bound, provided the prior information that is used is correct. On the other hand the resulting error bound is proven to be non–conservative under certain conditions, which means that no smaller bound for the model error can be derived from the information available.

Next in the same setting the problem is considered of identifying an H_∞-optimal model, i.e. a nominal model with minimal corresponding error bound. An approximate solution to this problem is obtainable in two steps. In the first step frequency response data are calculated using the notion of central estimate. In the second step a nominal model of the desired order is calculated with a frequency domain curve–fit procedure, minimizing a maximum absolute value criterion.

The outline of the paper is as follows. In the next section the a priori information assumed available is summarized. In section 3 it is described how this information, including the measurement data, is processed, such that it can be used in the worst–case analysis. Then in section 4 a solution is given for the problem of identifying an upper bound for the H_∞-norm of the model error. In section 5 we consider the problem of identifying a new nominal model with minimal error bound. Then in section 6 an example is given of the entire procedure developed. The paper ends with conclusions.

2 A Priori Knowledge

We consider a discrete time, asymptotically stable, linear, time-invariant, causal SISO system $G_0(q) = \sum_{k=0}^{\infty} g_0(k)q^{-k}$ (where q is the forward shift operator) with additive bounded output noise. The input–output behaviour of the plant is assumed to be given by the equation

$$y(t) = G_0(q)u(t) + H(q)e(t), \quad e(t) \in [e_l(t), e_u(t)], \tag{1}$$

where $u(t)$ is the measured input signal, $y(t)$ is the measured output signal, $e(t)$ is the noise, only known to be bounded by $e_l(t)$, $e_u(t)$. $H(q)$ is some (a priori given) noise model, that can be used to bring in a priori knowledge about the frequency distribution of the noise.

For identification purposes we need measurements of the input signal $u(t)$ and the output signal $y(t)$ acting on the system, $t = 1, 2, \ldots, N$. There are no prior restrictions whatsoever on $u(t)$, it may for example be generated in closed loop. Here the situation is considered that one data sequence is available. It is however straightforward to extend to the case that more measurement sequences are available.

We consider the uncertainty configuration

$$G_0(q) = \hat{G}(q) + \Delta_{\hat{G}}(q)W(q), \tag{2}$$

where $\hat{G}(q)$ is some a priori given nominal model, constructed by any identification or modelling procedure and $W(q)$ is an a priori specified fixed weighting function. The system $G_0(q)$ and the model error $\Delta_{\hat{G}}(q)$ are unknown. All transfer functions in (2) are assumed to be stable. We require the weight $W(q)$ and the noise model $H(q)$ to be minimum–phase. Without loss of generality we further require $W(q)$ to be biproper. The (possibly infinite) pulse response sequences of the transfer functions will be denoted by the corresponding lower–case characters. Hence (2) defines the pulse responses g_0, $\hat{g}$, $\delta_{\hat{G}}$ and w.

Next we assume to know an $M > 0$ and $\rho > 1$ such that

$$|\delta_{\hat{G}}(k)| \leq M\rho^{-k}, \quad \forall\, k \geq 0. \tag{3}$$

If more information is available about the pulse response of the model error this may be included as well. It is for example possible to consider an interval bound on $\delta_{\hat{G}}(k)$ independent of the bound for other values of k.

Finally we assume to know upper bounds on past (unmeasured) data $u(t)$ and $y(t)$,

$$|u(t)| \leq \bar{u}, \ |y(t)| \leq \bar{y}, \quad \forall\, t \leq 0. \tag{4}$$

If the system is at rest at $t = 0$, $\bar{u}$ can be chosen to be equal to 0.

Notice that no model order assumption has been imposed on the system $G_0(q)$, neither any statistical properties have been assumed for the noise $e(t)$.

The information obtained so far does not uniquely determine the system $G_0(q)$ and the model error $\Delta_{\hat{G}}(q)$. There is a set of systems $G(q)$ and corresponding model errors $\Delta(q)$ consistent with the data and the prior information. We accordingly define

$$\Delta_{\hat{G},C} = \{\Delta(q) \mid (1),\ t = 1, \ldots, N,$$
$$(2),\ (3) \text{ and } (4) \text{ are satisfied}\}, \tag{5}$$

with the property $\Delta_{\hat{G}}(q) \in \Delta_{\hat{G},C}$.

3 Processing the Information

The idea now is to formulate the identification problems as constrained optimization problems. However the set $\Delta_{\hat{G},C}$ has a complicated (implicit) structure and is not well suited for numerical optimization techniques. In this section it is described how a set $\Delta_{\hat{G},L}$ consisting of a number of linear constraints, can be obtained, that is a close outer approximation of the set $\Delta_{\hat{G},C}$. This set of linear constraints will then be used in numerical optimization techniques, or more specifically linear programming, in order to calculate an upper bound on the H_∞-norm of the model error.

In order to obtain a finite dimensional optimization problem the number of unknowns in $\Delta_{\hat{G}}(q)$ has to be reduced to a finite number $n+1$. For that reason the (pulse response of the) model error $\Delta_{\hat{G}}(q)$ is split into two parts:

$$\Delta_{\hat{G}}(q) = \tilde{\Delta}_{\hat{G}}(q) + \bar{\Delta}_{\hat{G}}(q),$$

$$\tilde{\Delta}_{\hat{G}}(q) = \sum_{k=0}^{n} \delta_{\hat{G}}(k) q^{-k}, \ \bar{\Delta}_{\hat{G}}(q) = \sum_{k=n+1}^{\infty} \delta_{\hat{G}}(k) q^{-k}, \tag{6}$$

where n is a design variable which influence will be discussed later on.

We substitute (2) into (1), divide by $H(q)$ and introduce $\tilde{H}(q) = H^{-1}(q)$, $\tilde{G}(q) = H^{-1}(q)\hat{G}(q)$ and $\tilde{W}(q) = H^{-1}(q)W(q)$, yielding

$$\tilde{H}(q)y(t) = \tilde{G}(q)u(t) + \Delta_{\hat{G}}(q)\tilde{W}(q)u(t) + e(t),$$

$$e(t) \in [e_l(t), e_u(t)]. \tag{7}$$

When calculating various signals a distinction will be made between the known part of a signal and the unknown part. Bounds will be calculated for these unknown parts and their influence will be captured in the bounded output noise. Using (4) in order to calculate the worst-case influence of the initial conditions, we write for the terms appearing in (7),

$$\tilde{H}(q)y(t) = x(t) + a(t), \ \ x(t) = \sum_{k=0}^{t-1} \tilde{h}(k) y(t-k),$$

$$|a(t)| \le \bar{a}(t) = \sum_{k=t}^{\infty} |\tilde{h}(k)| \bar{y}, \ \ t = 1, \ldots, N, \tag{8}$$

$$\tilde{G}(q)u(t) = v(t) + b(t), \ \ v(t) = \sum_{k=0}^{t-1} \tilde{g}(k) u(t-k),$$

$$|b(t)| \le \bar{b}(t) = \sum_{k=t}^{\infty} |\tilde{g}(k)| \bar{u}, \ \ t = 1, \ldots, N,$$

$$\tilde{W}(q)u(t) = w(t) + c(t), \ \ w(t) = \sum_{k=0}^{t-1} \tilde{w}(k) u(t-k),$$

$$|c(t)| \le \bar{c}(t) = \sum_{k=t}^{\infty} |\tilde{w}(k)| \bar{u}, \ \ t = -n+1, \ldots, N,$$

with the additional property that

$$\bar{c}(-t) = \ldots = \bar{c}(0) \ge \bar{c}(1) \ge \ldots \ge \bar{c}(t),$$

$$w(-t) = 0, \ \forall\, t \ge 0.$$

In fact $\bar{a}(t)$, $\bar{b}(t)$ and $\bar{c}(t)$ are decreasing functions of t.

We now obtain

$$\Delta_{\hat{G}}(q)\tilde{W}(q)u(t) = (\tilde{\Delta}_{\hat{G}}(q) + \bar{\Delta}_{\hat{G}}(q))(w(t) + c(t)) =$$

$$= \tilde{\Delta}_{\hat{G}}(q)w(t) + d(t) + f(t),$$

$$d(t) = \tilde{\Delta}_{\hat{G}}(q)c(t), \ \ f(t) = \bar{\Delta}_{\hat{G}}(q)(w(t) + c(t)),$$

where, using (3), $d(t)$ can be bounded by

$$|d(t)| \le \sum_{k=0}^{n} |\delta_{\hat{G}}(k)||c(t-k)| \le$$

$$\le \sum_{k=0}^{n} M\rho^{-k}\bar{c}(t-k) = \bar{d}(t), \ \ t = 1, \ldots, N,$$

which is also a decreasing function of t, and $f(t)$ can be bounded by

$$|f(t)| \le \sum_{k=n+1}^{\infty} |\delta_{\hat{G}}(k)|(|w(t-k)| + |c(t-k)|) \le$$

$$\le \sum_{k=n+1}^{\infty} M\rho^{-k}(|w(t-k)| + \bar{c}(t-k)) =$$

$$= \sum_{k=n+1}^{t-1} M\rho^{-k}(|w(t-k)| + \bar{c}(t-k)) + \sum_{k=t}^{\infty} M\rho^{-k}\bar{c}(0) =$$

$$= \sum_{k=n+1}^{t-1} M\rho^{-k}(|w(t-k)| + \bar{c}(t-k)) +$$

$$+ M\rho^{-t+1}(\rho - 1)^{-1}\bar{c}(0) = \bar{f}(t), \ \ t = 1, \ldots, N,$$

that will generally not vanish for increasing t, especially due to the contribution of $|w(t-k)|$.

With these results equation (7) can be written as

$$x(t) + a(t) = v(t) + b(t) + \tilde{\Delta}_{\hat{G}}(q)w(t) +$$

$$+ d(t) + f(t) + e(t), \ \ t = 1, \ldots, N,$$

$$e(t) \in [e_l(t), e_u(t)], \ |a(t)| \le \bar{a}(t), \ |b(t)| \le \bar{b}(t),$$

$$|d(t)| \le \bar{d}(t), \ |f(t)| \le \bar{f}(t). \tag{9}$$

If we now introduce extended noise bounds

$$\begin{aligned} n_l(t) &= x(t) - v(t) - e_u(t) - \bar{a}(t) - \bar{b}(t) + \\ &\quad - \bar{d}(t) - \bar{f}(t), \\ n_u(t) &= x(t) - v(t) - e_l(t) + \bar{a}(t) + \bar{b}(t) + \\ &\quad + \bar{d}(t) + \bar{f}(t), \end{aligned}$$

then (3) and (9) yield a set of (linear inequality) constraints for the unknown pulse response parameters $\delta_{\hat{G}}(k)$, $\Delta_{\hat{G}}(q) \in \mathbf{\Delta}_{\hat{G},L}$, where

$$\mathbf{\Delta}_{\hat{G},L} = \{\Delta(q) \mid n_l(t) \leq$$

$$\leq \sum_{k=0}^{n} \delta(k) w(t-k) \leq n_u(t),\ t = 1, \ldots, N,$$

$$-M\rho^{-k} \leq \delta(k) \leq M\rho^{-k},\ k = 0, \ldots, \infty\}.$$

The set $\mathbf{\Delta}_{\hat{G},L}$ has been constructed in such a way that $\mathbf{\Delta}_{\hat{G},C} \subseteq \mathbf{\Delta}_{\hat{G},L}$ as each $\Delta(q)$ satisfying the constraints in (5) also satisfies the constraints of the set $\mathbf{\Delta}_{\hat{G},L}$. In general the set $\mathbf{\Delta}_{\hat{G},L}$ will be a fairly tight approximation of the set $\mathbf{\Delta}_{\hat{G},C}$ provided n has been chosen large enough, as in that case the signals $\bar{a}(t)$, etc. remain small (compared to the noise level $e_l(t)$, $e_u(t)$). The set $\mathbf{\Delta}_{\hat{G},L}$ is even identical to $\mathbf{\Delta}_{\hat{G},C}$ if $\bar{u} = 0$, $H(q) = 1$ and $n \geq N - 1$ as in that case the signals $\bar{a}(t)$, $\bar{b}(t)$, $\bar{c}(t)$, $\bar{d}(t)$ and $\bar{f}(t)$ are zero $\forall\, t$. At the price of some conservatism we thus have obtained a set of linear constraints, which contains information from the data and the prior information, that is well suited for usage in numerical optimization techniques.

4 Identification of an Upper Bound for the H_∞-norm of the Model Error

The first problem we focus on is the estimation of an upper bound on the H_∞-norm of the model error. This will only be an upper bound as the true model error is unknown. To derive an upper bound we will use the fact that $\Delta_{\hat{G}} \in \mathbf{\Delta}_{\hat{G},C} \subseteq \mathbf{\Delta}_{\hat{G},L}$ and hence

$$\|\Delta_{\hat{G}}\|_\infty = \sup_{\omega \in [0,\pi]} |\Delta_{\hat{G}}(e^{i\omega})| \leq$$

$$\leq \max_{\Delta \in \mathbf{\Delta}_{\hat{G},C}} \|\Delta\|_\infty \leq \max_{\Delta \in \mathbf{\Delta}_{\hat{G},L}} \|\Delta\|_\infty . \qquad (10)$$

In this section we will focus on deriving a bound for the last term in this formula.

In the sequel we will often use the following lemma.

Lemma 4.1 *Consider the function* $f_m(x) : \mathbb{C} \to \mathbb{R}$, *defined by*

$$f_m(x) = \max_{k=1,\ldots,m} \mathrm{Re}(c_{m,k} x),$$

with $c_{m,k} = e^{2\pi \frac{k}{m} i}$, $k = 1, 2, \ldots, m \geq 3$, *where* $\mathrm{Re}(\cdot)$ *denotes the real part of* $\cdot$, *then*

$$\text{(i)}\ \ f_m(x) \leq |x| \leq \frac{f_m(x)}{\cos\left(\frac{\pi}{m}\right)},$$

$$\text{(ii)}\ \ \lim_{m \to \infty} f_m(x) = |x|.$$

Proof: For any x and any $c_{m,k}$ with $|c_{m,k}| = 1$, $\mathrm{Re}(c_{m,k}x) \leq |c_{m,k}x| \leq |c_{m,k}||x| = |x|$, which proves the left–hand inequality of (i). Further for any x there exist an integer l and $\delta \in [-\frac{\pi}{m}, \frac{\pi}{m})$ such that $x = |x| e^{(2\pi \frac{l}{m} + \delta) i}$, yielding

$$\mathrm{Re}(c_{m,k}x) = \mathrm{Re}(e^{2\pi \frac{k}{m} i} |x| e^{(2\pi \frac{l}{m} + \delta) i}) =$$

$$= |x| \mathrm{Re}(e^{(2\pi \frac{k+l}{m} + \delta) i}) = |x| \cos(2\pi \tfrac{k+l}{m} + \delta).$$

If we now choose $k = k^*$ such that $k^* + l = nm$ for some integer n, we obtain

$$\mathrm{Re}(c_{m,k^*}x) = |x| \cos(2\pi n + \delta) =$$

$$= |x| \cos(\delta) \geq |x| \cos(\tfrac{\pi}{m}) \Leftrightarrow |x| \leq \frac{\mathrm{Re}(c_{m,k^*}x)}{\cos(\frac{\pi}{m})},$$

which proves the right–hand inequality of part (i). Finally part (ii) immediately follows from part (i) for $m \to \infty$. □

Moreover it is easy to show that the bounds in (i) are tight in the sense that there exists an x such that the lower bound becomes equality, and there is an x such that the upper bound becomes equality. The lemma in fact says that the amplitude of a complex number can be calculated approximately by checking a number of different directions in the complex plane.

We will derive bounds for the model error by evaluating $|\Delta(e^{i\omega})|$ for a finite number of frequencies. The behaviour between the frequencies will later on be estimated by means of a worst–case interpolation argument. The set of frequencies is given by

$$\Omega = \{\omega_1, \ldots, \omega_l\},\ 0 \leq \omega_1 < \cdots < \omega_l \leq \pi.$$

For each frequency ω_j the model error is bounded by $\Delta_{\hat{G}}(e^{i\omega_j}) \in \mathbf{\Delta}_{\hat{G},j}$, where

$$\mathbf{\Delta}_{\hat{G},j} = \{\Delta(e^{i\omega_j}) \mid \Delta(q) \in \mathbf{\Delta}_{\hat{G},L}\},$$

which is a convex set as the set $\Delta_{\hat{G},L}$ is convex. Now for each frequency ω_j, $j = 1,\ldots,l$ the frequency domain uncertainty set $\Delta_{\hat{G},j}$ will be evaluated using the tool provided in lemma 4.1. With the $c_{m,k}$ as defined in lemma 4.1 we calculate

$$\mu_k(\omega_j) = \max_{\Delta\in\Delta_{\hat{G},L}} \mathrm{Re}(c_{m,k}\tilde{\Delta}(e^{i\omega_j})) =$$

$$= \max_{\Delta\in\Delta_{\hat{G},L}} \mathrm{Re}(c_{m,k}\sum_{k'=0}^{n}\delta(k')e^{-ik'\omega_j}) =$$

$$= \max_{\Delta\in\Delta_{\hat{G},L}} \sum_{k'=0}^{n}\delta(k')\mathrm{Re}(c_{m,k}e^{-ik'\omega_j}),$$

$$k = 1,\ldots,m,\ j = 1,\ldots,l, \qquad (11)$$

with $\mu_{k+m} = \mu_k$, which requires solving ml linear programming problems for $n+1$ unknowns subject to $2(N+n+1)$ linear inequality constraints (see Luenberger (1984) for details about linear programming). In this way for each frequency ω_j a convex polytope $\mathbf{P}_{m,j}$ in the complex plane is determined,

$$\mathbf{P}_{m,j} = \{\tilde{\Delta}(\omega_j) \mid$$

$$\mathrm{Re}(c_{m,k}\tilde{\Delta}(\omega_j)) \le \mu_k(\omega_j),\ k = 1,\ldots,m\}.$$

The convex polytope has vertices $v_k(\omega_j)$, $k = 1,\ldots,m$ which satisfy

$$\mathrm{Re}(c_{m,k}v_k(\omega_j)) = \mu_k(\omega_j),$$

$$\mathrm{Re}(c_{m,k+1}v_k(\omega_j)) = \mu_{k+1}(\omega_j),\ k = 1,\ldots,m. \qquad (12)$$

This set has the property that it contains the exact uncertainty set for the truncated model error,

$$\{\tilde{\Delta}(e^{i\omega_j}) \mid \Delta(q)\in\Delta_{\hat{G},L}\} \subseteq \mathbf{P}_{m,j},$$

and hence $\tilde{\Delta}_{\hat{G}}(e^{i\omega_j}) \in \mathbf{P}_{m,j}$. Moreover due to the convexity of the exact uncertainty set and the fact that $\lim_{n\to\infty}\tilde{\Delta}(q) = \Delta(q)$ the following convergence property holds,

$$\lim_{n,m\to\infty} \mathbf{P}_{m,j} = \Delta_{\hat{G},j}. \qquad (13)$$

For the case $m = 4$ it simply means that for each frequency ω_j the minimum and maximum of the real and imaginary parts of the model error $\tilde{\Delta}(\omega_j)$ are calculated, which yields a box in the complex plane. Notice that the model error is evaluated in the frequency domain without transforming the measurement data to the frequency domain.

The following lemma establishes the bound obtainable in this way.

Lemma 4.2 *Let $\mu_k(\omega_j)$ be defined by (11) and $v_k(\omega_j)$ by (12), then*

$$\text{(i)}\ \max_k \mu_k(\omega_j) \le \max_{\Delta\in\Delta_{\hat{G},L}} |\tilde{\Delta}(e^{i\omega_j})| \le \max_k |v_k(\omega_j)| \le \max_k \frac{\mu_k(\omega_j)}{\cos(\frac{\pi}{m})},$$

$$\text{(ii)}\ \lim_{m\to\infty}\max_k \mu_k(\omega_j) = \max_{\Delta\in\Delta_{\hat{G},L}} |\tilde{\Delta}(e^{i\omega_j})| = \lim_{m\to\infty}\max_k |v_k(\omega_j)|.$$

Proof: The first inequality in part (i) directly follows from the definition of $\mu_k(\omega_j)$ and lemma 4.1. The second inequality follows from the definition of $v_k(\omega_j)$. The bound defined by the second inequality is the tightest bound that can be derived from the set $\mathbf{P}_{m,j}$. Noting that $\max_k \frac{\mu_k(\omega_j)}{\cos(\frac{\pi}{m})}$ is also an upper bound according to lemma 4.1, we conclude that the third inequality must hold, which proves part (i). Next the statement in part (ii) is proven by noting that the left–hand expression in (i) converges to the right–hand expression for $m \to \infty$. □

In this way we have established a frequency dependent bound on the model error $\tilde{\Delta}_{\hat{G}}(q)$ for a finite number of frequencies. Taking into account the worst–case influence of the tail $\bar{\Delta}_{\hat{G}}(q)$ and of the intersample behaviour of the model error, an upper bound for $\|\Delta_{\hat{G}}\|_\infty$ can readily be derived. Introduce the parameter λ_j for the intersample frequency distance

$$\lambda_j = \max\{\omega_j - \omega_{j-1}, \omega_{j+1} - \omega_j\},\ j = 1,\ldots,l. \qquad (14)$$

Now a bound on the H_∞-norm of the model error is established in the following theorem.

Theorem 4.3 *Let $\beta(n,\Omega,m)$ be defined by*

$$\beta(n,\Omega,m) = \max_j \left\{\max_k |v_k(\omega_j)| + \frac{1}{2}\lambda_j\frac{M\rho}{(\rho-1)^2}\right\} + \frac{M\rho^{-n}}{\rho-1},$$

with $v_k(\omega_j)$ defined by (12) and λ_j by (14) then

$$\text{(i)}\ \|\Delta_{\hat{G}}\|_\infty \le \max_{\Delta\in\Delta_{\hat{G},L}} \|\Delta\|_\infty \le \beta(n,\Omega,m),$$

$$\text{(ii)}\ \lim_{\Omega\to[0,\pi]}\lim_{n,m\to\infty}\beta(n,\Omega,m) = \max_{\Delta\in\Delta_{\hat{G},L}} \|\Delta\|_\infty.$$

Proof: The first inequality in part (i) has been established in (10). Next (6) yields

$$\|\Delta_{\hat{G}}\|_\infty \le \left\|\tilde{\Delta}_{\hat{G}}\right\|_\infty + \left\|\bar{\Delta}_{\hat{G}}\right\|_\infty,$$

and using the fact that the ℓ_1-norm upper bounds the H_∞-norm,

$$\max_{\Delta\in\Delta_{\hat{G},L}} \left\|\bar{\Delta}\right\|_\infty \le \max_{\Delta\in\Delta_{\hat{G},L}} \left\|\bar{\Delta}\right\|_{\ell_1} =$$

$$= \sum_{k=n+1}^{\infty} M\rho^{-k} = \frac{M\rho^{-n}}{\rho - 1}.$$

In De Vries and Van den Hof (1992) it has been shown that assumption (3) implies that

$$\left|\frac{\mathrm{d}\,|\Delta_{\hat{G}}(e^{i\omega})|}{\mathrm{d}\,\omega}\right| \leq \left|\frac{\mathrm{d}\,\Delta_{\hat{G}}(e^{i\omega})}{\mathrm{d}\,\omega}\right| \leq \frac{M\rho}{(\rho-1)^2},\ \forall\omega.$$

Worst–case interpolation considerations now give

$$|\bar{\Delta}_{\hat{G}}(e^{i\omega})| \leq |\bar{\Delta}_{\hat{G}}(e^{i\omega_j})| + \frac{M\rho}{(\rho-1)^2}|\omega_j - \omega|,\ \forall\omega,\omega_j,$$

which in combination with lemma 4.2 yields the desired result (i). Next, using lemma 4.2, we obtain

$$\lim_{\Omega\to[0,\pi]}\lim_{n\to\infty}\max_{j,k}\mu_k(\omega_j) \leq \max_{\Delta\in\mathbf{\Delta}_{\hat{G},L}}\|\Delta\|_\infty \leq$$

$$\lim_{\Omega\to[0,\pi]}\lim_{n\to\infty}\beta(n,\Omega,m) = \lim_{\Omega\to[0,\pi]}\lim_{n\to\infty}\max_{j,k}|v_k(\omega_j)| \leq$$

$$\leq \lim_{\Omega\to[0,\pi]}\lim_{n\to\infty}\max_{j,k}\frac{\mu_k(\omega_j)}{\cos(\frac{\pi}{m})},$$

which proves part (ii) by noting that the right–hand side expression converges to the left–hand side expression for $m \to \infty$. □

We see that the total error in (i) consists of three parts. The first contribution, $\max_k |v_k(\omega_j)|$, consists of a kind of bias part and a kind of variance part. The bias part is the true model error $\bar{\Delta}_{\hat{G}}(e^{i\omega_j})$ and the variance part stems from the fundamental uncertainty in the data (the noise level). The bias part can only be reduced by the choice of a more accurate nominal model. This problem will be considered in the next section. The variance part can basically only be reduced by using more informative data or a priori information (besides a small reduction obtainable by choosing a large value for m). The second contribution to the error in (i), $\frac{1}{2}\lambda_j\frac{M\rho}{(\rho-1)^2}$, comes from the fact that only a finite number of frequencies is evaluated and the inter-sample behaviour is analyzed by some worst–case interpolation argument. This error can be reduced by evaluating more frequencies (which can be done for the same data set) or doing a more careful interpolation analysis, see De Vries and Van den Hof (1992). However it should be emphasized that often this interpolation contribution is much too conservative and that generally a more realistic indication of the model error is obtained by simply linearly interpolating the computed model error between two subsequent frequencies. The third contribution, $\frac{M\rho^{-n}}{\rho-1}$, follows from the truncation in the parametrization of the model error and reduction of this error requires an increase in the computational effort as the size of the linear programming problems increases. However this can also be performed for the same data set.

5 Identification of an H_∞-Suboptimal Model

5.1 Introduction

In the previous section we have presented a procedure to determine an upper bound on the H_∞-norm of the model error. A natural way to continue now is to determine a new nominal model $\hat{G}_N(q)$ that minimizes the H_∞-norm of the worst–case model error. For a fixed weight $W(q)$ the newly identified model satisfies the equation

$$\hat{G}_N(q) + \Delta_{\hat{G}_N}(q)W(q) = G_0(q) =$$
$$= \hat{G}(q) + \Delta_{\hat{G}}(q)W(q).$$

Accordingly the new uncertainty set $\mathbf{\Delta}_{\hat{G}_N,L}$ is given by

$$\mathbf{\Delta}_{\hat{G}_N,L} = \{\Delta_N(q) \mid \Delta_N(q) = \Delta(q) +$$
$$+ \left(\hat{G}(q) - \hat{G}_N(q)\right)W^{-1}(q),\ \Delta(q) \in \mathbf{\Delta}_{\hat{G},L}\},$$

and the new frequency domain uncertainty set by

$$\mathbf{\Delta}_{\hat{G}_N,j} = \{\Delta_N(e^{i\omega_j}) \mid \Delta_N(q) \in \mathbf{\Delta}_{\hat{G}_N,L}\} =$$
$$= \{\Delta_N(\omega_j) \mid \Delta_N(\omega_j) = \Delta(\omega_j) +$$
$$+ \left(\hat{G}(e^{i\omega_j}) - \hat{G}_N(e^{i\omega_j})\right)W^{-1}(e^{i\omega_j}),\ \Delta(\omega_j) \in \mathbf{\Delta}_{\hat{G},j}\}.$$

Notice that this new frequency domain uncertainty set can be evaluated directly using the polytopes $\mathbf{P}_{m,j}$ that already have been calculated. In other words to calculate the worst–case model error for some new nominal model no new set of linear programming problems need to be solved.

Now the problem of finding an optimal nominal model $\hat{G}_N(q)$ can be formulated as

$$\hat{G}_N(q) = \arg\min_{\hat{G}'_N\in\mathcal{M}}\max_{\Delta_N\in\mathbf{\Delta}_{\hat{G}'_N,L}}\|\Delta_N\|_\infty, \qquad (15)$$

where $\mathcal{M}$ is a prespecified model set.

We will present an approximate solution for this identification problem by adopting a two–step procedure. Due to this approximation the resulting model will be suboptimal rather than optimal. In the first step we will calculate the complex–valued so–called central estimate,

$$\hat{G}_C(\omega_j) = \arg\min_{\hat{G}'_C(e^{i\omega_j})}\max_{\Delta_C(\omega_j)\in\mathbf{\Delta}_{\hat{G}'_C,j}}|\Delta_C(\omega_j)|,\ \forall\omega_j \qquad (16)$$

which is in fact a nonparametric frequency domain description of the optimal nominal model. In the second step we will perform frequency domain model fitting in H_∞-norm,

$$\hat{G}_N(q) =$$

$$\arg \min_{\hat{G}'_N \in \mathcal{M}} \max_{\omega \in [0,\pi]} \left| \left(\hat{G}_C(\omega) - \hat{G}'_N(e^{i\omega}) \right) W^{-1}(e^{i\omega}) \right|. \quad (17)$$

The motivation for this two–step procedure lies in the fact that

$$\max_{\omega_j \in [0,\pi]} \max_{\Delta_C(\omega_j) \in \mathbf{\Delta}_{\hat{G}_C,j}} |\Delta_C(\omega_j)| +$$

$$+ \max_{\omega_j \in [0,\pi]} \left| \left(\hat{G}_C(e^{i\omega_j}) - \hat{G}_N(e^{i\omega_j}) \right) W^{-1}(e^{i\omega_j}) \right| \geq$$

$$\geq \max_{\omega \in [0,\pi]} \max_{\Delta_C \in \mathbf{\Delta}_{\hat{G}_C,L}} \left| \Delta_C(e^{i\omega}) + \right.$$

$$\left. + \left(\hat{G}_C(e^{i\omega}) - \hat{G}_N(e^{i\omega}) \right) W^{-1}(e^{i\omega}) \right| =$$

$$= \max_{\omega \in [0,\pi]} \max_{\Delta \in \mathbf{\Delta}_{\hat{G},L}} \left| \Delta(e^{i\omega}) + \left(\hat{G}(e^{i\omega}) - \hat{G}_C(e^{i\omega}) \right) \cdot \right.$$

$$\left. \cdot W^{-1}(e^{i\omega}) + \left(\hat{G}_C(e^{i\omega}) - \hat{G}_N(e^{i\omega}) \right) W^{-1}(e^{i\omega}) \right| =$$

$$= \max_{\omega \in [0,\pi]} \max_{\Delta \in \mathbf{\Delta}_{\hat{G},L}} \left| \Delta(e^{i\omega}) + \right.$$

$$\left. + \left(\hat{G}(e^{i\omega}) - \hat{G}_N(e^{i\omega}) \right) W^{-1}(e^{i\omega}) \right| =$$

$$= \max_{\omega \in [0,\pi]} \max_{\Delta_N \in \mathbf{\Delta}_{\hat{G}_N,L}} |\Delta_N(e^{i\omega})| = \max_{\Delta_N \in \mathbf{\Delta}_{\hat{G}_N,L}} \|\Delta_N\|_\infty .$$

As the two contributions on the left are minimized by (16) resp. (17), also a small (though not necessarily minimal) value on the right is obtained, which is exactly the objective (15). In the next two subsections the two subproblems (16) and (17) are considered respectively.

5.2 The Central Estimate

In this subsection we will consider subproblem (16), the problem of calculating the central estimate for each frequency. We will present a procedure which approximately solves the problem, with the property that asymptotically the exact problem is solved. We utilize the polytopes $\mathbf{P}_{m,j}$ as calculated in the previous section. Define for each $\omega_j \in \Omega$ the (complex–valued) center of the polytope $\mathbf{P}_{m,j}$ as

$$\hat{\Delta}_C(\omega_j) = \arg \min_{\hat{\Delta}'_C(\omega_j)} \max_{\Delta(\omega_j) \in \mathbf{P}_{m,j}} |\Delta(\omega_j) - \hat{\Delta}'_C(\omega_j)| =$$

$$= \arg \min_{\hat{\Delta}'_C(\omega_j)} \max_{k=1,\ldots,m} |v_k(\omega_j) - \hat{\Delta}'_C(\omega_j)|, \quad (18)$$

and define

$$\hat{\hat{G}}_C(\omega_j) = \hat{G}(e^{i\omega_j}) + \hat{\Delta}_C(\omega_j) W(e^{i\omega_j}),\ \omega_j \in \Omega. \quad (19)$$

The intersample frequency behaviour of $\hat{\hat{G}}_C(\omega)$ is defined by linear interpolation,

$$\hat{\hat{G}}_C(\omega) = \frac{\omega - \omega_j}{\omega_{j+1} - \omega_j} \left(\hat{\hat{G}}_C(\omega_{j+1}) - \hat{\hat{G}}_C(\omega_j) \right) +$$

$$+ \hat{\hat{G}}_C(\omega_j),\ \omega \in [\omega_j, \omega_{j+1}]. \quad (20)$$

Then pointwise and uniform convergence to the central estimate can be proven.

Proposition 5.1 *Consider $\hat{G}_C(\omega)$ defined by (16) and $\hat{\hat{G}}_C(\omega)$ defined by (19) and (20) then*

(i) $\lim_{n,m \to \infty} \hat{\hat{G}}_C(\omega_j) = \hat{G}_C(\omega_j),\ j = 1, \ldots, l.$

(ii) $\lim_{\Omega \to [0,\pi]} \lim_{n,m \to \infty} \hat{\hat{G}}_C(\omega) = \hat{G}_C(\omega),\ \omega \in [0,\pi]$

Proof: Using (13) we obtain that for $n, m \to \infty$,

$$\max_{\Delta(\omega_j) \in \mathbf{P}_{m,j}} |\Delta(\omega_j) - \hat{\Delta}_C(\omega_j)| =$$

$$= \max_{\Delta(\omega_j) \in \mathbf{\Delta}_{\hat{G},j}} |\Delta(\omega_j) - \hat{\Delta}_C(\omega_j)| =$$

$$\max_{\Delta(\omega_j) \in \mathbf{\Delta}_{\hat{G},j}} \left| \Delta(\omega_j) + \left(\hat{G}(e^{i\omega_j}) - \hat{\hat{G}}_C(\omega_j) \right) W^{-1}(e^{i\omega_j}) \right|$$

$$= \max_{\Delta_C(\omega_j) \in \mathbf{\Delta}_{\hat{G}_C,j}} |\Delta_C(\omega_j)|,$$

from which we conclude that the minimization (18) is identical to the minimization (16), which proves part (i). The second part follows from the first part and the fact that both $\hat{\hat{G}}_C(\omega)$ and $\hat{G}_C(\omega)$ are continuous functions of ω and have bounded first derivatives. More specifically the left and right first derivatives of the real and imaginary parts are bounded. □

Now the problem remains how to calculate the solution to (18). For the case $m = 4$ it is not so difficult as calculating the center of a box is an easy thing to do. For the general case we present an algorithm to calculate the center of the polytope $\mathbf{P}_{m,j}$ approximately, within any accuracy desired.

Proposition 5.2 *Consider for some $m' \geq 3$ and for some $\omega_j \in \Omega$ the linear programming problem*

$$\min_{\mu_j, a_j, b_j} \mu_j \quad s.t.$$

$$\mathrm{Re}(c_{m',k'} v_k(\omega_j)) - \mathrm{Re}(c_{m',k'}) a_j - Im(c_{m',k'}) b_j \leq \mu_j,$$

$$k = 1, \ldots, m,\ k' = 1, \ldots, m',$$

where $v_k(\omega_j)$ are defined in (12). Let the optimal solution of this LP problem be given by $\mu_{j,o}$, $c(\omega_j) = a_{j,o} + b_{j,o} i$ and let $\hat{\Delta}_C(\omega_j)$ be given by (18), then

(i) $\mu_{j,o} \leq \max_k |v_k(\omega_j) - \hat{\Delta}_C(\omega_j)| \leq$

$$\max_k |v_k(\omega_j) - c(\omega_j)| \leq \frac{\mu_{j,o}}{\cos(\frac{\pi}{m'})},$$

(ii) $\lim_{m' \to \infty} c(\omega_j) = \hat{\Delta}_C(\omega_j)$.

Proof: The second inequality in part (i) arises from the definition of $\hat{\Delta}_C(\omega_j)$. Next we notice that

$$\mathrm{Re}(c_{m',k'}v_k(\omega_j)) - \mathrm{Re}(c_{m',k'})a_j - \mathrm{Im}(c_{m',k'})b_j =$$

$$= \mathrm{Re}(c_{m',k'}(v_k(\omega_j) - a_j - b_j i)),$$

and hence the optimal solution has the property

$$\mu_{j,o} = \max_k f_{m'}(v_k(\omega_j) - c(\omega_j)),$$

which with lemma 4.1 yields the third inequality. Finally optimality of $c(\omega_j)$ implies that for some k^*,

$$f_{m'}(v_{k^*}(\omega_j) - \hat{\Delta}_C(\omega_j)) \geq \mu_{j,o},$$

which again with lemma 4.1 yields the first inequality of part (i). For $m' \to \infty$ the right–hand side in (i) converges to the left–hand side and hence, as $\hat{\Delta}_C(\omega_j)$ is a unique complex number, $c(\omega_j)$ converges to $\hat{\Delta}_C(\omega_j)$, which proves part (ii). □

This means that for m' large enough the complex number $c(\omega_j)$ resulting from the linear programming problem presented here is a very good approximation of $\hat{\Delta}_C(\omega_j)$, the center of the polytope $\mathbf{P}_{m,j}$. It can be used to calculate $\hat{\hat{G}}_C(\omega_j)$ in (19), which in turn is a very good approximation of the exact central estimate $\hat{G}_C(\omega_j)$ provided that n and m have been chosen large enough.

5.3 Frequency Domain Curve Fitting

In this subsection we consider subproblem (17), the problem of H_∞-optimal model fitting. We will present a procedure which approximately solves this problem. Asymptotically it will be shown to be an exact solution for (17). The procedure consists of fitting a parametrized transfer function to a finite number of frequency response data minimizing a maximum absolute value criterion function, which is closely related to the H_∞-norm optimization criterion. The intersample frequency behaviour of the resulting model will be bounded.

We restrict to linearly parametrized models, that is we consider the model set

$$\mathcal{M} : \hat{G}'_N(q) = \frac{x(q)}{d(q)}, \quad x(q) = \sum_{k=0}^{p} x(k)q^{-k},$$

$$-x_m \leq x(k) \leq x_m, \ \forall k,$$

where $d(q)$ is an a priori given denominator of order p with all roots within the unit circle and the parameters in the numerator are bounded as specified.

Let there be given a continuous complex valued frequency response function $\hat{G}_C(\omega)$ such that the (left and right) first derivatives of its real and imaginary parts are bounded. With some abuse of terminology we simply say that the first derivative of $\hat{G}_C(\omega)$ is bounded. We consider the objective function

$$\hat{\hat{G}}_N(q) =$$

$$\arg \min_{\hat{G}'_N \in \mathcal{M}} \max_{\omega_j \in \Omega} \left| (\hat{G}_C(\omega_j) - \hat{G}'_N(e^{i\omega_j}))W^{-1}(e^{i\omega_j}) \right|, \tag{21}$$

which implies that in the optimization use is made of only a finite number of frequencies. The nominal model $\hat{\hat{G}}_N(q)$ defined by (21) has a bounded intersample behaviour and is moreover asymptotically equal to the optimal model $\hat{G}_N(q)$ as formulated in the next theorem.

Theorem 5.3 *Consider the optimal model $\hat{G}_N(q)$ defined by (17) and $\hat{\hat{G}}_N(q)$ defined by (21).*

(i) *The H_∞-norm of $\hat{\hat{G}}_N$ is a priori bounded by*

$$\left\| \hat{\hat{G}}_N \right\|_\infty \leq \frac{(p+1)x_m}{\inf_{|z|=1} |d(z)|},$$

(ii) $\lim_{\Omega \to [0,\pi]} \hat{\hat{G}}_N(q) = \hat{G}_N(q)$,

where it is allowed that $x_m \to \infty$ provided that $(\max_j \lambda_j)x_m \to 0$, where λ_j has been defined in (14).

Proof: Let $\hat{\hat{G}}_N(q) = \frac{x_o(q)}{d(q)}$, then

$$\left\| \hat{\hat{G}}_N \right\|_\infty = \sup_{|z|=1} \left| \frac{x_o(z)}{d(z)} \right| \leq$$

$$\leq \frac{\sup_{|z|=1} \left| \sum_{k=0}^{p} x_o(k)z^{-k} \right|}{\inf_{|z|=1} |d(z)|} \leq \frac{(p+1)x_m}{\inf_{|z|=1} |d(z)|},$$

which proves part (i). Next,

$$\left| \frac{\mathrm{d}\, x_o(e^{i\omega})}{\mathrm{d}\,\omega} \right| = \left| \frac{\mathrm{d} \sum_{k=0}^{p} x_o(k)e^{-i\omega k}}{\mathrm{d}\,\omega} \right| =$$

$$= \left| \sum_{k=0}^{p} x_o(k)(-ik)e^{-i\omega k} \right| \leq$$

$$\leq \sum_{k=0}^{p} |k x_o(k)| \leq x_m \sum_{k=0}^{p} k = x_m \frac{p(p+1)}{2},$$

yielding

$$\left|\frac{\mathrm{d}\,\hat{\hat{G}}_N(e^{i\omega})}{\mathrm{d}\,\omega}\right| = \left|\frac{\mathrm{d}\,\frac{x_o(e^{i\omega})}{d(e^{i\omega})}}{\mathrm{d}\,\omega}\right| =$$

$$= \left|d^{-2}(e^{i\omega})\left(d(e^{i\omega})\frac{\mathrm{d}\,x_o(e^{i\omega})}{\mathrm{d}\,\omega} - x_o(e^{i\omega})\frac{\mathrm{d}\,d(e^{i\omega})}{\mathrm{d}\,\omega}\right)\right| \leq$$

$$\leq \left|d^{-1}(e^{i\omega})\right|\left|\frac{\mathrm{d}\,x_o(e^{i\omega})}{\mathrm{d}\,\omega}\right| +$$

$$+ \left|d^{-2}(e^{i\omega})\frac{\mathrm{d}\,d(e^{i\omega})}{\mathrm{d}\,\omega}\right|\left|x_o(e^{i\omega})\right| \leq$$

$$\leq x_m\frac{p(p+1)}{2}\left\|d^{-1}\right\|_\infty + x_m(p+1)\left\|d^{-2}\frac{\mathrm{d}\,d}{\mathrm{d}\,\omega}\right\|_\infty, \ \forall\omega.$$

Hence,

$$\left|\frac{\mathrm{d}\left|\left(\hat{G}_C(\omega) - \hat{\hat{G}}_N(e^{i\omega})\right)W^{-1}(e^{i\omega})\right|}{\mathrm{d}\,\omega}\right| \leq$$

$$\leq \left|\frac{\mathrm{d}\,\hat{G}_C(\omega)W^{-1}(e^{i\omega})}{\mathrm{d}\,\omega}\right| + \left|\frac{\mathrm{d}\,\hat{\hat{G}}_N(e^{i\omega})}{\mathrm{d}\,\omega}W^{-1}(e^{i\omega})\right| +$$

$$+ \left|\hat{\hat{G}}_N(e^{i\omega})\frac{\mathrm{d}\,W^{-1}(e^{i\omega})}{\mathrm{d}\,\omega}\right| \leq c_1 + c_2x_m, \ \forall\omega,$$

for some constants c_1 and c_2. Applying the same interpolation argument as in theorem 4.3 we obtain

$$\max_{\omega\in[0,\pi]}\left|\left(\hat{G}_C(\omega) - \hat{\hat{G}}_N(e^{i\omega})\right)W^{-1}(e^{i\omega})\right| \leq$$

$$\leq \max_j\left\{\left|\left(\hat{G}_C(\omega_j) - \hat{\hat{G}}_N(e^{i\omega_j})\right)W^{-1}(e^{i\omega_j})\right| + \right.$$

$$\left. + \frac{1}{2}\lambda_j(c_1 + c_2x_m)\right\},$$

which yields the desired result (ii) by noting that the first quantity on the right is minimized in the interpolation procedure (21) and the second quantity converges to zero for $\lambda_j,\ \lambda_jx_m \to 0$. □

Finally the problem remains how to calculate the solution to problem (21). We propose a linear programming procedure which yields the desired result within any accuracy desired.

Proposition 5.4 *Consider for some $m'' \geq 3$ the linear programming problem*

$$\min_{\mu,x(k)} \mu \ s.t.$$

$$\mathrm{Re}\left(c_{m'',k''}\hat{G}_C(\omega_j)W^{-1}(e^{i\omega_j})\right) +$$

$$- \sum_{k=0}^{p} x(k)\mathrm{Re}\left(c_{m'',k''}\frac{e^{-i\omega_jk}}{d(e^{i\omega_j})}W^{-1}(e^{i\omega_j})\right) \leq \mu,$$

$$k'' = 1,\ldots,m'',\ j = 1,\ldots,l,$$

$$-x_m(k) \leq x(k) \leq x_m(k),\ k = 0,\ldots,p,$$

and let the optimal solution be given by μ_o, $x_o(k)$. Moreover consider $\hat{\hat{G}}_N(q)$ defined by (21), then

(i) $\mu_o \leq \max_{\omega_j\in\Omega}\left|(\hat{G}_C(\omega_j) - \hat{\hat{G}}_N(e^{i\omega_j}))W^{-1}(e^{i\omega_j})\right| \leq$

$$\max_{\omega_j\in\Omega}\left|\left(\hat{G}_C(\omega_j) - \frac{\sum_{k=0}^{p} x_o(k)e^{-i\omega_jk}}{d(e^{i\omega_j})}\right)W^{-1}(e^{i\omega_j})\right|$$

$$\leq \frac{\mu_o}{\cos(\frac{\pi}{m''})},$$

(ii) $\lim_{m''\to\infty}\dfrac{\sum_{k=0}^{p} x_o(k)q^{-k}}{d(q)} = \hat{\hat{G}}_N(q).$

Proof: The second inequality in part (i) arises from the definition of $\hat{\hat{G}}_N(\omega_j)$. Next we notice that

$$\mathrm{Re}\left(c_{m'',k''}\hat{G}_C(\omega_j)W^{-1}(e^{i\omega_j}\right) +$$

$$- \sum_{k=0}^{p} x(k)\mathrm{Re}\left(c_{m'',k''}\frac{e^{-i\omega_jk}}{d(e^{i\omega_j})}W^{-1}(e^{i\omega_j})\right) =$$

$$\mathrm{Re}\left(c_{m'',k''}\left(\hat{G}_C(\omega_j) - \frac{\sum_{k=0}^{p} x(k)e^{-i\omega_jk}}{d(e^{i\omega_j})}\right)W^{-1}(e^{i\omega_j})\right),$$

and hence the optimal solution has the property

$$\mu_o = \max_{\omega_j\in\Omega}$$

$$f_{m''}\left(\left(\hat{G}_C(\omega_j) - \frac{\sum_{k=0}^{p} x_o(k)e^{-i\omega_jk}}{d(e^{i\omega_j})}\right)W^{-1}(e^{i\omega_j})\right),$$

which yields the third inequality by applying lemma 4.1. Finally, optimality of $x_o(k)$ implies that for some j^*,

$$f_{m''}\left(\left(\hat{G}_C(\omega_{j^*}) - \hat{\hat{G}}_N(e^{i\omega_{j^*}})\right)W^{-1}(e^{i\omega_{j^*}})\right) \geq \mu_o,$$

which yields the first inequality of part (i) by again applying lemma 4.1. For $m'' \to \infty$ the right–hand side in (i) converges to the left–hand side, which proves part (ii). □

This means that for m'' large enough the estimated model is a very good approximation of the curve fit model $\hat{\hat{G}}_N(q)$, which in turn is a very good approximation of the H_∞-optimal model $\hat{G}_N(q)$ if enough frequencies are used in the curve fitting procedure.

6 Example

In this section an example is presented which shows the applicability of the theory developed. First for a given nominal model we evaluate the model error in the frequency domain, yielding an upper bound on the H_∞-norm of the model error. Next we identify an H_∞-suboptimal model by first calculating the central estimate and then applying the curve fitting algorithm derived in the previous section.

In figure 1 a Bode diagram is given of the 5th order system $G_0(q)$, the 3rd order nominal model $\hat{G}(q)$ and the 7th order weighting function $W(q)$ that have been chosen (quite randomly). Starting from zero initial conditions ($\bar{u} = 0$), a simulation experiment has been performed with a Gaussian white noise input signal (variance 1) and a uniformly distributed additive output noise ($e(t) \in [-0.3, 0.3]$, $H(q) = 1$, hence the choice of $\bar{y}$ is irrelevant as $\bar{a}(t) = 0$, $\forall t$ in (8)). We chose $M = 2$, $\rho = 1.1$, which is a very conservative choice. We used 1000 samples for identification purposes and chose $n = 130$ (which implies that the contribution of $\bar{\Delta}(q)$ to the model error is almost zero) and $m = 4$. We calculated the worst-case model error for 100 frequencies logarithmically distributed between 0.01 and π. This means that 400 linear programming problems had to be solved for 131 unknowns subject to 2262 linear inequality constraints. This has been done on a VAX workstation 3100 using the linear programming software in the Fortran NAG library. Solving one such linear programming problem takes about 4 minutes CPU time.

The result is shown in the Nyquist plot of figure 2, where the calculated uncertainty regions are shown, together with the true model error $\Delta_{\hat{G}}(q)$, which is of course inside the uncertainty regions. In figure 3 the upper bound on the amplitude of the model error is plotted in a Bode diagram together with the amplitude of the true model error. The influence of the interpolation contribution to the worst-case model error in theorem 4.3 has not been taken into account here. The H_∞-norm of the worst-case model error is 0.65 whereas the H_∞-norm of the true model error is 0.57. We conclude that a tight error bound has been obtained.

Next we calculated the central estimate and performed curve fitting with maximum absolute value criterion as described in section 5.3. The central estimate is easily obtained by calculating the centers of the boxes in figure 2. The curve fit model has been chosen a 10th order model with all poles a priori fixed to 0.5. We chose $m'' = 8$. Hence one linear programming problem had to be solved for 12 unknowns subject to 800 inequality constraints, which took a few seconds computing time.

In figure 4 the amplitude of the worst-case model error for the new nominal model is shown in a Bode diagram together with the amplitude of $\Delta_{\hat{G}_N}(q)$, the new true model error. In figure 5 a Bode diagram is shown of the new nominal model and the true system, which appear to be very close. The H_∞-norm of the worst-case model error of the new nominal model is 0.32 whereas the H_∞-norm of the true model error is 0.02. We conclude that the worst-case error is not tight for this new nominal model. In this case the nominal model is much closer to the true system than expected from the worst-case analysis.

7 Conclusions

An identification procedure has been developed which yields an upper bound for the H_∞-norm of the model error, starting from measurement data and some a priori information. This prior information consists of a time domain bound on the noise and information about the decay rate of the pulse response of the model error. There are no restrictions on the shape of the input signal. Numerically it requires solving a set of linear programming problems. The bound is a guaranteed upper bound on the model error and moreover under certain conditions it is non-conservative, i.e. no smaller bound can be obtained using the information available.

Also a procedure has been developed to identify a new nominal model $\hat{G}_N(q)$ in such a way that the upper bound on the H_∞-norm of the model error is small. This is performed in two steps. In the first step the central estimate is computed and in the second step curve fitting in H_∞-norm is performed. This curve fitting problem can again be solved using linear programming if the nominal model is linear in the parameters.

In an example the complete procedure has been illustrated. Tight frequency domain error bounds were obtained with some computational effort. It appeared that the estimated nominal model $\hat{G}_N(q)$ may be a lot closer to the true system than indicated by the error bounds. This is mainly due to the worst-case character of the analysis, the noise is always assumed to have the worst possible value. Current investigations show that the error bounds can be reduced by utilizing more prior information about the noise, more specifically the fact that the noise is known to be uncorrelated to the input signal (in open loop) or some external reference signal

(in closed loop). Current research also focusses on extensions to the MIMO case and extending the curve fit algorithm of section 5.3 to the case of a fully parametrized transfer function.

Acknowledgement

The author gratefully acknowledges the helpful comments of Douwe de Vries of the Delft University of Technology.

References

Bai, E. (1991). Adaptive quantification of model uncertainties by rational approximation. *IEEE Trans. Autom. Contr.*, Vol. AC–36, pp. 441–453.

De Vries, D.K. and P.M.J. Van den Hof (1992). Quantification of model uncertainty from data: input design, interpolation and connection with robust control design specifications. *Proc. Am. Contr. Conf.*, Chicago, U.S.A., pp. 3170–3175.

Goodwin, G.C., M. Gevers and B.M. Ninness (1990). Optimal model order selection and estimation of model uncertainty for identification with finite data. *Proc. Conf. Dec. Contr.*, Honolulu, U.S.A., pp. 285–290.

Gu, G. and P.P. Khargonekar (1992). A class of algorithms for identification in H_∞. *Automatica*, Vol. 28, pp. 299–312.

Hakvoort, R.G. (1992). Worst–case system identification in ℓ_1: error bounds, optimal models and model reduction. *Sel. Topics in Id., Mod. and Contr.*, Vol. 5, eds. O.H. Bosgra and P.M.J. Van den Hof, Delft Univ. Press. Also to appear in *Proc. Conf. Dec. Contr.*, Tucson, U.S.A., 1992.

Helmicki, A.J., C.A. Jacobson and C.N. Nett (1991). Control oriented system identification: a worst–case/deterministic approach in H_∞. *IEEE Trans. Autom. Contr.*, Vol. AC–36, pp. 1163–1176.

Helmicki, A.J., C.A. Jacobson and C.N. Nett (1992). Worst–case/deterministic identification in H_∞: the continous–time case. *IEEE Trans. Autom. Contr.*, Vol. AC–37, pp. 604–610.

Lamaire, R.O., L. Valavani, M. Athans and G. Stein (1991). A frequency domain estimator for use in adaptive control systems. *Automatica*, Vol. 27, pp. 23–38.

Lau, M., R. Kosut and S. Boyd (1990). Parameter set estimation of systems with uncertain nonparametric dynamics and disturbances. *Proc. Conf. Dec. Contr.*, Honolulu, U.S.A., pp. 3162–3167.

Luenberger, D.G. (1984). *Linear and Nonlinear Programming*, Addison Wesley, U.K., 2nd edition.

Maciejowski, J.M. (1989). *Multivariable Feedback Design*, Addison Wesley, U.K.

Ninness, B.M. and G.C. Goodwin (1992). Robust frequency response estimation accounting for noise and undermodelling. *Proc. Am. Contr. Conf.*, Chicago, U.S.A., pp. 2847–2851.

Partington, J.R. (1991). Robust identification and interpolation in H_∞. *Int. J. of Contr.*, Vol. 54, pp. 1281–1290.

Van den Boom, T., M. Klompstra and A. Daamen (1991). System identification for H_∞-robust control design. *Proc. 9th IFAC Symp. Ident. and Syst. Par. Est.*, Budapest, Hungary, pp. 1431–1436.

Wahlberg, B. and L. Ljung (1991). On estimation of transfer function error bounds. *Proc. European Contr. Conf.*, Grenoble, France, pp. 1378–1383.

Younce, R.C. and C.E. Rohrs (1992). Identification with nonparametric uncertainty. *IEEE Trans. Autom. Contr.*, Vol. AC–37, pp. 715–728.

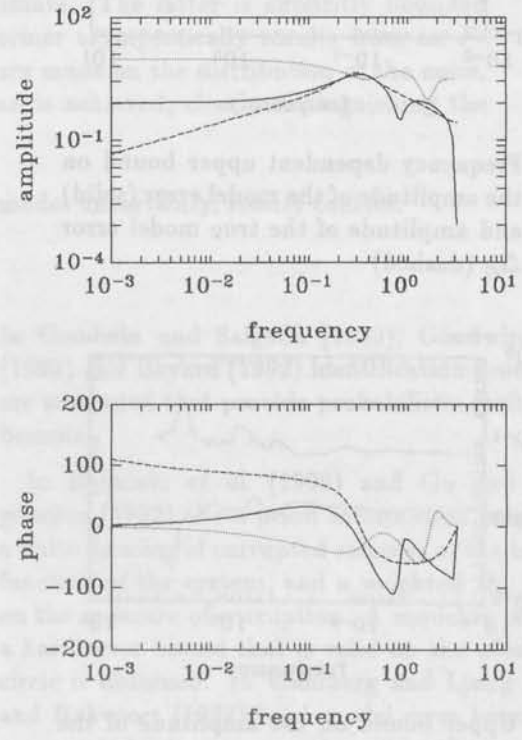

Fig. 1: Bode diagram system G_0 (solid), nominal model $\hat{G}$ (dashed) and weight W (dotted)

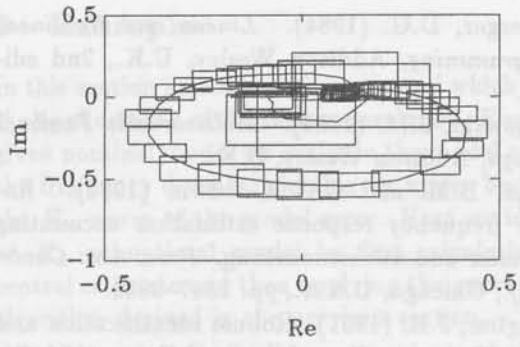

Fig. 2: Nyquist diagram frequency dependent uncertainty regions $\mathbf{P}_{m,j}$ (boxes) and true model error $\Delta_{\hat{G}}$ (solid line)

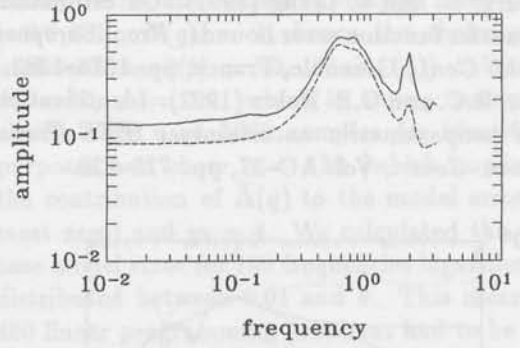

Fig. 3: Frequency dependent upper bound on the amplitude of the model error (solid) and amplitude of the true model error $\Delta_{\hat{G}}$ (dashed)

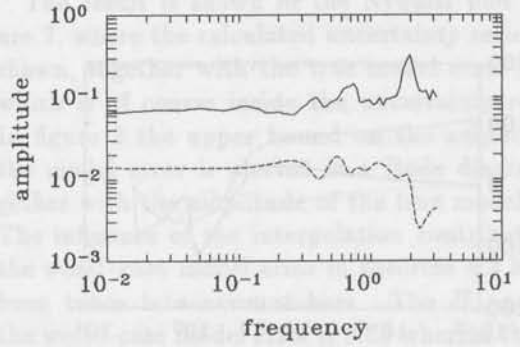

Fig. 4: Upper bound on the amplitude of the model error for the new nominal model (solid) and amplitude of the new true model error $\Delta_{\hat{G}_N}$ (dashed)

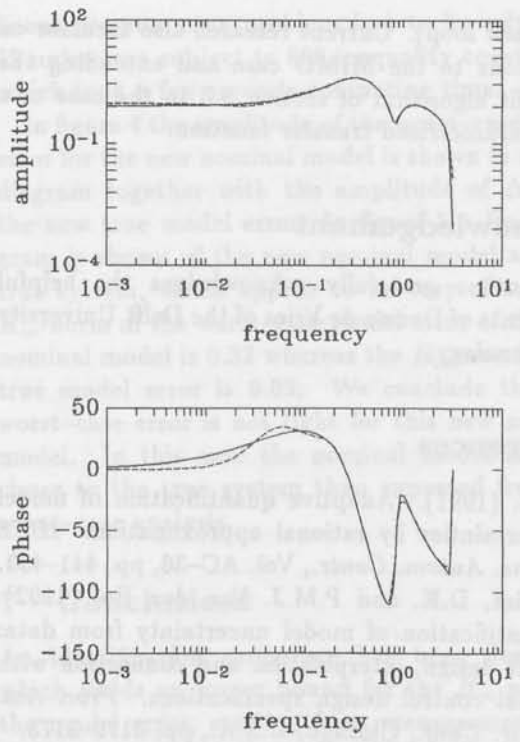

Fig. 5: Bode diagram system G_0 (solid) and identified new nominal model $\hat{G}_N$ (dashed)

Selected Topics in Identification, Modelling and Control
Vol. 5, December 1992

A mixed deterministic-probabilistic approach for quantifying uncertainty in transfer function estimation

Douwe K. de Vries and Paul M.J. Van den Hof

Mechanical Engineering, Systems and Control Group,
Delft University of Technology, Mekelweg 2, 2628 CD Delft, The Netherlands.

Abstract. A procedure is presented to obtain an estimate of the transfer function of a linear system together with an upper bound on the error, using only limited a priori information on the data generating process. By employing a periodic input signal, together with a non-parametric Emperical Transfer Function Estimate (ETFE) over each period, and by averaging over a number of estimates, the statistics of the resulting model asymptotically can be obtained from the data. The model error consists of two parts: a probabilistic part, due to the stochastic noise disturbance on the data, and a deterministic part, due to the bias in the estimate. The latter is explicitly bounded with a deterministic error bound, while the former asymptotically results from an F-distribution. For this analysis no assumptions are made on the distribution of the noise. A mixed deterministic-probabilistic error bound is achieved, clearly distinguishing the different sources of uncertainty.

Keywords. Identification, frequency domain, model uncertainty, robust control.

1 Introduction

In the systems and control community there is a growing interest in merging the problems of system identification and (robust) control system design. This interest is based on the conviction that, in many situations, models obtained from process experiments will be used as a basis for control system design. On the other hand, in model-based robust control design, models and model uncertainties have to be available that are essentially provided by, or at least validated by, measurement data from the process.

Recently several approaches to the identification problem have been presented, considering the identification in view of the control design. By far the most attention has been paid to the construction of deterministic (hard) error bounds, see e.g. Helmicki *et al.* (1990), Gu and Khargonekar (1992), Wahlberg and Ljung (1991) and Hakvoort (1992). In Goodwin and Salgado (1989), Goodwin *et al.* (1992) and Bayard (1992) identification procedures are presented that provide probabilistic (soft) error bounds.

In Helmicki *et al.* (1990) and Gu and Khargonekar (1992) the a priori information consists of a finite number of corrupted samples of the transfer function of the system, and a weighted H_∞ bound on the measure of corruption. A model in H_∞ and a hard error bound that is valid on the whole unit circle is obtained. In Wahlberg and Ljung (1991) and Hakvoort (1992) hard model error bounds are constructed using an upper bound on the amplitude of the noise in the time domain. In Wahlberg and Ljung (1991) the hard error bound on the system's transfer function is obtained using a least squares FIR estimate and parameter set estimation techniques, whereas in Hakvoort (1992) the bound is obtained by directly calculating the worst-case uncertainty from the time domain data using linear

programming. In deVries and Van den Hof (1992a) a frequency domain estimation procedure based on the ETFE is proposed, by which a frequency dependent hard quantification of the model uncertainty can be obtained for a prespecified nominal model. The a priori information on the noise that is necessary (a hard bound on the DFT of the noise) however will be hard to obtain in practice.

In Goodwin and Salgado (1989) and Goodwin *et al.* (1992) a stochastic embedding approach is used. The distribution of the error is assumed to be known, up to a number of free parameters. The free parameters of the distribution are estimated from the data, together with a least squares estimate of the system. The model error due to undermodelling is represented as a zero mean stochastic process. This results in a probabilistic description of the error in the least squares estimate. In Bayard (1992) a periodic input signal is used, and an ETFE is made over each period of the input signal. The average over a number of these ETFE's provides the final estimate, and a probabilistic describtion of the error in this final estimate is presented. However, it is assumed that the noise is normally distributed, that the noise filter is known, and that the steady-state situation is reached before experimental data is taken.

In this paper we will use a stochastic description of the disturbances, based on the same and, in the authors' opinion, definitely sound arguments that are given in Goodwin *et al.* (1992). We will however consider the errors due to undermodelling, as deterministic. The input signal is also considered to be deterministic, because the input signal is known in the measurement interval. Hence, for the influence of the noise we will use a probabilistic description, whereas the errors due to undermodelling and unknown past inputs will be bounded with deterministic bounds. This constitutes the main deviation from existing methods: in the current literature on identification with error bounds either both the errors due to undermodelling and noise are considered as being deterministic, or they are both considered as being stochastic. As a result, the approach presented in this paper will yield error bounds that consist of elements with a probabilistic nature, and elements with a deterministic nature. We will call this kind of error bound a mixed deterministic-probabilistic error bound.

In this paper the ETFE is used to obtain a nonparametric frequency domain estimate $\hat{G}(e^{j\omega_k})$, which is only defined at a finite number of frequency points ω_k, and an error bound. The asymptotic distribution of this estimate is obtained through application of the central limit theorem, cf. Brillinger (1981), and by mutually comparing the information arising from different sections of the measured input-output data. This way of extracting the statistical properties of the noise is enabled by using a periodic input signal. Using a periodic input signal and distinguishing different sections of the data set can be thought of as a repetition of similar experiments, which is a very appealing way to separate structural phenomena present in the data (i.e. the input-output system) from random effects due to disturbances.

In comparison with previous work on hard error bounds, the probabilistic setting used in this paper has the advantage that we do need only minor a priori information. We do not need a hard error bound on the noise in the time or frequency domain. Actually, through the repetition of experiments, a corresponding probabilistic bound is estimated from the data. As opposed to Goodwin *et al.* (1992), the method proposed here has the property that the form of the distribution of the error is induced by the estimation procedure itself, so that we do not have to choose it a priori. As parameters we have the frequency dependent variance of the noise, which is estimated from the data, and whose estimation error is taken into account. As opposed to Bayard (1992), the noise is not assumed to be normally distributed, nor is the noise filter assumed to be known, and the deviation from a steady-state situation is taken into account.

For brevity, all proofs are omitted; the reader is referred to deVries and Van den Hof (1992b).

2 Preliminaries

It is assumed that the plant, and the measurement data that is obtained from this plant, allow a description

$$y(t) = G_o(q)u(t) + v(t) \qquad (1)$$

with $y(t)$ the output signal, $u(t)$ a bounded deterministic input signal, $v(t)$ an additive output noise, q^{-1} the delay operator, and G_o the proper transfer function of the system, being time-invariant and exponentially stable. The transfer function can be written in its Laurent expansion around $z = \infty$, as

$$G_o(z) = \sum_{k=0}^{\infty} g_o(k) z^{-k} \qquad (2)$$

with $g_o(k)$ the impulse response of the plant. We will consider scalar (single input, single output) systems. The output disturbance $v(t)$ is represented as

$$v(t) = H_o(q)e(t) \qquad (3)$$

where $\{e(t)\}$ is a sequence of independent identically distributed random variables with zero mean values, finite variance σ_e^2, and bounded moments of order $2+\delta$ for some $\delta > 0$, and where H_o is a proper transfer function that is strictly stable. The noise filter $H_o(z)$ can be written in its Laurent expansion around $z = \infty$, as

$$H_o(z) = 1 + \sum_{k=1}^{\infty} h_o(k) z^{-k} \tag{4}$$

Throughout the paper we will consider discrete time intervals for input and output signals denoted by the integer intervals $T^N := [0, N-1]$, $T_{N_s}^N := [N_s, N+N_s-1]$ with N and N_s appropriate integers. We will frequently use a partitioning of the time interval $T_{N_s}^N$ with $N = rN_o$ in r time-intervals of length N_o, denoting $T_i := [(i-1)N_o + N_s, iN_o + N_s - 1]$, $i = 1, .., r$.
With the subscript i we will indicate a variable that originates from the i-th time interval T_i, e.g.

$$x_i(t) = x(t + (i-1)N_o + N_s) \quad \text{where} \quad t \in T^{N_o} \tag{5}$$

$$X_i(e^{j\omega}) = \frac{1}{\sqrt{N_o}} \sum_{t=0}^{N_o-1} x_i(t) e^{-j\omega t} \tag{6}$$

For a signal $x(t)$, defined on T^N, we will denote the N-point Discrete Fourier Transform (DFT) by

$$X(e^{j\frac{2\pi k}{N}}) = \frac{1}{\sqrt{N}} \sum_{t=0}^{N-1} x(t) e^{-j\frac{2\pi k}{N}t} \quad \text{for} \quad k \in T^N \tag{7}$$

Some specific sets of frequencies that arise in the DFT are denoted as

$$\Omega_N := \{\omega_k = \frac{2\pi k}{N}, \, k = 0, 1, ..., N-1\} \tag{8}$$

$$\Omega_{N_o}^{u_i} := \{\omega_k \in \Omega_{N_o} \mid |U_i(e^{j\omega_k})| \neq 0\} \tag{9}$$

Finally we will denote

$$\max_{t \in T^{N+N_s}} |u(t)| = \bar{u}$$

Throughout this paper we will adopt a number of additional assumptions on the system and the generated data.

Assumption 2.1 *We have as a priori information that*

i. there exists a finite and known $\bar{u}^p \in \mathbb{R}$, such that $|u(t)| \leq \bar{u}^p$ for $t < 0$

ii. there exist finite and known M and ρ, with $M, \rho \in \mathbb{R}$, $\rho > 1$, such that $|g_o(k)| \leq M\rho^{-k}$, for $k \in \mathbb{Z}_+$

The a priori information on M and ρ need not be very tight in first instance, as it can be improved using the measurement data. This will be discussed later on. The a priori information on $\bar{u}^p$ is given by the actuator constraints.

3 The DFT of the Noise

In this section we will present a theorem dealing with the properties of the DFT of the output disturbance. This theorem is also given in Brillinger (1981), see Brillinger (1981) theorem 4.4.1 and exercise 4.8.23, using slightly different conditions. This theorem will be essential in the sequel of this paper.

Theorem 3.1 *Consider $v_i(t)$ as defined in (3), (4), (5) and let $V_i(e^{j\omega_k})$ be the N_o-point DFT of $v_i(t)$ with $\omega_k \in \Omega_{N_o}$. Let*

$$\check{V}_{N_o} = \begin{bmatrix} Re\{V_i(e^{j\omega_k})\} \\ Im\{V_i(e^{j\omega_k})\} \\ Re\{V_i(e^{j\omega_\ell})\} \\ Im\{V_i(e^{j\omega_\ell})\} \\ Re\{V_m(e^{j\omega_\ell})\} \\ Im\{V_m(e^{j\omega_\ell})\} \end{bmatrix}$$

Then, for $\omega_k, \omega_\ell \in \Omega_{N_o}$, $\omega_k \neq \omega_\ell$, $i, m = 1, ..., r$ and $i \neq m$, there holds

$$\check{V}_{N_o} \in As\mathcal{N}(0, \Lambda)$$

where Λ is a diagonal matrix with diagonal elements given by

$$\begin{aligned}
var[Re\{V_i(e^{j\omega_k})\}] &= \tfrac{\sigma_e^2}{2}|H_o(e^{j\omega_k})|^2 && \omega_k \neq 0, \pi \\
var[Im\{V_i(e^{j\omega_k})\}] &= var[Re\{V_i(e^{j\omega_k})\}] && \omega_k \neq 0, \pi \\
var[Re\{V_i(e^{j\omega_k})\}] &= \sigma_e^2|H_o(e^{j\omega_k})|^2 && \omega_k = 0, \pi \\
var[Im\{V_i(e^{j\omega_k})\}] &= 0 && \omega_k = 0, \pi
\end{aligned}$$

The theorem states that the DFT of the noise is asymptotically normally distributed, with real and imaginary parts that are uncorrelated, and have equal variance for $\omega_k \neq 0, \pi$. Furthermore, asymptotically the DFT's of the noise for different frequencies are uncorrelated, and the DFT's of the noise over different intervals are uncorrelated. Note that uncorrelated jointly normally distributed random variables are independent.

4 Error Bound for Transfer Function Estimate

4.1 Introduction

In this section we will construct a nonparametric estimate $\hat{G}$ of the system's transfer function G_o, by

averaging over a set of ETFE's. This procedure is similar to Bartlett's procedure of periodogram averaging, see Brillinger (1981), and is also proposed by Ljung (1985). Note that the ETFE is only defined at a finite number of frequency points. We will establish an error bound $\alpha(\omega_k)$ such that

$$|G_o(e^{j\omega_k}) - \hat{G}(e^{j\omega_k})| \leq \alpha(\omega_k) \qquad (10)$$

for a finite set of frequencies that will be specified later on. As mentioned in Sect. 1, we will use a probabilistic description of the noise, whereas both the error due to undermodelling and the input signal are considered as being deterministic. This results in an upper bound on the error which has both soft (probabilistic) and hard (deterministic) components, and consequently a statement as (10) can only be made within a prespecified probability. In order to arrive at an error bound (10), we will pursue the following strategy. Experimental data is available over a time set of length N. This time set is composed of a first interval of length N_s, not used for identification, and consecutively r intervals of length N_o. We consider an input signal that is periodic with period N_o, such that in each of the r intervals the same input signal is applied. This repetition of experiments offers the opportunity to mutually compare the information arising from different intervals of the data, and consequently to formulate the statistics of the estimated transfer function. In other words: the noise contribution on the data is also identified on the basis of the experiments. As a result an error bound (10) can be specified without heavily relying on a priori knowledge of the noise.
Because of the periodicity of the input signal u it follows that

$$\Omega^{u_i}_{N_o} = \Omega^{u}_{N_o} \quad \text{for all} \quad i = 1, ..., r$$

4.2 A Transfer Function Estimate

Define the following estimates for $\omega_k \in \Omega^u_{N_o}$

$$\hat{G}_i(e^{j\omega_k}) = \frac{Y_i(e^{j\omega_k})}{U_i(e^{j\omega_k})} \quad \text{for} \quad i = 1, 2, ..., r \qquad (11)$$

$$\hat{G}(e^{j\omega_k}) = \frac{1}{r}\sum_{i=1}^{r} \hat{G}_i(e^{j\omega_k}) \qquad (12)$$

Note that we do not average over different frequencies, we only average over different estimates $\hat{G}_i(e^{j\omega_k})$ of $G_o(e^{j\omega_k})$ at the same frequency ω_k. Employing the system's equations, similar as in deVries and Van den Hof (1992a), it follows that

$$Y_i(e^{j\omega_k}) = G_o(e^{j\omega_k})U_i(e^{j\omega_k}) + R_i(e^{j\omega_k}) + V_i(e^{j\omega_k}) \qquad (13)$$

with $R_i(e^{j\omega_k})$ a component which is due to unknown past inputs, i.e. input samples outside the time interval that is considered. In deVries and Van den Hof (1992a) it is shown that for $\omega_k \in \Omega_{N_o}$ this term is bounded by

$$|R_i(e^{j\omega_k})| \leq \frac{\bar{u}^P + \bar{u}}{\sqrt{N_o}} \frac{M\rho(1-\rho^{-N_o})}{(\rho-1)^2} \rho^{-(i-1)N_o - N_s} \qquad (14)$$

if $u(t)$ is periodic with period N_o for $t \in T^{N+N_s}$, and

$$|R_i(e^{j\omega_k})| \leq \frac{\bar{u}^P + \bar{u}}{\sqrt{N_o}} \frac{M\rho(1-\rho^{-N_o})}{(\rho-1)^2} \qquad (15)$$

if $u(t)$ is not periodic. Using (11) and (13) we can write

$$\hat{G}_i(e^{j\omega_k}) = G_o(e^{j\omega_k}) + S_i(e^{j\omega_k}) + \frac{V_i(e^{j\omega_k})}{U_i(e^{j\omega_k})} \qquad (16)$$

with

$$S_i(e^{j\omega_k}) = \frac{R_i(e^{j\omega_k})}{U_i(e^{j\omega_k})} \qquad (17)$$

the error due to the unknown past inputs for the i-th estimate $\hat{G}_i$. Because S_i only depends on the input and the system, it is a deterministic term. This yields the following result.

Proposition 4.1 *Consider the estimates $\hat{G}_i(e^{j\omega_k})$, $i = 1, ..., r$. For all $\omega_k \in \Omega^u_{N_o}$ there holds*

a. $\mathbb{E}[\hat{G}_i(e^{j\omega_k})] = G_o(e^{j\omega_k}) + S_i(e^{j\omega_k})$ *, where $S_i(e^{j\omega_k})$ is given by* (17) *and is bounded using* (14) *or* (15)

b. $var[\hat{G}_i(e^{j\omega_k})] = \dfrac{var[V_i(e^{j\omega_k})]}{|U_i(e^{j\omega_k})|^2}$

c. $\hat{G}_i(e^{j\omega_k})$ *asymptotically in N_o is normally distributed*

The above proposition states that the Emperical Transfer Function Estimate (ETFE) is asymptotically normally distributed, and asymptotically unbiased. However, the variance does not decrease with N_o in general, it is just the noise to signal ratio in the frequency domain. The averaging (12) is introduced in order to obtain an estimate with decreasing variance. However, $S_i(e^{j\omega_k})$ is unknown and varies with i, even if $U_i(e^{j\omega_k})$ is independent of i for $i = 1, ..., r$. Furthermore, $var[V_i(e^{j\omega_k})]$ is unknown, and $var[\hat{G}_i(e^{j\omega_k})]$ varies with i if $U_i(e^{j\omega_k})$ varies with i. Moreover, if the input is not periodic, the uncertainty due to the unknown past inputs $S_i(e^{j\omega_k})$ typically will dominate the error bound, see (15). Hence in general the estimate $\hat{G}(e^{j\omega_k})$ will

be heavily biased, and it is not possible to obtain a satisfactory estimate of its variance.

In order to improve upon the above situation, we will use a periodic input signal. We will split up the analysis into two parts: first we will derive the properties of an intermediate variable, and next we will analyse the properties of the estimate (12). Define the intermediate variable $\tilde{G}_i(e^{j\omega_k})$ as

$$\tilde{G}_i(e^{j\omega_k}) = \hat{G}_i(e^{j\omega_k}) - S_i(e^{j\omega_k}) \quad (18)$$

$$= G_o(e^{j\omega_k}) + \frac{V_i(e^{j\omega_k})}{U_i(e^{j\omega_k})} \quad (19)$$

Proposition 4.2 *Consider the intermediate variables $\tilde{G}_i(e^{j\omega_k})$, $\omega_k \in \Omega^u_{N_o}$. Let $u(t)$ be a periodic input signal with period N_o for all $t \in T^{N+N_s}$. Then asymptotically in N_o the random variables $\tilde{G}_i(e^{j\omega_k})$ and $\tilde{G}_\ell(e^{j\omega_k})$ are independent and identically distributed for all $i, \ell = 1, ..., r$, $i \neq \ell$.*

We denote the averaged intermediate variable, averaged over the different time intervals, as

$$\tilde{G}(e^{j\omega_k}) = \frac{1}{r}\sum_{i=1}^{r} \tilde{G}_i(e^{j\omega_k}) \quad \text{for} \quad \omega_k \in \Omega^u_{N_o} \quad (20)$$

This averaged intermediate is going to be used in determining an error bound as meant in (10)

$$|G_o(e^{j\omega_k}) - \hat{G}(e^{j\omega_k})| \quad (21)$$

$$\leq |G_o(e^{j\omega_k}) - \tilde{G}(e^{j\omega_k})| + |\tilde{G}(e^{j\omega_k}) - \hat{G}(e^{j\omega_k})|$$

$$= |G_o(e^{j\omega_k}) - \tilde{G}(e^{j\omega_k})| + |S(e^{j\omega_k})| \quad (22)$$

with

$$S(e^{j\omega_k}) = \frac{1}{r}\sum_{i=1}^{r} S_i(e^{j\omega_k})$$

Considering the inequality (22), the first term on the right hand side is the variance contribution to the error due to the noise disturbance. The second term on the right hand side of (22) is a bias contribution, due to unknown past inputs. This deterministic term can be bounded by using (14). For a periodic input signal this term can be made small by choosing N_s. A bound on the first (stochastic) term has to be determined on the basis of its distribution. For the distribution of $\tilde{G}(e^{j\omega_k})$ we have the following results.

Proposition 4.3 *Consider the situation as in Proposition 4.2. Then for all $\omega_k \in \Omega^u_{N_o}$ there holds*

a. $\mathbb{E}[\tilde{G}(e^{j\omega_k})] = G_o(e^{j\omega_k})$

b. Asymptotically in N_o

$var[\tilde{G}(e^{j\omega_k})] = \frac{1}{r} var[\tilde{G}_i(e^{j\omega_k})] = \frac{var[V_i(e^{j\omega_k})]}{r|U_i(e^{j\omega_k})|^2}$, *independent of i*

c. $\sqrt{r}\,\tilde{G}(e^{j\omega_k})$ *asymptotically in N is normally distributed*

As a result the asymptotic distribution of the estimate $\tilde{G}(e^{j\omega_k})$ is specified, although its variance still remains to be unknown. In the next steps we will quantify this variance on the basis of measurement data. To this end we use the following two estimates

$$\hat{\sigma}^2_r(\hat{G}(e^{j\omega_k})) = \frac{\sum_{\ell=1}^{r} |\hat{G}(e^{j\omega_k}) - \hat{G}_\ell(e^{j\omega_k})|^2}{r(r-1)} \quad (23)$$

$$\hat{\sigma}^2_r(\tilde{G}(e^{j\omega_k})) = \frac{\sum_{\ell=1}^{r} |\tilde{G}(e^{j\omega_k}) - \tilde{G}_\ell(e^{j\omega_k})|^2}{r(r-1)} \quad (24)$$

Note that the first one of these estimates indeed can be calculated from data. However the second one is not available.

Proposition 4.4 *Consider the situation as in Proposition 4.2. Then the estimate $\hat{\sigma}^2_r(\tilde{G}(e^{j\omega_k}))$ is a consistent estimate of $var[\tilde{G}(e^{j\omega_k})]$. Asymptotically in N_o the variance of the estimate $\hat{\sigma}^2_r(\tilde{G}(e^{j\omega_k}))$ decays as $\frac{1}{r-1}$.*

Although this estimate is not available from data, we can bound the difference between the two estimates (23), (24).

Lemma 4.5 *Consider the estimates $\hat{\sigma}^2_r(\hat{G}(e^{j\omega_k}))$, $\hat{\sigma}^2_r(\tilde{G}(e^{j\omega_k}))$ as defined in (23), (24). Let $u(t)$ be a periodic input signal with period N_o for all $t \in T^{N+N_s}$. Then*

$$|\hat{\sigma}^2_r(\tilde{G}(e^{j\omega_k})) - \hat{\sigma}^2_r(\hat{G}(e^{j\omega_k}))| \leq \epsilon(\omega_k) \quad (25)$$

with

$$\epsilon(\omega_k) = \frac{\sum_{i=1}^{r} 2|A_i(e^{j\omega_k})||B_i(e^{j\omega_k})| + |B_i(e^{j\omega_k})|^2}{r(r-1)} \quad (26)$$

and

$$|A_i(e^{j\omega_k})| = |\hat{G}(e^{j\omega_k}) - \hat{G}_i(e^{j\omega_k})|$$

$$|B_i(e^{j\omega_k})| = \frac{1}{r}\sum_{m=1}^{r} |S_m(e^{j\omega_k})| + \frac{r-2}{r}|S_i(e^{j\omega_k})|$$

$$|S_i(e^{j\omega_k})| \leq \frac{\bar{u}^P + \bar{u}}{|U_i(e^{j\omega_k})|} \frac{M\rho(1-\rho^{-N_o})}{(\rho-1)^2} \frac{\rho^{-(i-1)N_o - N_s}}{\sqrt{N_o}}$$

Clearly the difference between $\hat{\sigma}^2_r(\tilde{G}(e^{j\omega_k}))$ and $\hat{\sigma}^2_r(\hat{G}(e^{j\omega_k}))$ is due to the $S_i(e^{j\omega_k})$, i.e. the influence of the unknown past input signals. The difference is small if the $S_i(e^{j\omega_k})$ are small, which for a periodic input signal can be obtained by choosing N_s.

Using only the unknown intermediate transfer function $\tilde{G}(e^{j\omega_k})$, and its estimated variance

$\hat{\sigma}_r^2(\tilde{G}(e^{j\omega_k}))$, an error bound with respect to the system's transfer function can be calculated asymptotically in N_o. Due to the fact that the intermediate variables $\tilde{G}_i(e^{j\omega_k})$ are independent and identically distributed, see Proposition 4.2, this results in an F distribution for the error, as formulated in the following lemma.

Lemma 4.6 *Consider the intermediate transfer function* $\tilde{G}(e^{j\omega_k})$, (20), (19), *and the estimate of its variance* (24). *Let the input signal be periodic with period* N_o *for* $t \in T^{N+N_s}$, *and let* $r > 1$. *Then as* $N_o \to \infty$

$$\frac{|G_o(e^{j\omega_k}) - \tilde{G}(e^{j\omega_k})|^2}{\hat{\sigma}_r^2(\tilde{G}(e^{j\omega_k}))} \to \begin{cases} F(2,2(r-1)) & \omega_k \neq 0,\pi \\ F(1,r-1) & \omega_k = 0,\pi \end{cases}$$

for all $\omega_k \in \{\omega \in \Omega_{N_o}^u \mid \hat{\sigma}_r^2(\tilde{G}(e^{j\omega})) > 0\}$, *where* $F(n,d)$ *denotes the* F *distribution with* n *degrees of freedom in the numerator and* d *degrees of freedom in the denominator.*

Note that no assumptions are made on the distribution of the noise, and that the uncertainty in the estimated variance is taken into account by the F-distribution.

Combining Lemma's 4.5 and 4.6 and (22) leads to an error bound that can be calculated on the basis of data, in terms of a confidence interval. In formulating this confidence interval, we will adopt the following notation

$$F_\alpha(m,n) = \{P[x \leq \alpha]\,,\ x \in F(m,n)\}$$

which means that $F_\alpha(m,n)$ is the probability that $x \in F(m,n)$ is smaller than α.

Theorem 4.7 *Consider the estimated transfer function* $\hat{G}(e^{j\omega_k})$, (12), (11), *and the estimate of its variance* (23). *Let the input signal be periodic with period* N_o *for* $t \in T^{N+N_s}$, *and let* $r > 1$. *Asymptotically in* N_o *there holds*

$$|G_o(e^{j\omega_k}) - \hat{G}(e^{j\omega_k})| \leq \gamma_\alpha(\omega_k) + |S(e^{j\omega_k})|$$
$$w.p. \geq \begin{cases} F_\alpha(2,2r-2) & \omega_k \neq 0,\pi \\ F_\alpha(1,r-1) & \omega_k = 0,\pi \end{cases}$$

for all $\omega_k \in \{\omega \in \Omega_{N_o}^u \mid \hat{\sigma}_r^2(\hat{G}(e^{j\omega})) > \epsilon(\omega)\}$, *where*

$$\gamma_\alpha(\omega_k) = \sqrt{\alpha}\left(\hat{\sigma}_r^2(\hat{G}(e^{j\omega_k})) + \epsilon(\omega_k)\right)^{\frac{1}{2}}$$
$$|S(e^{j\omega_k})| \leq \frac{1}{r\sqrt{N_o}} \frac{\bar{u}^P + \bar{u}}{|U_i(e^{j\omega_k})|} \frac{M\rho(1-\rho^{-N})}{(\rho-1)^2} \rho^{-N_s}$$

and $\epsilon(\omega_k)$ *is given by* (26).

The deterministic error terms are $\epsilon(\omega_k)$ and $S(e^{j\omega_k})$, where $\epsilon(\omega_k)$ is a function of the $S_i(e^{j\omega_k})$. These terms are due to the unknown past inputs, and typically will be small in comparison with the error due to the noise $\sqrt{\alpha}\,\hat{\sigma}_r(\hat{G}(e^{j\omega_k}))$. This is due to the fact that $S(e^{j\omega_k})$ and $S_i(e^{j\omega_k})$ have exponential convergence to zero with N_s. For the error due to the noise we have that, asymptotically in N_o, the variance decays as $1/r$ and the variance of the estimated variance decays as $1/(r-1)$.

Note that the above estimate is only defined at the finite number of frequency points $\Omega_{N_o}^u$. Theorem 4.7 can very well be used to provide an estimate of the a priori information needed by e.g. Helmicki *et al.* (1990) and Gu and Khargonekar (1992), to obtain a model in H_∞ and a hard error bound that is valid on the whole unit circle. Note however that the error bound formulated in theorem 4.7 is a soft one, while the bound needed by e.g. Helmicki *et al.* (1990) and Gu and Khargonekar (1992) is a hard one.

5 Additional Results

Using a similar procedure as in Sect. 4, together with Theorem 3.1, we have obtained a number of additional results:

- By estimating a Finite Impulse Response (FIR) model on each $\hat{G}_i$ a set of FIR models can be obtained. Averaging over this set results in a FIR model with an error bound on the estimated parameters. Hence, an estimate with an error bound of the impulse response of the system is obtained, which can be used to improve the prior information M and ρ.
- An error bound for the transfer function of an estimated FIR model can be obtained. This results in an error bound that is valid on the whole unit circle, whereas the error bound of Theorem 4.7 is only defined at a finite number of frequency points.
- Estimates with an error bound of the response of the system to arbitrary input signals can be obtained. This is useful for validation, simulation and fault detection purposes.

6 Example

To illustrate our results a simulation was made of a fifth order system

$$G_o(z) = \frac{N_o(z)}{D_o(z)}$$

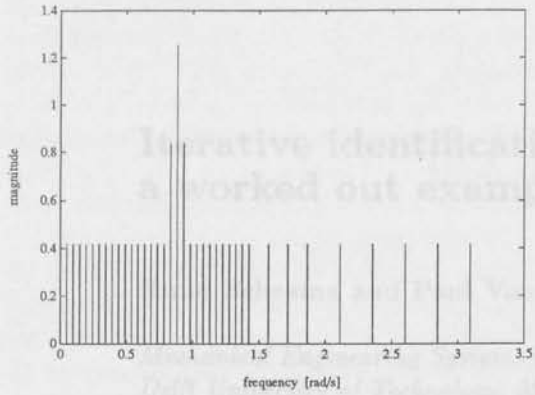

Fig. 1: Magnitude of the DFT over one period of the input signal, $|U_i(e^{j\omega_k})|$.

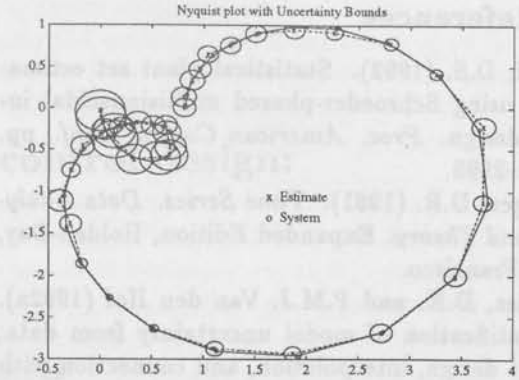

Fig. 2: Estimate $\hat{G}(e^{j\omega_k})$ with error bound, and true system $G_o(e^{j\omega_k})$ for $\omega_k \in \Omega^u_{N_o}$.

$$
\begin{aligned}
N_o(z) &= 0.7027 - 0.8926z^{-1} + 0.24z^{-2} \\
&\quad + 0.5243z^{-3} - 0.9023z^{-4} + 0.4z^{-5} \\
D_o(z) &= 1 - 2.4741z^{-1} + 2.8913z^{-2} \\
&\quad - 1.9813z^{-3} + 0.8337z^{-4} - 0.1813z^{-5}
\end{aligned}
$$

whose impulse response $g_o(k)$ satisfies a bound given by $M_o = 2$ and $\rho_o = 1.23$. There was 10 percent (in amplitude) *uniformly* distributed colored noise (highpass filtered white noise) on the output.

As a priori information on the impulse response we choose $M = 3$ and $\rho = 1.2$. A periodic input signal was applied to the system. The input signal was chosen to obey $\bar{u}^p = 2$ and $\bar{u} = 1$. We used 1074 points with $N = 1024$, $N_o = 128$ and $N_s = 50$. The magnitude of the DFT of the input signal over one period, $|U_i(e^{j\omega_k})|$, is given in Fig. 1. Note that the frequency points where $|U_i(e^{j\omega_k})| > 0$ are not equidistant. The magnitude and frequency grid of the input express that we are especially interested in the behaviour of the system around $\omega = 0.88$ rad/s, and that we do not expect the system behaviour to change rapidly with frequency for the higher frequencies.

In Fig. 2 a Nyquist plot of the estimate $\hat{G}(e^{j\omega_k})$ of Theorem 4.7 is given, together with the estimated error bound and the true system. The probability level for the error bound is 99 %. Note that a very good estimate is obtained for those frequencies where $|U_i(e^{j\omega_k})|$, the magnitude of the DFT of the input signal, was chosen to be large. Note also that the error bound is tight, i.e. the actual error can be close to the upper bound.

7 Conclusions

In this paper a procedure is presented to obtain an estimate, together with an error bound, of the transfer function of a system, using only minor a priori information. The basis of our results is the derivation of the asymptotic distribution of a Discrete Fourier Transform (DFT) of a filtered sequence of independent random variables, the seperation of the error in a deterministic and a probabilistic part, and the use of a periodic input signal.

By employing a periodic input signal a repetition of experiments is obtained. This repetition offers the possibility to mutually compare the information arising from different intervals of the data, and consequently to formulate the statistics of the estimated transfer function. More specifically, a non-parametric Emperical Transfer Function Estimate (ETFE) is made over each period of the input signal. Due to the periodicity of the input signal these estimates are approximately independent and identically distributed. Averaging over the estimates, which provides the final estimate of the system, now results in a fast decrease of the variance of the final estimate with the number of averages. Moreover, the final estimate is almost unbiased and its variance can be estimated consistently. The error in this final estimate can be seperated into two parts: a probabilistic part, due to the noise disturbance on the data, and a deterministic part, due to the bias in the estimate. The latter is explicitly bounded with a deterministic error bound. The former asymptotically has an F-distribution, so that a confidence interval can be specified. This results in a mixed deterministic-probabilistic error bound, which clearly distinguishes the different sources of uncertainty. No assumptions are made on the distribution of the noise, and the uncertainty in the estimated variance is taken into account by the F-distribution.

8 References

Bayard, D.S. (1992). Statistical plant set estimation using Schroeder-phased multisinusoidal input design. *Proc. American Control Conf.*, pp. 2988–2995.

Brillinger, D.R. (1981). *Time Series. Data Analysis and Theory.* Expanded Edition, Holden-Day, San Francisco.

De Vries, D.K. and P.M.J. Van den Hof (1992a). Quantification of model uncertainty from data: input design, interpolation, and connection with robust control design specifications. *Proc. American Control Conf.*, pp. 3170–3175.

De Vries, D.K. and P.M.J. Van den Hof (1992b). Quantification of uncertainty in transfer function estimation. *Report N-410, Mechanical Engineering Systems and Control Group, Delft Univ. Technology, The Netherlands, Submitted to Automatica.*

Goodwin, G.C., M. Gevers and B. Ninness (1992). Quantifying the error in estimated transfer functions with application to model order selection. *IEEE Trans. Automatic Contr.*, AC–37, pp. 913–928.

Goodwin, G.C. and M.E. Salgado (1989). Quantification of uncertainty in estimation using an embedding principle. *Proc. American Control Conf.*, pp. 1416–1421.

Gu, G. and P.P. Khargonekar (1992). A class of algorithms for identification in H_∞. *Automatica*, vol. 28, pp. 299–312.

Hakvoort, R.G. (1992). Worst-case system identification in H_∞: error bounds and optimal models. *Selected Topics in Identification, Modelling and Control, 5.* Delft University Press, The Netherlands.

Helmicki, A.J., C.A. Jacobson and C.N. Nett (1990). Identification in H_∞: a robustly convergent, nonlinear algorithm. *Proc. American Control Conf.*, pp. 386–391.

Ljung, L. (1985). On the estimation of transfer functions. *Automatica*, vol. 21, pp. 677–696.

Wahlberg, B. and L. Ljung (1991). On estimation of transfer function error bounds. *Proc. European Control Conf.*, pp. 1378–1383.

Selected Topics in Identification, Modelling and Control
Vol. 5, December 1992

Iterative identification and control design: a worked out example ‡

Ruud Schrama and Paul Van den Hof

Mechanical Engineering Systems and Control Group
Delft University of Technology, Mekelweg 2, 2628 CD Delft, The Netherlands.

Abstract. The topic of this paper is the synthesis of a high performance controller for a plant with unknown dynamics by means of approximate identification and model-based control design. For this purpose, identification and control design have to be treated together as the joint problem of deriving a nominal model that gives rise to a compensator which achieves a high performance for the plant under consideration. Using a fairly general measure of performance we establish a link between the performance designed for the nominal model and the performance actually achieved for the plant. Hereupon we propose an iterative scheme of repeated identification and control design, that will be illustrated with a simulation example.

Keywords. Control-relevant identification; closed-loop identification; robust control.

1 Introduction

Recently it has been motivated that the problem of designing a high performance control system for a plant with unknown dynamicics through separate stages of (approximate) identification and model based control design requires iterative schemes to solve the problem, see e.g. Zang *et al.*(1991), Schrama (1992a, 1992b), Lee *et al.*(1992). The underlying idea is that there actually is a joint problem of finding an appropriate model $\hat{P}$ of the plant P, and a controller $C_{\hat{P}}$ based on $\hat{P}$, such that $C_{\hat{P}}$ achieves a high performance for the modelled plant P and a similar performance for the nominal model $\hat{P}$. The former is the true control objective; the latter is needed in order that we are confident about the compensator $C_{\hat{P}}$. Simultaneous high performances are accomplished, if the feedback system composed of the nominal model $\hat{P}$ and its own high performance compensator $C_{\hat{P}}$ approximately describes the feedback system containing the plant P and the same compensator $C_{\hat{P}}$. The quality of each candidate nominal model depends on its own compensator and vice versa. Hence the problem of designing a high performance compensator for an imprecisely known plant boils down to a *joint problem* of approximate identification and model-based control design. Solving this joint problem through separate stages of identification and control design can be done, only if these procedures are embedded in an iterative scheme. We elaborate an iterative scheme, in which each identification is based on new data collected while the plant is controlled by the latest compensator. Each new nominal model is used to design an improved compensator, which replaces the old compensator.

A few iterative schemes proposed in literature have been based on the prediction error identification method, together with LQG/LTR control design (Bitmead *et al.*, 1990) and with LQG control design (Hakvoort, 1990; Zang *et al.*, 1991; Hakvoort *et al.*, 1992). Alternatively, in Liu and Skelton (1990) the identification and control design are based on covariance data. In Lee *et al.*(1992) the IMC-design

‡To appear in *Proc. NSF/AFOSR Sponsored Workshop on The Modelling of Uncertainty in Control Systems*, University of California, Santa Barbara, CA, June 18-20, 1992. Springer Verlag.

method is employed, and the identification step is replaced by a model reduction based on full plant knowledge. Alternatively, in Rivera (1991) an iteration is used to build prefilters for a control-relevant prediction error identification from one open-loop dataset.

Our iterative scheme is composed of a robust control design method and a frequency domain identification technique that are conceived in terms of coprime factorizations. We will discuss the iterative scheme, and show an extensive simulation example. For more details on the approach presented, the reader is referred to Schrama (1992a).

2 A Link Between Identification and Control Design

We adopt the following control design paradigm from Bongers and Bosgra (1990) and McFarlane and Glover (1988). The feedback configuration of interest is the interconnection $H(\hat{P}, C)$, which is depicted in Fig. 1. The transfer matrix $T(\hat{P}, C)$ defined as

$$T(\hat{P}, C) \doteq \begin{bmatrix} \hat{P}(I+C\hat{P})^{-1}C & \hat{P}(I+C\hat{P})^{-1} \\ (I+C\hat{P})^{-1}C & (I+C\hat{P})^{-1} \end{bmatrix} \quad (1)$$

maps $\mathrm{col}(r_2, r_1)$ into $\mathrm{col}(\hat{y}, \hat{u})$. This transfer matrix is called the nominal *feedback matrix*, because it embodies all feedback properties like disturbance and noise attenuation, sensitivity, stability and robustness margins. The model-based controller $C_{\hat{P}}$ is derived from the nominal model $\hat{P}$ according to

$$C_{\hat{P}} = \arg\min_{C} \|T(\alpha\hat{P}, C/\alpha)\|_\infty \quad (2)$$

with $\alpha \in \Re$ a scalar weight. The resulting controller is optimally robust against stable perturbations of the normalized right coprime factors of $\alpha\hat{P}$, see Bongers and Bosgra (1990) and Vidyasagar (1985) for details. At the same time this controller $C_{\hat{P}}$ pursues some traditional control objectives like a small sensitivity at the lower frequencies and a small complementary sensitivity at the higher frequencies. C_i optimizes robustness for a nominal performance level associated with α. The resulting designed feedback system has its bandwidth close to the cross-over frequency of $\alpha\hat{P}$ (McFarlane and Glover, 1988), and thus a large α corresponds to a high nominal performance.

Conformably to (2) the nominal performance is high, if $\|T(\alpha\hat{P}, C_{\hat{P}}/\alpha)\|_\infty$ is small. We examine the performance norm of the actual plant P by the triangular inequalities:

$$\Big|\|T(\alpha\hat{P}, C_{\hat{P}}/\alpha)\| - \|T(\alpha P, C_{\hat{P}}/\alpha) - T(\alpha\hat{P}, C_{\hat{P}}/\alpha)\|\Big| \leq$$

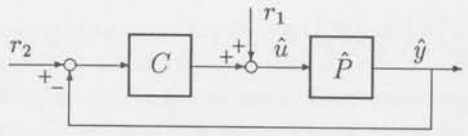

Fig. 1: Feedback configuration $H(\hat{P}, C)$ for control design

$$\leq \|T(\alpha P, C_{\hat{P}}/\alpha)\| \leq$$

$$\leq \|T(\alpha\hat{P}, C_{\hat{P}}/\alpha)\| + \|T(\alpha P, C_{\hat{P}}/\alpha) - T(\alpha\hat{P}, C_{\hat{P}}/\alpha)\| \quad (3)$$

The middle term reflects the performance of the controlled plant. The nominal performance norm $\|T(\alpha\hat{P}, C_{\hat{P}}/\alpha)\|_\infty$ is minimized by the design of (2); and $\|T(\alpha P, C_{\hat{P}}/\alpha) - T(\alpha\hat{P}, C_{\hat{P}}/\alpha)\|$ is the 'worst-case' performance degradation due to the fact that $C_{\hat{P}}$ has been designed for the nominal model $\hat{P}$ rather than for the plant P. With the above inequalities we can make more precise the implications of the high performance control design problem. The point is to find a nominal model $\hat{P}$ with an induced controller $C_{\hat{P}}$ such that

$$\|T(\alpha\hat{P}, C_{\hat{P}}/\alpha)\| \text{ is small} \quad (4)$$

$$\|T(\alpha P, C_{\hat{P}}/\alpha) - T(\alpha\hat{P}, C_{\hat{P}}/\alpha)\| \ll \|T(\alpha\hat{P}, C_{\hat{P}}/\alpha)\|. \quad (5)$$

The requirement of (4) pertains to a high *nominal* performance. The strong inequality of (5) embodies the demand of a *robust* performance: if (5) is satisfied, then there is only a relatively small difference between the feedback properties of the designed and actual feedback systems $T(\hat{P}, C_{\hat{P}})$ and $T(P, C_{\hat{P}})$. The two requirements (4) and (5) can not simply be separated. Note that for a given nominal model $\hat{P}$, (4) refers to a control design problem, and for a given controller C, (5) refers to a (closed loop) approximate identification problem. This will be clarified later on.

As the control design of (2) pursues a small nominal performance norm $\|T(\alpha\hat{P}, C_{\hat{P}}/\alpha)\|_\infty$, the remaining task for the approximate identification would be to find such a nominal model $\hat{P}$ that the performance degradation

$$\|T(\alpha P, C_{\hat{P}}/\alpha) - T(\alpha\hat{P}, C_{\hat{P}}/\alpha)\|_\infty$$

is relatively small. This approximate identification problem cannot be solved straightforwardly, because the compensator $C_{\hat{P}}$ is not available prior to the identification. This explains once more that the problems of approximate identification and model-based control design have to be treated as a joint problem.

Note that the bounds of (3) are used to express the identification objective in terms of the control objective of (2). The same approach applies to any other control design method that optimizes a norm or a distance function of the nominal feedback matrix $T(\hat{P}, C_{\hat{P}})$. As explained in Schrama (1992a) these methods include LQ control design and the H_∞-optimization of a weighted sensitivity.
As the choice of α refers to a required nominal performance level, we will not fix its value a priori, e.g. aiming at a very high but unachievable performance, but we will gradually increase α during the iteration process. A motivation for this will be given later on.

We propose the following iterative scheme to tackle the joint problem of approximate identification and model-based control design.

Step i. Given $\hat{P}_{i-1}$, C_{i-1}, α_{i-1}

(a) Obtain data from the plant, while it operates under feedback by C_{i-1}. The nominal model $\hat{P}_i$ is identified with an identification scheme that asymptotically obtaines $\hat{P}_i = \arg\min_{P \in \mathcal{P}(\theta)}$

$$\|T(\alpha_{i-1}P, C_{i-1}/\alpha_{i-1}) - T(\alpha_{i-1}\bar{P}, C_{i-1}/\alpha_{i-1})\|_2 \quad (6)$$

where $\mathcal{P}(\theta)$ is the set of parameterized candidate models.

(b) Determine $\alpha_i > \alpha_{i-1}$ and design a new controller C_i according to

$$C_i = \arg\min_C \|T(\alpha_i \hat{P}_i, C/\alpha_i)\|_\infty. \quad (7)$$

such that the performance degradation $\|T(\alpha_i P, C_i/\alpha_i) - T(\alpha_i \hat{P}_i, C_i/\alpha_i)\|_\infty$ is kept small.

(c) Perform a robust stability test to verify whether the plant P will be stabilized by the new controller C_i, prior to implementing it.

Note that we have replaced the infinity-norm with a 2-norm in (6). This is done since there exists no identification technique yet that can handle an H_∞ (or L_∞) approximation. The rationale for this replacement is that the L_2 approximation yields a reasonably good nominal model in an L_∞ sense, provided that the error-term is sufficiently smooth. This observation is backed up by the result in Caines and M. Baykal-Gürsoy (1989) on the L_∞ consistency of L_2 estimators.
Since the control design scheme does not take account of model uncertainties directly, the design weight is used to tune the design. We intend to gradually increase the design weight during the iteration in order to keep the performance degradation small at each iteration step. In this way we guarantee that in the control design step, there remains a good resemblance between the feedback properties of $H(\hat{P}_i, C_i)$ and $H(P, C_i)$.
The different steps in the iterative scheme will be described in more detail in the next sections.

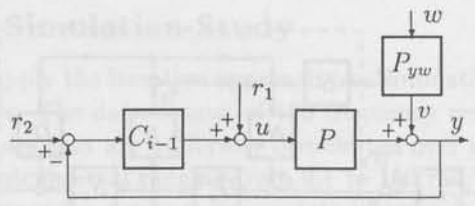

Fig. 2: Feedback configuration for identification

3 Control-Relevant Identification

We consider the feedback configuration of Fig. 2, in which the plant P is stabilized by the controller C_{i-1}. The feedback system is driven by the exogenous inputs r_1 and r_2 and the additive output noise v. The noise v is uncorrelated with r_1 and r_2 and it is modelled as $v = P_{yw}w$, where w is a white noise.
The problem of concern is to identify a nominal model $\hat{P}_i$ from measurements of u and y such that the asymptotic identificationm criterion reflects

$$\hat{P}_i = \arg\min_{\bar{P} \in \mathcal{C}(\theta)} \|T(P, C_{i-1}) - T(\bar{P}, C_{i-1})\|_2. \quad (8)$$

Only for notational simplicity we use $\alpha_{i-1} = 1$. We recall from the previous sections that we actually use system identification to find an approximate description of the feedback properties of $H(P, C_{i-1})$. Therefore we concentrate on the so-called "asymptotic bias distribution" due to undermodelling.
Since $P \notin \mathcal{P}(\theta)$ the minimization in (8) from u and y combines all problems that are encountered in approximate identification and in closed-loop identification. The desired $\hat{P}_i$ cannot be derived by a direct application of some standard identification method to u and y. In order to obviate this problem we first represent the plant P by a right coprime factorization (definitions are provided in Vidyasagar (1985)).
The plant P is known to be stabilized by the latest controller C_{i-1}. As P belongs to the set of all systems that are stabilized by C_{i-1}, it can be represented by a coprime factorization that is dual to the (Youla-) parameterization of all stabilizing compensators (Vidyasagar, 1985). This dual parameterization can be extended to incorporate the

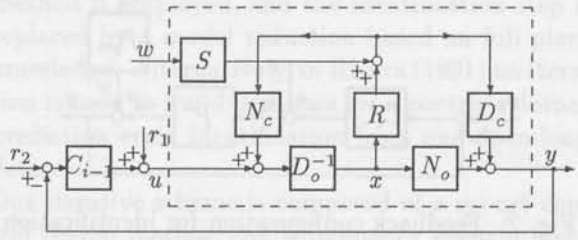

Fig. 3: Coprime factor representation of P and P_{yw}.

"noise filter" P_{yw}, (Schrama *et al.*, 1992; Schrama, 1992a). A similar parameterization has been used by Hansen (1989) for closed-loop experiment design.

This parametrization of P is sketched in Fig. 2, with P_0 an auxiliary model that is stabilized by C_{i-1}; $P_o = N_0(D_o)^{-1}$, and $C_{i-1} = N_c(D_c)^{-1}$ are right coprime factorizations, and R, S any stable transfer functions. For notational convenience we define

$$N \doteq N_o + D_c R; \quad D \doteq D_o - N_c R, \tag{9}$$

so that $P = ND^{-1}$, which is the dual of the Youla parameterization. The following result can now be employed.

Proposition 3.1 *(Schrama, 1992a; Schrama and Van den Hof, 1992). Consider the notation and parametrization as presented above. Then*

(a)

$$\begin{pmatrix} y \\ u \end{pmatrix} = \begin{bmatrix} N \\ D \end{bmatrix} x + \begin{bmatrix} D_c \\ -N_c \end{bmatrix} Sw \tag{10}$$

(b)

$$x = (D_o + C_{i-1}N_o)^{-1}(u + C_{i-1}y) \tag{11}$$
$$= (D_o + C_{i-1}N_o)^{-1}(r_1 + C_{i-1}r_2) \tag{12}$$

and x is uncorrelated with w provided that w is uncorrelated with r_1, r_2;

(c)

$$T(P, C_{i-1}) = \begin{bmatrix} N \\ D \end{bmatrix} (D_o + C_{i-1}N_o)^{-1} \begin{bmatrix} C_{i-1} & I \end{bmatrix}. \tag{13}$$

The proposition shows that the signal x can be reconstructed from the measured signals u and y, and that x is "designed" through appropriate choice of r_1 and/or r_2. Since x is uncorrelated with w, (10) shows that identification of the coprime factors (N, D) actually is an open loop identification problem. This creates the possibility of approximate identification of $P = ND^{-1}$ with an asymptotic identification criterion that is not influenced by w.

Application of an output error identification algorithm to (10) with a prefilter L, shows an asymptotic identification criterion (for SISO systems):

$$\int_\omega [|N(j\omega) - \hat{N}(j\omega)|^2 + |D(j\omega) - \hat{D}(j\omega)|^2] \Phi_x(\omega) |L(j\omega)|^2 d\omega \tag{14}$$

Through the choice of a prefilter L, satisfying

$$|L(j\omega)|^2 = \frac{1 + |C_{i-1}(j\omega)|^2}{\Phi_{r_1}(\omega) + |C_{i-1}(j\omega)|^2 \Phi_{r_2}(\omega)} \tag{15}$$

the expression (14) can be shown to be equal to $\|T(P, C_{i-1}) - T(\hat{P}, C_{i-1})\|_2^2$.

In the example shown later on, we will employ (10) to construct a non-parametric estimate of the frequency response of $N(j\omega)$, $D(j\omega)$; this estimate is substituted for P in (8), in order to construct a low order $\hat{P}_i$ through nonlinear optimization. This latter minimization problem is all but trivial, because the nominal model $\bar{P}_i$ appears in $T(\bar{P}_i, C_{i-1})$ in a multiple and non-linear fashion. The problem is attacked by the Newton-Raphson method in Schrama (1992a). Due to its highly non-linear character the utility of this particular optimization hinges on a good initial estmate. In Schrama (1992a) such an estimate is obtained by parametrizing $\bar{P}_i$ in (8) in terms of its coprime factors.

Finally we have to verify whether the estimated model $\hat{P}_i$ induces a performance degradation

$$\|T(\alpha_{i-1}P, C_{i-1}/\alpha_{i-1}) - T(\alpha_{i-1}\hat{P}_i, C_{i-1}/\alpha_{i-1})\|_\infty$$

that is sufficiently small with respect to the nominal performance. If this is not true, we might have to increase the order of the model. The evaluation of this degradation is done by replacing P by its estimated frequency response, and evaluating the norm for the available frequency response data points.

4 Enhancement of the Controller

We have a system $H(\hat{P}_i, C_{i-1})$ that provides a good description of $H(P, C_{i-1})$ in view of the weighted performance norm. We may expect that this holds also if C_{i-1} is slightly changed. Hence we design an improved controller C_i for $\hat{P}_i$ in such a way that C_i does not differ too much from the old controller C_{i-1}. The change of the compensator will be moderate if the performance requirements are increased moderately. Hence we may choose α_i a bit larger than α_{i-1}. We outline how, in essence, this selection

of α_i is guided by a frequency response estimate of P (details can be found in Schrama (1992a)). We build this estimate from the frequency response estimates of N and D used in the previous section. Then we evaluate the ratio of maximum singular values

$$\frac{\bar{\sigma}\{T(\alpha_i P, C_{i-1}/\alpha_i)(j\omega)\}}{\bar{\sigma}\{T(\alpha_i P, C_i/\alpha_i)(j\omega)\}} \Big/ \frac{\bar{\sigma}\{T(\alpha_i \hat{P}_i, C_{i-1}/\alpha_i)(j\omega)\}}{\bar{\sigma}\{T(\alpha_i \hat{P}_i, C_i/\alpha_i)(j\omega)\}}$$

and a similar ratio for the upper bound of (3). We choose α_i such that these ratios are bounded for every frequency response sample of P. Thereby C_i changes $H(P, C_{i-1})$ similarly to $H(\hat{P}_i, C_{i-1})$. In the example shown later on, these bounds are chosen to be $0.7 - 1.3$.

As the choice of α_i is based on a "prediction" of the frequency response of $T(P, C_i)$, the feedback systems $H(\hat{P}_i, C_i)$ and $H(P, C_i)$ are expected to be similar in an L_∞-sense. However, stability still has to be ascertained.

5 Robustness Analysis

Before the enhanced compensator C_i is actually applied to the plant P, we have to ascertain the stability of the new control system $H(P, C_i)$. This stability test is necessary anyway, because the optimization of robustness against stable coprime factor perturbations is an unconstrained optimization, without the guarantee of obtaining sufficient robustness. We employ the following result from Schrama *et al.*(1992).

Proposition 5.1 *Let $\hat{P}_i = \hat{N}\hat{D}^{-1}$ be stabilized by $C_i = \tilde{Y}^{-1}\tilde{X}$, the latter being a normalized coprime factorization, such that $\tilde{Y}\hat{D} + \tilde{X}\hat{N} = I$. Denote $P_\Delta = N_\Delta D_\Delta^{-1}$ with $N_\Delta = \hat{N} + \Delta N$, $D_\Delta = \hat{D} + \Delta D$. Then $H(P_\Delta, C_i)$ is stable for all P_Δ such that* $\left\| \begin{bmatrix} \Delta_N \\ \Delta_D \end{bmatrix} \right\|_\infty < 1.$

The result is used as follows. Knowing $\hat{P}_i$ and C_i, we can construct $\hat{N}$, $\hat{D}$. For N_Δ, D_Δ we substitue the estimated frequency response of the coprime factors (N, D) of P. If there exists a stable filter Q such that $\left\| \begin{bmatrix} \hat{N} - N_\Delta Q \\ \hat{D} - D_\Delta Q \end{bmatrix} \right\|_\infty < 1$, the stability of $H(P, C_i)$ can be concluded. In practice the 2-norm of the expression is minimized over stable Q, and the inequality is verified for the ∞-norm (Schrama, 1992a; Schrama *et al.*, 1992).

6 Simulation Study

We apply the iterative approach to a simulation example. The data consist of 100 frequency response samples that are uniformly distributed over a logarithmic interval ranging from 0.1 to 100 rad/s. We use exact frequency response data in order to stress the effects due to undermodelling. We merely list the results of this iterative high performance control design procedure, which is investigated in much more detail in Schrama (1992a).

The continuous-time plant P under investigation has a transfer function $n(s)/d(s)$ with

$$\begin{aligned} n(s) &= 30s^6+3020s^5+30538s^4+40373s^3+74041s^2+ \\ &\quad 41972s+12467 \\ d(s) &= s^8+26.023s^7+321.70s^6+2635.9s^5+10412s^4+ \\ &\quad +3091.4s^3+11032s^2+306.81s+986.86. \end{aligned}$$

In order to simulate a real application we pretend that the plant P is imprecisely known. Accordingly we do not use any knowledge of the plant's number of poles or (unstable) zeros; we just know that P is open-loop stable. Hence we cannot tell a priori how complex a compensator must be in order to obtain some performance. Conversely we do not know what performance is achievable with a compensator of constrained complexity. The iteration commences with an open-loop identification of $\hat{P}_1$. Fig. 4 shows the Bode log-magnitude plots of P (—) and $\hat{P}_1$ (--). The nominal model $\hat{P}_1$ provides an accurate description of the low frequency behavior of P. The mismatch at the higher frequencies hardly contributes to the identification criterion of (8) with $C_0 = 0$, because this criterion measures an additive error on a linear scale. From $\hat{P}_1$ we design the compensator C_1 as in (7) with $\alpha_i = 0.113$. We apply C_1 to P, we obtain new data, and we subsequently derive several nominal models and compensators. The iteration ends with the nominal model $\hat{P}_5(s) = \hat{n}(s)/\hat{d}(s)$, where

$$\begin{aligned} \hat{n}(s) &= 8.8\cdot 10^{-4}s^5 - 4.77\cdot 10^{-2}s^4 + 34.7s^3 + 2494s^2 + \\ &\quad 1663s + 6028 \\ \hat{d}(s) &= s^5 + 13.3s^4 + 156.3s^3 + 712.4s^2 + 131.3s + 369.4, \end{aligned}$$

with the compensator $C_5(s) = n_c(s)/d_c(s)$, where

$$\begin{aligned} n_c(s) &= 71.407s^4 + 2182.1s^3 + 28718s^2 + 23854s + \\ &\quad +68457 \\ d_c(s) &= s^4 + 129.16s^3 + 4829.0s^2 + 3344.1s + 11571, \end{aligned}$$

and with $\alpha_5 = 20$. The evolution of the nominal models and of the controllers are illustrated respectively in Fig. 4 and Fig. 5. The latter figure displays the gradual increase of control action. The former figure reveals that during the iteration the

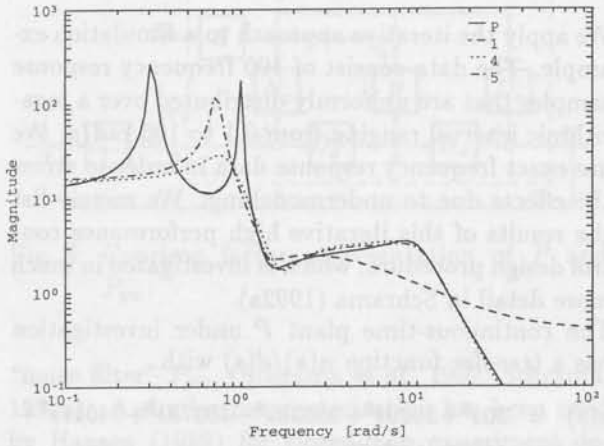

Fig. 4: Log-magnitudes of P (—), $\hat{P}_1$ (--), $\hat{P}_4$ (····) and $\hat{P}_5$ (-·-).

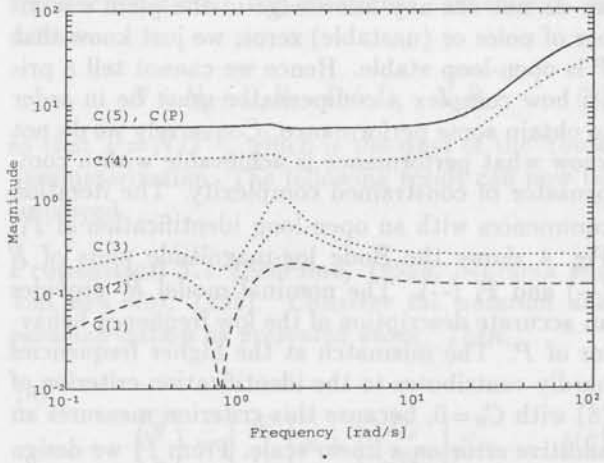

Fig. 5: Log-magnitudes of the designed controllers.

accuracy of the nominal model is improved in the high frequency range at the expense of a large mismatch for the lower frequencies. Despite the large open-loop mismatch between P and $\hat{P}_5$ (see again Fig. 4), the nominal model $\hat{P}_5$ is suited for high performance control design. This is illustrated in Fig. 6, which shows the log-magnitudes of $T(P, C_5)$ and of $T(\hat{P}_5, C_5)$. Considering the logarithmic scale we may conclude that P and $\hat{P}_5$ have very similar high performances under feedback by C_5. Hence the couple $\hat{P}_5$,C_5 is a solution to the joint problem of approximate identification and model-based control design.

Note that the model error that appears in the low frequency range is due to the fact that we have chosen a model order that is too small to capture all system dynamics. If one additionally to the

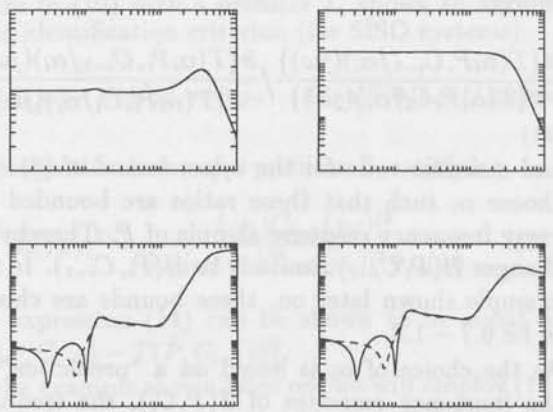

Fig. 6: Log-magnitudes of $T(P, C_5)$ (—) and $T(\hat{P}_5, C_5)$ (--).

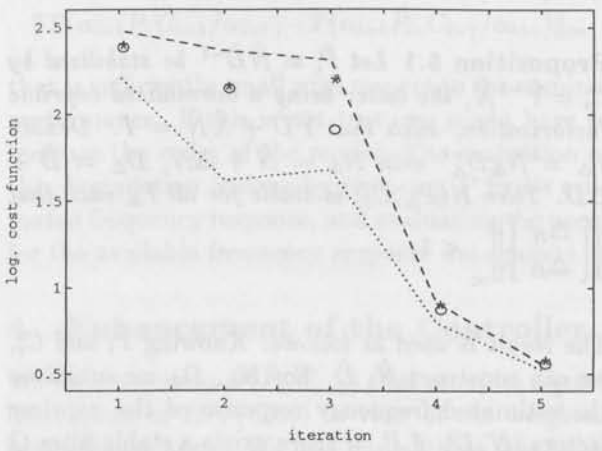

Fig. 7: Logarithm of the performance norms.

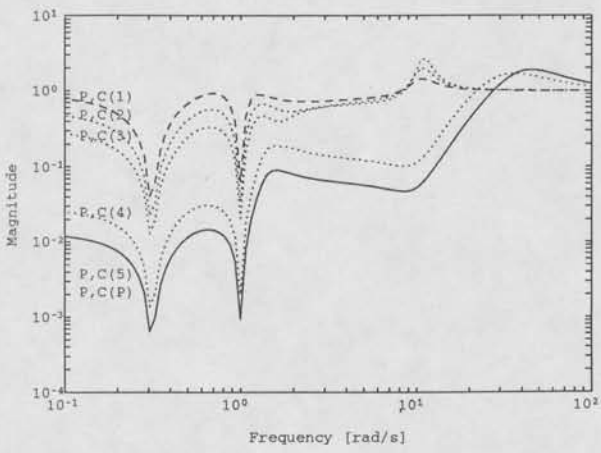

Fig. 8: Sensitivities achieved for the plant P.

high performance control requirements, would require the estimated model to have a similar open loop response as the plant, one has to "pay" for that in terms of a higher model order.

We evaluate the performance norms for all pairs of nominal models and compensators in regard of α_5. That is, we determine for instance $\|T(\alpha_5 P, C_i/\alpha_5)\|$ as the maximum singular value over all frequency reponse samples. These performance norms have been plotted in Fig. 7. The indices at the horizontal axis indicate the iteration step. The performance norms corresponding to $T(\hat{P}_i, C_i)$ and $T(P, C_i)$ are marked respectively by 'o' and '$\star$'. The upper bound of (3), indicated by (--), and the analogous lower bound (····) disclose that the approximation of $T(P, C_i)$ by $T(P_i, C_i)$ is relatively accurate. This is a direct consequence of the frequency reponse based controller enhancement of Section 4. The figure also displays that the "worst-case" performance (--) is improved in each step of the iteration. Finally Fig. 8 shows the evolution of the sensitivity that is achieved for the plant P.

We complete the evaluation by using the method of (7) and α_5 to design also the compensator C_P of order 4 directly from the plant P. In regard of α_5 this C_P is the optimal compensator of order 4 that can be designed for and from the plant P. In Fig. 5 we see that the frequency responses of C_P and C_5 are indiscernible, which produces indiscernible sensitivities for P (see Fig. 8). Thus the iteratively designed high performance compensator C_5 is almost identical with the optimal plant-based compensator C_P, even though no exact knowledge of P nor any information of C_P has been used to achieve C_5.

Lastly we elucidate the need of an iteration to solve the joint problem of approximate identification and model-based control design. The left upper term of $T(P, C_5) - T(\hat{P}_5, C_5)$, which equals $PC_5(I+PC_5)^{-1} - \hat{P}_5 C_5 (I+\hat{P}_5 C_5)^{-1}$, can be rewritten to $(I+PC_5)^{-1}(P-\hat{P}_5)C_5(I+\hat{P}_5 C_5)^{-1}$. Similar expressions can be derived for the other elements of $T(P, C_5)$ and $T(\hat{P}_5, C_5)$. Hence $\hat{P}_5$,C_5 make a *couple* that produces a small mismatch

$$W_L(P, C_5)\ (P-\hat{P}_5)\ W_R(\hat{P}_5, C_5),$$

where W_L and W_R are weighting functions depending on P, $\hat{P}_5$ and C_5. It is tempting to suggest that $\hat{P}_5$ could have been obtained directly from a weighted open-loop identification. However, $W_L(P, C_5)$ and $W_R(\hat{P}_5, C_5)$ depend on the outcome of the iteration, and thus the required weighting functions are not available at the outset.

7 Concluding remarks

We addressed the problem of designing a high performance compensator for an imprecisely known plant. We tackled this problem by an iterative scheme of repeated identification and control design. At each stage of the iteration data is obtained from the plant while it is controlled by the latest compensator. As the iterative design procedure evolves, it learns about the control-relevant dynamics of the plant in question. The resulting nominal model is accurate near the cross-over frequency and, at least as important, the large mismatch at other frequencies does not impair the control design. In addition the iteration reveals the performance that is attainable for the imprecisely known plant.

References

P.M.M. Bongers and O.H. Bosgra (1990). Low order robust H_∞ controller synthesis. *Proc. 29th IEEE Conf. Decision and Control*, Honolulu, HI, pp. 194-199.

R.R. Bitmead, M. Gevers and V. Wertz (1990). *Adaptive Optimal Control, The Thinking Man's GPC.* Prentice Hall, Englewood Cliffs, NJ.

P.E. Caines and M. Baykal-Gürsoy (1989). On the L_∞ consistency of L_2 estimators. *Syst. Control Lett.*, vol.12, pp. 71-76.

F.R. Hansen (1989). *A Fractional Representation Approach to Closed Loop System Identification and Experiment Design.* Ph.D.-Thesis, Stanford University, Stanford, CA, March 1989.

R.G. Hakvoort (1990). Optimal experiment design for prediction error identification in view of feedback design. *Selected Topics in Identification,*

Modelling and Control, vol. 2. Delft University Press, pp. 71-78.

R.G. Hakvoort, R.J.P. Schrama and P.M.J. Van den Hof (1992). Approximate identification in view of LQG feedback design. *Proc. 1992 American Control Conf.*, June 26-28, 1992, Chicago, IL, pp. 2824-2828.

W.S. Lee, B.D.O. Anderson, R.L. Kosut and I.M.Y. Mareels (1992). On adaptive robust control and control-relevant system identification. *Proc. 1992 American Control Conf.*, June 26-28, 1992, Chicago, IL, pp. 2834-2841.

K. Liu and R.E. Skelton (1990). Closed loop identification and iterative controller design. *Proc. 29th IEEE Conf. Decision and Control*, Honolulu, HI, pp. 482-487.

D. McFarlane and K. Glover (1988). An H_∞ design procedure using robust stabilization of normalized coprime factors. *Proc. 27th IEEE Conf. Decision and Control*, Austin, TX, pp. 1343-1348.

D.E. Rivera (1991). Control-relevant parameter estimation: a systematic procedure for prefilter design. *Proc. 1991 American Control Conf.*, Boston, MA, pp. 237-241.

R.J.P. Schrama (1992a). *Approximate Identification and Control Design with Application to a Mechanical System.* Dr. Dissertation, Delft University of Technology, May 1992.

R.J.P. Schrama (1992b). Accurate models for control design: the necessity of an iterative scheme. *IEEE Trans. Automat. Contr., AC-37*, pp. 991-994.

R.J.P. Schrama and P.M.J. Van den Hof (1992). An iterative scheme for identification and control design based on coprime factorizations. *Proc. 1992 American Control Conf.*, June 24-26, 1992, Chicago, IL, pp. 2842-2846.

R.J.P. Schrama, P.M.M. Bongers and D.K. de Vries (1992). Assessment of robust stability from experimental data. *Proc. 1992 American Control Conf.*, Chicago, IL, pp. 266-270.

M. Vidyasagar (1985). *Control System Synthesis: A Factorization Approach.* M.I.T.-Press, Cambridge, MA.

Z. Zang, R.R. Bitmead and M. Gevers (1991). H_2 iterative model refinement and control robustness enhancement. *Proc. 30th IEEE Conf. Decision and Control*, Brighton, UK, pp. 279-284.

CONTENTS Volume 5, December 1992

Parametric uncertainty modelling using LFTs
P.F. Lambrechts, J. Terlouw, S. Bennani and M. Steinbuch 1

Robustness of feedback systems under simultaneous plant and controller perturbation
P.M.M. Bongers 11

Stability robustness for simultaneous perturbations of linear plant and controller: beyond the gap metric
R.J.P. Schrama, P.M.M. Bongers and O.H. Bosgra 19

Generalized frequency weighted balanced reduction
P.M.R. Wortelboer and O.H. Bosgra 29

On orthogonal basis functions that contain system dynamics
P.S.C. Heuberger, P.M.J. Van den Hof and O.H. Bosgra 37

Partial validation of a flexible wind turbine model
G.E. van Baars and P.M.M. Bongers 45

Heat balance reconciliation in chemical process operation
E.A.J.Ch. Baak, J. Krist and S. Dijkstra 53

Worst-case system identification in l_1: error bounds, optimal models and model reduction
R.G. Hakvoort 63

Worst-case system identification in H_∞: error bounds, interpolation and optimal models
R.G. Hakvoort 73

A mixed deterministic-probabilistic approach for quantifying uncertainty in transfer function estimation
D.K. de Vries and P.M.J. Van den Hof 85

Iterative identification and control design: a worked out example
R.J.P. Schrama and P.M.J. Van den Hof 93

TU Delft

Delft University of Technology